Random matrix methods in complex systems analysis

Belga Fedeli, Sirio

Awarding institution:
King's College London

Random Matrix Methods in Complex Systems Analysis

Sirio Belga Fedeli

King's College London

A thesis submitted for the degree of
Doctor of Philosophy

Supervisor:
Prof. Yan V. Fyodorov

London 2021

Abstract

Natural systems consist of many interacting degrees of freedom. The corresponding dynamical behaviour is frequently erratic, i.e. strongly influenced by minute changes in system's parameters, like e.g. boundary conditions. In quantum systems this may lead to huge sample-to-sample fluctuations of observable properties while in classical systems to changes in topological characteristic of the dynamical flow. This intrinsic stochasticity and disorder require statistical tools to achieve a quantitative description of the system's behaviour. In these regards, Random Matrix Theory is the leitmotif of the whole thesis as it provides powerful and versatile techniques for such studies and it connects the investigated topics. The first chapter of this thesis contains the relevant analytical results from Random Matrix Theory necessary for the comprehension of the following chapters. Particular emphasis is devoted to averages of characteristic polynomials of different random matrix ensembles.

The first topic presented in this thesis is the description of quantum scattering in systems with wave chaos. This is an area of active experimental interest and provides one of the best verification of Random Matrix Theory. In particular, we will focus on the presence of uniform absorption, with and without the hypothesis of time-reversal invariance. We computed the distributions of the real and imaginary parts for off-diagonal entries of the Wigner reaction matrix. Such calculations were made possible by previous results for characteristic polynomials of well-known random matrix ensembles and the use of Berezin integrals. We published this work in [1].

The next chapter is devoted to the description of the phase portrait and chaos in classical disordered systems. After a brief overview of recent models and May's work in 1972, we go beyond the linear approximation supported by the Hartman-Grobman theorem, around equilibrium points. We connect this problem and the notion of topological complexity with the mean number of real roots of random multivariate Kac polynomials. A fine tuning of the free parameters reveals the existence of a "resilience radius". Assuming the origin to be stable, the number of fixed points within such radius is exponentially suppressed as the size of the system grows. This represents a measure of the resilience for disordered systems. In ecological terms, we show that the study of resilience of randomly assembled systems has to go through the investigations

of higher order interactions among species. This work has culminated into a paper available at [2]. This chapter is ended with three subsections. In the first one, we introduce a dynamical mean field approach to address and describe the co-existence of fixed points and chaotic motion. However, what presented requires additional work before reaching a publication level. In the second subsection, we investigate the phase portrait for systems whose dynamics is generated by the superposition of random periodic potentials with random amplitudes and wave vectors. This model represents a first connection between dynamical systems and the spectrum of generalized Wishart matrices. The coexistence of more sources of disorder has several implications. Qualitative and few analytical results lead to a rather different statistical picture compared to the behaviour of the models above. Indeed, the energy landscape does not seem to undergo abrupt topological changes, as for any values of the control parameter, the fixed points remain, on average, exponentially abundant. This project is in preparation for publication [3]. The last subsection contains few remarks on May's model with delayed response.

Lastly, the project described in chapter 4 remains, at present, to a preliminary stage. The aim of this chapter is the investigation of critical values for a random, constrained and quadratic function. The complexity of this problem is contained in the definition and tractability of the feasible set. Additionally, difficulties reside in the numerical validation of the analytical results obtained by the replica trick.

This thesis does not include the following second-author publications:

- G.Gradoni, S.Belga Fedeli, M.Richter, O.Legrand, "Mutual Information Statistics for Wireless MIMO Propagation Channels in Confined Environments". *In final review before submission-2021.*

Statement of Originality

I, Sirio Belga Fedeli, confirm that the content of this thesis is my original work. This was done in collaboration with my supervisor Prof. Yan Fyodorov while external contributions and collaborators have been acknowledged and clearly indicated.

date: 18/06/2021

Signature: Sirio Belga Fedeli

Acknowlegements

The four years I spent in London, in the department of mathematics at King's College London, have represented an incredible journey and part of my life. Looking back to my first months in England, I had the opportunity to meet extremely special people, researchers, academics and staff members who soon became friends. Hence, I want here to mention and acknowledge their contribution.

Firstly, my immense gratitude goes to my supervisor Prof. Yan Fyodorov for his continuous support, his immense knowledge, patience and surely for our countless meetings. My appreciation goes beyond these formalities, I'm grateful for encouraging me and celebrating even the smallest achievements behind this work, for giving me that curiosity and instilling that astonishment which are behind any researcher and I hope to preserve them in my academic future.

Special thanks also go to Dr. Mihail Poplavskyi and Dr. Jesper Ipsen for their friendship, their extremely helpful advice and chats, for sharing their time, ideas and knowledge with me.

I'm grateful to the whole Disordered Systems group and CANES CDT, in particular to Dr. Pierpaolo Vivo, Prof. Chris Lorenz, Prof. Reimer Khün, Dr. Valeria De Marco, Joanna Pauk and Prof. Peter Sollich for their support during my master and my PhD at King's.

My gratitude goes to Prof. Boris Khoruzhenko and Prof. Oleg Zaboronski for having accepted the request of being the examiners of my PhD thesis. I want to send a special thanks to Prof. Rondoni for his continuous support since my early days of master at Politecnico di Torino.

A special thank goes to Prof. Gabriele Gradoni for his friendship and for sharing his knowledge with me, for his warm welcome in his group in Nottingham.

I want to say thank you to Prof. Stanislas Leibler for his advice and remarks on chapter 3, for the seminar invitation, for welcoming me in his group in Princeton.

The time spent in the "S5.20" and "4KL12" offices has been extremely precious and enriched by several friends and colleagues. Their presence, words and support were extremely important to me and, I can openly say, they positively contribute to the person I'm today. I'm referring to Francois, Gioia, Rob and Vito. You are really special friends to me and people I know I can count on. Our friendship goes far beyond the university, I feel honoured and deeply lucky to have met you in this journey to London.

I want to say thank you to my old flatmates of The Limes Avenue flat: Fahim, Francois(again!) and Sam. We have shared so many nice memories and celebrations. With nostalgia, I think of those days and I miss living with you. More generally, I express my gratitude to all the friends and colleagues of the third CANES Cohort (2016).

My journey to London has challenged several friendships and relationships born in Italy. I want to deeply thank Andrea for his endless calls, texts but, mostly, for his visit in London. I hope it was a good one. I'm grateful to Marco for his continuous offers to visit Turin (I will come soon hopefully!). A special mention goes to my friends Marianna, Tommaso and Giada, for being extremely patient listeners.

There are people whose support has been fundamental. I want to dedicate this work to the following people. The first is my fiancée Amina (London hasn't just given me degrees and friends eheh...). You are a real companion for life; we will share many more memories in the future. My thoughts go to my grandfather, my grandmothers, my mum, my dad and my brother. They are and will always be an infinite source of support and inspiration.

Lastly, I acknowledge funding by the Centre for Doctoral Training in Cross Disciplinary Approaches to Non-Equilibrium Systems (Engineering and Physical Sciences Research Council through-CANES, Grant Nr. EP/L015854/1).

Contents

List of Figures

Introduction

The first chapter of this thesis contains a quick introduction to Random Matrix Theory and Statistical Physics tools used for the subsequent chapters. The results are presented in a simple way in order to make this work self-contained and accessible. The reader might want to skip these initial parts as the necessary mathematical results will be outlined and will be referred when necessary. The aim of the subsequent chapters is to show how a random matrix approach, in particular by characteristic polynomials of certain random matrix ensembles, is capable of describing some features of different phenomena: quantum chaos, disordered dynamical systems and constrained optimization.

Chapter 1

Random Matrix Theory

From its early stage in 1950s, Random Matrix Theory(RMT) has gradually become a mathematical research field on its own. Benefiting from a very large community of mathematicians and physicists, its success is due to its versatility to describe and embrace several fields of science and engineering. We start by summarizing its history, in particular considering those events which have relevancy for this thesis. We refer the reader to [6] [7] and references therein for more accurate reviews.

1.1 The overview of Classical RMT

The foundation of RMT trace back to 1928 with a work, in Statistics, on finite size Gaussian matrices by J.Wishart [8]. However, the symbolical roots of RMT, as subfield in nuclear Physics, are attributed to Wigner in the 1950s [9]. Interested in heavy nuclei under strong interactions, Wigner realized that a random matrix could be introduced to model the Hamiltonian, i.e. he replaced the self-adjoint operator with a random matrix sufficiently large. Such a matrix, since we are interested in energy levels and, in order to conform to physical principles of probability conservation, has to be Hermitian. Initially Wigner considered the simplest case where the main diagonal is null while the off diagonal entries take value ± 1 with equal probability. He proved, by combinatorics, that the limit spectral density of this matrix converges to the semicircle law. Later it became clear that the semicircle law was valid for any Hermitian matrix whose independent entries are i.i.d. random variables, provided the latter are distributed according to sufficiently fast decaying probability density function. This was the first universality result in RMT[1]. Remarkable achievements were later ob-

[1]we will retrieve this result differently for the Gaussian case by using Supersymmetry in section 1.1.1.4.

tained by Mehta in [10] and Dyson in [11] followed by several other publications. If one assumes the distribution of a Hermitian random matrix $\mathbf{H}$ to be written as the product of the densities of its independent entries, and invariant with respect to any change of the basis, then such probability density function must be proportional to the exponential of the trace of $\mathbf{H}\mathbf{H}^T$. This is the foundation of the Gaussian ensembles further discussed in this chapter. Dyson showed the existence, by Group Theory, of three symmetry ensembles labelled by the Dyson index β. The probability distribution of the latter remains invariant under orthogonal $\beta = 1$, unitary $\beta = 2$ or unitary symplectic $\beta = 4$ transformations. This "Threefold way" was obtained initially for the circular ensembles whose eigenvalues reside on the unitary circle in the complex plane. However, this classification goes beyond the unitary ensembles and is valid for the Gaussian Ensembles above and other distributions. In a nutshell, this is due to the appearance in the joint distribution of the eigenvalues of a repulsion term, coming from the so-called Vandermonde determinant, namely, $|\lambda_i - \lambda_j|^\beta$ (see section 1.1.1.1). Despite its initial motivations in nuclear physics and the results above random matrix theory had a setback due to the discrepancies with experiments for the energy states of Uranium 228 and Erbium 166. In 1967, simultaneously to the publication of the celebrated Mehta's book [12], however not receiving the deserved attention, Marcenko and Pastur retrieved the limit distribution of the singular value of rectangular random matrices [13]. Subsequently, just before the '70s, Ginibre established the circular law for matrices with i.i.d with Guassian entries giving rise to a new thriving period for RMT [14]. The latter includes influences from and to other fields as the emblematic Montgomery's hypothesis on the correlation of zeros of the Riemann zeta function coinciding with the corresponding correlation of random Hermitian matrices [15]. It is also worth to mention, for this thesis, May's seminal paper in ecology [16] (see section 3.1.1). The latter partially explained the discrepancy between experiments and simulations in ecology. Around a decade later, a remarkable milestone in RMT was achieved by the discovery of Free probability [17, 18]. Founded by Voiculescu, such theory aimed to tackle the non-commutative nature of matrices. Introducing the concept of asymptotic freeness, the limit spectral density of the sum of two matrices can be obtained starting from the spectral densities of the single matrices. Similar conclusions hold concerning the product of two *free* matrices. While the bulk regime of the spectrum of Hermitian matrices has marked the beginning of RMT, the edge regime was considered almost 50 years after. The distribution of the maximal eigenvalue, depends on β and was obtained by Tracy and Widom from the solution of a Painleve equation [19][20]. At the beginning of the last century, the spectral properties for the Gaussian and Wishart ensembles were generalized to sparse tri-diagonal random matrix models for non integer β [21]. Last to mention, the circular law was generalized by Tao in [22] including outliers for finite rank perturbed random matrices. More generally, many results mentioned above, with time, have been enriched of proofs and generalizations. Nowadays, RMT have applications in many fields, beyond the Reimann hypothesis, in stochastic calculus, condensed matter and statistical physics, chaos, ecology and signal processing to name few. Beyond the scope of this work, we will mention the most influential papers to this thesis in each section and project separately as necessary. We now review the necessary literature in Random Matrix theory.

1.1.1 Gaussian Ensembles

We start with the $G\beta$E matrices (see [12]). Each component of the entry of the latter is a centered Gaussian random variable of variance J. The probability density function of such matrices is then proportional to the exponential of the trace of $\mathbf{H}^2$, i.e.

$$d\mu(\mathbf{H}) = C_{G\beta E} e^{-\frac{\beta N}{4J^2} \operatorname{Tr} \mathbf{H}^2} d\mathbf{H} \tag{1.1}$$

where the constant $C_{G\beta E} = \frac{1}{2^{N/2}} \left(\frac{2^{\beta-2} N}{\pi J^2} \right)^{\frac{N}{4}(\beta N + 2 - \beta)}$ provides the right normalization in eq(**1.1**). Hence we have:

- Gaussian Orthogonal Ensemble (GOE)$\beta = 1$: the matrix $\mathbf{H}$ is symmetric and its entries are real. For these matrices the measure in eq(**1.1**) is invariant under transformations $\mathbf{H} \to \mathbf{O}^T \mathbf{H} \mathbf{O}$ with $\mathbf{O} \in O(N)$ and $d\mathbf{H} = \prod_{i=1}^N dH_{ii} \prod_{i<j} dH_{ij}$. The matrix $\mathbf{O}^T$ is the transpose of $\mathbf{O}$, i.e. $(\mathbf{O}^T)_{ij} = \mathbf{O}_{ji}$.

- Gaussian Unitary Ensemble (GUE)$\beta = 2$: the matrix $\mathbf{H}$ is Hermitian. For these matrices eq(**1.1**) is invariant under transformations $\mathbf{H} \to \mathbf{U}^\dagger \mathbf{H} \mathbf{U}$ with $\mathbf{U} \in U(N)$ and $d\mathbf{H} = \prod_{k \le j} d \operatorname{Re} H_{kj} \prod_{k<j} d \operatorname{Im} H_{kj}$. $\mathbf{U}^\dagger$ is the conjugate transpose of $\mathbf{U}$, i.e. $(\mathbf{U}^\dagger)_{ij} = \mathbf{U}^*_{ji}$.

- Gaussian Symplectic Ensemble (GSE)$\beta = 4$: the matrix $\mathbf{H}$ is self dual Hermitian matrix. For these matrices eq(**1.1**) is invariant under automorphism: $\mathbf{H} \to \mathbf{W}^R \mathbf{H} \mathbf{W}$ with $\mathbf{W} \in Sp(2N)$ and $d\mathbf{H} = \prod_{k \le j} dH^{(1)}_{kj} \prod_{\ell=2}^4 \prod_{k<j} dH^{(\ell)}_{kj}$. $(\cdot)^R$ is defined as follows. If we consider $\mathbf{W}$ to be a $N \times N$ matrix with 2×2 entries $w_{jk} = \begin{bmatrix} a_{jk} & b_{jk} \\ c_{jk} & d_{jk} \end{bmatrix}$, then $(\mathbf{W}^R)_{kj} = \begin{bmatrix} d_{jk} & -b_{jk} \\ -c_{jk} & a_{jk} \end{bmatrix}$.

For any random variable, x, and its probability density function, $p(x)$, we will indicate the expectation as

$$\mathbb{E}_x[g(x)] = \int_{supp\{p\}} p(x)g(x)dx$$

for sufficiently nice function $g(x)$. The form of eq(**1.1**) is particularly useful whenever we need to compute $\mathbb{E}_{G\beta E}[e^{\mathrm{Tr}\,\mathbf{AH}}]$. By expanding the definition of the trace, assuming for simplicity $J = 1$, and performing a multivariate Gaussian integral, it is straightforward to prove:

$$\mathbb{E}_{GUE(N)}\left[e^{\mathrm{Tr}\,\mathbf{AH}}\right] = \exp\left(\frac{1}{2N}\,\mathrm{Tr}\,\mathbf{A}^2\right) \tag{1.2}$$

and

$$\mathbb{E}_{GOE(N)}\left[e^{\mathrm{Tr}\,\mathbf{AH}}\right] = \exp\left(\frac{1}{4N}\,\mathrm{Tr}(\mathbf{A}+\mathbf{A}^T)^2\right) \tag{1.3}$$

For $g(x)$ invariant under the transformations mentioned above it is sufficient to compute the average $\mathbb{E}_{\mathbf{H}}[g(\mathbf{H})]$ with respect to the joint probability density function of the eigenvalues of $\mathbf{H}$. Examples of such gs include function of the trace of power of $\mathbf{H}$ and functions of the characteristic polynomial of $\mathbf{H}$. Remarkably, the probability density function of $\mathbf{H}$, written in terms of its eigenvectors and eigenvalues, factorizes into the product of the corresponding probability densities, implying that eigenvalues and eigenvectors are independent.

1.1.1.1 Joint PDF of the Eigenvalues

To retrieve the joint probability density function of the eigenvalues we need to compute the Jacobian of the change of variables (see [23]). In what follow we consider, for simplicity the case $\beta = 1$, although similar considerations lead to the distribution of the eigenvalues for the remaining ensembles $\beta = 2$ and $\beta = 4$. Any symmetric matrix $\mathbf{H}$ can be decomposed as the product $\mathbf{O\Lambda O}^T$ where $\mathbf{O} \in O(N)$ while $\mathbf{\Lambda}$ is the diagonal matrix collecting the eigenvalues of $\mathbf{H}$. The differential of $\mathbf{H}$ is given by the chain rule,

$$d\mathbf{H} = d\mathbf{O\Lambda O}^T + \mathbf{O}d\mathbf{\Lambda O}^T + \mathbf{O\Lambda}d\mathbf{O}^T$$

Since $\mathbf{OO}^T = \mathbf{1}_N$ one retrives that $d(\mathbf{OO}^T) = d\mathbf{O}^T\mathbf{O} + \mathbf{O}^T d\mathbf{O} = 0$. It follows

$$d\mathbf{H} = \mathbf{O}(d\mathbf{\Lambda} + [\mathbf{O}^T d\mathbf{O}, \mathbf{\Lambda}])\mathbf{O}^T$$

where we introduced the commutator $[a, b] = ab - ba$. If we relabel $\mathbf{O}^T d\mathbf{O} = d\mathbf{\Phi}$, due to the diagonal form of Λ, the Euclidean line element is given by

$$(ds)^2 = (d\mathbf{H}^T d\mathbf{H}) = ((d\mathbf{\Lambda} + [\mathbf{O}^T d\mathbf{O}, \mathbf{\Lambda}])^T(d\mathbf{\Lambda} + [\mathbf{O}^T d\mathbf{O}, \mathbf{\Lambda}])) \tag{1.4}$$

Since

$$\sum_{i,j}[d\mathbf{\Lambda}^T]_{ij}(d\mathbf{\Phi}\mathbf{\Lambda}-\mathbf{\Lambda}d\mathbf{\Phi})_{ij}=\sum_{ij}[d\mathbf{\Lambda}^T]_{ii}(d\Phi_{ii}\Lambda_i-\Lambda_i d\Phi_{ii})=0$$

$([d\mathbf{\Phi},\mathbf{\Lambda}]^T)_{ij}=[d\mathbf{\Phi},\mathbf{\Lambda}]_{ji}$ and $[d\mathbf{\Phi},\mathbf{\Lambda}]_{ij}=(\Lambda_j-\Lambda_i)d\Phi_{ij}$, then the quadratic term of the commutator in eq(**1.4**) simplifies to $\mathrm{Tr}([\mathbf{O}^T d\mathbf{O}, d\mathbf{\Lambda}]^T,[\mathbf{O}^T d\mathbf{O}, d\mathbf{\Lambda}])=\sum_{ij}(\Lambda_i-\Lambda_j)^2(d\Phi_{ij})^2$. Finally:

$$(ds)^2=\sum_i(d\Lambda_i)^2+\sum_{ij}(\Lambda_i-\Lambda_j)^2(d\Phi_{ij})^2$$

The line element does not contain terms of the form $(d\Lambda_i)(d\Phi_{ij})$. This implies that the Jacobian matrix is a block matrix and its determinant is given by the product of the determinants of two squared blocks. The Jacobian $|\mathcal{J}|_{\beta=1}$ is therefore given by the Vandermonde determinant, $\Delta(\mathbf{\Lambda})=\prod_{i<j}|\Lambda_i-\Lambda_j|$. A similar result holds for the GUE and GSE ensembles. In the first case each entry of $\mathbf{\Phi}$ is a complex variable, in the second case the entries of $\mathbf{\Phi}$ are quaternion parametrize by four variables. Therefore $|\mathcal{J}|_{\beta=2}=\prod_{i<j}|\Lambda_i-\Lambda_j|^2$ and $|\mathcal{J}|_{\beta=4}=\prod_{i<j}|\Lambda_i-\Lambda_j|^4$. By integrating out $\mathbf{O}$ one obtain the probability density function of the eigenvalues, namely:

Theorem :*(see [12]) the joint probability density function for the eigenvalues of matrices drawn from the Gaussian Orthogonal($\beta=1$), the Gaussian Unitary($\beta=2$) and the Gaussian Symplectic($\beta=4$) Ensembles is given by:*

$$p_{N\beta}(x_1,..,x_N)=C_{N\beta}\exp\Big(-\frac{\beta}{2}\sum_{j=1}^N x_j^2\Big)\prod_{j<i}|x_j-x_i|^\beta \tag{1.5}$$

The constant $C_{N\beta}$ is chosen such that $p_{N\beta}$ is normalised, i.e.:

$$\int_{\mathbb{R}^N}p_{N\beta}(x_1,..,x_N)dx_1..dx_N=1$$

At this point, one can obtain the distribution of the single eigenvalue by integrating out the remaining $N-1$ variables from eq(**1.5**). Additionally, passing to the limit $N\to+\infty$, one retrieves the semicircle law, $\rho_{sc}(x)$. Following Wigner's initial spirit, the latter can be derived by explicitly computing, to the leading order, the average of the trace of the powers of $\mathbf{H}$. These powers are associated with the sequence of Catalan numbers. Alternatively, the spectral density, for finite N, can be obtained by introducing the set of Hermite polynomials and re-write the joint probability density function as a determinantal($\beta=2$) or Pfaffian($\beta=1,4$) point process with a given kernel ([24, 25]). The joint density function for k of the N eigenvalues drawn from eq(1.5) satisfies

$$p_{N2}(x_1, ..., x_k) = \frac{N!}{(N-k)!}\det\left(K_N^{(2)}(x_i, x_j)_{i,j=1}^k\right)$$

for $\beta = 2$, and

$$p_{N\beta}(x_1, ..., x_k) = \frac{N!}{(N-k)!}\,\mathrm{Pf}\left(\mathbf{K}_N^{(\beta)}(x_i, x_j)_{i,j=1}^k\right)$$

for $\beta = 1, 4$ and where the functions $K_N^{(2)}$ and $\mathbf{K}_N^{(\beta)}$ are scalar and 2×2 matrix kernels respectively[2]. The complexity of such expressions can be considerably reduced, with the help of the Christoffel-Darboux formula to the single eigenvalue distribution. We take this opportunity to introduce two powerful tools which will be essential in the following chapters. We will retrieve the semicircle by introducing the so called replica trick and a set of anticommuting Grassmann variables. As it will be pointed out, this lacks the mathematical rigour. However, the most general and complete result will be promptly presented.

We define the limiting spectral density of an ensemble of random Hermitian matrices $\mathbf{H}$, $\rho(x)$, as

$$\rho(x) = \lim_{N\to+\infty}\frac{1}{N}\mathbb{E}\left[\sum_{i=1}^N \delta(\lambda_i - x)\right]$$

where λ_i are the eigenvalues of $\mathbf{H}$. Since $\mathrm{Im}\left(\lim_{\varepsilon\to 0^+}\frac{1}{x-i\varepsilon}\right) = \pi\delta(x)$, $\rho(x)$ can be written by introducing the resolvent $G_N(x) = \frac{1}{N}\mathrm{Tr}\,\frac{1}{\mathbf{H}-x\mathbf{1}_N}$ where $\mathbf{1}_N$ is the identity matrix. Hence, the semicircle law is obtained as

$$\rho_{sc}(x) = -\frac{1}{\pi}\lim_{\varepsilon\to 0^+}\mathrm{Im}\,\mathbb{E}_{GUE}\left[G_{+\infty}(x - i\varepsilon)\right]$$

Lastly, the average of the resolvent can be written in terms of

$$-\frac{1}{N}\frac{d}{dx}\mathbb{E}_{GUE}\left[\log\det(\mathbf{H}_N - x\mathbf{1}_N)\right] \tag{1.6}$$

The average of a logarithm is clearly unpleasant and one would like to find an alternative way to compute such average. Ideally, if one could possibly move and interchange the logarithm with the expectation the calculation would simplify considerably. Inheriting its name from Physics, this approach is called *annealed*. In what follows we will perform a more justifiable calculation, the *quenched* calculation by the replica trick.

[2]For an exhaustive treatise on determinantal and Pfaffian point processes we refer the reader to [26]

1.1.1.2 Replica Trick

Firstly, we consider a positive random variable $\mathcal{Z}$, for which the integral $\mathbb{E}[\log \mathcal{Z}] = \int_0^{+\infty} dx p_{\mathcal{Z}}(x) \log x$ is well defined and convergent. Since such integral is usually challenging we can make use of the following identity for positive variable:

$$\log \mathcal{Z} = \lim_{n \to 0} \frac{\mathcal{Z}^n - 1}{n}$$

We plug this expression inside the average. Then the calculation of the expectation of the logarithm is equivalent to the calculation of $\mathbb{E}[\mathcal{Z}^n]$ and clearly

$$\mathbb{E}[\log \mathcal{Z}] = \lim_{n \to 0} \frac{\mathbb{E}[\mathcal{Z}^n] - 1}{n} \tag{1.7}$$

Going back to the initial problem one easily identifies $\mathcal{Z}(x)$ with $\det(\mathbf{H} - x\mathbf{1}_N)$. If one knows $\mathbb{E}[\mathcal{Z}^n]$ for any real n then $\mathbb{E}[\log(\mathcal{Z})]$ easily follows. As it will be presented in the next section, the average of the power of this characteristic polynomial is again tricky and it is usually known only for integer values of n. We overcome this difficulty in the following way. As our main goal is to retrieve ρ_{sc}, we need to take the limit $N \to +\infty$. Firstly, we assume that, by taking the latter for $\mathbb{E}[\mathcal{Z}^n]$, there is, to the leading order, an analytical continuation from natural to the real numbers in n for such average. Indeed, we address the limit $N \to +\infty$ in the saddle-point framework, taking the replica limit $n \to 0$ in the end. For sake of clarity, we will omit the details of the saddle point approximation. The latter, together with more complete and exhaustive results, will be the subject of section 1.2.

To motivate the content of the next chapters, we temporally turn our attention to a useful example of the replica trick. This is an adapted version of an example contained in [27]. We consider a model for which the replica trick holds in order to illustrate its essential features.

Replicas of Harmonic Oscillator:
We start computing the partition function $\mathcal{Z}$ of the system described by the following quadratic Hamiltonian

$$H(x,p) = \frac{\lambda^2 x^2}{2} + \frac{p^2}{2} \tag{1.8}$$

We assume that the frequency of the oscillator, λ, is a positive random variable with probability density function $f(\lambda) = \frac{2}{\pi}\frac{1}{1+\lambda^2}$, i.e. one side Cauchy distributed. We introduce an additional variable, the inverse temperature, β, and compute the partition function

$$\mathcal{Z} = \int_{\mathbb{R}} dx \int_{\mathbb{R}} dp \exp\left(-\beta H(x,p)\right) \tag{1.9}$$

The Gaussian integrals above, for a fixed realization of λ, give $\mathcal{Z} = \frac{2\pi}{\beta\lambda}$. Therefore, after performing the average in λ, we have, from the definition of secant function, for $n < 1$,

$$\mathbb{E}[\mathcal{Z}^n] = \left(\frac{2\pi}{\beta}\right)^n \sec\left(\frac{n\pi}{2}\right) \tag{1.10}$$

We now forget the result above and we replicate the system above n-times, namely ($n \in \mathbb{N}$),

$$\mathbb{E}[\mathcal{Z}^n] = \mathbb{E}_\lambda \left[\int \prod_{i=1}^{n} dx_i dp_i \exp\left(\sum_{i=1}^{n} H(x_i, p_i)\right)\right] \tag{1.11}$$

The integration over all p_i is simply $(\frac{2\pi}{\beta})^n$. Therefore,

$$\mathbb{E}[\mathcal{Z}^n] = \left(\frac{2\pi}{\beta^{1/2}}\right)^n \frac{1}{\Gamma\left(\frac{n}{2}\right)} \int_0^{+\infty} dR R^{n-1} \int_0^{+\infty} d\lambda e^{-\lambda^2 \frac{\beta R^2}{2}} f(\lambda) \tag{1.12}$$

For simplicity we perform the integration over λ first. This is equivalent to

$$\exp\left(\frac{\beta R^2}{2}\right) \operatorname{erfc}\left(\frac{\beta^{1/2} R}{2}\right)$$

Lastly, the integral in R is convergent for $n < 1$. This is perfectly fine as n does not need to be an integer anymore. Therefore,

$$\mathbb{E}[\mathcal{Z}^n] = 2\left(\frac{\pi}{\beta}\right)^n \frac{\Gamma\left(\frac{1-n}{2}\right)\Gamma(n)}{\sqrt{\pi}\,\Gamma\left(\frac{n}{2}\right)} \tag{1.13}$$

For $n < 1$, eq(**1.10**) and eq(**1.13**) are equal.

1.1.1.3 Supersymmetry Approach

In order to compute the expectation of $\det(H_N - x\mathbf{1}_N)^n$ the simplest way is to rewrite the latter making use of the formulas at the beginning of section 1.1.1. To do so, we introduce the Supersymmetry Method. This approach finds its roots and vocabulary in particle Physics as adapted to condensed matter theory in the work of Efetov[28][29]. In this regard, for the purpose of this thesis we only briefly discuss the Fermionic formulation. Systems of Fermions can be described by a set of Grassmann variables ψ_i. Any pair of these anticommutes i.e.

$$\psi_i \psi_j = -\psi_j \psi_i.$$

Instead, usual variables commute with ψ_i. Taking $j = i$ in the equality above implies that any ψ_i is nilpotent since for the square and any other greater power n, $\psi_i^n = 0$. Therefore, any analytic function of ψ_i reduces, by its Taylor expansion, to a finite order polynomial. For our purpose a meaningful example is

$$\exp(x\psi_i\psi_j) = 1 + x\psi_i\psi_j$$

Considering n Grassmann variables, any function of the latter is truncated to the first 2^n terms. Lastly, we introduce the operation of integration over such variables. This integral, called Berezin integral, cannot be formulated in the usual way, as Lebesque or Riemann integral, since ψ_i are only symbolic variables and do not have numerical values. The integral over ψ_i is formally defined by postulating two properties, i.e.

- $\int D\psi = 0$
- $\int D\psi\psi = 1$

Any change of variable within the integral requires a counter intuitive differential. In fact, in order to have the value of the integral unique and keep the properties above, for $x\psi_i = \tilde{\psi}$ we need to impose $d\psi_i = xd\tilde{\psi}$. The generalisation to multivariate integral follows straightforwardly recalling that each differential is a Grassmann variable and therefore anticommutes with all the other Grassmann variables as well. Hence, any function of ψ_j can be integrated. Indeed, the analogy with usual integral is only formal as the Berezin integral does not require any notion of convergence. This stems from the fact that the integral of a generic function is obtained by the integral of its Taylor expansion. As an example

$$\int D\psi_i \int D\psi_j e^{x\psi_j\psi_i} = \int D\psi_i \int D\psi_j(1 + x\psi_j\psi_i) = x$$

In analogy with the one dimensional case, if we replace x with the determinant of a any $N \times N$ matrix $\mathbf{A}$ with commuting entries, and introduce two set of anti-commuting Grassmann vectors $\boldsymbol{\psi}^T = (\psi_1, ..., \psi_N)$ and $\tilde{\boldsymbol{\psi}}^T = (\tilde{\psi}_1, ..., \tilde{\psi}_N)$ we have

$$\det(\mathbf{A}) = \int D\boldsymbol{\psi} D\tilde{\boldsymbol{\psi}} \exp\left(\tilde{\boldsymbol{\psi}}^T \mathbf{A} \boldsymbol{\psi}\right)$$

The argument in the exponential is equivalent to $\tilde{\boldsymbol{\psi}}^T \mathbf{A} \boldsymbol{\psi} = -\operatorname{Tr} \boldsymbol{\psi}\tilde{\boldsymbol{\psi}}^T \mathbf{A}$. We are now able to compute the average over the Gaussian ensembles of eq(**1.6**), we just need to introduce n *replicas* of the Berezin integral.

1.1.1.4 The Semicircle Law

As already stated, the validity of the result we are going to present goes beyond the Gaussian ensemble and a complete stand-alone theorem is presented at the end of this section. However, this section gives us the opportunity to master the theory so far introduced. The ingredients presented so far allows one to retrieve the semicircle for the Gaussian Ensembles easily. From eq(1.7), the resolvent of the matrix $\mathbf{H}$ reads

$$\mathbb{E}_{GUE(N)}\left[G_N(x)\right] = -\frac{1}{N}\frac{d}{dx}\lim_{n\to 0^+}\frac{1}{n}\mathbb{E}_{GUE(N)}\left[\det(\mathbf{H}-x\mathbf{1}_N)^n\right]$$

where, for simplicity, we assume $\mathbf{H}$ is drawn from the Gaussian Unitary ensemble. Without issues of convergence, the argument of the logarithm can be written as integrals of Grassmann variables $(\boldsymbol{\psi}, \boldsymbol{\psi}^\dagger)$, namely:

$$\mathbb{E}_{GUE(N)}\left[\det(\mathbf{H}-x\mathbf{1}_N)^n\right] = \frac{1}{i^N}\mathbb{E}_{GUE(N)}\left[\int\prod_{j=1}^{n} D\boldsymbol{\psi}_j D\boldsymbol{\psi}_j^\dagger e^{i\sum_{j=1}^{n}\boldsymbol{\psi}_j^\dagger(\mathbf{H}-x\mathbf{1}_N)\boldsymbol{\psi}_j}\right]$$

performing the ensemble average of $\exp\left(-i\,\mathrm{Tr}\,\mathbf{H}(\sum_{j=1}^{n}\boldsymbol{\psi}\boldsymbol{\psi}^\dagger)\right)$ from eq(1.2) we obtain:

$$\mathbb{E}_{GUE(N)}\left[\det(\mathbf{H}-x\mathbf{1}_N)^n\right] = \frac{1}{i^N}\int\prod_{j=1}^{n} D\boldsymbol{\psi}_j D\boldsymbol{\psi}_j^\dagger \left(e^{-ix\sum_{j=1}\boldsymbol{\psi}_j^\dagger\boldsymbol{\psi}_j}\right) e^{\frac{1}{2N}\mathrm{Tr}\,\mathbf{Q}^2} \tag{1.14}$$

where:

$$\mathbf{Q} = \begin{bmatrix} \boldsymbol{\psi}_1^\dagger\boldsymbol{\psi}_1 & \boldsymbol{\psi}_1^\dagger\boldsymbol{\psi}_2 & \dots \\ \vdots & \ddots & \\ \boldsymbol{\psi}_n^\dagger\boldsymbol{\psi}_1 & & \boldsymbol{\psi}_n^\dagger\boldsymbol{\psi}_n \end{bmatrix}$$

So far, up to a constant factor, the equations above are exact for any dimension N. If one prefers to work with exact formulas, it is possible to pass from the set of matrices $\mathbf{Q}$ with nilpotent entries to an integration over the manifold of standard unitary matrices according to the rotational symmetries of the integrand. This procedure is called Superbosonization and it will be the subject of the next chapter. To obtain the circular law, we are interested in the leading order, as $N \to +\infty$, of the integral above. Therefore, we proceed as follows. The last term in eq(1.14) can be linearized by the Hubbard-Stratonovich transformation as

$$e^{\frac{1}{2N}\mathrm{Tr}\,\mathbf{Q}^2} \propto \int_{Herm(n)} d\hat{\mathbf{Q}} e^{-\frac{N}{2}\mathrm{Tr}\,\hat{\mathbf{Q}}^2 + \mathrm{Tr}\,\hat{\mathbf{Q}}\mathbf{Q}}$$

where the integration runs over the set of $n \times n$ Hermitian matrices and the omitted proportionality constant depends upon N and n. However, the latter contains sub-leading terms as we take $N \to +\infty$ and $n \to 0^+$. Substituting back into eq(**1.14**) and exchanging the order of the integrals we obtain:

$$\mathbb{E}_{GUE(N)}\left[\det(\mathbf{H} - x\mathbf{1}_N)^n\right] \propto \int_{Herm(n)} d\hat{\mathbf{Q}} e^{-\frac{N}{2}\operatorname{Tr}\hat{\mathbf{Q}}^2} \int \prod_{j=1}^{n} D\boldsymbol{\psi}_j D\boldsymbol{\psi}_j^\dagger$$

$$\times \exp\left(\begin{bmatrix} \boldsymbol{\psi}_1 \\ \boldsymbol{\psi}_2 \\ \vdots \\ \boldsymbol{\psi}_n \end{bmatrix}^\dagger \begin{bmatrix} (\hat{\mathbf{Q}}_{11} - ix)\mathbf{1}_N & \hat{\mathbf{Q}}_{12}\mathbf{1}_N & \dots & \hat{\mathbf{Q}}_{1n}\mathbf{1}_N \\ \hat{\mathbf{Q}}_{12}\mathbf{1}_N & \ddots & & \vdots \\ \vdots & & & \\ \hat{\mathbf{Q}}_{1n}\mathbf{1}_N & \dots & \dots & (\hat{\mathbf{Q}}_{nn} - ix)\mathbf{1}_N \end{bmatrix} \begin{bmatrix} \boldsymbol{\psi}_1 \\ \boldsymbol{\psi}_2 \\ \vdots \\ \boldsymbol{\psi}_n \end{bmatrix} \right) \tag{1.15}$$

The matrix above can be written as $(\hat{\mathbf{Q}} - ix) \otimes \mathbf{1}_N$ and its determinant is equal to $(\det(\hat{\mathbf{Q}} - ix\mathbf{1}_N))^N$. Therefore we obtain:

$$\mathbb{E}_{GUE(N)}\left[\det(\mathbf{H} - x\mathbf{1}_N)^n\right] \propto \int d\hat{\mathbf{Q}} e^{-\frac{N}{2}\operatorname{Tr}\hat{\mathbf{Q}}^2 + N\log\det(\hat{\mathbf{Q}} - ix\mathbf{1}_n)}$$

We have reduced the complexity of our calculation as we started from the integral over $2nN$ (Grassmannian variables). Since $\hat{\mathbf{Q}}$ is Hermitian and the integrand in eq(**1.15**) is unitary invariant, we can perform a final change of variables $\hat{\mathbf{Q}} = \mathbf{U}\boldsymbol{\Lambda}\mathbf{U}^\dagger$, i.e. $d\hat{\mathbf{Q}} = \prod_{i<k} |\lambda_i - \lambda_k|^2 (\mathbf{U}^\dagger d\mathbf{U}) d\boldsymbol{\Lambda}$. The integral above becomes[3]

$$\mathbb{E}_{GUE(N)}\left[\det(\mathbf{H} - x\mathbf{1}_N)^n\right] \propto \int d\mathbf{U} d\Lambda \prod_{i<k} |\lambda_i - \lambda_k|^2 e^{N\sum_{j=1}^{n}\mathcal{L}(\lambda_j)}$$

with $\mathcal{L}(\lambda) = -\frac{1}{2}\lambda^2 + \log(\lambda - ix)$. As $N \gg 1$, the main contribution to the integral above stems from the saddle points of the argument at the exponent. In fact, it has to be noted that the Vandermonde determinant is not taken into account to find the position of such points as it consists of only $n(n-1)$ terms and it doesn't scale with N. So we can write $\mathbb{E}_{GUE(N)}\left[\det(\mathbf{H} - x\mathbf{1}_N)^n\right] \propto \exp\{Nn\Phi(x)\}$ for some $\Phi(x)$. A critical points of $\mathcal{L}(\lambda)$ is given by $\lambda_{sd} = \frac{1}{2}(ix + \sqrt{4 - x^2})$. Therefore, in a neighbourhood of the latter[4]

$$\mathcal{L}(\lambda) \approx \mathcal{L}(\lambda_{sd}) + \frac{1}{2}\left(x^2 - 4 - ix\sqrt{4 - x^2}\right)(\lambda - \lambda_{sd})^2.$$

[3]See section 1.1.1.1

[4]We postpone and provide the details of this technique in section 1.2.2

We can modify the contour of integration in order to approach λ_{sd} with angles $\theta = -\frac{\varphi}{2} + (2k+1)\frac{\pi}{2}$ with $k = 0, 1$. The phase of $\frac{d^2\mathcal{L}}{d\lambda^2}(\lambda_{sd})$, φ, is given by

$$\varphi = \begin{cases} \pi \text{ for } x \leq -2 \\ \pi - \arctan\left(\frac{x\sqrt{4-x^2}}{x^2-4}\right) \text{ for } -2 < x \leq 0 \\ -\pi - \arctan\left(\frac{x\sqrt{4-x^2}}{x^2-4}\right) \text{ for } 0 < x \leq 2 \\ 0 \text{ for } x > 2 \end{cases} \tag{1.16}$$

One can easily see that $\mathcal{L}(\lambda_{sd})$ is exactly $\Phi(x)$. So we are left with the evaluation of

$$\int_{-\infty}^{+\infty} dz_{j=1}^{n} \prod_{i<k} |z_i - z_k|^2 e^{-\frac{N\alpha}{2}\sum_{j=1}^{n} z_j^2} \tag{1.17}$$

with $\alpha = \left|\frac{d^2\mathcal{L}}{d\lambda^2}\right|(\lambda_{sd})$. Integral in eq(**1.17**) can be computed exactly. Moreover, one observes that it is proportional to the normalizing factor in eq(**1.5**) and it does not represent a matter of concern. We can now substitute these results back into the resolvent, namely $\lim_{N\to+\infty} \mathbb{E}\left[G_N(x)\right] = -\frac{d}{dx}\Phi(x) = -\frac{1}{2}(x + i\sqrt{4-x^2})$. Lastly:

$$\begin{aligned} \rho_{sc}(x) &= \frac{1}{2\pi} \lim_{\varepsilon\to 0^+} \operatorname{Im}\{(x - i\varepsilon) + i\sqrt{4-(x-i\varepsilon)^2}\} \\ &= \frac{\sqrt{4-x^2}}{2\pi} \text{for } |x| < 2 \end{aligned} \tag{1.18}$$

This is the semicircle law obtained from the Gaussian Unitary Ensemble. Similar calculations occur for the other two invariant ensembles.

We conclude this section with a generalized and more rigorous version, beyond the Gaussian ensembles, of this result. Let's consider $\frac{N(N+1)}{2}$ i.i.d. real and centered random variables $X_{i\leq j}$ drawn from two distributions, one for X_{ii} and another one for $X_{i<j}$ respectively, with finite second moment. We rescale such variables by $1/\sqrt{N}$, rearrange them in a $N \times N$ symmetric matrix $\mathbf{M}_N$ according to the indexes above and compute its spectral empirical distribution $R_N(x) = \frac{1}{N}\sum_{i=1}^{N}\delta(x-\lambda_i)$ where λ_i are the eigenvalues of $\mathbf{M}_N$. Then, the random measure R_N converges in probability to the semicircle law, i.e.

Theorem: *([30]) Given the ensemble of matrices with the properties above, a bounded continuous function f and $\delta > 0$ the following limit holds*

$$\lim_{N\to+\infty} p(|(R_N, f) - (\rho_{sc}, f)| > \delta) = 0$$

1.1.1.5 Ratio of Characteristics Polynomials

While we will address the corresponding applications in Physics later in this thesis, the mathematical results on characteristics polynomials are interesting on their own. In particular, the mean value of ratio of characteristics polynomials of certain ensembles provides a wonderful insight in the statistical description of quantum chaos with uniform absorption. For unitary invariant Hermitian matrices, whose probability density function is of the form $\exp(-N\,\mathrm{Tr}\,V(\mathbf{H}))$, such ratios have a determinantal form given by integrable kernels. The latter are defined by orthogonal polynomials and the associate Cauchy transform. For the purpose of this thesis, we want an explicit formula for

$$\mathcal{F}^K(\boldsymbol{\mu},\boldsymbol{\varepsilon}) = \mathbb{E}_{Herm(N),V}\left[\prod_{j=1}^{K}\frac{\det(\mu_j\mathbf{1}_N-\mathbf{H})}{\det(\varepsilon_j\mathbf{1}_N-\mathbf{H})}\right] \tag{1.19}$$

To obtain this quantity, [31] rewrote such expression as function of the correlation among products of characteristic polynomials only. Consider $\mathrm{Im}\,\varepsilon_j \neq 0$ for $j = 1,..,K$, then

$$\mathcal{F}^K(\boldsymbol{\varepsilon},\boldsymbol{\mu}) = (-1)^{K(K-1)/2}\left(-\frac{2\pi i}{c_{N-1}^2}\right)^K \frac{\Delta(\boldsymbol{\varepsilon},\boldsymbol{\mu})}{\Delta^2(\boldsymbol{\varepsilon})\Delta^2(\boldsymbol{\mu})}\det[W_N(\varepsilon_i,\mu_j)]_{i,j=1}^K$$

where the kernel $W_N(\varepsilon,\mu)$ is given by:

$$W_N(\varepsilon,\mu) = \frac{h_N(\varepsilon)\pi_{N-1}(\mu) - h_{N-1}(\varepsilon)\pi_N(\mu)}{\varepsilon-\mu},$$

The constant c_j is the normalization for the monic polynomials $\pi_j(x) = x^j + ..$ orthogonal with respect to the meausure $e^{-NV(x)}dx$. The term $h_j(x)$ is its Cauchy transform

$$h_j(x) = \frac{1}{2\pi i}\int \frac{e^{-NV(y)}\pi_j(y)}{y-x}dy \text{ with } x \in \mathbb{C}/\mathbb{R}$$

Dyson limit for $\mathcal{F}(\boldsymbol{\mu},\boldsymbol{\varepsilon})$:

The previous result is exact for any finite N. However, we will be interested in $K = 2$ and the large N regime, at the scale of the mean separation length between two eigenvalues. This corresponds to the Dyson limit

$$\mathcal{F}^K\left(x+\frac{\boldsymbol{\xi}}{N\rho(x)}, x+\frac{\boldsymbol{\eta}}{N\rho(x)}\right) = (-1)^{K(K-1)/2}e^{-\alpha(x)\sum_{i=1}^K(\xi_i-\eta_i)} \times \frac{\Delta(\xi,\eta)}{\Delta^2(\xi)\Delta^2(\eta)}\det[\mathbb{S}_{II}(\xi_i-\eta_j)]_{i,j=1}^K \tag{1.20}$$

where $\alpha(x) = \frac{V'(x)}{2\rho(x)}$ and the kernel $\mathbb{S}_{II}(\xi - \eta)$ is given by

$$\begin{cases} \frac{e^{i\pi(\xi-\eta)}}{\xi-\eta} \text{ with } \operatorname{Im}\xi > 0 \\ \frac{e^{-i\pi(\xi-\eta)}}{\xi-\eta} \text{ with } \operatorname{Im}\xi < 0 \end{cases} \tag{1.21}$$

This was obtained again in [31] by adopting a Riemann-Hilbert approach.

1.1.1.6 Correlations for Determinants of GOE Matrices

To obtain new results concerning the average of ratios of characteristic polynomials for GOE matrices, we do not follow the techniques used in [31]. The difficulties in obtaining the correlations function of GOE characteristic polynomials are related to the absence of a Harish-Chandra-Itzykson-Zuber integral for orthogonal matrices (although see [32]) and the fact that the joint density of eigenvalues has a Pfaffian structure due to the De Brujin identities. However, even in this case, averages of products and ratios of determinants are known due to Borodin and Strahov [33]. Once again we don't need the finite N expression rather the Dyson limit of $\mathcal{Z}(\mu_1, \mu_2) = \det(\mathbf{H} - \mu_1 \mathbf{1}_N) \det(\mathbf{H} - \mu_2 \mathbf{1}_N)$. Such result was obtained by [34], i.e.

$$\lim_{N\to+\infty} \sqrt{2\pi} \frac{N^{N-3/2} e^{-N\xi^2/2}}{N!} \mathbb{E}_{GOE(N)} \left[\mathcal{Z}\left(\xi + \frac{\lambda_1}{N\rho_{sc}(\xi)}, \xi + \frac{\lambda_2}{N\rho_{sc}(\xi)} \right) \right] = \tag{1.22}$$

$$= e^{\xi(\lambda_1+\lambda_2)/(2\rho(\xi))} (2\pi\rho_{sc}(\xi))^3 \frac{1}{2} \left(\frac{\sin(\pi(\lambda_1-\lambda_2))}{(\pi(\lambda_1-\lambda_2))^3} - \frac{\cos(\pi(\lambda_1-\lambda_2))}{(\pi(\lambda_1-\lambda_2))^2} \right)$$

where $\xi \in (-2, 2)$.

We will provide an example for which $\mathbf{H}$ is symmetric but its entries are strongly correlated so this (Dyson) rescaling does not hold (see section 1.3.3).

1.1.1.7 Half-integer Powers of Characteristic Polynomials

In investigating the chaotic scattering of quantum systems we will assume the presence or absence of time symmetry. The presence of such symmetry poses challenging tasks for the calculation of the statistics of the entries of the Wigner reaction matrix (we postpone its definition and investigation to chapter 2). The most successful approach to describe this quantity is by its characteristic function. The latter is proportional to the average of ratios of characteristic polynomials of GOE matrices. In principle, after obtaining the characteristic function is sufficient to compute its Fourier transform. This procedure contains several limitations due to the complicated form of the functions involved. For these reasons an explicit formula for these averages represents a hard task. Remarkable results were obtained in [35] motivated by study of scattered waves without an absorbing environment. More precisely they obtained

$$\lim_{\varepsilon\to 0, N\to+\infty} \mathbb{E}\left[\frac{\det(\mathbf{H}^2)}{\det(\mathbf{H}^2+\frac{x^2}{N^2})^{1/2}\det(\mathbf{H}^2+\frac{\varepsilon^2}{N^2})^{1/2}}\right] = \frac{2}{\pi}\left(|x|K_0(|x|)+\int_{|x|}^{+\infty} dy K_0(y)\right) \tag{1.23}$$

Where $K_0(x)$ is the modified Bessel function of the second kind. This result was extended to include further complex shift of the spectrum of $\mathbf{H}$ (see [1] and section 1.1.1.7). This will allow us to include the presence of absorption for the mentioned problem.

1.1.2 Circular Law and Outliers

We now turn our attention to fully asymmetric random matrices whose entries are again normally distributed. These correspond to the Ginibre ensembles. For the present work it is sufficient to consider the real ensemble (GinOE) such that each entry is i.i.d. and $G_{ij} \sim \mathcal{N}(0,1)$. The probability density function of the entries can re-arranged similarly to GβE as

$$d\mu(\mathbf{G}) = (\sqrt{2\pi})^{-N^2} e^{-\frac{1}{2}\operatorname{Tr}\mathbf{G}\mathbf{G}^T} d\mathbf{G}$$

Analogously to the Hermitian case one can work out the expectation of the trace:

$$\mathbb{E}_{GinOE}\left[e^{\operatorname{Tr}(\mathbf{G}\mathbf{A}+\mathbf{G}^T\mathbf{B})}\right] = e^{\frac{1}{2}\operatorname{Tr}(\mathbf{A}^T\mathbf{A}+\mathbf{B}^T\mathbf{B}+2\mathbf{A}\mathbf{B})}$$

The probability density function above is invariant under $\mathbf{G} \to \mathbf{O}\mathbf{G}\mathbf{V}$ with $\mathbf{O}, \mathbf{V} \in Orth(N)$. To obtain the distribution of the eigenvalues one can proceed similarly to the case for Hermitian matrices considering $\mathbf{G} = \mathbf{U}(\mathbf{\Lambda}_d + \mathbf{\Lambda}_s)\mathbf{U}^T$. $\mathbf{\Lambda}_d$ is a diagonal block matrix and $\mathbf{\Lambda}_s$ has non null blocks above the blocks in $\mathbf{\Lambda}_d$. One then arrives to the joint distribution of the eigenvalues, distributed over $\mathbb{C}$ (see [6]),

$$dp(\lambda_1, ..., \lambda_N) \propto \prod_{i<j} |\lambda_i - \lambda_j| \prod_{i=1}^{N} \sqrt{\operatorname{erfc}\left(\frac{|\lambda_i - \lambda_i^*|}{\sqrt{2}}\right)} e^{-\frac{1}{2}(\lambda_i^2 + \lambda_i^{*2})} \tag{1.24}$$

One notices that the spectrum is clearly symmetric with respect to the real axis and the presence, once again, of a repelling term between each pair of eigenvalues. It can be further shown ([6]) that the eigenvalues of such matrices display properties of a so-called Pfaffian process, as marginal densities can be expressed via the so-called

Pfaffians. In particular, joint probability function of the eigenvalues can be integrated and yields the density of complex and real eigenvalues respectively (see [36]),

$$R_1^C(z) = \frac{2|y|}{\sqrt{2\pi}} e^{2y^2} \operatorname{erfc}(\sqrt{2}|y|) \frac{\Gamma(N-1,|z|^2)}{\Gamma(N-1)} \tag{1.25}$$

and

$$R_1^R(x) = \frac{\Gamma(N-1,x^2)}{\sqrt{2\pi}\Gamma(N-1)} + \frac{1}{2^{N-1/2}\Gamma(N/2)} \nu\left(\frac{N-1}{2}, \frac{x^2}{2}\right) \tag{1.26}$$

with $\nu(N,x) = 1/x^N(1-\Gamma(N,x)/\Gamma(N))$ and $\Gamma(N,a) = \int_a^{+\infty} e^{-t}t^{N-1}dt$. The quantity above can be related to the averages of characteristic polynomials of the same ensemble of matrices:

$$R_1^C(x+iy) = C_N|y|e^{-\frac{1}{2}(x^2-y^2)} \operatorname{erfc}(\sqrt{2}|y|)\mathbb{E}_{GinOE}[\det((x\mathbf{1}_{N-1} - \mathbf{G}_{N-2})^2 + y^2\mathbf{1}_{N-1})] \tag{1.27}$$

for some normalizing constant C_N and

$$R_1^R(x) = \frac{1}{2^{N/2}\Gamma(N/2)} e^{-\frac{1}{2}x^2}\mathbb{E}_{GinOE}[|\det(x\mathbf{1}_{N-1} - \mathbf{G}_{N-1})|] \tag{1.28}$$

If in eq(**1.25**), we rescale $x \to \tilde{x}\sqrt{N}$ and $y \to \tilde{y}\sqrt{N}$, such that $\tilde{x}, \tilde{y} < +\infty$ (the bulk regime) and we use

$$\lim_{N\to+\infty} \frac{\Gamma(N-1,Na)}{(N-2)!} = \begin{cases} 1 \text{ if } 0 \leq a < 1 \\ 0 \text{ if } a > 1 \end{cases}$$

we obtain the circular law. We state the latter in the strong form, given by Tao [37]:

Theorem:*([37]) the spectral empirical distribution of a random matrix* $\frac{1}{\sqrt{N}}\mathbf{G}$ *with i.i.d entries such that* G_{ij} *is a centered complex random variable of unitary variance and* $\mathbb{E}[|G_{ij}|^{2+\eta}] < +\infty$ *for some* $\eta > 0$ *converges uniformly to*

$$\rho_c(z) = \begin{cases} \frac{1}{\pi} \text{ for } |z| < 1 \\ 0 \text{ otherwise} \end{cases}$$

This result is still valid if we replace the last assumption with $\mathbb{E}[|G_{ij}|^2(\log(2+|G_{ij}|))^\delta] < \infty$ for a sufficiently large $\delta > 0$ and the case of G_{ij} being independent but not identically distributed.

There is a secondary regime at the edge of the spectrum, namely, after we rescale $\tilde{x} = 1 + \frac{\delta}{\sqrt{N}}$, with $\delta = O(1)$. $R_1^R(x)$ becomes

$$R_1^R(x) \approx \frac{1}{2\sqrt{2\pi}}(1 - \operatorname{erf}(\delta\sqrt{2}) + \frac{1}{\sqrt{2}} e^{-\delta^2}(1 + \operatorname{erf}(\delta))) \tag{1.29}$$

where we used

$$\lim_{N\to+\infty}\frac{\Gamma(N-1,N(1+\delta N^{-1/2}))}{(N-2)!}=\frac{1}{\sqrt{2\pi}}\int_{\delta}^{+\infty}e^{-\frac{v^2}{2}}dv=\operatorname{erfc}\sqrt{2}\delta$$

Note that the absolute value of the determinants in eqs(**1.27**,**1.28**) formally involves the Ginibre matrix globally shifted by the spectral identity operator: $\lambda\mathbf{1}_N$.

However in chapter 3, we will need to evaluate such quantity additionally considering the Ginibre matrix deformed by a rank-1 perturbation. Such perturbation takes the deterministic form $\mathbf{M}=\boldsymbol{h}\otimes\boldsymbol{h}^{\dagger}$ where $|\boldsymbol{h}|=O(1)$ and does not alter the circular law, since

Theorem: *([22]) the convergence in probability to $\rho_c(z)$ of the empirical distribution is also preserved for matrices $\frac{1}{\sqrt{N}}\mathbf{G}+\mathbf{M}$ where $\left(\mathrm{Tr}\left(\mathbf{M}\mathbf{M}^{\dagger}\right)\right)^{1/2}=O(N^{1/2})$ and rank $(\mathbf{M})=o(N)$.*

However the perturbation $\mathbf{M}$ might be sufficient to generate a finite number of outliers in the spectrum:

Theorem: *([22]) consider $\mathbf{M}$ with rank$(\mathbf{M})=O(1)$ and operator norm $O(1)$. For $\varepsilon>0$, let assume that for large N there are no eigenvalue in the region $\{z\in C: 1+\varepsilon<|z|<1+3\varepsilon\}$ and there are $n=O(1)$ eigenvalues of $\mathbf{M}$ in $|z|\geq 1+3\varepsilon$. Then almost surely, for $N\gg 1$, there are n eigenvalues of $\frac{1}{\sqrt{N}}\mathbf{G}+\mathbf{M}$ in the region $|z|\geq 1+2\varepsilon$.*

Starting from these theorems and considerations, in section 1.3.2 we will address some statistics of the determinants of such matrices.

1.1.3 Generalized Wishart Matrices

We introduce the last class of random Hermitian matrices we will use in the second part of this thesis, namely $\mathbf{W}\in\mathbb{C}^{N,N}$ or $\mathbb{R}^{N,N}$ such that

$$\mathbf{W}=\mathbf{A}_N+\sum_{j=1}^{M}T_i\boldsymbol{w}_i\boldsymbol{w}_i^{\dagger}\tag{1.30}$$

where $\mathbf{A}_N$ is an Hermitian matrix, T_is are i.i.d random scalar with probability density $p_T(t)$ and $\boldsymbol{w}_j$ are random column vectors of N components. As we are interested in the spectral properties of $\mathbf{W}$ we will take $M,N\to+\infty$ such that $M/N=\alpha<+\infty$. The ensemble in eq(**1.30**) generalizes the ensemble of Wishart matrices[5][8]. We assume that $\mathbf{A}_N$ is null, to avoid any problem which may arise due to violation of rotational invariance of the resulting ensemble of random matrices. Similarly to the hypothesis for the semicircle and circular laws, we assume finite values for the fist four centered moments of $\boldsymbol{w}$, i.e.

$$\begin{cases} \mathbb{E}[\boldsymbol{w}_i^\dagger \boldsymbol{w}_j] = \frac{1}{N}\delta_{ij} + a_{ij}(N) \\ \mathbb{E}[\boldsymbol{w}_i^\dagger \boldsymbol{w}_j \boldsymbol{w}_l^\dagger \boldsymbol{w}_m] = \frac{1}{N^2}(\delta_{ij}\delta_{lm} + \delta_{im}\delta_{jl}) + \varphi_{il}(N)\varphi_{jm}^*(N) + b_{ijlm}(N) \end{cases} \tag{1.31}$$

We further impose, as $N \to +\infty$, the following scaling: $|a_{ij}|^2 \sim 1/N^{\varepsilon_1}$, $|\varphi|_{ij} \sim 1/N^{\varepsilon_2}$ and $|b_{ijlm}| \sim 1/N^{\varepsilon_3}$ with $\varepsilon_1 < 3$, $\varepsilon_2 < 2$ and $\varepsilon_3 < 6$ respectively. These guarantees the statistical unitary invariance of $\boldsymbol{w}$ and,

Theorem:*([13]) with the premises above, the spectral cumulative empirical density of* $\mathbf{W}$ *converges in probability to a function* $F(x,\alpha) = \int_{-\infty}^{x} \rho_\alpha(\xi) d\xi$ *for* $N \to +\infty$*. Its Stieltjes transform* $m(z,\alpha)$ *of* $\mathbf{B}_N$ *satisfies*

$$m(z,\alpha) = -\left(z - \alpha \int_0^1 \frac{t dF_T(t)}{1 + tm(z,\alpha)}\right)^{-1} \tag{1.32}$$

and it is analytic in z *in the region* $\operatorname{Im} z > 0$*.* $F_T(t)$ *is the cumulative distribution of* T_i*.*

The knowledge of $m(z,\alpha)$ allows one to compute the probability of observing the eigenvalue within an interval (x_1, x_2) in $\mathbb{R}$ by the inverse transform

$$F(x_2,\alpha) - F(x_1,\alpha) = \lim_{\eta \to 0^+} \frac{1}{\pi} \int_{x_2}^{x1} \operatorname{Im} m(\xi + i\eta, \alpha) d\xi \tag{1.33}$$

The calculation of $F(x,\alpha)$ by the formula above is not always an easy task. In the original paper [13], $F(x,\alpha)$ was retrieved for $\boldsymbol{w}$ being uniformly distributed on the unit sphere and three particular choices of $F_T(t)$: $\frac{dF_T}{dt}(t) = \delta(t-r)$(single point mass), $\frac{dF_T}{dt}(t) = \frac{1}{\pi\sqrt{1-t^2}}$(arcsine distribution) and $\frac{dF_T}{dt}(t) = \frac{1}{\pi(1+t^2)}$(Cauchy distribution). Interesting, regardless of the nature of T_i and the details on the behaviour at the edge of the spectrum, these examples seem to suggest the boundedness of the domain of $\frac{dF}{dx}(x,\alpha)$. This is not a universal behaviour (see section 1.3.3).

[5]These correspond to $T_i = 1$ in eq(**1.30**)

1.2 Overview of Existing Methods and Techniques

The following subsections are a collection of mathematical tools used in this thesis. Hence, the aim is to sketch some methods underlying results briefly mentioned in previous sections, and show the most relevant works which have lead to the original results of section 1.3.

1.2.1 Change of Variables For the Replica Methods

In many of our calculations, we will be left with evaluating integrals over the pair of complex vectors $(\boldsymbol{z}_j, \boldsymbol{z}_j^\dagger)$, each of dimension N, for $j = 1, ..., n$ which appears in the form of a $n \times n$ matrix $\tilde{\mathbf{Q}}$ whose entries are $\tilde{Q}_{ij} = \boldsymbol{z}_i^\dagger \boldsymbol{z}_j$. Namely, we will exploit the following identity given in [38, 39]:

$$\int \prod_{j=1}^{n} d\boldsymbol{z}_j d\boldsymbol{z}_j^\dagger f(\tilde{\mathbf{Q}}) = \frac{2\pi^{-n(n-1)/2}}{\prod_{j=1}^{n}(N-j)!} \int_{\mathbf{Q}\succ 0} d\mathbf{Q} \det(\mathbf{Q})^{N-n} f(\mathbf{Q}) \tag{1.34}$$

where the integration runs over the positive definite Hermitian matrices. Eq(**1.34**) was extended to the real case $\tilde{Q}_{ij} = \boldsymbol{x}_i^T \boldsymbol{x}_j$, namely [39]:

$$\int \prod_{j=1}^{n} d\boldsymbol{x}_j f(\tilde{\mathbf{Q}}) = \frac{2\pi^{-n(n-1)/4}}{\prod_{j=0}^{n-1}\Gamma\left(\frac{N-j}{2}\right)} \int_{\mathbf{Q}\succ 0} d\mathbf{Q} \det(\mathbf{Q})^{\frac{N-n-1}{2}} f(\mathbf{Q}) \tag{1.35}$$

This time considering $\mathbf{Q}$ being a positive definite symmetric matrices.

1.2.2 Saddle Point-Steepest Descent Approximation

In this chapter we made use of the saddle point approximation whenever we were interested in the large N behaviour. In what follows there will be frequently a need to approximate integrals and series as a function of a parameter, when the latter becomes sufficiently large. Here we briefly sketch the essence of the corresponding method. Let's consider a generic integral in the complex plane

$$I(\eta) = \oint_\gamma e^{\eta \mathcal{L}(z)} g(z) dz \tag{1.36}$$

where the integration occurs over a contour γ, not necessarily closed, in the complex plane. The idea is to the deform the latter such that the integrand, for large η, can be replaced by a simpler function. Qualitatively, as η increases, the main contribution to the integral arises from the neighbourhood dz where the real part of $\mathcal{L}$ reaches its maximum. For simplicity, let's assume $\mathcal{L}$ is holomorphic within the path γ. Therefore, we need to obtain the sets of points z_{sd} such that $\frac{d\mathcal{L}}{dz} = 0$ (see [40]). However, we need to approach such points carefully as the imaginary part of $\mathcal{L}$ leads to rapid oscillations. These points generate a set of surfaces $\operatorname{Re}\mathcal{L}(z_{sd}) = \operatorname{Re}\mathcal{L}(z)$ and $\operatorname{Im}\mathcal{L}(z_{sd}) = \operatorname{Im}\mathcal{L}(z)$. By virtue of Cauchy-Riemann equations we have $\nabla \operatorname{Im}\mathcal{L} = (-\partial_y \operatorname{Re}\mathcal{L}, \partial_x \operatorname{Re}\mathcal{L})^T$ and clearly $(\nabla \operatorname{Im}\mathcal{L})^T(\nabla \operatorname{Re}\mathcal{L}) = 0$. Therefore the direction of maximum increase of the real part of $\mathcal{L}$, namely $\nabla \operatorname{Re}\mathcal{L}$, is also the direction on which the imaginary part of $\mathcal{L}$ remains constant. We can include in this approach higher order saddle points. A $N-1$ order saddle point, is such that the first non-vanishing derivative is $\frac{d^N\mathcal{L}}{dz^N} \neq 0$ so that

$$\mathcal{L}(z) = \mathcal{L}(z_{sd}) + \frac{1}{N!}\frac{d^N\mathcal{L}}{dz^N}(z_{sd})(z - z_{sd})^N + o((z - z_{sd})^N). \tag{1.37}$$

We can rewrite any complex number as $z = z_{sd} + re^{i\theta}$ and $\frac{d^N\mathcal{L}}{dz^N}(z_{sd}) = se^{i\varphi}$. Therefore, $\mathcal{L}(z) - \mathcal{L}(z_{sd}) \simeq \frac{1}{N!}r^N se^{i(N\theta+\varphi)}$. The imaginary part of $\mathcal{L}$ remains constant on $\sin(N\theta + \varphi) = 0$. We now want to select the curves where $\operatorname{Re}(\mathcal{L}(z)) < \operatorname{Re}(\mathcal{L}(z_{sd}))$, this occurs for curves approaching z_{sd}:

$$\theta = -\frac{\varphi}{N} + (2k+1)\frac{\pi}{N} \tag{1.38}$$

for $k = 0, .., N-1$. Therefore to compute eq(**1.36**) we need to deform the path γ in order to approach and leave z_{sd} with the paths indicated by eq(**1.38**).

1.2.2.1 Generalization to $\mathbb{R}^N$

The saddle point approach can be generalized to $\mathbb{R}^N$. For the purpose of this thesis, we assume $\mathcal{L}$ is $C^2(\mathbb{R}^2)$ and has only first order saddle points. The Hessian of $\mathcal{L}$ computed in such points is negative definite. In particular, if the integration runs over a compact subset, U, and over the latter $\operatorname{Re}\mathcal{L}(z)$ has a single maximum at $\boldsymbol{x}_0$ such that the Hessian of $\mathcal{L}(z)$ is non singular, then ([41])

$$I(\eta) = \int_U g(\boldsymbol{x})e^{\eta\mathcal{L}(\boldsymbol{x})}d\boldsymbol{x} = \left(\frac{2\pi}{\eta}\right)^{N/2} \frac{e^{\eta\mathcal{L}(\boldsymbol{x}_0)}}{\sqrt{\det(-\nabla^2\mathcal{L}(\boldsymbol{x}_0))}}\left(g(\boldsymbol{x}_0) + o(1)\right) \tag{1.39}$$

for $\eta \gg 1$. Lastly, it might happen that the maximum of $\mathcal{L}(\boldsymbol{z})$ is achieved at an accumulation point of U. We present here the case $N = 2$ which is particular simple, making use of the Green Theorem:

$$I(\eta) = \frac{1}{\eta}\oint_{\partial U} e^{\eta\mathcal{L}(\boldsymbol{x}(s))} g_0(\boldsymbol{x}(s))\frac{\nabla\mathcal{L}}{|\nabla\mathcal{L}|^2}\cdot \boldsymbol{n}(\boldsymbol{x}(s))ds - \frac{1}{\eta}\int_U e^{\eta\mathcal{L}}\nabla\cdot\left(g_0(\boldsymbol{x}(s))\frac{\nabla\mathcal{L}}{|\nabla\mathcal{L}|^2}\right)dx \tag{1.40}$$

where $\boldsymbol{n}(\boldsymbol{x})$ is the outward normalised and orthogonal vector on ∂U. The second integral is of order $O(e^{\eta\mathcal{L}(\boldsymbol{x}_0)}\eta^{-2})$ while the first term is of order $O(e^{\eta\mathcal{L}(\boldsymbol{x}_0)}\eta^{-3/2})$ and therefore it is the leading contribution. With a local parametrization of ∂U around $\boldsymbol{x}_0$, i.e. the critical point of $\mathcal{L}(\boldsymbol{x})$ on ∂U, we obtain the leading order of $I(\eta)$,

$$I(\eta) = \sqrt{\frac{2\pi}{\eta^3}} g_0(\boldsymbol{x}_0) e^{\eta \mathcal{L}(\boldsymbol{x}_0)} \times \tag{1.41}$$

$$\left(\sqrt{|\partial_{x_1,x_1}\mathcal{L}(\partial_{x_2}\mathcal{L})^2 - 2\partial_{x_1,x_2}\mathcal{L}\partial_{x_1}\mathcal{L}\partial_{x_2}\mathcal{L} + \partial_{x_1,x_2}\mathcal{L}(\partial_{x_1}\mathcal{L})^2 \pm k|\nabla|^3|}\right)^{-1} (1 + o(1))$$

Where k is the curvature of ∂U at $\boldsymbol{x}_0$.

1.2.3 Watson's Lemma

The results contained in section 1.3.3.5 are expressed in terms of finite sums and hypergeometric function. To derive the large N behavior it is convenient to "transform" the sum into a proper integral. Such approximation is an inverse procedure of the Watson's lemma here presented. Hence, let's consider again a control parameter η, which takes sufficiently large values in $\mathbb{R}_+$ and a given integral (see [40])

$$I(\eta) = \int_0^b f(t) e^{-\eta t} dt, \text{with } b > 0 \tag{1.42}$$

As the critical point of $\mathcal{L}(t) = t$ is zero, we restrict our attention to those continuous functions f which admit a series representation for $t \to 0^+$, i.e.

$$f(t) \sim t^\alpha \sum_{n=0}^{+\infty} a_n t^{\beta n}$$

with $\alpha > -1$ and $\beta > 0$. Then $I(\eta)$ for $\eta \to +\infty$ behaves as

$$I(\eta) \sim \sum_{n=0}^{+\infty} a_n \frac{\Gamma(\alpha + \beta n + 1)}{\eta^{\alpha+\beta n+1}}$$

To derive this result we introduce $I(\eta, \delta) = \int_0^\delta f(t) e^{-\eta t} dt$ and we impose δ to be sufficiently small such that we have, for $0 \le t \le \delta$

$$\left| f(t) - t^\alpha \sum_{n=0}^{N} a_n t^{\beta n} \right| \le C t^{\alpha+\beta(N+1)}$$

For some $C > 0$. Replacing the statements above into the formula for $I(\eta)$:

$$\left| I(\eta, \delta) - \sum_{n=0}^{N} a_n \int_0^\delta t^{\alpha+\beta n} e^{-\eta t} dt \right| \le C \int_0^\delta t^{\alpha+\beta(N+1)} e^{-xt} dt$$

the r.h.s. is bounded by $C\frac{\Gamma(\alpha+\beta+\beta N+1)}{\eta^{\alpha+\beta+\beta N+1}}$. So we can take $\delta \to +\infty$ and $\eta \to +\infty$ and observe that, therefore, the l.h.s. is bounded by $\eta^{-\alpha-\beta N-1}$. If $b \to +\infty$ we also need to impose $f(t) \ll e^{vt}$ as $t \to +\infty$.

1.2.4 Kac-Rice Formula

The investigations of dynamical systems necessarily require to identify those states which do not change with time. These are called equilibrium or fixed points. For discrete systems, with $\boldsymbol{x}^{(n+1)} = \boldsymbol{f}\left(\boldsymbol{x}^{(n)}\right)$, the latter satisfy $\boldsymbol{x} = \boldsymbol{f}(\boldsymbol{x})$. Similarly, for a continuous dynamical system, with $\frac{d\boldsymbol{x}}{dt} = \boldsymbol{f}(\boldsymbol{x})$, such states belong to the set of solutions of $\boldsymbol{f}(\boldsymbol{x}) = \boldsymbol{0}$. In both cases, the analysis of the number of fixed points clearly reduces to finding the real zeros of a vector field which describes the evolution of such systems. Before addressing this problem, we start from the simplest one dimensional case for a more general counting problem (see [42]). This is equivalent to finding the real roots of a function, $f(x)$, on a feasible interval on the real line. Let's consider the case for which $f(x)$ is continuous and with continuous derivative on the real line. Furthermore $f(x)$ is assumed to have a finite number of turning points. This guarantees that the set of fixed points is countable. We further introduce the rectangular function $\psi_\varepsilon(x)$ such that

$$\psi_\varepsilon(x) = \begin{cases} 1 \text{ for } -\varepsilon < x < +\varepsilon \\ 0 \text{ otherwise} \end{cases} \tag{1.43}$$

With these premises, $f(x)$ defines a family of u open sets I_i on the real line where $-\varepsilon < f(x) < +\varepsilon$. We take ε sufficiently small so that each I_i contains a single zero of $f(x)$. On each of these sufficiently small interval follows $\int_{I_i} |f'(x)|dx = 2\varepsilon$. We can sum the latter on any interval (a, b) such that a and b are not the zeros of f, and divide by a common factor 2ε in order to obtain

$$\frac{1}{2\varepsilon}\sum_{i=1}^{u}\int_{I_i} |f'(x)|dx$$

The sum can be replaced with the indicating function $\psi(x)$ inside the integral. Lastly, with hypothesis on $f(x)$, we can take the limit $\varepsilon \to 0^+$. This is equivalent in the sense of the distributions, to replace $1/(2\varepsilon)\psi_\varepsilon(x) \to \delta(x)$. Therefore the number of zeros of $f(x)$ within (a, b) is given by

$$\mathcal{N}_f(a, b) = \int_a^b \delta(f(x)) \left|\frac{df}{dx}(x)\right| dx \tag{1.44}$$

If in addition, as it is the case in this thesis, f is a random function, we may wish to compute the mean (expected) number of fixed points. Hence, for this we need to compute $\mathbb{E}_f\left[\delta(f(x))\left|\frac{df}{dx}(x)\right|\right]$. In [42], Kac investigated the real zeros of the following algebraic polynomial

$$p_\xi(x) = \xi_0 + \xi_1 x + \xi_2 x^2 + ... + \xi_{N-1}x^{N-1} = 0 \tag{1.45}$$

where ξ_n are random coefficients whose distribution is given by $p(\xi_n) \propto e^{-\xi_n^2}$. Indeed, functions as in eq(**1.45**) are called univariate Kac Polynomials. By using the formulae above, the mean number of real zeros, for finite N, is given by

$$\mathcal{N}_p(\mathbb{R}) = \frac{4}{\pi} \int_0^1 \frac{(1 - N^2(x^2(1-x^2)/(1-x^{2N}))^2)^{1/2}}{1-x^2} dx \tag{1.46}$$

and for $N \gg 1$, it behaves as (see [42])

$$\mathcal{N}_p(\mathbb{R}) = \frac{2}{\pi} \log N + O(1) \tag{1.47}$$

In this thesis, we generalize the result above to a set of multivariate Kac polynomials, i.e.

$$p_{\boldsymbol{\xi},n}(\boldsymbol{x}) = -\mu x_n + \sum_{k=1}^{\Omega} \sigma_k \sum_{i_1,..,i_k=1}^{N} \xi_{n,i_1,...,i_k} x_{i_1} \cdots x_{i_k} = 0 \tag{1.48}$$

for $n = 1, ..., N$. In this case the large N behaviour of $\mathcal{N}_p(\mathbb{R}^N)$ is given by

$$\mathcal{N}_p(\mathbb{R}^N) = e^{\frac{N}{2}\log\Omega}(1 + o(1)) \tag{1.49}$$

See appendix C.4. To obtain the result above we exploit the well-known multivariate Kac-Rice formula. The natural generalization of the formula eq(**1.44**) to multivariate setting is provided by replacing $|\frac{df}{dx}|dx$ with the elementary volume $|\det(f'(\boldsymbol{x}))|d\boldsymbol{x}$. The mean number of real zeros of a random function $\boldsymbol{f}(\boldsymbol{x}; \mu)$ on $V \subseteq \mathbb{R}^N$ is given by

$$\mathcal{N}_{\boldsymbol{f}}(V) = \int_V d\boldsymbol{x} \mathbb{E}\left[\prod_{k=1}^{N} \delta(f_k(\boldsymbol{x}; \mu)) \left| \det\left(\frac{\partial f_i}{\partial x_j}(\boldsymbol{x}; \mu)\right)_{i,j=1}^{N} \right|\right] \tag{1.50}$$

We also mention here a more general result:

Theorem:*([43]) Given $N, M \geq 1$, consider the random fields $\boldsymbol{f} = (f_1, ..., f_N)$ and $\boldsymbol{g} = (g_1, ..., g_M)$ and fix $T \subset \mathbb{R}^N$ and $B \subset \mathbb{R}^M$ and assume, for some $\boldsymbol{u} \in \mathbb{R}^N$, that*

- *$\boldsymbol{f}, \boldsymbol{g}, \nabla \boldsymbol{f}$ are almost surely continuous and of finite variance. For any $\boldsymbol{x} \in \mathbb{R}^N$, the density $p_{\boldsymbol{f}(\boldsymbol{x})}(t)$ of $\boldsymbol{f}(\boldsymbol{x})$ is continuous in $\boldsymbol{t} = \boldsymbol{u}$.*

- *the conditional density of $\boldsymbol{f}(\boldsymbol{x})$ given $\nabla \boldsymbol{f}(\boldsymbol{x})$ and $\boldsymbol{g}(\boldsymbol{x})$ is bounded by above and continuous in $\boldsymbol{u}$, uniformly over T.*

- *the conditional density of $\det(\nabla \boldsymbol{f}(\boldsymbol{x}))$ given $\boldsymbol{f}(\boldsymbol{x}) = \boldsymbol{t}$ is continuous in the neighbourhood of zero and for $\boldsymbol{t}$ in the neighbourhood of $\boldsymbol{u}$, uniformly over T.*

- *in addition, we require:*

$$\sup_{\boldsymbol{x}\in\mathbb{R}^N} \max_{1\leq i,j\leq N} \mathbb{E}\left[|\partial_j f_i(\boldsymbol{x})|^N\right] < +\infty \tag{1.51}$$

- *given the Euclidean metric $d(\boldsymbol{x},\boldsymbol{y})$ on T, defining $\omega_{\boldsymbol{f}}(\delta) = \sup_{d(\boldsymbol{x},\boldsymbol{y})\leq\delta} |\boldsymbol{f}(\boldsymbol{x}) - \boldsymbol{f}(\boldsymbol{y})|$ we assume, for sufficiently small δ,*

$$p(\omega_q(\delta) > \varepsilon) = o(\delta^N) \tag{1.52}$$

  with $q = \boldsymbol{f}, \nabla\boldsymbol{f}$ and $\boldsymbol{g}$.

Then the mean number of points $\boldsymbol{x}$ in T satisfying $\boldsymbol{f}(\boldsymbol{x}) = \boldsymbol{u}$ and $\boldsymbol{g}(\boldsymbol{x}) \in B \subset \mathbb{R}^M$ is given by

$$\mathbb{E}\left[\mathcal{N}_u\right] = \int_T \left(\int_{\mathbb{R}^D:\boldsymbol{v}\in B} |\det(\nabla\boldsymbol{y})| p_{\boldsymbol{f},\nabla\boldsymbol{f},\boldsymbol{g}}(\boldsymbol{u},\nabla\boldsymbol{y},\boldsymbol{v}) d(\nabla\boldsymbol{y}) d\boldsymbol{v}\right) d\boldsymbol{x} \tag{1.53}$$

where $p_{\boldsymbol{f},\nabla\boldsymbol{f},\boldsymbol{g}}$ is the joint probability density function of $\boldsymbol{f}, \nabla\boldsymbol{f}$ and $\boldsymbol{g}$ computed in $\boldsymbol{x}$ and $D = N(N+1)/2 + M$.

We will use eq(**1.53**) or the multivariate version of eq(**1.44**) at our convenience. Both of the latter are valid for any random field satisfying the hypothesis above. However, we will only consider applications involving random Gaussian fields $\boldsymbol{f}$.

1.2.5 Random Fields

Eqs(**1.45**,**1.48**) are just examples of Gaussian random fields. Later, in section 3.1.3, we will encounter dynamical systems whose evolution is described by random functions. The mean number of fixed point is clearly an average over the realization of these functions. In our calculations, we will heavily rely upon the theory of random fields (see [43]). The latter can be thought as a random process which occur in a coordinate space, in our case a subspace $U \subseteq \mathbb{R}^N$. More precisely,

Definition: A random field f, over a set U of a dimension $N > 1$, is a set of random variables parameterized by the elements of U.

In virtue of the Kolmogorov extension theorem, analogously to real random variables, a real Gaussian random field, $\boldsymbol{\varphi}(\boldsymbol{x})$, is defined by the first two moments:

$$\boldsymbol{\mu}(\boldsymbol{x}) = \mathbb{E}[\boldsymbol{\varphi}(\boldsymbol{x})] \tag{1.54}$$

$$\boldsymbol{\Sigma}(\boldsymbol{x}, \boldsymbol{y}) = \mathbb{E}[(\boldsymbol{\varphi}(\boldsymbol{x}) - \boldsymbol{\mu}(\boldsymbol{x}))(\boldsymbol{\varphi}(\boldsymbol{y}) - \boldsymbol{\mu}(\boldsymbol{y}))^T] \tag{1.55}$$

As an example, for a real Gaussian field $\varphi(\boldsymbol{x})$ with value in $\mathbb{R}$ with $\boldsymbol{x} \in \mathbb{R}^N$ this means, given K observations, that

$$\begin{bmatrix} \varphi(\boldsymbol{x}_1) \\ \vdots \\ \varphi(\boldsymbol{x}_K) \end{bmatrix} \sim \mathcal{N}\left(\begin{bmatrix} \mu(\boldsymbol{x}_1) \\ \vdots \\ \mu(\boldsymbol{x}_K) \end{bmatrix}, [\Sigma(\boldsymbol{x}_i, \boldsymbol{x}_j)]_{i,j=1}^K \right)$$

As classic Gaussian random variables, a linear combination of Gaussian fields is a Gaussian field. More generally any linear operator preserves (in mean-square sense) Gaussianity, this includes differentiation and integration with respect to $\boldsymbol{x}$. Provided $\boldsymbol{\mu}(\boldsymbol{x})$ and $\boldsymbol{\Sigma}(\boldsymbol{x}, \boldsymbol{y})$ are differentiable functions, the derivatives of $\varphi(\boldsymbol{x})$ are again Gaussian with the statistics given by:

$$\mathbb{E}[\partial_{x_i} \varphi(\boldsymbol{x})] = \partial_{x_i} \mu(\boldsymbol{x}) \tag{1.56}$$

$$\mathbb{E}[\partial_{x_i} \varphi(\boldsymbol{x}) \partial_{y_j} \varphi(\boldsymbol{y})] = \partial_{x_i} \partial_{y_j} \Sigma(\boldsymbol{x}, \boldsymbol{y}) \tag{1.57}$$

We notice in obtaining the quantities above that $\varphi(\boldsymbol{x})$ and $\nabla \varphi(\boldsymbol{x})$ are correlated, in fact,

$$\mathbb{E}[\varphi(\boldsymbol{x}) \partial_{y_j} \varphi(\boldsymbol{y})] = \partial_{y_j} \Sigma(\boldsymbol{x}, \boldsymbol{y}) \tag{1.58}$$

As our goal is to apply the multivariate Kac-Rice formula, it is useful to investigate the conditions under which the random field and its derivatives are uncorrelated. For our purpose, we assume the Gaussian field to be centered, i.e. $\mu(\boldsymbol{x}) = 0$. Since the random field and its derivatives are Gaussian, un-correlation implies statistical independence. They are uncorrelated if:

- φ is homogeneous, i.e. the correlation function is invariant under spatial translation, i.e. $\mathbb{E}[\varphi(\boldsymbol{x})\varphi(\boldsymbol{y})] = \Phi(\boldsymbol{x} - \boldsymbol{y})$.
- φ is isotropic, i.e. the correlation function is invariant for any rotation $\mathbf{O} \in O(N)$ of the coordinates, i.e. for $\boldsymbol{x} \to O\boldsymbol{x}$ and $\boldsymbol{y} \to O\boldsymbol{y}$, we have

$$\mathbb{E}[\varphi(\boldsymbol{x})\varphi(\boldsymbol{y})] = \mathbb{E}[\varphi(O\boldsymbol{x})\varphi(O\boldsymbol{y})] \tag{1.59}$$

If the two properties above are satisfied then the field and its derivatives are statistically independent.

1.2.6 Superbosonization

For the introductory calculation of the semicircle law we made use of the replica trick, generating n copies of the Fermionic partition function. Afterward, we send the number of replicas to zero and successively N to infinity. We omitted further generalizations of such technique not essential for understanding of the content of this thesis, such as notion of supermatrices, containing both bosonic and fermionic entries. We now consider a more general picture, which allows one to easily deal with matrices such as those appearing in eq(**1.30**) for finite value of n and N. Before doing so, following the notation introduced in section 1.1.1, we introduce the circular ensembles CβE:

- Orthogonal ensemble $\beta = 1$: it corresponds to the unitary and symmetric $n \times n$ matrices $\mathbf{U}$ whose unique measure is invariant under $\mathbf{U} \to \mathbf{W}^T \mathbf{U} \mathbf{W}$ where $\mathbf{W}$ is a $n \times n$ unitary matrix.

- Unitary ensemble $\beta = 2$: it corresponds to the unitary $n \times n$ matrices $\mathbf{U}$ whose unique measure is invariant under $\mathbf{U} \to \mathbf{W}\mathbf{U}\mathbf{V}$ where $\mathbf{W}$ and $\mathbf{V}$ are $n \times n$ unitary matrix.

- Symplectic ensemble $\beta = 4$: it corresponds to the self-dual unitary quaternion $n \times n$ matrices $\mathbf{U}$ whose unique measure is invariant under $\mathbf{U} \to \mathbf{W}^R \mathbf{U} \mathbf{W}$ where $\mathbf{W}$ is a $n \times n$ unitary quaternion matrix.

Let's now consider the following integral,

$$\mathcal{I}_\beta(\hat{F}) = \int \prod_{j=1}^{n} D\boldsymbol{\psi}_j D\tilde{\boldsymbol{\psi}}_j \hat{F}(\{\boldsymbol{\psi}_j, \tilde{\boldsymbol{\psi}}_j\}_{j=1}^{p}). \tag{1.60}$$

This Berezin integral involves n Grassmannian pairs vectors of size N. As we deal with β rotationally invariant ensemble, we assume the Grassmannian entries can be re-arrange such that the integrand $\hat{F}$ is function of the block matrix

$$\hat{\boldsymbol{Q}} = \begin{bmatrix} \tilde{\boldsymbol{\psi}}_i^T \boldsymbol{\psi}_j & \tilde{\boldsymbol{\psi}}_i^T \tilde{\boldsymbol{\psi}}_j \\ -\boldsymbol{\psi}_i^T \boldsymbol{\psi}_j & -\boldsymbol{\psi}_i^T \tilde{\boldsymbol{\psi}}_j \end{bmatrix} \tag{1.61}$$

Namely $\hat{F}(\{\boldsymbol{\psi}_j, \tilde{\boldsymbol{\psi}}_j\}_{j=1}^{n}) = F_\beta(\hat{\mathbf{Q}})$. The subscript β is introduced to take into account the symmetries of $\hat{F}$. With these premises we have ([44][45] and [46])

$$\mathcal{I}_\beta(F) = \frac{\int_{U_n} (\mathbf{U}^\dagger d\mathbf{U}) \det(\mathbf{U})^{-\frac{2N}{\beta}} F_\beta(\mathbf{U})}{\int_{U_n} (\mathbf{U}^\dagger d\mathbf{U}) \det(\mathbf{U})^{-\frac{2N}{\beta}} e^{\frac{2}{\beta} \operatorname{Tr} \mathbf{U}}} \tag{1.62}$$

The differential $(\mathbf{U}^\dagger d\mathbf{U})$ denotes the normalised Haar measure over the corresponding group:

- For $\beta = 1$: $U_n = CSE(2n)$, i.e. the integrals run over the group of $2n \times 2n$ unitary matrices $\mathbf{U}$ with skew symmetric sub-blocks, satisfying

$$\mathbf{P}^{-1}\mathbf{U}\mathbf{P} = \mathbf{U}^T \tag{1.63}$$

where $\mathbf{P} = \begin{bmatrix} \mathbf{0}_n & -\mathbf{1}_n \\ \mathbf{1}_n & \mathbf{0}_n \end{bmatrix}$. Therefore $\mathbf{U}$ has the following block form:

$$\mathbf{U} = \begin{bmatrix} \mathbf{U}_{11} & \mathbf{U}_{12} \\ \mathbf{U}_{21} & \mathbf{U}_{11}^T \end{bmatrix}$$

with $\mathbf{U}_{12}, \mathbf{U}_{21} \in Skew(\mathbb{C}^{n,n})$. This group corresponds to the unitary matrix of the circular symplectic ensemble CSE(n). Validity of eq(**1.62**) can be demonstrated by introducing a shift operator and the $N \times N$ skew-symmetric matrix $\mathbf{A} = \sum_{i=1}^{n} \boldsymbol{\psi}_i \boldsymbol{\psi}_i^T$, and observe the following identity

$$\int D\boldsymbol{\psi} F_1\left(\sum_{i=1}^{n} \boldsymbol{\psi}_i \boldsymbol{\psi}_i^T\right) = \int D\boldsymbol{\psi} \exp\left(\mathrm{Tr} \sum_{i=1}^{n} \boldsymbol{\psi}_i \boldsymbol{\psi}_i^T \frac{\delta}{\delta \mathbf{A}}\right) F_1(\mathbf{A})|_{\mathbf{A}=0} \tag{1.64}$$

The integral operator can be written in terms of Pfaffian so the equation is proportional to

$$\det\left(2\frac{\delta}{\delta \mathbf{A}}\right)^{n/2} F_1(\mathbf{A})\Bigg|_{\mathbf{A}=0} \tag{1.65}$$

- In a similar way one can treat the complex case ($\beta = 2$). In this case the integrand can be written as a function of $\hat{\boldsymbol{Q}}$ which only consists of the $n \times n$ upper left block of eq(**1.61**). Namely, the Berezin integral is replaced by an integral over the group of the $n \times n$ unitary matrices and $U_n = CUE(n)$.

Clearly if $F_\beta(\mathbf{U})$ is unitary invariant, the formula eq(**1.62**) above can be expressed in terms of the eigenvalues of Circular β-Ensemble. The joint probability density function of the latter is given by

$$p_n(\{e^{i\theta_j}\}_{j=1}^n) = \frac{1}{C_{\beta,n}} \prod_{j<k} |e^{i\theta_j} - e^{i\theta_k}|^\beta \tag{1.66}$$

with $C_{\beta,n} = (2\pi)^n \Gamma(\beta n/2 + 1)/(\Gamma(\beta/2+1))^n$ with $\theta_j \in (0, 2\pi)$. Before finding an explicit formula for some choices of $\hat{F}$, it is useful to include the following digression for $N \gg 1$. Let suppose that $F_\beta(x)$ can be written as $e^{\mathrm{Tr}\, x} f_\beta(x)$ with $f_\beta(x)$ homogeneous in the size N, i.e. $f_\beta(Nx) = N^\alpha f_\beta(x)$ for some parameter $\alpha \in \mathbb{R}$. An example is simply given by the denominator of eq(**1.62**) for which $f_\beta(x) = 1$. If that is the case, we can perform a saddle point approximation as $N \gg 1$ observing that the main contribution to the closed contour integrals is given by the critical point of $\mathcal{L}(z) = z - \log z$, i.e. $z = 1$. Such point is crossed at angles $\{\frac{\pi}{2}, \frac{3\pi}{2}\}$. Therefore, for $N \gg 1$, the numerator (equivalently the denominator) is proportional to,

$$\int_{-\infty}^{+\infty} \prod_{j=1}^{n} dx_j \prod_{j<k} |x_j - x_k|^\beta \prod_{j=1}^{n} \frac{e^{-\frac{N}{2}x_j^2}}{1 + ix_j} f_\beta\left((1 + ix_1), ..., (1 + ix_n)\right) \tag{1.67}$$

This shows that the integration over CβE can be effectively reduced to integration over the corresponding Gaussian matrices. Therefore after some calculations, for $N \gg 1$, up to a constant depending on N, we arrive to

$$\mathcal{I}_\beta(F) \propto \mathbb{E}_{G\beta E}\left[\frac{f_\beta\left(N\left(\mathbf{1}_{2/\beta n} + i\sqrt{\frac{n}{N}}\mathbf{H}\right)\right)}{\det\left(\mathbf{1}_{2/\beta n} + i\sqrt{\frac{n}{N}}\mathbf{H}\right)}\right] \tag{1.68}$$

For finite N and generic F_β we need to parametrize the entries of CβE matrices.

1.2.7 Parametrization of Unitary Matrices

We have given the probability distribution of the eigenvalues of CβE matrices. However, the integrand in eq(**1.62**) is not necessarily unitary invariant. Therefore a parametrization of such matrices is required. For this purpose we will sketch the parametrization proposed in [47] and [48]. Any $n \times n$ unitary matrix $\mathbf{U}$ is described by $(n-1)^2$ real parameter and can be written as follows

$$\mathbf{U} = \begin{bmatrix} ae^{i\varphi} & \mathbf{b} \\ \mathbf{c} & \mathbf{D} \end{bmatrix} \tag{1.69}$$

where $0 \leq a \leq 1$ and $\varphi \in (0, 2\pi)$, $\mathbf{b} \in \mathbb{C}^{1,n-1}$, $\mathbf{c} \in \mathbb{C}^{n-1,1}$ and $\mathbf{D} \in \mathbb{C}^{n-1,n-1}$ and subject to the constraints

$$\begin{cases} |a|^2 + \mathbf{b}\mathbf{b}^\dagger = 1 \\ |a|^2 + \mathbf{c}^\dagger\mathbf{c} = 1 \\ \mathbf{c}\mathbf{c}^\dagger + \mathbf{D}\mathbf{D}^\dagger = \mathbf{1}_{n-1} \end{cases} \tag{1.70}$$

where $0 \leq a \leq 1$ and $\varphi \in (0, 2\pi)$. The block matrices in $\mathbf{U}$ are contractions. Therefore, $a = \mathbf{U}_{11}$ admits a defect operator $d_a = (1 - |a|^2)^{1/2}$. This fixes the norm of $\mathbf{b}$ and $\mathbf{c}$ and their entries since: $\mathbf{b} = d_a\mathbf{u}$ and $\mathbf{c} = d_a\mathbf{v}$ where $\mathbf{u}$ and $\mathbf{v}$ are normalized vectors belonging to $\mathbb{C}^{1,n-1}$ and $\mathbb{C}^{n-1,1}$. The vectors $\mathbf{u}$ and $\mathbf{v}$ are isometric and admit diagonalizable defect operators $\mathbf{D}_v = (\mathbf{1}_{n-1} - \mathbf{v}\mathbf{v}^\dagger)^{1/2}$ and $\mathbf{D}_u = (\mathbf{1}_{n-1} - \mathbf{u}^\dagger\mathbf{u})^{1/2}$. The eigenvalues of the latter are $\lambda = 1$ with multiplicity $n-2$ and $\lambda = 0$ with multiplicity one. If we substitute these results back in the last equation of eq(**1.70**) we obtain the last block matrix $\mathbf{D}$, i.e.

$$\mathbf{D} = -ae^{-i\varphi}\mathbf{v}\mathbf{u} + \mathbf{K_1}\begin{bmatrix} \mathbf{U}_\star & \mathbf{0} \\ \mathbf{0} & \mathbf{0} \end{bmatrix}\mathbf{K_2}^\dagger \tag{1.71}$$

the matrix $\mathbf{U}_\star$ is an *arbitrary* unitary $(n-2)\times(n-2)$. The matrix $\mathbf{K}_1$ and $\mathbf{K}_2$ diagonalize $\mathbf{D}_{\mathbf{v}^\dagger}$ and $\mathbf{D}_{\mathbf{u}}$ respectively. To obtain the parametrization of CSE(n) matrices we additionally impose the constraints of eq(**1.63**). Iteratively, we obtain:

For $CUE(n)$:

- $n=1$: $U=e^{i\theta}$ with $\theta\in(0,2\pi)$
- $n=2$: $\mathbf{U}=\begin{bmatrix} e^{i(\psi_{11}+\psi_{12})}\cos\varphi & e^{i\psi_{12}}\sin\varphi \\ -e^{i(\psi_{11}+\psi_{22})}\sin\varphi & e^{i\psi_{22}}\cos\varphi \end{bmatrix}$ with $i,j=1,2$, $\psi_{ij}\in(0,2\pi)$ and $\varphi\in(0,\pi/2)$

For $CSE(n)$:

- $n=1$: $\mathbf{U}=\begin{bmatrix} e^{i\theta} & 0 \\ 0 & e^{i\theta} \end{bmatrix}$ with $\theta\in(0,2\pi)$
- $n=2$: $\mathbf{U}=\begin{bmatrix} \mathbf{U}_{11} & \mathbf{U}_{12} \\ -\mathbf{U}_{12}e^{i(\varphi_{12}+\varphi_{21}-2\varphi_{14})} & \mathbf{U}_{11}^t \end{bmatrix}$ with

$$\mathbf{U}_{11}=\begin{bmatrix} e^{i\varphi_{11}}h & e^{i\varphi_{22}}d\sqrt{1-h^2} \\ e^{i\varphi_{21}}d\sqrt{1-h^2} & -e^{-i(\varphi_{11}-\varphi_{21}-\varphi_{22})}h \end{bmatrix}$$

  and

$$\mathbf{U}_{12}=e^{i\varphi_{14}}\sqrt{1-h^2}\sqrt{1-d^2}\begin{bmatrix} 0 & -1 \\ 1 & 0 \end{bmatrix}$$

  with $h,d\in(0,1)$ and $\varphi_{11},\varphi_{21},\varphi_{22},\varphi_{14}\in(0,2\pi)$.

1.3 Overview of Original RMT Results

We now turn our attention to the original technical results of this thesis concerning properties of random matrices (these results will form the basis for applications in the rest of the thesis). These represent extensions and generalizations of what stated so far.

1.3.1 Extension of Eq(1.23)

In section 1.1.1.7, we introduced the ratios of half integer powers of determinants for the Gaussian Orthogonal ensemble. Eq(**1.23**) can be used for obtaining the characteristic function of the entries of the Wigner reaction matrix in absence of absorption. We want to generalize it and include uniform absorption in the scattering region. We postpone further discussing the physical meaning of these results for chapter 2. Here for convenience of the reader, we provide the mathematical results. In particular, later on we will exploit the following equalities and limits derived by us in ([1]):

$$\lim_{N\to+\infty} \mathbb{E}_{GOE(N)}\left[\frac{\det((\lambda\mathbf{1}_N-\mathbf{H})^2+\frac{\alpha^2}{N^2}\mathbf{1}_N)}{\prod_{\ell=1}^2\det((\lambda\mathbf{1}_N-\mathbf{H})^2+\frac{\omega_\ell^2}{N^2}\mathbf{1}_N)^{1/2}}\right]= \tag{1.72}$$

$$-\int_{\mathbb{R}_+}dq_1\int_{\mathbb{R}_+}dq_2|q_1-q_2|J_0\Big(s\alpha(q_1-q_2)\Big)\times\ e^{-\frac{1}{4}(q_1+q_2)\left((q_1q_2)^{-1}+4\alpha^2\right)}$$
$$\times\frac{D(q_1,q_2,\alpha)\sinh(2\alpha)-2\alpha C(q_1,q_2,\alpha)\cosh(2\alpha)}{512\sqrt{\pi}q_1^3q_2^3(q_1+q_2)^{5/2}\alpha^3}$$

where $\omega_1^2=\alpha^2-i\alpha s$, $\omega_2^2=\alpha^2+i\alpha s$ and

$$\lim_{N\to+\infty} \mathbb{E}_{GOE(N)}\left[\frac{\det((\lambda\mathbf{1}_N-\mathbf{H})^2+\frac{\alpha^2}{N^2}\mathbf{1}_N)}{\prod_{\ell=1}^2\det((\lambda\mathbf{1}_N-\mathbf{H})^2+i(-1)^\ell\frac{k}{N}(\lambda 1_N-\mathbf{H})+\frac{\omega_\ell^2}{N^2}\mathbf{1}_N)^{1/2}}\right]= \tag{1.73}$$

$$-\int_{\mathbb{R}_+}dq_1\int_{\mathbb{R}_+}dq_1dq_2|q_1-q_2|I_0\Big(k\sqrt{\frac{k^2}{4}+\alpha^2}(q_1-q_2)\Big)\ e^{-\frac{1}{4}(q_1+q_2)\left((q_1q_2)^{-1}+2(k^2+2\alpha^2)\right)}$$
$$\times\frac{D(q_1,q_2,\alpha)\sinh(2\alpha)-2\alpha C(q_1,q_2,\alpha)\cosh(2\alpha)}{512\sqrt{\pi}q_1^3q_2^3(q_1+q_2)^{5/2}\alpha^3}$$

with:

$$C(q_1,q_2,\alpha)=q_2^2-4q_2^3+4q_1^3(4q_2-1)+2q_1q_2(1-4q_2+8q_2^2)+q_1^2(1-8q_2+44q_2^2) \tag{1.74}$$
$$-4(q_1+q_2)\left(-q_2^3+q_1^2q_2(4q_2-5)+q_1q_2^2(4q_2-5)+q_1^3(4q_2-1)\right)\alpha^2+16q_1^2q_2^2(q_1+q_2)^2\alpha^4$$

and

$$D(q_1,q_2,\alpha) = C(q_1,q_2,\alpha) - 8(q_1+q_2)^2\alpha^2\left(q_1+q_2-2q_1q_2+4q_1q_2(q_1+q_2)\alpha^2\right)$$

The function $J_0(x)$ is the Bessel function of order zero and $I_0(x)$ is the modified counterpart. In the process of derivation, presented in full in appendix B.4, we made use of eq(**1.22**), firstly assuming $\lambda = 0$ and successively introducing the Dyson limit (see appendix B.4). For $\alpha \to 0^+$ in eq(**1.72**) and eq(**1.73**), one returns to eq(**1.23**).

1.3.2 New Results for Non-Hermitian Matrices

The results of section 1.1.2 are clearly non-exhaustive and insufficient to infer the statistics of the characteristic polynomials of $\lambda\mathbf{1}_N + \varepsilon\boldsymbol{e}_1\otimes\boldsymbol{e}_1^T - \mathbf{G}$. One can start addressing this problem by computing $\mathbb{E}_{GinOE}[\det(\lambda\mathbf{1}_N + \varepsilon\boldsymbol{e}_1\otimes\boldsymbol{e}_1^T - \mathbf{G})]$ where $\boldsymbol{e}_1 = (1,0,...,0)^T$. This is a simple task as the determinant is a linear function of the entries and its average is equal to $\lambda^{N-1}(\lambda+\varepsilon)$. Therefore, the outlier contributes to the expectation only if it is of the order of the shift λ. More important, the asymptotics $N \gg 1$ is dominated by $|\lambda|$ being smaller(bulk regime) or greater(outer regime) than one. The expectation of higher powers and the absolute value of the determinant require a more sophisticated approach. The calculation of the latter is contained in appendix A and [2]. The essential idea is the "Hermitization" of the non Hermitian matrix $\mathbf{G}$ and to re-write the determinant by introducing pairs of Grassmannian vectors in order to obtain (fig(**1.1**))

$$\mathbb{E}_{GinOE}[\det(\lambda\mathbf{1}_N + \varepsilon\boldsymbol{e}_1\otimes\boldsymbol{e}_1^T - \mathbf{G})^2] = \lambda^{2N} + (N+\varepsilon^2+2\lambda\varepsilon)e^{\lambda^2}\Gamma(N,\lambda^2) \tag{1.75}$$

Once again $|\lambda|$ discriminates the two regimes. Our attention, for the purpose of this thesis, is devoted to the expectation of the absolute value, namely (fig(**1.1**))

$$\mathbb{E}_{GinOE}[|\det(\lambda\mathbf{1}_N + \varepsilon\boldsymbol{e}_1\otimes\boldsymbol{e}_1^T - \mathbf{G})|] = \frac{2^{-\frac{N}{2}-1}e^{-\lambda^2}}{\sqrt{\pi}\Gamma(\frac{N+1}{2})}\int_{\mathbb{R}} dx_1 \int_{\mathbb{R}+} dx_2 e^{\mathcal{L}(x_1,x_2)} g(x_1,x_2) \tag{1.76}$$

where we found [2]

$$g(x_1,x_2) = x_2^{\frac{N-3}{2}}(x_1^2+x_2+1)^{-\frac{N}{2}-2}\Big(+\lambda^{2N}(\varepsilon^2x_2+(N-1)(x_2+x_1^2+1))+2\varepsilon\lambda^{2N+1}x_2+$$
$$+e^{\lambda^2}\Gamma(N,\lambda^2)(\lambda^2((1-N)(x_2+x_1^2)-x_2\varepsilon^2)+(N-1)(\varepsilon^2(x_2+1)+N(x_2+x_1^2+1))+$$
$$+2\varepsilon\lambda(N-1)(x_2+1)-2\lambda^3x_2\varepsilon)\Big)$$

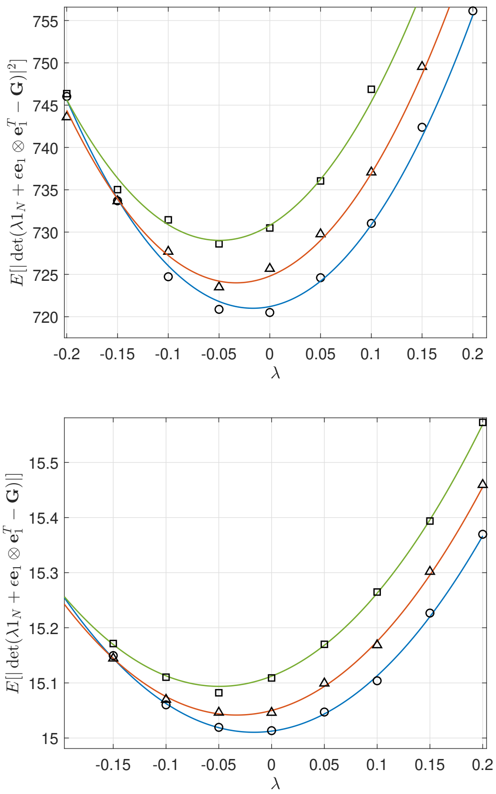

Figure 1.1: Eq(**1.75**) (top) and Eq(**1.76**) (bottom) against simulations of the ensemble *GinOE* indicated by markers for $N = 6$, $\varepsilon = 0.1$(blue), $\varepsilon = 0.2$(red) and $\varepsilon = 0.3$(green). # Samples matrices=50000.

and

$$\mathcal{L}(x_1, x_2) = \frac{-\varepsilon^2 x_1^2 - 2\varepsilon\lambda x_1^2 + \lambda^2(x_2 + x_1^2 + 2)}{2(x_2 + x_1^2 + 1)}.$$

As it will be clear in the following chapters, averages of absolute values of determinants of random matrices and operators is of fundamental importance in counting problems by using the Kac-Rice method (see section 1.2.4 and [49, 50, 36, 51]). Eq(**1.76**), although exact for any N, is unpleasant due to the double integration. The two regimes can be obtained by rescaling $\lambda \to \sqrt{N}\lambda$ and $\varepsilon \to \sqrt{N}\varepsilon$ and take $N \gg 1$, i.e.

- $|\lambda| > 1$

$$\mathbb{E}_{GinOE}\left[\left|\det\left(\lambda \mathbf{1}_N + \varepsilon \boldsymbol{e}_1 \otimes \boldsymbol{e}_1^T - \frac{1}{\sqrt{N}}\mathbf{G}\right)\right|\right] = |\lambda|^{N-1}|\varepsilon + \lambda|(1 + o(1)). \quad (1.77)$$

- $|\lambda| < 1$

$$\mathbb{E}_{GinOE}\left[\left|\det\left(\lambda \mathbf{1}_N + \varepsilon \boldsymbol{e}_1 \otimes \boldsymbol{e}_1^T - \frac{1}{\sqrt{N}}\mathbf{G}\right)\right|\right] = \sqrt{2}e^{\frac{N}{2}(\lambda^2-1)}\sqrt{\varepsilon^2 + 2\lambda\varepsilon + 1}(1+o(1)). \quad (1.78)$$

These results are consistent with the asymptotics for $R_1^R(x)$ with $\varepsilon \to 0$ in the equations above. Remarkably, the case $|\lambda| > 1$ is equivalent, up to a function of N, to the asymptotics of $(\mathbb{E}_{GinOE}[\det(\lambda \mathbf{1}_N + \varepsilon \boldsymbol{e}_1 \otimes \boldsymbol{e}_1^T - \mathbf{G})^2])^{1/2}$. For completeness, we now consider the edge of the spectrum, $|\lambda| = 1$. We further rescale $\lambda \to 1 + \frac{\lambda}{\sqrt{N}}$ and $\varepsilon \to 1 + \frac{\varepsilon}{\sqrt{N}}$. We assume that the new variables λ and ε are real and of order one. Again by performing a saddle point approximation for eq(**1.76**),

- for $\lambda < 0$:

$$\mathbb{E}_{GinOE}\left[\left|\det\left(\lambda \mathbf{1}_N + \varepsilon \boldsymbol{e}_1 \otimes \boldsymbol{e}_1^T - \frac{1}{\sqrt{N}}\mathbf{G}\right)\right|\right] = \sqrt{2} e^{\sqrt{N}\lambda + \frac{\lambda^2}{2}} \operatorname{erfc}(\sqrt{2}\lambda)(1 + o(1)) \tag{1.79}$$

- for $\lambda > 0$:

$$\mathbb{E}_{GinOE}\left[\left|\det\left(\lambda \mathbf{1}_N + \varepsilon \boldsymbol{e}_1 \otimes \boldsymbol{e}_1^T - \frac{1}{\sqrt{N}}\mathbf{G}\right)\right|\right] = 2\left(1 + \frac{\lambda}{\sqrt{N}}\right)^{N-1}(1 + o(1)) \tag{1.80}$$

1.3.3 New Results for Wishart Matrices

The examples in [13] and mentioned at the end of section 1.1.3 suggested the boundedness of the domain of $\frac{dF}{dx}(x, \alpha)$. We show now that this is not a universal behaviour. Here and in section 3.1.5, we consider the ensemble of $\mathbf{W}$ in eq(**1.30**) generated by $\boldsymbol{w}_i = \frac{1}{\sqrt{N}}(w_{i,1}, ..., w_{i,N})$ where w_{ij} and T_i are real independent identically distributed normal random variables of unitary variance. For this choice $F(x, \alpha)$ can not be obtained analytically by inversion. The Stieltjes transform satisfies

$$z = \frac{\alpha - 1}{m(z)} - \frac{i\alpha}{m^2(z)}\Psi\left(\frac{i}{\sqrt{2}m(z)}\right) \tag{1.81}$$

where $\Psi(x) = \sqrt{\frac{\pi}{2}} e^{\frac{1}{x}}(1 + \operatorname{erf}(x))$. The inversion of this equation is a hard task for finite values of x and α. Nevertheless, it is enough to shed light on the behaviour of ρ_α. We firstly show that $\rho_\alpha(x)$ does not have compact support. Given $z = x + iy$, for $x \gg 1$ follows $\operatorname{Re}(m) \approx -\frac{1}{x}$ and $\operatorname{Im}(m) \propto \exp -\frac{1}{2\operatorname{Re}^2(m)}$. Since we expect ρ_α to be symmetric and that can be obtained from $\rho(x) = \frac{1}{\pi}\frac{d}{dx}\lim_{y\to 0^+}\int dx \operatorname{Im} m(x + iy)$ we have that

$$\rho_\alpha(x) \propto e^{-\frac{x^2}{2}} \text{ for } |x| \gg 1. \tag{1.82}$$

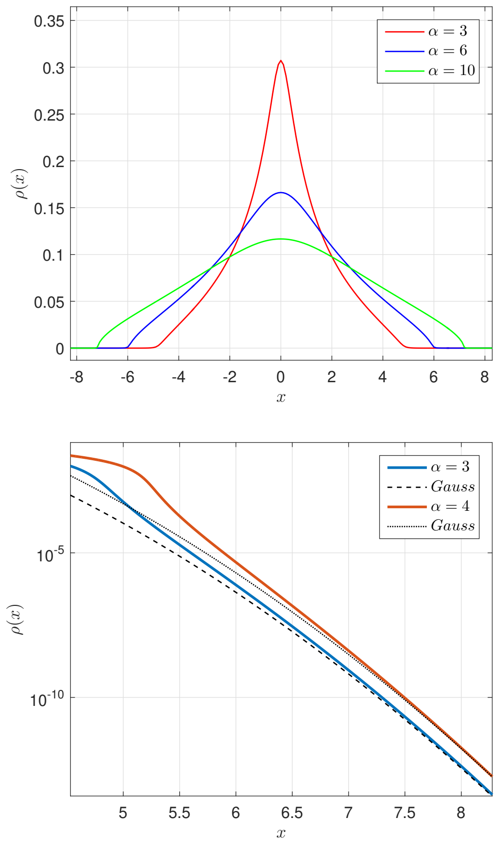

Figure 1.2: Top: limit spectral density of eq(**1.30**) for $T_j \sim \mathcal{N}(0,1)$ obtained numerically by fixed point equation eq(**1.81**). Bottom: detail of the Gaussian tails.

where the constant depends on α. Therefore $\rho_\alpha(x)$ has Gaussian tails. Fig(**1.2**) shows different regimes. At $x = 0$, $\rho_{\alpha,0} = \rho_\alpha(0)$ satisfies

$$1 - \frac{e^{\frac{1}{2\pi^2\rho_{\alpha,0}^2}}}{\sqrt{2\pi}\rho_{\alpha,0}} \operatorname{erfc}\left(\frac{1}{\sqrt{2\pi}\rho_{\alpha,0}}\right) = \frac{1}{\alpha} \tag{1.83}$$

Not surprising, for $\alpha = 1$, $\rho_\alpha \to +\infty$ for $x \to 0$. This is present also in the Marchenko–Pastur distribution. For $\alpha = 1 + \varepsilon$ with $\varepsilon \to 0^+$, we have

$$\rho(x) \approx \frac{1}{\varepsilon\sqrt{2\pi}} - \sqrt{\frac{\pi}{2}}\frac{x^2}{\varepsilon^5} + o(x^2)$$

For $\alpha \gg 1$, $\rho_{\alpha,0} \approx \frac{1}{\pi\sqrt{\alpha-3}}$. From the expansion of the real and imaginary part of eq(**1.81**) for $|x| \ll 1$ we have:

$$\rho_\alpha(x) \approx \frac{1}{\pi\sqrt{\alpha-3}}\left(1 - \frac{x^2}{2(\alpha-3)}\right) + o(x^2) \tag{1.84}$$

The range of finite value for x is not easily accessible. Lastly, we see, from numerical calculations of the first moments, defined by $\mathbb{E}[x^n] = \int \rho_\alpha(x) x^n dx$, that[6] $\mathbb{E}[x^2] = \alpha$ and $\mathbb{E}[x^4] = \alpha(2\alpha + 3)$.

This example leaves us with the question: which properties of $\boldsymbol{w}_i$ and T_i determine the domain of the spectral limit density? In what follows we will try to shed some light on this question.

1.3.3.1 Level Spacing

The tail of the distribution poses question regarding how the eigenvalues are arranged on the real line. To investigate the correlation among the eigenvalues we numerically evaluate the statistics of the mean separation of the latter. In fact the Gaussian tails do not confine the eigenvalues within a bounded segment of the real line as the size of the matrix grows. In particular we know that for bounded-support spectral densities, as GβE and the Laguerre β-ensembles, in the bulk $|\lambda_i - \lambda_j| \sim \frac{1}{N}$. For $\mathbf{W}$, we have to abandon the strict notion of the spectral bulk. We investigated the level spacing between the eigenvalues around zero by adopting the approach contained in [52] we introduce

$$r_j = \frac{\min\{s_j, s_{j+1}\}}{\max\{s_j, s_{j-1}\}}$$

where $s_j = \lambda_{j+1} - \lambda_j$. Such choice has the advantage, respect to the simple spacing s_j to be less sensitive to sample fluctuations [52]. For $N = 400$, we consider sequences 16 consecutive eigenvalues from the middle of the spectrum yielding a collection of r_j values for 20000 disorder realizations. The distribution of r_j is show in fig(1.3) and in table(1). As α grows the expectation of r increases and approaches the expectation for GOE $\mathbb{E}[r] \simeq 0.53068 \pm 0.00001$ with $N = 100$. For GOE, in fact, $P(r) \propto (r + r^2)/(1 + r + r^2)^{5/2}$ ([52]). The eigenvalues around the maximum

Table 1.1: Numerical evaluation of $\mathbb{E}[r]$ for $N = 100$, # Samples=200000.

α	Ensemble eq(1.30) and $T_i \sim \mathcal{N}(0,1)$	Real Wishart Matrices
1	0.5201±0.0001	0.5304±0.0001
3	0.5304±0.0001	0.5306±0.0001
6	0.5306±0.0001	0.5306±0.0001

[6]The moments were numerically tested up to $\alpha = 15$. The series were provided by the OEIS Foundation http://oeis.org/

of $\rho_\alpha(x)$ form spectral sequences similar to the known random matrix ensemble mentioned above. The extreme eigenvalues remain de-localized due to the presence of the tails.

1.3.3.2 The Largest Eigenvalue

Another question left by ρ_α is the behaviour of the largest eigenvalue. The absence of an explicit formula for the joint density of the eigenvalues of $\mathbf{W}$ prevents any analytical consideration over the largest eigenvalue λ_{max}. For the unscaled β ensembles presented at the beginning of section 1.1.1, the latter behaves as

$$\lambda_{max} \approx \sqrt{2N} + \frac{c_\beta}{N^{1/6}}\ell$$

where ℓ is a random variable with Tracy-Widom distribution, i.e.

$$p(\ell < x) = F_\beta(x)$$

For $\beta = 2$, $F_2(x)$ is equal to $\exp\left(-\int_x^{+\infty}(s-x)q^2(s)ds\right)$, where $q(x)$ is the solution of the Painlevé type II equation (see [19][20])

$$\frac{d^2q}{dx^2}(x) = xq(x) + 2q^3(x)$$

Without further details, from these results we get

$$\begin{cases} F_1(x) = e^{E(x)}F_2^{1/2}(x) \\ F_4 = \cosh\left(E(x)\right)F_2^{1/2}(x) \end{cases} \tag{1.85}$$

with $E(x) = -1/2\int_x^{+\infty} q(s)ds$. If we consider the statistics of $\lambda_{\max} - \mathbb{E}[\lambda_{\max}]$, we observe the matching with $\frac{dF_1}{dx}(x)$ around the peak (fig(**1.3**)). This is not a surprising result, but interesting such observation is *not* obtained by a rescaling with N as it happened for the GβE matrices. The distribution includes two asymmetric exponential tails.

1.3.3.3 Characteristic Polynomials

Similarly to the investigations on Hermitian and non Hermitian random matrices of the sections above, we want to investigate the correlations among characteristic polynomials of $\mathbf{W} = \sum_{j=1}^{M} T_j \boldsymbol{w}_j \boldsymbol{w}_j^\dagger$. We assume as in section 1.1.3, $p(\boldsymbol{w}) \propto e^{-\frac{\beta N}{2}\boldsymbol{w}^\dagger \boldsymbol{w}}$. In principle, we would like to compute (see section 3.1.5 for further details)

$$\mathbb{E}_{\mathbf{w}}\left[|\det(\lambda \mathbf{1}_N - \mathbf{W})|\right]$$

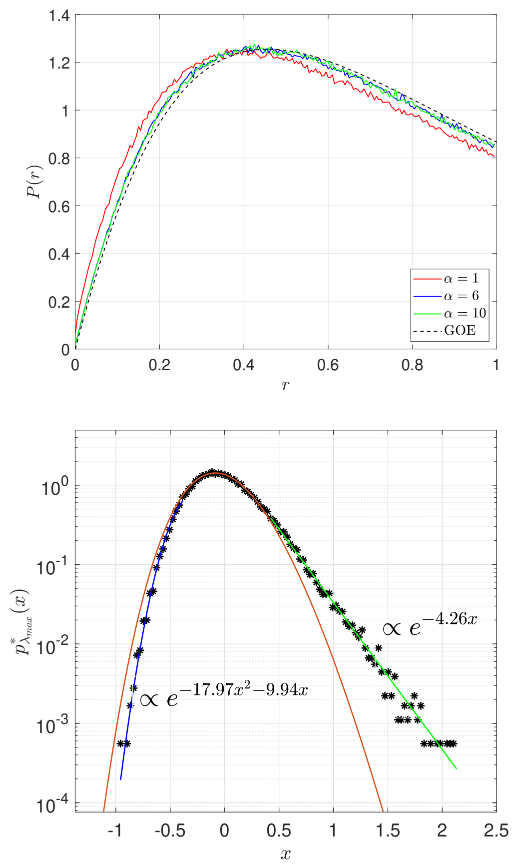

Figure 1.3: Top: Mean level spacing among eigenvalues surrounding zero. Bottom: Empirical distribution of the (centered) largest eigenvalue for $\alpha = 1, N = 600, \beta = 1$, i.e $\lambda_{max} - \mathbb{E}[\lambda_{max}]$(markers), Tracy-Widom distribution(red), fitting of the left(blue) and right (green) tails of the distribution. # Samples=200000.

for $p(T) \propto e^{-T^2/2}$. This quantity is related to a counting problem in section 3.1.5. However, this appeared to be an extremely hard task and any approach attempted in this thesis was unsuccessful. Alternatively one can try to obtain the joint probability density function of the (real) eigenvalues, x_j, of $\mathbf{W}$ for $\beta = 2$. In order to obtain the latter one can start by recalling the measure $p(\mathbf{W})d\mathbf{W}$ and apply the change of variables in section 1.1.1.1, introduce residues and the Harish-Chandra identity([53]). One arrives at

$$p(\boldsymbol{x}) \propto \int_{\mathbf{K}\in\mathrm{Herm}(N)} e^{i\,\mathrm{Tr}\,\mathbf{KX}} \left(\sum_{j=1}^{N} \frac{e^{\frac{N^2}{2\omega_j^2}}}{|\omega_j| \prod_{k\neq j} \left(1 - \frac{\omega_k}{\omega_j}\right)} \Gamma\left(\frac{1}{2}, \frac{N^2}{2\omega_j^2}\right) \right)^M$$

where ω_j are the eigenvalues of $\mathbf{K}$ and $\mathbf{X} = \mathrm{diag}(x_1, ..., x_N)$. It is not clear how to simplify the integral above. Nevertheless, this ensemble is of interest on its own and we follow an alternative route. Aiming to shed some light on this ensemble, in this section we discuss the p-th correlation function of the characteristic polynomial:

$$\mathcal{Z}_{\beta,p}(\boldsymbol{\lambda};\mathbf{T}) = \mathbb{E}_{\mathbf{w}}\left[\prod_{j=1}^{p}\det(\lambda_j \mathbf{1}_N - \mathbf{W})\right] \tag{1.86}$$

where $\mathbb{E}_{\mathbf{w}}[...]$ is the average over all $\boldsymbol{w}_j$ for $j = 1, ..., M$. For now we fix a finite sequence $\mathbf{T} = (T_1, ..., T_M)$. We will consider the average over T_js later on. We emphasize that T_j is not required to be necessarily strictly positive. Each term above in the expectation can be written as Berezin integral by introducing p pairs of Grassmanian vectors. By Bosonization (eq(**1.62**)), eq(**1.86**) can be reduced to evaluating the expectation over the circular unitary ensembles by (see appendix A.2).

$$\mathcal{Z}_{\beta,p}(\boldsymbol{\lambda};\mathbf{T}) = \frac{\int_{C(4/\beta)E(p)}(\mathbf{U}^\dagger d\mathbf{U})\det\mathbf{U}^{-\frac{\beta N}{2}} e^{\frac{\beta}{2}\operatorname{Tr}\boldsymbol{\Lambda}\mathbf{U}}\prod_{a=1}^{M}\Theta_a(\mathbf{U})}{\int_{C(4/\beta)E(p)}(\mathbf{U}^\dagger d\mathbf{U})\det\mathbf{U}^{-\frac{\beta N}{2}} e^{\frac{\beta}{2}\operatorname{Tr}\mathbf{U}}} \tag{1.87}$$

where $\Theta_{a,\beta}(\mathbf{U}) = \det(\mathbf{1}_{(2/\beta)p} - \frac{T_a}{N}\mathbf{U})^{\beta/2}$ and

$$\boldsymbol{\Lambda} = \mathbf{1}_{2/\beta} \otimes \begin{bmatrix} \lambda_1 & 0 & \dots & 0 \\ 0 & \lambda_2 & \dots & 0 \\ \vdots & \vdots & \ddots & \vdots \\ 0 & 0 & \dots & \lambda_p \end{bmatrix}$$

If $\boldsymbol{\Lambda}$ is proportional to the identity matrix, i.e. $\lambda_j = \lambda$, the integrals in eq(**1.87**) are unitary invariant and can be written in terms of the eigenvalues of $\mathbf{U}$. In order to present the results given below we introduce the hypergeometric function of a matrix argument (see [26]). For any $N \times N$ matrix $\mathbf{M}$ of eigenvalues $\boldsymbol{x}$

$${}_pF_q^{(\beta)}(\boldsymbol{a},\boldsymbol{b};\mathbf{M}) = \sum_{k=0}^{\infty}\sum_{\kappa\vdash k}\frac{\prod_{j=1}^{p}(a_j)_\kappa^{(\beta)}}{|k|!\prod_j^q(b_j)_\kappa}C_\kappa^{(\beta)}(\boldsymbol{x}) \tag{1.88}$$

where $(a_j)_\kappa^{(\beta)}$ is the generalized Pochhammer symbol, $C_\kappa^{(\beta)}(\boldsymbol{x})$ is the C-normalized Jack polynomial and $\kappa \vdash k$ represents the sum over the partitions of k. For $a_j < 0$, the infinite sum over k is replaced by a finite order algebraic polynomial in the variables $\boldsymbol{x}$. If the latter is a scalar the hypergeometric function reduces to a more familiar:

$${}_pF_q(a_1, ..., a_p; b_1, ..., b_q; x) = \sum_{k=0}^{+\infty}\frac{\prod_{j=1}^{p}(a_j)_k}{\prod_{j=1}^{q}(b_j)_k}\frac{x^k}{k!}$$

From the definition of $\Theta_{a,\beta}$, for $\beta = 1$, we choose the branch cut of $\sqrt{(\cdot)}$ to be the negative real semi-axis and, to simplify the calculations, we further assume that

$$\operatorname{Re}\left(\det\left(\mathbf{1}_{2p} - \frac{T}{N}\mathbf{U}\right)\right) \geq 0. \tag{1.89}$$

For N sufficiently large and bounded Ts this assumption is justified. However, for $N \gg 1$, the results concerning the asymptotic behaviour of eq(**1.86**) presented below are shown to be valid even for unbounded support of certain sufficiently nice probability density function of T.

1.3.3.4 Fixed T

We first state the case of $\mathbf{T}$ being fixed, not necessarily real, and $\lambda_j = \lambda$. The integrands above in eq(**1.87**) become unitary invariant. Therefore introducing the diagonalization $\mathbf{U} = \mathbf{V}e^{i\mathbf{\Theta}}\mathbf{V}^\dagger$ and integrating out the unitary matrix $\mathbf{V}$, those integrals only depend on the distribution of the eigenvalues of $\mathbf{U}$. If we consider $\lambda \neq 0$ the correlation acquires a determinantal structure for the complex case (See appendix A.3)

$$\mathcal{Z}_{\beta=2,p}(\lambda;\mathbf{T}) = \frac{\det\left[g_N(k-j)\right]_{j,k=1}^{p}}{\det\left[h_N(k-j)\right]_{j,k=1}^{p}} \tag{1.90}$$

and Pfaffian structure for the real case

$$\mathcal{Z}_{\beta=1,p}(\lambda;\mathbf{T}) = \frac{\text{Pf}\left[(j-k)g_N(2p+1-(k+j))\right]_{j,k=1}^{2p}}{\text{Pf}\left[(j-k)h_N(2p+1-(k+j))\right]_{j,k=1}^{2p}} \tag{1.91}$$

where

$$\begin{cases} g_N(x) = \lambda^{N+x}\sum\limits_{u=0}^{N+x}\frac{(-1)^u}{(N+x-u)!}e_u\left(\frac{\boldsymbol{T}}{N\lambda}\right) \\ h_N(x) = \frac{1}{(N+x)!} \end{cases} \tag{1.92}$$

and $e_u(x)$ is the u-th elementary symmetric polynomial. Figs(**1.4**) provide an example of the formulas above with

$$\mathbf{T}^{(1)} = (0.4339, 1.0562, -0.3710, 0.3090, -0.8655, -1.0482, -1.6036, -0.7595, 1.1370, -1.0643)^T \tag{1.93}$$

and

$$\mathbf{T}^{(2)} = (0.4339, 1.0562, -0.3710, 0.3090, -0.8655, -1.0482, -1.6036, -0.7595)^T \tag{1.94}$$

For $\lambda = 0$, a directly application of the Selberg integral and of the definition of Jack and quaternion zonal polynomials leads to following formulas ([26]):

$$\mathcal{Z}_{\beta=2,p}(0;\mathbf{T}) = (-1)^{pN}\frac{{}_2F_1^{(1)}\Big(-p, N; -(p-1)-(1-N); \frac{\mathbf{T}}{N}\Big)}{{}_1F_1^{(1)}(-N, p-N; 1)} \tag{1.95}$$

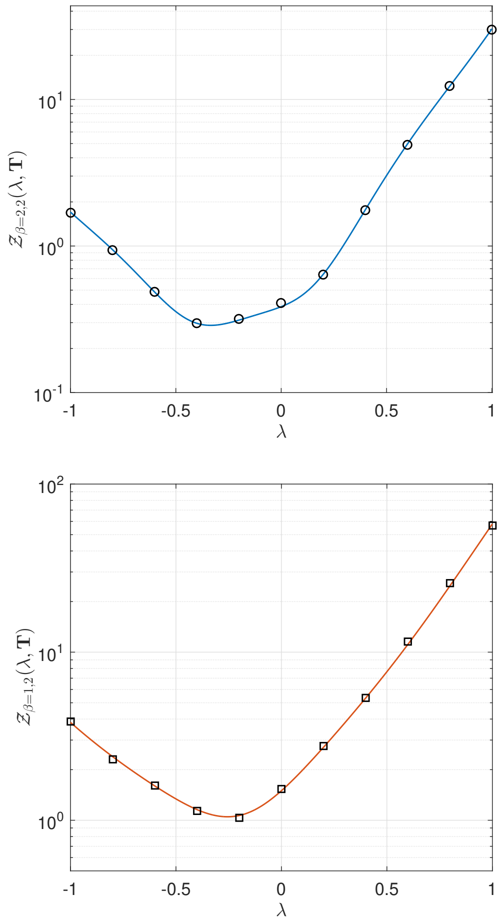

Figure 1.4: Top: Evaluation of $\mathcal{Z}_{2,2}(\lambda,\mathbf{T})$ from eq(**1.90**) (dark line) with $\mathbf{T}^{(1)}$ (eq(**1.93**)), $N=5,\alpha=2$ against numerical simulations (markers). Bottom: Evaluation of $\mathcal{Z}_{1,2}(\lambda,\mathbf{T})$ from eq(**1.91**) (dark line) with $\mathbf{T}^{(2)}$ (eq(**1.94**)),$N=4,\alpha=2$ against numerical simulations (markers). For each figure, # Samples=100000.

$$\mathcal{Z}_{\beta=1,p}(0;\mathbf{T}) = (-1)^{pN} \frac{{}_2F_1^{(2)}\Big(-p, \frac{N}{2}; -(p-1)-1/2(1-N); \frac{\mathbf{T}}{N}\Big)}{{}_1F_1^{(1/2)}(-N,-N+1+2(p-1);1)} \tag{1.96}$$

We use these calculation for [3].

1.3.3.5 Random T

We now turn to the original case of $\mathbf{T}$ being a random diagonal matrix with i.i.d main diagonal entries. We consider again N to be finite, with the hypothesis so far introduced $\mathbb{E}_{\mathbf{T}}[\mathcal{Z}_{\beta,p}]$ depends on the first p moments of $\mathbf{T}$. This property results in a certain "universality". Different distributions of $\mathbf{T}$, continuous or discrete, with the same first p centered moments result in $\mathbb{E}_{\mathbf{T}}[\mathcal{Z}_{\beta,p}]$ being the same. In what follows we

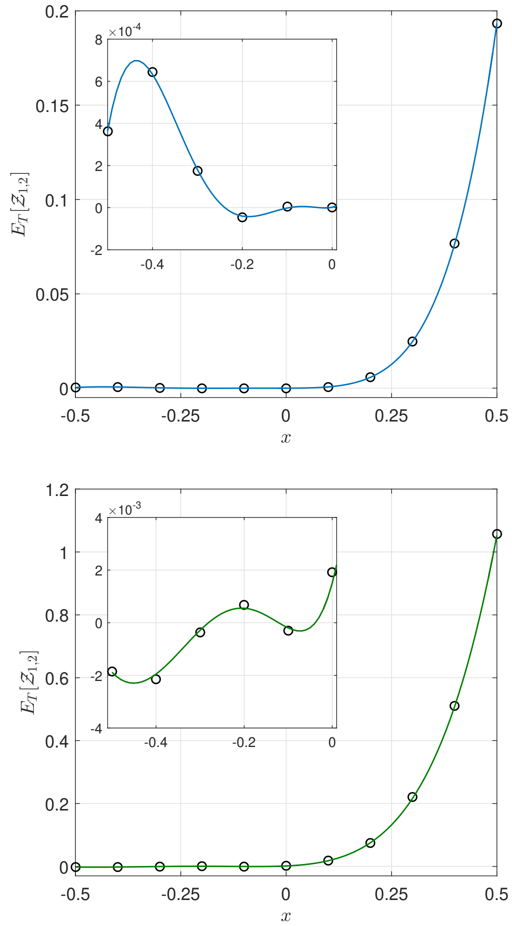

Figure 1.5: Evaluation of $\mathbb{E}_T[\mathcal{Z}_{1,2}]$ from eq(**1.98**) dark line and numerical evaluation (markers); $\alpha = 1$(blue),$\alpha = 2$(green), $x = \lambda_1\lambda_2$ $\mathbb{E}[T^2] = 0.5, \mathbb{E}[T] = 0, N = 6$. For each figure, # Samples=6000000.

give results for $p = 1$ and $p = 2$ therefore we will require $\mathbb{E}[|T|] < +\infty$ and $\mathbb{E}[T^2] < +\infty$.

- $p = 1$: in this case $\mathbf{U}$ is a 1×1 and a 2×2 diagonal matrix for $\beta = 2$ and $\beta = 1$ respectively. For $\beta = 1$, we assume that $|T/N| < 1$ almost surely. The only relevant moment of T is the mean $\mathbb{E}_T[T]$. However, $\mathbb{E}_{\mathbf{T}}[\mathcal{Z}_{\beta,1}(\lambda; \mathbf{T})]$ does not depend on the choice of β:

$$\mathbb{E}_{\mathbf{T}}[\mathcal{Z}_{\beta,1}(\lambda; \mathbf{T})] = \left(\frac{\mathbb{E}[T]}{N}\right)^N \Omega_{\alpha 1}F_1\left(-N; 1 + (\alpha - 1)N; \frac{\lambda N}{\mathbb{E}[T]}\right) \tag{1.97}$$

with $\Omega_\alpha = \frac{(\alpha N)!}{((\alpha-1)N)!}$. For $\mathbb{E}[T] = 0$ this simplifies to

$$\mathbb{E}_{\mathbf{T}}[\mathcal{Z}_{\beta,1}(\lambda; \mathbf{T})] = \lambda^N$$

- $p = 2$: in this case the relevant moments of T are $\mathbb{E}[T]$ and $\mathbb{E}[T^2]$. We introduce the vector $\boldsymbol{\lambda} = (\lambda_1, \lambda_2)$. Whenever the latter are distinct, eq(**1.87**) requires a direct parametrization of the circular unitary and symplectic **U**s. For $\beta = 1$, we further assume that $1 + \frac{T}{N}(\cos\theta_1 + \cos\theta_2) + \frac{T^2}{N^2}\cos(\theta_1 + \theta_2) > 0$ for $\theta_{j=1,2} \in (-\pi, +\pi)$. This is necessary to guarantee that eq(**1.89**) is satisfied. Lastly, assuming $\mathbb{E}[T] = 0$, the 2-point correlation function is given by:

$$\mathbb{E}_{\mathbf{T}}[\mathcal{Z}_{\beta,2}(\boldsymbol{\lambda}; \mathbf{T})] = \left(\frac{\mathbb{E}[T^2]}{N^2}\right)^N \Gamma\left(N + \frac{2}{\beta} + 1\right) \frac{\beta\Omega_\alpha}{2} \times \\ {}_1F_2\Big(-N; \frac{2}{\beta} + 1, 1 + (\alpha - 1)N; -\frac{\lambda_1\lambda_2 N^2}{\mathbb{E}[T^2]}\Big) \quad (1.98)$$

Here we would like to draw the attention to an unusual dependence of $\mathbb{E}_{\mathbf{T}}[\mathcal{Z}_{\beta,2}(\boldsymbol{\lambda}; \mathbf{T})]$ on the spectral parameters $\boldsymbol{\lambda} = (\lambda_1, \lambda_2)$. In fact, for the well known GβE matrix ensembles in the limit $N \gg 1$, $\mathbb{E}_{\mathbf{T}}[\mathcal{Z}_{\beta,2}(\boldsymbol{\lambda}; \mathbf{T})]$ becomes a function of the difference $|\lambda_1 - \lambda_2|$ rather than their product (see [6]). Figs(**1.5**) provide numerical evidence of this behaviour. This lays the ground for new investigations concerning the associated kernel of $\mathbb{E}_{\mathbf{T}}[\mathcal{Z}_{\beta,2}(\boldsymbol{\lambda}; \mathbf{T})]$ and consequent scalings for $N \gg 1$.

1.3.3.6 Asymptotic of a Large Deviation Type

We now take the limit $N \to +\infty$ such that $\alpha = M/N$ is finite. Therefore we expect that the following results also hold, for sufficiently nice and fast-decaying probability density function of T, when $\mathrm{Re}\left(\det(\mathbf{1}_{2p} - \frac{T_a}{N}\mathbf{U})\right) > 0$ is not satisfied pointwise for $\beta = 1$. The objective is to extract the leading exponential behaviour of the moments of $\mathbb{E}_{\mathbf{T}}[\mathcal{Z}_{\beta,p}]$. This reduces to saddle point approximations of the results above:

- $p = 1$: We introduce $x = \lambda/\mathbb{E}[T]$ and define the intervals $S_1 = (-\infty, (1 - \sqrt{\alpha})^2)$, $S_2 = [(1 - \sqrt{\alpha})^2, (1 + \sqrt{\alpha})^2]$ and $S_3 = ((1 + \sqrt{\alpha})^2, +\infty)$, for $x \in S_j$ we have:

$$\lim_{N \to +\infty} \frac{1}{N} \log|\mathbb{E}_{\mathbf{T}}[\mathcal{Z}_{\beta,1}(\lambda, \mathbf{T})]| = \log|\mathbb{E}[T]| + \frac{f_j(\alpha, x)}{2} - 1 \quad (1.99)$$

where:

$$\begin{cases} f_1(\alpha, x) = -(\alpha - 1)\log(4x^2) - \log Z_+^2 + Z_+ + \alpha \log S_-^2 \\ f_2(\alpha, x) = -(\alpha - 1)(\log x + 1) + \alpha \log \alpha + x \\ f_3(\alpha, x) = -(\alpha - 1)\log(4x^2) - \log Z_-^2 + Z_- + \alpha \log S_+^2 \end{cases}$$

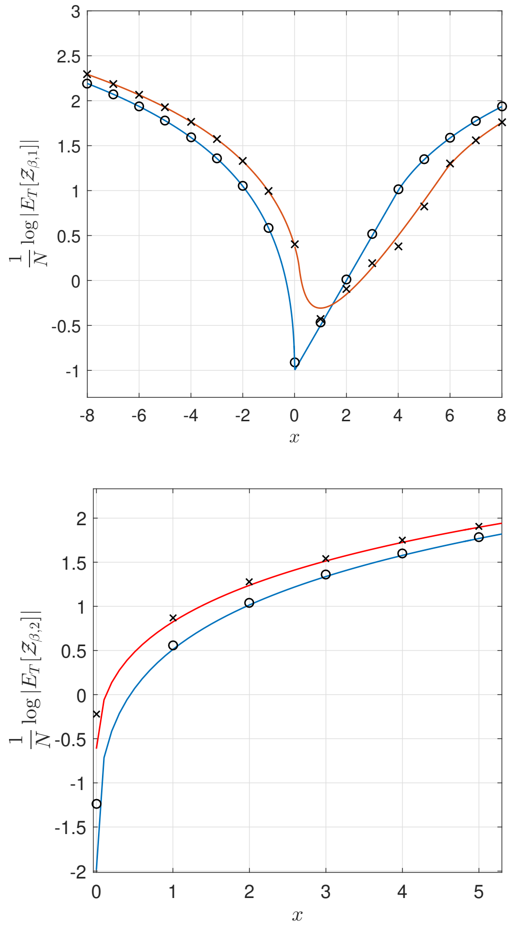

Figure 1.6: Top: Large deviations for $\mathcal{Z}_{\beta,1}$ of eq(**1.97**) for $\alpha = 1$(blue),$\alpha = 2$(red), and numerical simulations (markers) for $N = 20, \mathbb{E}[T] = 1$. Bottom: Large deviations for $\mathcal{Z}_{\beta,2}$ (eq(**1.98**)) for $\alpha = 1$(blue), $\alpha = 2$(red), and numerical simulations (markers) for $N = 100, \mathbb{E}[T] = 0, \mathbb{E}[T^2] = 1$. For each figure, # Samples=10^7.

with $S_\pm = \alpha \pm \sqrt{\Delta} + x - 1$, $Z_\pm = -\alpha \pm \sqrt{\Delta} + x + 1$ and $\Delta = (\alpha - 1 - x)^2 - 4x$. For $\alpha = 1$ in S_2, $f_2(\alpha, x)$ simplifies to x becoming linear (see fig(**1.6**)). Interestingly, the intervals of the different regimes are separated by the boundaries of the finite support of the Marchenko-Pastur distribution, i.e. $(1 \pm \sqrt{\alpha})^2$, regardless of the distribution of T. For $|x| \gg 1$, we have:

$$\frac{f_{1,3}(\alpha, x)}{2} \sim -\frac{\alpha}{x} + \log|x| + 1 \tag{1.100}$$

Conversely, if $\mathbb{E}[T] = 0$, the result simplifies to:

$$\lim_{N\to+\infty} \frac{1}{N} \log|\mathbb{E}_{\mathbf{T}}[\mathcal{Z}_{\beta,1}(\lambda, \mathbf{T})]| = \log|\lambda|$$

- $p = 2$: In the limit $N \to +\infty$, assuming $\alpha \geq 1$, $\mathbb{E}[T] = 0$, $\mathbb{E}[T^2] = 1$ and $x = |\lambda_1 \lambda_2|$, a saddle point approximation reveals (fig(1.6))

$$\lim_{N\to+\infty} \frac{1}{N} \log |\mathbb{E}_{\mathbf{T}}[\mathcal{Z}_{\beta,2}(\boldsymbol{\lambda}; \mathbf{T})]| = \mathcal{L}(\eta^*) \tag{1.101}$$

where:

$$\begin{cases} \eta^* = \frac{1-\alpha}{3} - \frac{\sqrt[3]{2}\Theta}{3\sqrt[3]{\Delta+\sqrt{\Delta^2+4\Theta^3}}} + \frac{\sqrt[3]{\Delta+\sqrt{\Delta^2+4\Theta^3}}}{3\sqrt[3]{2}} \\ \mathcal{L}(\eta) = \alpha\log\alpha - (\alpha+\eta-1)\log(\alpha+\eta-1) + \eta\log x + \\ +(\eta-1)\log(1-\eta) + 2(\eta - \eta\log\eta - 1) \\ \Delta = -2\alpha^3 + 6\alpha^2 - 6\alpha + 9\alpha x + 18x + 2 \\ \Theta = 3x - (\alpha-1)^2 \end{cases}$$

The asymptotic behaviour clearly depend on the absolute value of $\lambda_1\lambda_2$ and not on their signs. It has to be noticed that such result does not depend on the choice of β, i.e. of $\mathbf{W}$. In particular for $x \to 0^+$, $\lim_{N\to+\infty} \frac{1}{N} \log \mathbb{E}_{\mathbf{T}}[\mathcal{Z}_{\beta,2}(\boldsymbol{\lambda}; \mathbf{T})] = -2 + \log(\alpha-1) - \alpha\log(\alpha-1) + \alpha\log\alpha$. Conversely, for $x \to +\infty$, in analogy to $p = 1$, $\lim_{N\to+\infty} \frac{1}{N} \log \mathbb{E}_{\mathbf{T}}[\mathcal{Z}_{\beta,2}(\boldsymbol{\lambda}; \mathbf{T})] \sim \frac{\alpha}{x} + \log|x|$.

We numerically investigated eq(1.101) for i.i.d. Ts normal random variables and $\beta = 1$. This breaks the condition in eq(1.89). As N increases, the average in eq(1.101) requires an increased number of trials in order to control and suppress the sample variance. However, even in this case, the exponential behaviour of eqs(1.99,1.101) above is fulfilled.

Chapter 2

Wigner Reaction Matrix

2.1 Introduction

Firstly born to represent nuclear scattering, quantum chaotic scattering has become a paradigm for describing large quantum systems. In particular, the chaotic resonance scattering of quantum waves has been at the center of many investigations in literature both theoretical and experimental for the last thirty years (to cite a few reviews [54, 55, 56, 57] and [58]). Before being able to describe this phenomenon we proceed by steps, eventually introducing the RMT approach to the problem. We assume that the state of a system is described by a superposition of vectors (indicated as $|\varphi\rangle$) in a Hilbert space. Adopting the bra-ket notation for such vectors, for a given spectral parameter (energy) λ, in the proximity of a scattering region, the system can be described by M scattering open (incoming, outgoing and evanescent) channels (see fig(**2.1**)):

$$|\varphi\rangle = \sum_{n=1}^{M} \psi_n^{in} |\varphi_n^{in}\rangle + \sum_{n=1}^{M} \psi_n^{out} |\varphi_n^{out}\rangle + \sum_{n} \psi_n^{e} |\varphi_n^{e}\rangle \tag{2.1}$$

A linear and unitary transformation, *the scattering matrix*, $\mathbf{S}(\lambda)$ linearly couples the states $\psi_n^{\bullet}$ on the r.h.s. in eq(**2.1**). Therefore, the most interesting object to investigate is $\mathbf{S}$ and its statistics. The conservation of probability of the states requires $\mathbf{S}(\lambda \in \mathbb{R})$ to be unitary, i.e. $\mathbf{S}^{\dagger}(\lambda)\mathbf{S}(\lambda) = \mathbf{1}_M$. Additionally, the causality forces the resonances, i.e. the poles of $\mathbf{S}$, at complex energies to have negative imaginary part. We focus our attention to the statistics of the scattering observables for energy scales of the same order as the mean separation among positions of neighbouring resonances. The features concerning the scattering matrix can be dealt with many different tools. Examples are the Green function and the wave matching approaches. However, under our assumptions, the most suitable way to our goal is via the 'Heidelberg approach'.

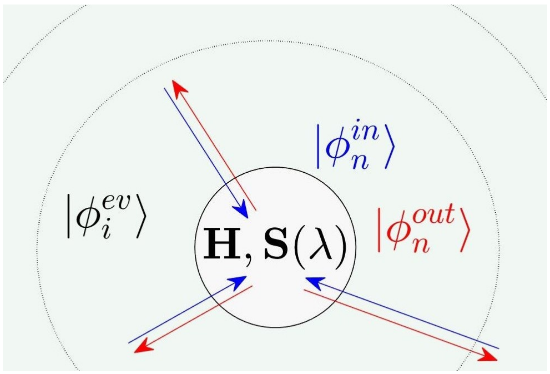

Figure 2.1: The system is described by M scattering channels and evanescent states.

Statistics of fluctuations of the scattering observables over an energy interval comparable with a typical separation between resonances can be most successfully achieved in the framework of the so called 'Heidelberg approach'. We refer the reader to the seminal work [59],[60], [61] and [62] to cite a few. The main idea is to re-write and investigate the resonance part of the scattering matrix in terms of the Cayley transform of the $M \times M$ Wigner reaction matrix $\mathbf{K}$. The latter contains $\mathbf{W}$, i.e. the $N \times M$ matrix which couples the open channels with the closed part of the scattering system. The latter is encoded in the resolvent of the Hamiltonian $\mathbf{H}$. Abandoning for now the bra-ket notations, one can show the validity of the following formulas

$$\mathbf{S}(\lambda) = \frac{\mathbf{1}_M - i\mathbf{K}}{\mathbf{1}_M + i\mathbf{K}}, \quad \text{with} \quad \mathbf{K} = \mathbf{W}^\dagger \frac{1}{\lambda \mathbf{1}_N - \mathbf{H}_N} \mathbf{W}, \tag{2.2}$$

Within the Heidelberg approach, one can see that $\mathbf{S}(\lambda \in \mathbb{R})$ being unitary follows from the Hermitian property of the Hamiltonian. Introducing at this point the RMT framework with the aim of investigating the fluctuations arising for the chaotic wave scattering, $\mathbf{H}$ can be chosen correspondingly as a $N \times N$ self-adjoint random matrix $\mathbf{H}_N$. The properties of $\mathbf{H}_N$ are clearly inherited from the symmetries of the Hamiltonian operator $\mathbf{H}$ which describes the quantum chaotic behaviour of the closed counterpart of the scattering system. Hence, we assume that $\mathbf{H}_N$ is a $N \times N$ random matrix drawn from the Gaussian ensembles listed in section 1.1.1. Firstly, we will investigate systems with broken time reversal invariance requiring $\mathbf{H}_N$ to be a $GUE(N)$ matrix ($\beta = 2$). Later we re-introduce such time reversal symmetry and therefore we will draw $\mathbf{H}_N$ from the Gaussian Orthogonal Ensemble ($GOE(N), \beta = 1$). We assume the system has no further geometric symmetries. To define the problem we still need to describe the entries of the coupling matrix $\mathbf{W}$. There are two main approaches in literature.

Verbaarschot et al. ([59]) fixed its columns $\boldsymbol{w}_a,\ a = 1, .., M$ to be non-random (complex for $\beta = 2$ or real for $\beta = 1$) orthogonal vectors. However, in the present thesis will follow a different path. In line with [63], we require the entries of vectors $\boldsymbol{w}_a$ to be i.i.d. Gaussian random variables orthogonal on average. *Regardless* of the choice (i.e. fixed vs random), the assumptions above lead to practically the same results whenever M is sufficiently smaller than N, i.e. $M \ll N \to \infty$. For the last decades, the advantages of this approach have been exploited in many works which make use of RMT and Supersymmetry (see [64, 65] and recent [66, 67, 35, 68, 69]). The power of these results have shed light on several experiments involving chaotic electromagnetic resonators, microcavities and acoustic reverberation cameras. It is worth mentioning their versatility in predicting properties of numerical models for scattering in quantum chaotic graphs [70] and the experimental counterpart with microwaves [71, 72, 73, 74, 4]. An important feature of this approach is the fact that the statistics of the Wigner reaction matrix can be determined experimentally as such matrix can be written in terms of the entries of the impedance matrix [75, 76, 77]. Recently, our results presented in section 2.2.1 has been observed experimentally by [4]. In general, a source of discrepancy with the previously existing theory arises from the fact that the experiments on the scattering face energy losses, i.e. absorption. This is given by imperfections or by losses in the conducting walls of the resonator. We assume that such energy losses are uniform and do not have a spatial dependency. The implication is the scattering matrix being not unitary anymore. Moreover, this presents serious challenges to the interpretation given above. The absorption has to be incorporated into the Heidelberg approach. To do so λ is replaced in eq(**2.2**) by $\lambda \to \lambda + i\alpha/N \in \mathbb{C}$ for some $\alpha > 0$ [65]. The consequences of this substitution are the following. The Wigner matrix $\mathbf{K}$ is no longer Hermitian and it has complex entries even in the case of preserved time-reverse invariance, i.e. for $\beta = 1$. The rescaling $1/N$ in λ is introduced to investigate the regime in which absorption appears with the order of magnitude of the mean separation between eigenvalues of $\mathbf{H}$. The statistics of the main diagonal entries of $\mathbf{K}$ is well understood thanks to several theoretical publications (see [78, 79, 80]). Many experimental works have followed for both for $\beta = 1$, especially in microwave cavities ([81, 75, 76, 77]), and for $\beta = 2$ (see [82]). In this chapter, we want to investigate the statistics of the off diagonal terms of $\mathbf{K}$. This is a hard task which has not been addressed before for $\beta = 1$ except for the limit of zero absorption ([35]) or for the mean value and variance of $|\mathbf{K}_{ab}|^2 = (\operatorname{Im} \mathbf{K}_{a\neq b})^2 + (\operatorname{Re} \mathbf{K}_{a\neq b})^2$ [83]. We want to address this problem and retrieve, particularly for $\beta = 1$, the joint distribution of $\mathrm{Re}\,\mathbf{K}_{a\neq b}$ and $\mathrm{Im}\,\mathbf{K}_{a\neq b}$ with non-vanishing absorption where

$$\mathbf{K}_{a,b} = \mathrm{Tr}\left\{ \left(\left(\lambda + i\frac{\alpha}{N}\right)\mathbf{1}_N - \mathbf{H}_N \right)^{-1} \boldsymbol{w}_b \otimes \boldsymbol{w}_a^T \right\} \tag{2.3}$$

for $N \to +\infty$. Before addressing the case $\beta = 1$, we consider the case of broken time reversal invariance. The aim is to complete and generalize eqs.(11)-(13) in [84] for the first statistics of $|\mathbf{K}_{ab}|^2$ for $a \neq b$. In the latter work they derived the full distribution of $|K_{a\neq b}|^2$ for $\beta = 2$. Additionally, we introduce the case of correlated channel vectors (see eq(**2.10**)). This also represents an initial benchmark to attempt the case $\beta = 1$. Before we provide the detail of our work, we point out that the case of correlated channel vectors represents a violation of the orthogonality on average. This results in a non diagonal mean scattering matrix $\mathbf{S}$ and shows the presence of "direct" scattering [85]. For the "Heidelberg model" this case is essentially new in literature (see [86]). In appendix B.3, we give particular emphasis on the "perfect coupling", obtained by either changing the strength of the channel couplings or increasing correlations between channels.

2.2 Characteristic Function for $\mathbf{K}_{ab}$

We now investigate the statistics for $\mathbf{K}_{ab}$ for the two choices of $\boldsymbol{w}_a$. Such choices will lead to different results. In particular, we are able to present a closed form expression only for $\beta = 2$ while leaving the result in a form of an integral representation for $\beta = 1$.

2.2.1 Systems with broken time-reversal invariance

In this case, the entries of $\mathbf{H}_N$ are complex and the probability density function is given by eq(**1.1**) for $J = 1$. Therefore, the expectation over this ensemble is given by $\mathbb{E}_{GUE(N)}[(...)] := \int(...)dp(\mathbf{H}_N)$ where $dp(\mathbf{H}_N) \propto e^{-N/2\,\mathrm{Tr}\,\mathbf{H}_N\mathbf{H}_N^\dagger} d\mathbf{H}_N$. To complete the description, firstly, we randomly choose the channel vectors $\boldsymbol{w}_a$ and $\boldsymbol{w}_b$ to be uncorrelated and centered complex Gaussian random variables of variance $1/N$. The expectation over the realization of these vectors is indicated by the overbar. We will eventually relax the assumption of independence: the correlation among channels is introduced by a given 2×2 covariance matrix. In both cases, instead of directly addressing the distribution of $\mathbf{K}_{a,b}$, we will investigate the characteristic function of the real and imaginary parts, given by the Fourier transform

$$\mathcal{R}(q,q^*) = \mathbb{E}_{GUE(N)}\overline{\left[\exp\frac{i}{2}\left(q\mathbf{K}^*_{a,b} + q^*\mathbf{K}_{a,b}\right)\right]}. \tag{2.4}$$

The statistics are given by the derivative of eq(**2.4**) in q or q^* and setting $q, q^* \to 0$. We will present explicit expressions for the probability density functions when possible.

2.2.1.1 Uncorrelated channel vectors $\boldsymbol{w}_a$ and $\boldsymbol{w}_b$.

The expectation over the complex components of the channel vectors $\boldsymbol{w}_a$ in eq(**2.4**) leads to a ratio of determinants involving a single realization of the Hamiltonian $\mathbf{H}_N$. A subsequent average over the latter belonging to the Gaussian Unitary ensemble (see appendix B.1 for details) leads to

$$\mathcal{R}(q,q^*) = \mathbb{E}_{GUE(N)}\left[\frac{\det\left((\mathbf{H}_N - \lambda\mathbf{1}_N)^2 + \frac{\alpha^2}{N^2}\mathbf{1}_N\right)}{\det\left((\mathbf{H}_N - \lambda\mathbf{1}_N)^2 + \frac{\alpha^2+|q/2|^2}{N^2}\mathbf{1}_N\right)}\right] \tag{2.5}$$

We have encountered this quantity and its Dyson limit in the first chapter (see eq(**1.20**) and it is of great significance in RMT ([31, 87, 33]). One can retrieve from the mentioned works the characteristic function $\mathcal{R}(q,q^*) \equiv \mathcal{R}(|q|)$. Indeed, for $N \to +\infty$ and a given spectral parameter $\lambda \in (-2,2)$, within the bulk regime of the GUE spectrum:

$$\mathcal{R}(|q|) = \frac{|q/2|^4 \exp\left(-2\pi\rho(\lambda)\sqrt{\alpha^2+|q/2|^2}\right)}{4\alpha\sqrt{\alpha^2+|q/2|^2}} \times \\ \times \left(\frac{\exp\left(2\pi\rho(\lambda)\alpha\right)}{(\sqrt{\alpha^2+|q/2|^2}-\alpha)^2} - \frac{\exp\left(-2\pi\rho(\lambda)\alpha\right)}{(\sqrt{\alpha^2+|q/2|^2}+\alpha)^2}\right), \tag{2.6}$$

with $\rho_{sc}(\lambda) = 1/(2\pi)\sqrt{4-\lambda^2}$ defined in eq(**1.18**). Eq(**2.6**) is numerically checked against Monte-Carlo simulations of eq(**2.5**) in fig(**2.2**). Eq(**2.6**) can be inverted to get the joint probability density function of $\mathbf{K}_{a,b}$ and $\mathbf{K}^*_{a,b}$. In order to express the most convenient form for the latter, we define the operator

$$\hat{\mathcal{D}}_x = \sinh(x)\left(1 + \frac{d^2}{dx^2}\right) - 2\cosh(x)\frac{d}{dx}$$

Then, the joint probability density function of $(\mathbf{K}_{ab}, \mathbf{K}^*_{ab})$ for systems with broken time-reversal invariance and uncorrelated channel vectors is given by

$$p(\mathbf{K}_{a,b}, \mathbf{K}^*_{a,b}) = \frac{\alpha^2}{\pi}\lim_{x\to 2\pi\rho(\lambda)\alpha}\hat{\mathcal{D}}_x\frac{\exp\left(-\sqrt{x^2+4\alpha^2|\mathbf{K}_{a,b}|^2}\right)}{\sqrt{x^2+4\alpha^2|\mathbf{K}_{a,b}|^2}} \tag{2.7}$$

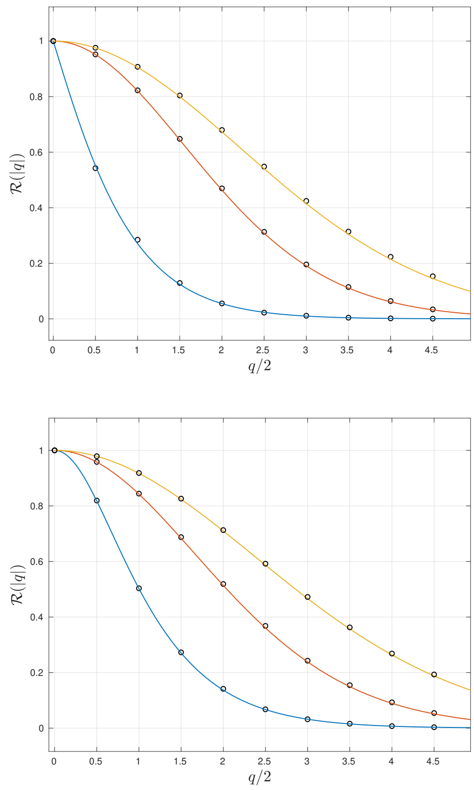

Figure 2.2: Characteristic function given by eq(2.6) for systems with broken time-reversal invariance for $\alpha = 1$(blue), $\alpha = 5$(red), $\alpha = 10$(yellow) and $\lambda = 0$ (top), $\lambda = 1$(bottom) versus direct numerical simulations ($N = 100$, # samples=50000, circular markers).

From eq(2.7), we can recover the statistics in absence of absorption by taking $\alpha \to 0^+$, namely $p(\mathbf{K}_{a,b}, \mathbf{K}^*_{a,b})$ becomes

$$p\left(\mathrm{Re}\,\mathbf{K}_{a,b}, \mathrm{Im}\,\mathbf{K}_{a,b}\right) = \frac{\rho(\lambda)}{4} \frac{|\mathbf{K}_{a,b}|^2 + 4\pi^2\rho^2(\lambda)}{(|\mathbf{K}_{a,b}|^2 + \pi^2\rho^2(\lambda))^{5/2}}$$

From the joint probability one can obtain the distribution of $\mathrm{Re}\,\mathbf{K}_{a,b}$ and $\mathrm{Im}\,\mathbf{K}_{a,b}$ separately. Indicating the latter as u_1 and u_2 respectively, we have

$$p(u_i) = \frac{\rho(\lambda)}{2} \frac{u_i^2 + 3\pi^2\rho^2(\lambda)}{(u_i^2 + \pi^2\rho^2(\lambda))^2} \tag{2.8}$$

Due to the limit in eq(2.7), the results above could have been obtained assuming $\lambda = 0$ and then retrieving the entire bulk $\lambda \in (-2, 2)$ by a further rescaling $\alpha \to \alpha\eta$ and $|q| \to |q|\eta$ with the ratio $\eta = \rho(\lambda)/\rho(0)$. In random matrix theory, this phenomenon is well-known under the name of *spectral universality* property. We will then assume the

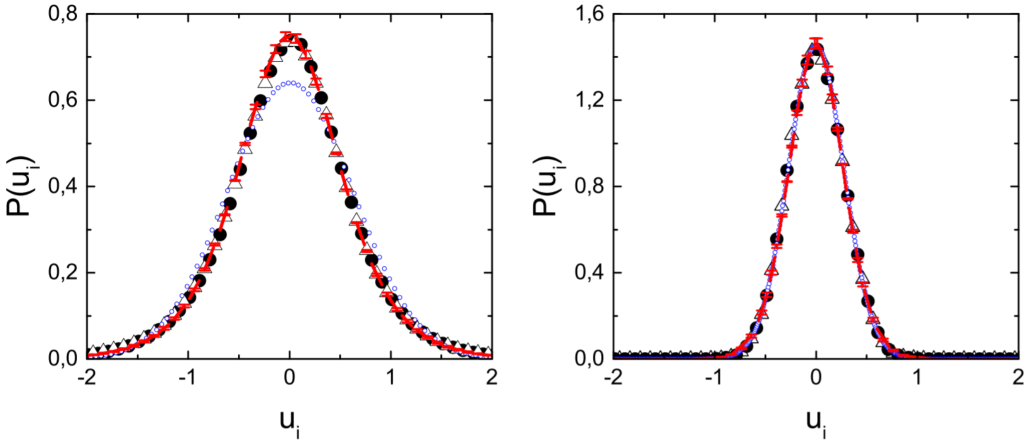

Figure 2.3: From [4], experimental verification of eq(**2.8**) with $\alpha = 1.35 \pm 0.05$(left) and $\alpha = 6.80 \pm 0.23$(right). Black circles represent the experiment, blue circles are the corresponding Gaussian approximation and the red lines are given by eq(**2.8**).

same rescaling universality also holds for systems with preserved time-reversal invariance. Indeed, the associated scattering problem is more challenging and it will require a different approach. The results presented in this section, in particular eq(**2.8**), have been experimentally tested in [4], for a 2×2 reaction matrix, by using microwave networks graphs. The latter can be considered as a physical realizations of Quantum graphs introduced by Pauling [88] since the Schrodinger equation and the telegraph equation are essentially equivalent (see [71]). In [4], the experimental setup was assembled connecting six microwave joints by coaxial cables and phase shifters. Lastly, the time reversal symmetry is broken by the presence of circulators while absorption is controlled by attenuators. In [4], they reported $\alpha = 1.35 \pm 0.05$ and $\alpha = 6.80 \pm 0.23$ (fig(**2.3**)).

2.2.1.2 Correlated channel vectors $\boldsymbol{w}_a$ and $\boldsymbol{w}_b$.

We now turn our attention to the case of correlated channel vectors. Firstly, we assume that each vector, $\boldsymbol{w}_n$, is independent from any other having a different energy level index n. Correlations then occur among its entries for the same value of n, i.e. between any pair $w_{a,n}$ and $w_{b,n}$ with $a \neq b$. Given the Gaussian nature of $\boldsymbol{w}_n$, it's sufficient to specify a correlation matrix $\mathbf{C^{-1}}$ whose entries are $\overline{w_{a,n}^* w_{b,n}} = \left(C^{-1}\right)_{ab}$. One can write down the probability density function as

$$p\left(w_{a,n}, w_{b,n}\right) \propto \exp\left(-N \begin{bmatrix} w_{a,n} \\ w_{b,n} \end{bmatrix}^\dagger \mathbf{C} \begin{bmatrix} w_{a,n} \\ w_{b,n} \end{bmatrix}\right)$$

Once again, following the uncorrelated approach above, one averages over the channel vectors and is left with a new ratio of characteristic polynomials, i.e.

$$\mathcal{R}(q,q^*) = \mathbb{E}_{GUE(N)}\left[\frac{\det\left((\lambda \mathbf{1}_N - \mathbf{H}_N)^2 + \frac{\alpha^2}{N^2}\mathbf{1}_N\right)}{\Pi_{l=1,2}\det\left((\lambda \mathbf{1}_N - \mathbf{H}_N) + \frac{i}{2N}(\hat{k} + (-1)^l\sqrt{\hat{k}^2+4\hat{s}})\mathbf{1}_N\right)}\right], \tag{2.9}$$

For simplicity of notation, we introduce:

$$\hat{k} = \mathrm{Re}\left(\frac{C_{ab}}{\det(\mathbf{C})}q^*\right)$$

$$\hat{s} = \alpha^2 - \alpha\,\mathrm{Im}\left(\frac{C_{ab}}{\det(\mathbf{C})}q^*\right) + \frac{|q|^2}{4\det(\mathbf{C})}$$

We note that we have lost the spherical symmetry as $\mathcal{R}(q,q^*)$ is now not written in terms of only $|q|$, as it was in eq(**2.6**). Additionally, a further simplification can be introduced, namely, $\frac{C_{ab}}{\det \mathbf{C}} = -\left(C^{-1}\right)_{ab}$. Then, one can easily see that taking the off-diagonal entry $C_{ab} \to 0$, eq(**2.5**) is retrieved. We now take the limit $N \to +\infty$ without rescaling the entries of $\mathbf{C}$, i.e. the latter are assumed to be of order one ($C_{i,j=a,b} = O(1)$). It is straightforward to perform the last expectation in eq(**2.9**), again using eq(**1.20**), we finally obtain:

$$\mathcal{R}(q,q^*) = \frac{1}{8(\sqrt{\hat{k}^2+4\hat{s}})\alpha}\exp\left(-\frac{1}{2}(i\hat{k}\lambda) - \pi\rho(\lambda)\left(\sqrt{\hat{k}^2+4\hat{s}}+2\alpha\right)\right)\times$$
$$\left((1-e^{4\pi\alpha\rho(\lambda)})\hat{k}^2 - \left(\sqrt{\hat{k}^2+4\tilde{s}}-2\alpha\right)^2 + e^{4\pi\alpha\rho(\lambda)}\left(\sqrt{\hat{k}^2+4\hat{s}}+2\alpha\right)^2\right) \tag{2.10}$$

The inversion of this expression, in order to recover $p(\mathbf{K}_{a,b},\mathbf{K}^*_{a,b})$, is far from trivial and can be achieved numerically. Our results for $\mathcal{R}(q,q^*)$ are plotted in figs(**2.4**,**2.5**,**2.6**). There, we consider the fixed covariance matrix

$$\mathbf{C}^{-1} = \begin{bmatrix} 2 & -i \\ i & 1 \end{bmatrix}$$

Unlike the case of uncorrelated channels, numerics reveals a slower convergence due to finite size effects, to the asymptotics $N \to +\infty$. In fact, simulations show that, as one increases the value for N, these discrepancies become less and less relevant. The higher is the value for α the more noticeable are these effects.

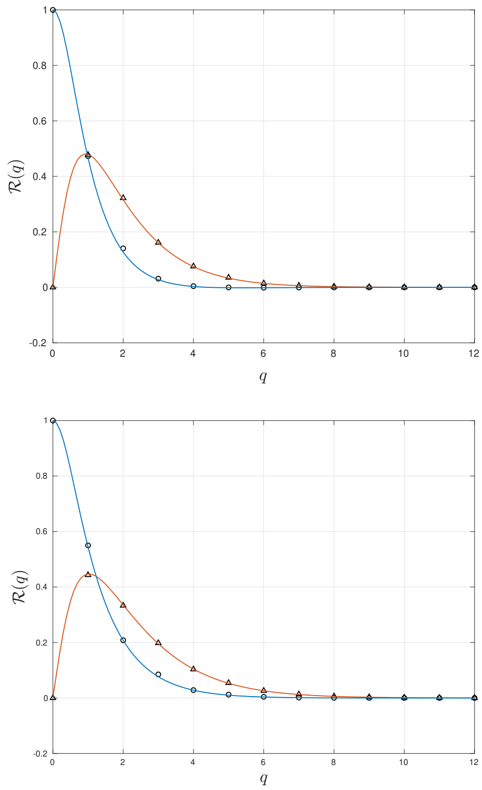

Figure 2.4: Real (blue) and imaginary (red) parts of the characteristic function eq(**2.10**) for $K_{a,b}$ in systems with broken time-reversal invariance and absorption $\alpha = 1$ with $q \in [0, 12]$ and the special choice of the channel covariance matrix, for $\lambda = 0$ (top),$\lambda = 1$ (bottom). Markers indicate numerical results involving # Samples=10000 for the matrix size N=100.

2.2.2 Systems with preserved time-reversal invariance

We now draw the random matrix $\mathbf{H}_N$ from the Gaussian Orthognal ensemble of section 1.1.1 with $\beta = 1$ and $J = 1$. Therefore, the probability density function is $dp(\mathbf{H}_N) \propto \exp(-\frac{N}{4}\operatorname{Tr}\mathbf{H}_N^2)d\mathbf{H}_N$. Within this framework, we only consider the case of uncorrelated channel vectors. Hence, the vectors $\boldsymbol{w}_n$ (and their entries) are assumed to be independent for $n \neq m$. The components are real i.i.d. centered Gaussian random variables of variance $1/N$. We introduce the average over channel vectors as $\overline{[...]} = \int\int [...] p(\boldsymbol{w}_n)p(\boldsymbol{w}_m)d\boldsymbol{w}_n d\boldsymbol{w}_m$. Again, we can only focus on the characteristic function of $\mathbf{K}_{a,b} = \operatorname{Re}\mathbf{K}_{a,b} + i\operatorname{Im}\mathbf{K}_{a,b}$. We introduce such characteristic function $\mathcal{R}(k, s)$ by replacing $q = k + is$ in eq(**2.4**) with $k, s \in \mathbb{R}$ and GOE average. We can analytically compute the expectation over the channel vectors. Since the latter is a real Gaussian integral, the result is given in terms of product of half integer power of

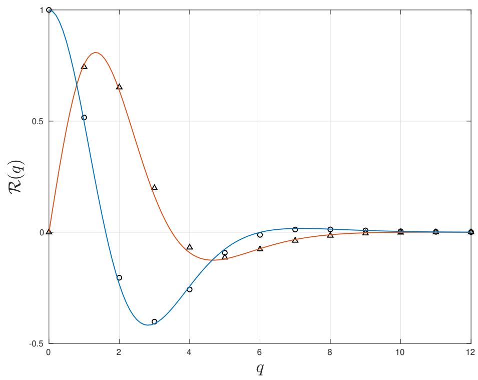

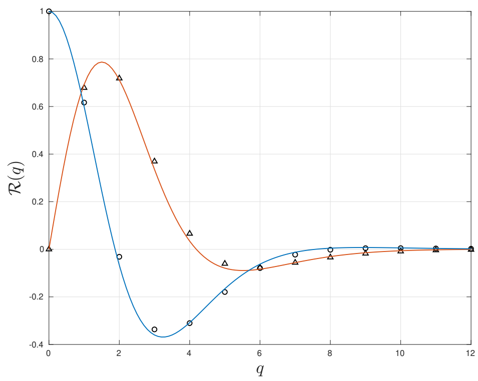

Figure 2.5: Real (blue) and imaginary (red) parts of the characteristic function eq(**2.10**) for $K_{a,b}$ in systems with broken time-reversal invariance and absorption $\alpha = 5$ with $q \in [0, 12]$ and the special choice of the channel covariance matrix, for $\lambda = 0$ (top),$\lambda = 1$ (bottom). Markers indicate numerical results involving # Samples=10000 for the matrix size N=100.

determinants, i.e.

$$\mathcal{R}(k,s) = \mathbb{E}_{GOE(N)}\left[\frac{\det\left((\lambda \mathbf{1}_N - \mathbf{H}_N)^2 + \frac{\alpha^2}{N^2}\mathbf{1}_N\right)}{\Pi_{l=1,2}\det^{1/2}\left((\lambda \mathbf{1}_N - \mathbf{H}_N)^2 + (-1)^l i\frac{k}{N}(\lambda \mathbf{1}_N - \mathbf{H}_N) + \frac{\omega_l^2}{N^2}\mathbf{1}_N\right)}\right], \tag{2.11}$$

with $\omega_1^2 = \alpha^2 - i\alpha s$ and $\omega_2^2 = \alpha^2 + i\alpha s$. The evaluation of the ensemble average over the $GOE(N)$ matrices can not be performed similarly to the case of broken time-reversal symmetry. The source of difficulties stems from the half-integer powers in the denominator. An attempt is presented in [35]. A Supersymmetry approach with finite N gives an integral representation, over 4×4 positive definite matrices, for eq(**2.11**) (see appendix B.5). However the evaluation by saddle point for $N \gg 1$ is a hard task and requires higher order expansions. Even neglecting correlations between the entries of $\boldsymbol{w}_n$ does not help to get the rotational invariance with respect to the complex variable

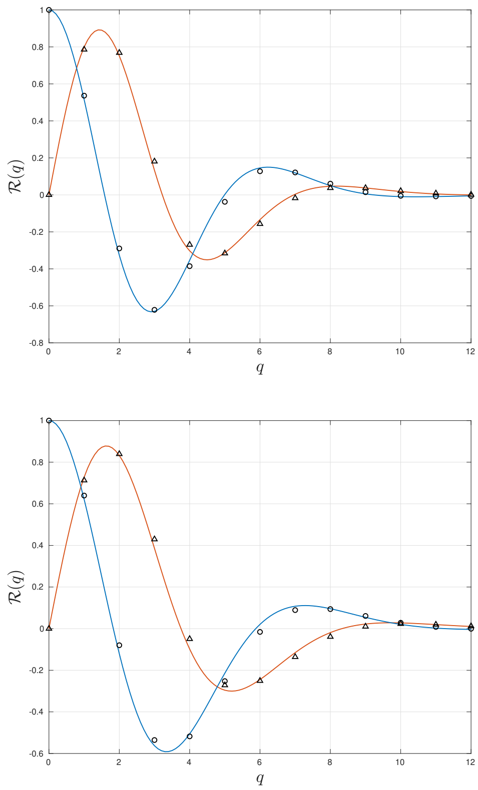

Figure 2.6: Real (blue) and imaginary (red) parts of the characteristic function Eq.(2.10) for $K_{a,b}$ in systems with broken time-reversal invariance and absorption $\alpha = 10$ with $q \in [0, 12]$ and the special choice of the channel covariance matrix, for $\lambda = 0$ (top),$\lambda = 1$ (bottom). Markers indicate numerical results involving # Samples=10000 for the matrix size N=100.

q, in contrast to $GUE(N)$ case. Indeed, $\mathcal{R}(k, s)$ cannot be written as a function of $|q| = \sqrt{k^2 + s^2}$. All these new features prevent us from obtaining the joint probability function and the joint characteristic function for the pair $(\mathbf{K}_{a,b}, \mathbf{K}^*_{a,b})$. Therefore, we abandon the idea of recovering the joint probability density and separately consider:

$$\mathcal{R}(s, 0) = \mathbb{E}_{GOE(N)}[\overline{\exp(is \operatorname{Im} \mathbf{K}_{a,b})}], \quad \mathcal{R}(0, k) = \mathbb{E}_{GOE(N)}[\overline{\exp(ik \operatorname{Re} \mathbf{K}_{a,b})}] \quad (2.12)$$

As the calculations for each of the latter requires to keep track of several terms, we only consider the spectral centre, i.e. $\lambda = 0$. This is sufficient for recovering the results for the entire spectrum ($\lambda \neq 0$) as one re-scales the absorption and the components of q, similarly to the $GUE(N)$ calculations, with η. This is a again a direct consequence of the universality. Using the results presented in section 1.1.1.7 and [35], we can summarise our calculations as follows (see appendix B.4). Firstly, we define the functions

$$C(q_1,q_2,\alpha) = q_2^2 - 4q_2^3 + 4q_1^3(4q_2-1) + 2q_1q_2(1-4q_2+8q_2^2) + q_1^2(1-8q_2+44q_2^2) \quad (2.13)$$

$$-4(q_1+q_2)\left(-q_2^3 + q_1^2q_2(4q_2-5) + q_1q_2^2(4q_2-5) + q_1^3(4q_2-1)\right)\alpha^2 + 16q_1^2q_2^2(q_1+q_2)^2\alpha^4$$

and

$$D(q_1,q_2,\alpha) = C(q_1,q_2,\alpha) - 8(q_1+q_2)^2\alpha^2\left(q_1+q_2-2q_1q_2+4q_1q_2(q_1+q_2)\alpha^2\right) \quad (2.14)$$

Then, in the limit $N\to\infty$, the characteristic function of the real and imaginary parts of $\mathbf{K}_{ab}$ for $\lambda = 0$ are

$$\lim_{N\to\infty} \mathbb{E}_{GOE(N)}\left[\overline{e^{ik\,\mathrm{Re}\,\mathbf{K}_{a,b}}}\right] = -\int_{\mathbb{R}_+} dq_1 \int_{\mathbb{R}_+} dq_1 dq_2 |q_1-q_2| I_0\left(k\sqrt{\frac{k^2}{4}+\alpha^2}(q_1-q_2)\right)$$
$$\times\; e^{-\frac{1}{4}(q_1+q_2)\left((q_1q_2)^{-1}+2(k^2+2\alpha^2)\right)}\,\frac{D(q_1,q_2,\alpha)\sinh(2\alpha)-2\alpha C(q_1,q_2,\alpha)\cosh(2\alpha)}{512\sqrt{\pi}q_1^3q_2^3(q_1+q_2)^{5/2}\alpha^3} \quad (2.15)$$

and

$$\lim_{N\to\infty} \mathbb{E}_{GOE(N)}\left[\overline{e^{is\,\mathrm{Im}\,\mathbf{K}_{a,b}}}\right] = -\int_{\mathbb{R}_+} dq_1 \int_{\mathbb{R}_+} dq_2 |q_1-q_2| J_0\Big(s\alpha(q_1-q_2)\Big)$$
$$\times\; e^{-\frac{1}{4}(q_1+q_2)\left((q_1q_2)^{-1}+4\alpha^2\right)}\,\frac{D(q_1,q_2,\alpha)\sinh(2\alpha)-2\alpha C(q_1,q_2,\alpha)\cosh(2\alpha)}{512\sqrt{\pi}q_1^3q_2^3(q_1+q_2)^{5/2}\alpha^3} \quad (2.16)$$

with $I_0(x)$ and $J_0(x)$ being Bessel and modified Bessel functions, respectively. In principle one can obtain the probability density function via the Fourier transform of the quantities above. However, as previously reported, these can only be approached numerically. A possible simplification can be made for the imaginary part. We can introduce the new variable $u = \alpha^{-1}\,\mathrm{Im}\,K_{ab}$. From the definition of Bessel function and denoting the integrand in eq(**2.16**) for $s = 0$ as $f(q_1,q_2;\alpha)$ one observes that the probability density function of u, can be written as

$$p(u) = \int_0^1\int_0^1 dp dt f\Big(\frac{|u|}{(2pt)}(t+1), \frac{|u|}{(2pt)}(1-t);\alpha\Big)\frac{|u|}{p^2t^2\sqrt{1-p^2}} \quad (2.17)$$

A similar formula for $\mathrm{Re}\,K_{ab}$ cannot be achieved due to the presence of $I_0(x)$ in eq(**2.15**). We can now recover the results for the full spectrum, i.e. $\lambda \in (-2,2)$, for characteristic functions $\mathbb{E}_{GOE(N)}\left[\overline{e^{is\,\mathrm{Im}\,\mathbf{K}_{a,b}}}\right]$ and $\mathbb{E}_{GOE(N)}\left[\overline{e^{ik\,\mathrm{Re}\,\mathbf{K}_{a,b}}}\right]$ from the case $\lambda = 0$ by rescalings $\alpha \to \eta\alpha$, $s \to \eta s$ and $k \to \eta k$. Hence,

$$\lim_{N\to\infty} \mathbb{E}_{GOE(N)}\left[\overline{e^{is\,\mathrm{Im}\,\mathbf{K}_{a,b}}}\right](\alpha,\lambda) = \lim_{N\to\infty} \mathbb{E}_{GOE(N)}\left[\overline{e^{i\eta s\,\mathrm{Im}\,\mathbf{K}_{a,b}}}\right](\eta\alpha, 0) \quad (2.18)$$

and

$$\lim_{N\to\infty} \mathbb{E}_{GOE(N)}\left[\overline{e^{ik\,\mathrm{Re}\,\mathbf{K}_{a,b}}}\right](\alpha,\lambda) = \lim_{N\to\infty} \mathbb{E}_{GOE(N)}\left[\overline{e^{i\eta k\,\mathrm{Re}\,\mathbf{K}_{a,b}}}\right](\eta\alpha,0) \tag{2.19}$$

This re-scale also applies to eq(**2.17**). If the latter is written as $p(\cdot;\alpha,\lambda)$ then, for $\lambda \neq 0$ and after rescaling $\tilde{u} = \eta^2 u$, one has $p(\tilde{u};\varepsilon,\lambda) = p(\tilde{u};\eta\alpha,0)$. Simulations show good agreements between eq(**2.16**) and eq(**2.11**) (see figs(**2.7**,**2.8**)). The case $\lambda \neq 0$, achieved by rescaling, is justified in [35] and in the appendix B.5. We can test the probability density function of $\mathrm{Im}\,\mathbf{K}_{a,b}$. For $\alpha \gg 1$, the probability density of $\mathrm{Im}\,\mathbf{K}_{a,b}$ approaches a Gaussian distribution. So it is sufficient to retrieve its variance. This secondary task turns out to be extremely simple, despite eq(**2.16**) and it is summarized in appendix B.6. We finally show this in fig(**2.9**) for $\lambda = 0$ and $\alpha = 50, 100$. We can push our analysis even forward. Clearly, we cannot recover the joint probability density function of $\mathrm{Re}\,\mathbf{K}_{a,b}$ and $\mathrm{Im}\,\mathbf{K}_{a,b}$. However, with the information so far acquired, we can infer the behaviour of the cross-correlations between the real and imaginary components of $\mathbf{K}_{ab}$ with the help of eq(24) in [83]. We report here the latter:

$$\mathbb{E}_{GOE}\left[|\mathbf{K}_{ab}|^4\right] = \frac{(\pi\rho(\lambda))^4}{\alpha^4}\left(5+28\alpha+7\alpha^2\right) - \frac{(\pi\rho(\lambda))^4}{\alpha^4}e^{-2\alpha}\left(5+2\alpha+\alpha^2\right) + \\ + \frac{(\pi\rho(\lambda))^4}{\alpha^4}e^{-\alpha}E_1(\alpha)(10+10\alpha+3\alpha^2+\alpha^3) + \frac{(\pi\rho(\lambda))^4}{\alpha^4}e^{\alpha}E_1(\alpha)(-10+10\alpha-3\alpha^2+\alpha^3) \tag{2.20}$$

with $E_1(x) = \int_x^{+\infty} \frac{e^{-s}}{s}ds$. Hence we can investigate the quantity (fig(**2.10**)):

$$\tau(\alpha) = \frac{\mathbb{E}_{GOE}\left[\overline{(\mathrm{Im}\,K_{a,b}\,\mathrm{Re}\,K_{a,b})^2}\right]}{\mathbb{E}_{GOE}\left[\overline{(\mathrm{Im}\,K_{a,b})^2}\right]\mathbb{E}_{GOE}\left[\overline{(\mathrm{Re}\,K_{a,b})^2}\right]} - 1, \tag{2.21}$$

The quantities at the denominator, $\mathbb{E}_{GOE}\left[\overline{(\mathrm{Im}\,K_{a,b})^2}\right]$ and $\mathbb{E}_{GOE}\left[\overline{(\mathrm{Re}\,K_{a,b})^2}\right]$ are known and reported in appendix B.6. As α grows the correlation between the real and imaginary parts decreases. One can also see that such correlation is stronger for small λ.

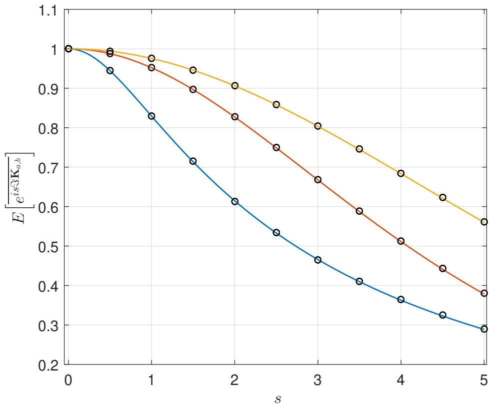

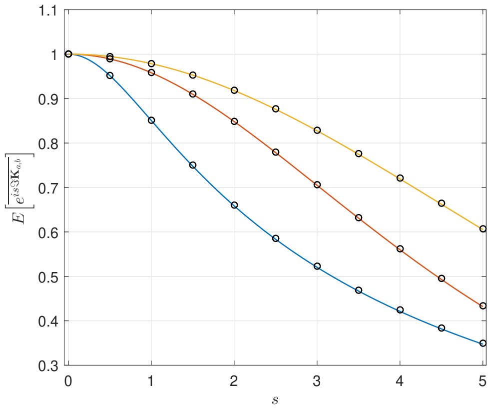

Figure 2.7: Characteristic function of Im $K_{a,b}$ as given by eq(**2.16**) vs. numerical simulations for systems with preserved time-reversal invariance at different level of absorption: $\alpha = 1(blue), 5(red), 10(yellow)$ (# Samples=80000, N=100, circular markers) for $\lambda = 0(\text{Top}), 1(\text{Bottom})$.

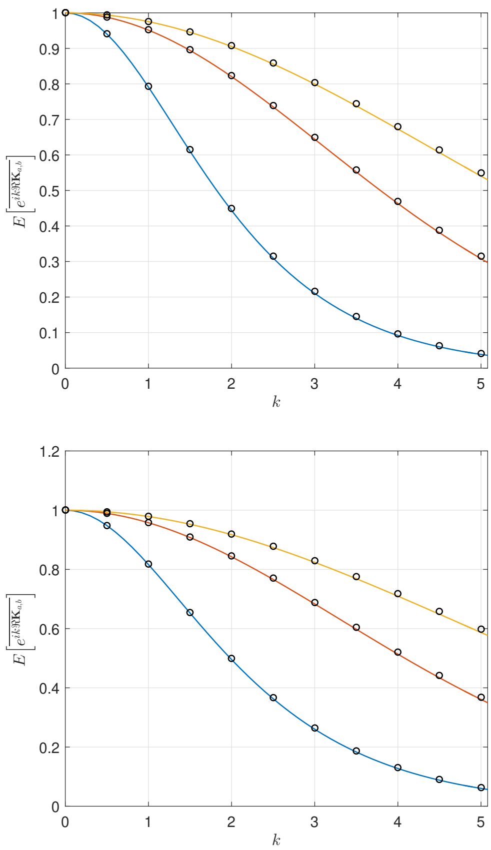

Figure 2.8: Characteristic function for $\mathrm{Re}\, K_{a,b}$ as given by eq(**2.15**) vs. numerical simulations for systems with preserved time-reversal invariance at different level of absorption: $\alpha = 1(blue), 5(red), 10(yellow)$ (# Samples=50000, $N = 300$, circular markers) for $\lambda = 0$ (Top), 1 (Bottom).

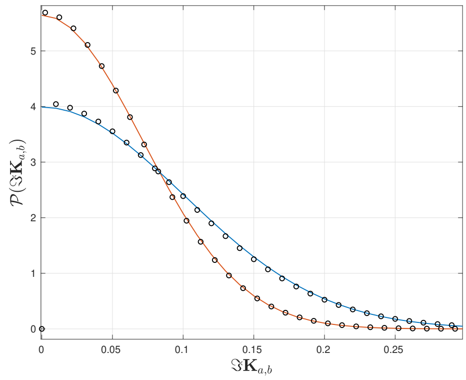

Figure 2.9: Comparison between the probability density of $\operatorname{Im} K_{a,b}$ (Eq(**2.17**)) for large absorption $\alpha = 50(blue), 100(red)$, and the Gaussian distribution $\mathcal{N}(0, 1/(2\alpha))$ (circular markers) ($\lambda = 0$).

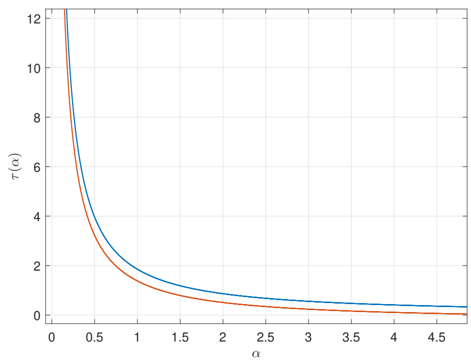

Figure 2.10: Behaviour of $\tau(\alpha)$ from eq(**2.21**) for $\lambda = 0(blue), 1(red)$

Chapter 3

Beyond May-Wigner Instability

3.1 Evolution of Ecosystems

For many years the idea that Nature would operate as an infinitely precise entity was predominant within the ecological communities. This perspective has produced remarkable results and has focused the attention on the first order interactions (and correlations) among species ([89, 90]). This intuitive idea of fine tuning behaviour finds its root in the second half of the twentieth century and since then it has been challenged. In fact, the ecological community has gradually abandoned the aforementioned idea of Nature being "infinitely" precise toward dynamical models of resilience. While the works mentioned above clearly remain a milestones in understanding of our world, they are clearly insufficient if one wants to investigate the dynamics behaviour of such systems. We will show later in this chapter that the investigations concerning the dynamics become more meaningful upon inclusion of the non-linear and multi-species interaction into account. To the best author's knowledge, such point of view is still at a preliminary stage of development and its consequences are not yet fully understood. The author believes that such inclusion would be necessary to tackle the new challenges of our time. We are experiencing multiple fast evolving phenomena in our environment. The most evident is climate change. The latter, due to human industrial activities, has provoked an alteration on the seasonal temperature fluctuations increasing the mean temperature by a few Celsius degrees. The second main ecological challenge is the loss of ecological diversity. The latter corresponds to the disappearance of species in our ecosystems. Due to several factors, many species have disappeared or are in danger of extinction. This process is occurring at a rate never experienced before since the late stages of the fossil era.

3.1.1 Linear Analysis

The first attempt to mathematically investigate the stability of biological systems was undertaken by Robert May in 1972 with his seminal and highly influential paper "*Will a large complex system be stable?*" ([16], see also [91]). He considered the linear stability of ecosystems, around a fixed point placed at the origin, i.e.

$$\frac{d\boldsymbol{x}}{dt} = -\mu\boldsymbol{x} + \frac{\sigma}{\sqrt{N}}\boldsymbol{\Xi x} + o(|\boldsymbol{x}^2|), \tag{3.1}$$

where the N dimensional vector $\boldsymbol{x} = (x_1, \dots, x_N)^T$ contains the state of each species, μ is the feedback relaxation parameter. This term is an inner feedback mechanism, i.e. as $\sigma = 0$ the system evolves toward the origin with a characteristic timescale μ^{-1}. In what follows we assume, without loss of generality, $\mu = 1$. The parameter σ is a positive constant measuring the strength of the interaction among species. The non-null entries of the connectivity matrix $\boldsymbol{\Xi} = (\xi_{nm})_{n,m}$, of connectance c, are i.i.d. random variables with zero mean and unit variance[1]. The factor $1/\sqrt{N}$ has been introduced to ensure that the first and second term are of the same order in a typical realization. Additionally, the assumptions on higher moments are also required albeit not explicitly mentioned in May's original paper to reach the conclusions below. According to the signs of the entries, the interaction has a mutualistic effect if ξ_{nm} and ξ_{mn} are positive. Conversely, if the latter are both negative the effect is competitive. Lastly, there is a parasitic effect if ξ_{nm} and ξ_{mn} have opposite signs. Clearly, this model is only qualitative as it does not take into account such meaningful and necessary ecological super-structures as food-web, hierarchies, trophic levels [92], modularities[93] and the choice of an equilibrium point [94][95] to cite a few. Despite these assumptions, May's work validated and corroborated the idea observed by early numerical simulations that ecological systems, randomly assembled, abruptly become unstable when either the connectivity c or the size of the system N reach a certain threshold. This is a consequence of the circular law, at that time accepted although not fully proven. In more details, the system is stable (unstable) almost surely if σ is greater (smaller) than $\frac{1}{Nc}$. This is a sharp transition which manifests itself in the limit $N \to +\infty$.

May also noticed that such large systems can be divided into classes. Given two systems S_1 and S_2 with (σ_1, c_1) and (σ_2, c_2) respectively, if $\sigma_1^2 c_1 \simeq \sigma_2^2 c_2$ then S_1 and S_2 belong to the same class. Namely, a system with a large number of interactions

[1] The connectance is the mean number of non-null terms in each column of the matrix $\boldsymbol{\Xi}$, it takes into account the sparsity of the interactions among species.

occurring with small strength qualitatively behaves as, the opposite, a system with few interactions and high strength. Some of these un-physical features have been recently mitigated in [96] and investigated for more general models ([97, 98, 99] and [100]). We can now move toward more complicated models.

3.1.2 Beyond the Linear Approximation: Previous Models

In order to shed light on the complexity of more general randomly assembled systems one can exploit the Kac-Rice formula in eq(**1.44**). This has been investigated in several contexts. In particular we want to mention, in the framework of neural network dynamics, the work of Wainrib et al. [101]. In this context the components of $\boldsymbol{x}$ are the firing rate of neurons and the interaction term with the community matrix in eq(**3.1**) is replaced by

$$\boldsymbol{f}_i = \sum_{j=1}^{N} J_{ij} S(x_j) \tag{3.2}$$

where $S(x)$ is an odd sigmoid function (synaptic nonlinearity) and J_{ij} is synaptic connectivity. The latter is chosen as i.i.d. centered Gaussian variables with variance σ^2. Similarly to the linear analysis, the fixed point at the origin is stable whenever $\sigma > 1$ and no other fixed points are present in this case. For $\sigma \to 1^+$, the authors of [101] computed the mean number of fixed points as

$$\mathcal{N}(\mathbb{R}^N) = e^{N(\sigma-1)^2}(1 + o(1))$$

Most of those points are located within a ball centered around original equilibrium at the origin, with the radius shrinking to zero as $\sigma \to 1^+$. Remarkably, the expression in the exponent above, called topological complexity, is equal to the dynamical complexity, i.e. the Lyapunov exponent $\lambda \sim (\sigma - 1)^2$. This is also confirmed for $\sigma \to +\infty$, since both the complexities scale as $\log(\sigma)$ for sufficiently large N. This behaviour poses a natural question to investigate, whether it is shared by other random models. Further generalizations were investigated by [50] and [5]. Again the linear interaction term in eq(**3.1**) is replaced by an isotropic, centered and homogeneous random Gaussian field

$$\boldsymbol{f}_i(\boldsymbol{x}) = -\frac{\partial V}{\partial x_i}(\boldsymbol{x}) + \frac{1}{\sqrt{N}} \sum_{j=1}^{N} \frac{\partial A_{ij}}{\partial x_j}(\boldsymbol{x}) \tag{3.3}$$

with $\mathbb{E}[V(\boldsymbol{x})V(\boldsymbol{y})] = v^2\Gamma_V(|\boldsymbol{x}-\boldsymbol{y}|^2)$, $\mathbb{E}[A_{ij}(\boldsymbol{x})A_{nm}(\boldsymbol{y})] = a^2\Gamma_A(|\boldsymbol{x}-\boldsymbol{y}|^2)(\delta_{in}\delta_{jm} - \delta_{im}\delta_{jn})$ and $\Gamma''_{V,A}(0) = 1$. Considering v and a to be the "strength" of the gradient

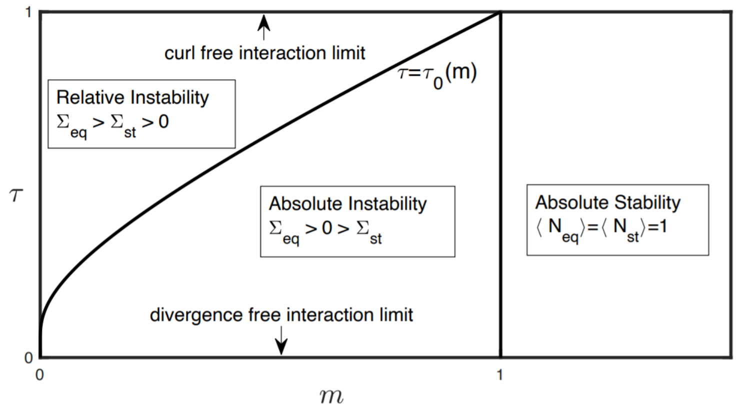

Figure 3.1: From [5], nature of the fixed points as function of μ, τ for eq(**3.4**).

and solenoidal parts of $\boldsymbol{f}(\boldsymbol{x})$, it is useful to introduce the parameters $\tau = \frac{v^2}{a^2+v^2}$ and $m = \frac{\mu}{2\sqrt{N}\sqrt{a^2+v^2}}$. With these assumptions, the first moment (the mean) of the number of fixed points is given by

$$\mathcal{N}_{eq}(\mathbb{R}^N) = \begin{cases} \gamma(\tau)e^{NL(m)} \text{ for } 0 < m < 1, \\ 1 \text{ for } m > 1 \\ \gamma(\tau)e^{k^2}\int_{-\infty}^{+\infty} e^{-t^2/2}\rho^{(r)}_{edge}\big(c(\tau)t + k\frac{\gamma(\tau)}{\sqrt{2}}\big)dt \text{ for } m \to 1 + \frac{k}{\sqrt{N}}, \end{cases} \tag{3.4}$$

with $k \in \mathbb{R}$,$\gamma(\tau) = \sqrt{\frac{2(1+\tau)}{1-\tau}}$, $c(\tau) = \sqrt{\frac{\tau}{1-\tau}}$ and $L(m) = \frac{(m^2-1)}{2} - \log m > 0$. The different regimes trace back to the existence of bulk and edge regimes for the elliptic law, similarly to eq(**1.76**). Very recently, the work [5] described the nature of the fixed points. Indicating with $\mathcal{N}_{st}(\mathbb{R}^N) \propto e^{N\Sigma_{st}}$ the mean number of stable fixed points, the complexity function, Σ_{st}, changes its sign across the line given in the parameter space by $\tau_0(m) = -\frac{1}{2}\frac{(1-m)^2}{1-m+\log m}$ (see fig(**3.1**)). In more details, for systems whose dynamics is governed by the gradient of a stationary isotropic Gaussian Lyapunov function $V(\boldsymbol{x})$, the variance of such function triggers the exponential growth of the number of local stable points. The introduction of solenoidal components of the field reshapes the phase portrait: most of the (exponentially many) critical points become unstable [5]. A fine tuning of the parameters reveals different phase transitions since the phase space landscape abruptly changes from exponentially many to a unique fixed point (topological trivialization). This results goes beyond the local analysis of May, it describes a *global* topological picture. The point $\boldsymbol{x} = \boldsymbol{0}$ is no longer a special point in such a model as $\boldsymbol{f}(\boldsymbol{0}) \neq \boldsymbol{0}$ almost surely. We now want to investigate where most of these points are located. To do so, we start from the Kac-Rice formula, namely, the mean number of fixed points with a ball of radius r centered at the origin (see eq(**1.50**)),

$$\mathcal{N}_{eq}(r) = \int_{|\boldsymbol{x}|<r} d\boldsymbol{x}\mathbb{E}[\delta^{(N)}(-\mu\boldsymbol{x} + \boldsymbol{f}(\boldsymbol{x}))|\det(-\mu\mathbf{1}_N + \boldsymbol{J}(\boldsymbol{x}))|] \tag{3.5}$$

For simplicity we indicate the variance of $\boldsymbol{f}$ as $\mathbb{E}[\boldsymbol{f}(\boldsymbol{x})\boldsymbol{f}^T(\boldsymbol{x})] = \sigma^2\mathbf{1}_N$ where $\sigma^2 = 2v^2|\Gamma'_V(0)| + 2a^2|\Gamma'_A(0)|\frac{N-1}{N}$. So we can isolate the dependency on $\boldsymbol{x}$ in the integrand above: $\mathcal{N}_{eq}(r) = \frac{1}{(2\pi\sigma^2)^{N/2}}\int_{|\boldsymbol{x}|<r} d\boldsymbol{x}e^{-\frac{\mu^2}{2\sigma^2}|\boldsymbol{x}|^2}\mathbb{E}[|\det(-\mu\mathbf{1}_N + \boldsymbol{J})|]$. We can introduce a spherical change of variables and readily integrate over the ball of radius r obtaining

$$\mathcal{N}_{eq}(r) = \left(1 - \frac{\Gamma\left(\frac{N}{2}, \frac{r^2\mu^2}{2\sigma^2}\right)}{\Gamma\left(\frac{N}{2}\right)}\right)\mathcal{N}_{eq}(\mathbb{R}^N) \tag{3.6}$$

The presence of the incomplete gamma function reflects a sharp change in the radial distribution of fixed points in $\mathbb{R}^N$. In fact, the radial distribution of fixed points is proportional to $r^{N-1}e^{-\frac{\mu^2}{2\sigma^2}r^2}$. This means that the fixed points are mainly distributed around the radius $r^* = \sqrt{N}\frac{\sigma}{\mu}$. Close to the origin (again $N \gg 1$) we have:

$$\mathcal{N}_{eq}(\varepsilon) = \mathcal{N}_{eq}(\mathbb{R}^N)\frac{\mu^N}{\sigma^N}\varepsilon^N\left(\frac{2}{2^{N/2}\Gamma(N/2)}\frac{1}{\varepsilon} + O(\varepsilon)\right) \tag{3.7}$$

Given the success of these models we now want to move to infer some characteristic of the dynamics by using the idea of the topological complexity.

3.1.3 Beyond the Linear Approximation: Full Taylor Expansion

In the last presented models there is a sort of universality. The tuning of the parameters reveals a *topological trivialization*, i.e. the system exhibits *globally* either a unique or exponentially many fixed points. We will question such a universality in section 3.1.5. However, we now want to investigate the dynamics by the topological complexity. The dynamics is likely to differ from model to model. The initial May's linear model is clearly unfeasible to this purpose as its analysis loses of significance once we leave a small neighbourhood of the origin. To shed light on this we include nonlinearities through higher-order interactions in eq(**3.1**). In this case $\mathbf{f}(\boldsymbol{x}) := \frac{1}{\sqrt{N}}\boldsymbol{\varphi}(\boldsymbol{x})$ replaces the linear interacting terms in eq(**3.1**) ([2]):

$$\varphi_n(\boldsymbol{x}) = \sum_{k=1}^{\infty}\sigma_k\sum_{i_1,\ldots,i_k=1}^{N}\xi_{n,i_1,\ldots,i_k}x_{i_1}\cdots x_{i_k} \tag{3.8}$$

The terms $\sigma_k > 0$ are positive constants quantifying the strength of the k-order interactions. The random $\xi_\bullet$ are centered i.i.d. Gaussian variables with unit variance, i.e.

$$\mathbb{E}[\xi_{n,i_1,\dots,i_k}] = 0 \tag{3.9}$$

$$\mathbb{E}[\xi_{n,i_1,\dots,i_k}\xi_{m,j_1,\dots,j_\ell}] = \delta_{nm}\delta_{k\ell}\delta_{i_1j_1}\cdots\delta_{i_kj_k}. \tag{3.10}$$

Each term in the expansion is clearly independently distributed. The above equalities define the following spatial covariance structure for the random vector field $\boldsymbol{\varphi}$:

$$\mathbb{E}[\varphi_n(\boldsymbol{x})] = 0, \qquad \mathbb{E}[\varphi_n(\boldsymbol{x})\varphi_m(\boldsymbol{y})] = \delta_{nm}C(\boldsymbol{x}^T\boldsymbol{y}) \tag{3.11}$$

with the (scalar) correlation function given by

$$C(\boldsymbol{x}^T\boldsymbol{y}) = \sum_{k=1}^{\infty}\sigma_k^2(\boldsymbol{x}^T\boldsymbol{y})^k. \tag{3.12}$$

This is completely different from the models above [50, 5] as we have lost the statistical invariance by spatial translations. Moreover, each $\varphi_n(\boldsymbol{x})$ is a multivariate Kac polynomial. Therefore it inherits the following properties:

- if we consider $k = 1$ in eq(**3.8**) then $\boldsymbol{\varphi}(\boldsymbol{x}) \approx \sigma_1\boldsymbol{J}\boldsymbol{x}$. Namely, we recover the original linear model. To address the global behaviour we need to include all the terms of the sequence. Therefore, for some choice of σ_k, we might need to define the convergence radius of C, R. We will also include the case of truncated summation with a cut off parameter Ω in the sum of eq(**3.12**).

- The field $\boldsymbol{\varphi}(\boldsymbol{x})$ is statistically bi-rotational invariant, since the functions in eq(**3.11**) are invariant under the transformation $\boldsymbol{\varphi}(\boldsymbol{x}) \mapsto \boldsymbol{V}\boldsymbol{\varphi}(\boldsymbol{U}\boldsymbol{x})$ for any rotation $\boldsymbol{U}, \boldsymbol{V} \in Orth(N)$. As we introduce the feedback mechanism term this symmetry is not preserved and breaks down to the ordinary rotational symmetry, with $\boldsymbol{V} = \boldsymbol{U}$.

The Gaussian hypothesis is merely introduced for the tractability as any moment simply depends on powers of the mean and variance. Despite this, we will show that major considerations will qualitatively hold for more general models. We know that when $\sigma_1 < \mu$ then the origin is locally stable. So clearly we expect the existence of a basin of attraction for it. Conversely, as the origin become unstable, i.e. the system crosses in the parameter space the so called 'tipping point' (see [102, 103]), the trajectories might become chaotic and have extreme sensitivity to initial conditions.

Similarly to eq(**3.6**), to characterize such basin of attraction qualitatively, we will compute the radial distribution of the mean number of fixed points. In this regard, we start by observing that the mean number of fixed points contained in a volume $D \subseteq \mathbb{R}^N$ can be written, introducing its density $\rho_\mu(\boldsymbol{x})$, as

$$\mathcal{N}(D) = \int_D d\boldsymbol{x}\, \rho_\mu(\boldsymbol{x}). \tag{3.13}$$

This time we use the form in eq(**1.53**) for the density of $\mathcal{N}_\mu$, i.e.

$$\rho_\mu(\boldsymbol{x}) = \int_{\mathbb{R}^{N\times N}} d\boldsymbol{M}\, p(\mu\sqrt{N}\boldsymbol{x}, \boldsymbol{M})|\det(\boldsymbol{M} - \mu\sqrt{N}\boldsymbol{1}_N)|, \tag{3.14}$$

The function $p(\boldsymbol{v}, \boldsymbol{M})$ is the joint (Gaussian) probability density function for $\boldsymbol{v} = \boldsymbol{\varphi}(\boldsymbol{x})$ and its gradient $\boldsymbol{M} = \nabla\boldsymbol{\varphi}(\boldsymbol{x})$ (see appendix C.1). We notice that the origin is always a fixed point of the dynamics. Excluding the latter, which contributes as a Dirac delta function with unit mass, and obtaining an explicit form for $\rho_\mu(\boldsymbol{x})$ (see below), eventually leads to

$$\rho_\mu(\boldsymbol{x} \neq 0) = \frac{1}{(2\pi)^{N/2}}\left(\frac{\Delta}{CC'}\right)^{\frac{1}{2}}\left(\frac{C'}{C}\right)^{\frac{N}{2}} e^{-N\mu^2\boldsymbol{x}^T\boldsymbol{x}/2C}\mathbb{E}_{\text{GinOE}}\left[|\det(\boldsymbol{\Xi} - \mu\sqrt{N}\boldsymbol{D})|\right], \tag{3.15}$$

where we imply $C = C(\boldsymbol{x}^T\boldsymbol{x})$ (similarly for its derivative),

$$\Delta = CC' + \left(CC'' - (C')^2\right)\boldsymbol{x}^T\boldsymbol{x} \tag{3.16}$$

and

$$\boldsymbol{D} = \text{diag}\left(\sqrt{\frac{C}{\Delta}}\left(1 - \frac{C'}{C}\boldsymbol{x}^T\boldsymbol{x}\right), \sqrt{\frac{1}{C'}}, \ldots, \sqrt{\frac{1}{C'}}\right) \tag{3.17}$$

is a diagonal matrix with two distinct eigenvalues. There are two considerations to bear in mind. The first one is the fact that the bi-rotational invariance of $\boldsymbol{\varphi}(\boldsymbol{x})$ is responsible for the rotational invariance of eq(**3.15**) as it is a scalar function of $r^2 = \boldsymbol{x}^T\boldsymbol{x}$. The second consideration is that $\mathbb{E}_{\text{GinOE}}[...]$ is taken over the realizations of $\boldsymbol{\Xi}$ whose entries are i.i.d. standard real mean-zero Gaussian variables. Therefore we need to compute the expectation of the absolute value of the characteristic polynomial of Ginibre matrices perturbed by a rank-one term [6]. For finite N, we can use the formula in eq(**1.76**). However, we are interested, in line with the results above, in large size systems. Before giving the final form of $\rho_\mu(\boldsymbol{x} \neq 0)$, we need to recall some properties of the correlation function $C(r^2)$. One can easily see that $C'(r^2)$ and $C(r^2)/r^2$ are continuous and strictly monotonically increasing for $0 < r < R$. For $r \to 0^+$ and $r \to R$, they tend to $\sigma_1^2 > 0$ and infinity, respectively. On the interval $0 < r < R$, the same hypothesis of continuity and monotonicity hold for

$$C'(r^2)r^2/C(r^2) \quad \text{and} \quad C'(r^2) - C(r^2)/r^2. \tag{3.18}$$

So we are ready to introduce two characteristic radii $r_\pm(\mu) \geq 0$. We will further assume that $r_\pm(\mu)$ are set to zero if $\mu \leq \sigma_1$. Conversely, for $\mu > \sigma_1$, the two radii are identified as the solutions of $C'(r_-^2) = \mu^2$ and $C(r_+^2) = \mu^2 r_+^2$, respectively. One can show from the properties above that $r_\pm(\mu)$ are uniquely defined, continuous and monotonically increasing functions of μ. Moreover, $0 < r_-(\mu) < r_+(\mu)$ for all $\mu > \sigma_1$; $r_\pm(\mu) \to 0$ for $\mu \to \sigma_1^+$ and $r_\pm(\mu) \to R$ for $\mu \to \infty$. We can now provide the final spherical form of the mean density of fixed points:

$$\widehat{\rho}_\mu(r) := \frac{2\pi^{N/2} r^{N-1}}{\Gamma(N/2)} \rho_\mu(r). \tag{3.19}$$

The ratio in the r.h.s. represents the surface of the hyper-sphere of dimension $N - 1$ of radius r. Once we plug the results of eqs(**1.77**,**1.78**) in eq(**3.15**), we have:

$$\widehat{\rho}_\mu(r) = \sqrt{\frac{N}{\pi}} \frac{h_{\mathrm{I}}(r^2)}{r} e^{+\frac{N}{2} L_{\mathrm{I}}(r^2)} (1 + o(1)) \tag{3.20}$$

for $0 < r < r_-$ and

$$\widehat{\rho}_\mu(r) = \sqrt{\frac{N}{\pi}} \frac{h_{\mathrm{II}}(r^2)}{r} e^{+\frac{N}{2} L_{\mathrm{II}}(r^2)} (1 + o(1)) \tag{3.21}$$

for $r_- < r < R$, where

$$h_{\mathrm{I}}(r^2) = \tfrac{C'}{C} r^2 - 1, \tag{3.22}$$

$$h_{\mathrm{II}}(r^2) = \left(\tfrac{2\Delta}{CC'}\right)^{\frac{1}{2}} \left(1 + \mu^2 \left(\tfrac{C}{\Delta} h_{\mathrm{I}}^2(r^2) - \tfrac{1}{C'}\right)\right)^{\frac{1}{2}}. \tag{3.23}$$

and

$$L_{\mathrm{I}}(r^2) = -f\left(\tfrac{\mu^2 r^2}{C}\right), \quad L_{\mathrm{II}}(r^2) = f\left(\tfrac{\mu^2}{C'}\right) - f\left(\tfrac{\mu^2 r^2}{C}\right) \tag{3.24}$$

with $f(x) = x - \log x - 1$ $(x > 0)$. The sign of $L_\bullet(r^2)$ determines the exponential explosion or suppression of the number of fixed points. This occurs on three different subsets $0 < r < r_-$, $r_- < r < r_+$, and $r_+ < r < R$, namely:

- For $r \in (0, r_-)$: $L_{\mathrm{I}}(r^2)$ is negative and monotonically increasing,

- For $r \in (r_-, r_+)$: $L_{\rm II}$ changes its sign since $L_{\rm II}(r_-^2) < 0 < L_{\rm II}(r_+^2)$.

  From the monotonicity in eq(**3.18**), one can verify that such change of sign occurs only once, in fact:

$$L'_{\rm II}(r^2) = \frac{(C' - \mu^2)C''}{(C')^2} + h_{\rm I}(r^2)\Big(\mu^2 - \frac{C}{r^2}\Big). \tag{3.25}$$

  The first term on the right-hand side in (3.25) is positive for $r_- < r < R$ and the second term on the right-hand side in (3.25) is positive for $0 < r < r_+$. Thus, $L_{\rm II}(r^2)$ is strictly monotonically increasing for $r_- < r < r_+$ and there exists a unique radius $r_* \in [r_-, r_+]$ such that $L_{\rm II}(r^2) < 0$ for $r < r_*$ and $L_{\rm II}(r^2) > 0$ for $r > r_*$.

- For $r_+ < r < R$, we can use the following properties of the function f: we have $f(x) - f(y) > 0$ for $x < y < 1$ and $f(x_2) - f(y_2) > f(x_1) - f(y_1)$ for $0 < y_2 - x_2 < y_1 - x_1$ and $x_2/y_2 < x_1/y_1 < 1$. It follows that $L_{\rm II}(r^2)$ is strictly positive and monotonically increasing.

Therefore, we observe that, as we increase N, the number of fixed points surrounding the origin within the radius r_* is exponentially suppressed. Conversely there are exponentially many of them as we consider any radius $r > r_*$. Interestingly, while the value of r_* where such transition occurs depends on the choice of C, its very existence is universal. This must not be confused with the topological trivialization of the models at the beginning of the chapter. Indeed, for finite μ, as one integrates over $\mathbb{R}^N$ the complexity function is positive or infinite. As we decided to "sit" at the origin, what we observe is rather a *local topological trivialization.* We can make these statements more precise and estimate the mean number of fixed point with a ball of radius r, $\mathcal{N}_\mu(r) = 1 + \int_{0<\tilde{r}<r} d\tilde{r}\, \widehat{\rho}_\mu(\tilde{r})$ as

$$\mathcal{N}_\mu(r) \leq 1 + (\tfrac{N}{\pi})^{\frac{1}{2}} c_1(r) e^{-N\kappa_1(r)} \qquad \text{for} \qquad r \in (0, r_*), \tag{3.26}$$

$$\mathcal{N}_\mu(r) \geq 1 + (\tfrac{N}{\pi})^{\frac{1}{2}} c_2(r) e^{+N\kappa_2(r)} \qquad \text{for} \qquad r \in (r_*, R). \tag{3.27}$$

for some positive and continuous real functions c_1, c_2, k_1 and k_2. With the functions

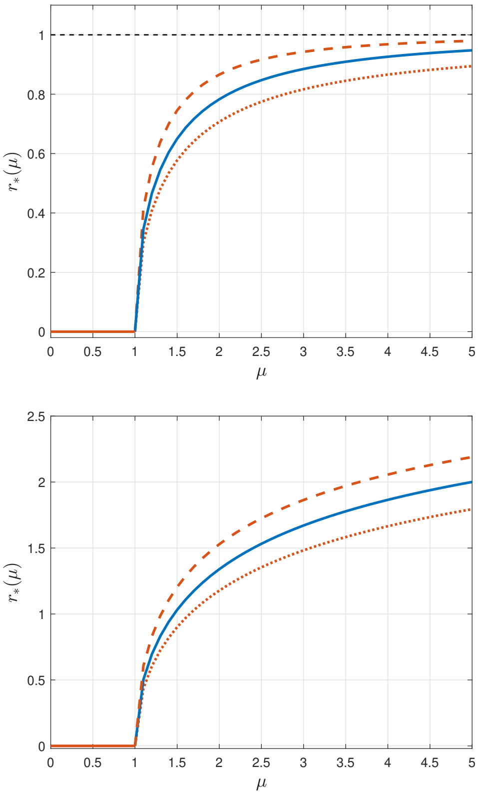

Figure 3.2: Resilience radius r_* as function of μ for eq(**3.32**)(top) and for eq(**3.33**)(bottom). Notice the interval $(r_-(\mu), r_+(\mu))$. $r_-(\mu)$ is the dotted curve and $r_+(\mu)$ is the dashed curve.

so far introduced the quantities entering eqs(**3.26**,**3.27**) are then given by

$$c_1(r) = \begin{cases} \int_0^r \frac{d\tilde{r}}{\tilde{r}} h_{\rm I}(\tilde{r}^2), & r < r_- \\ \int_0^{r_-} \frac{d\tilde{r}}{\tilde{r}} h_{\rm I}(\tilde{r}^2) + \int_{r_-}^r \frac{d\tilde{r}}{\tilde{r}} h_{\rm II}(\tilde{r}^2), & r > r_- \end{cases}, \tag{3.28}$$

$$c_2(r) = \int_{r_*}^r \frac{d\tilde{r}}{\tilde{r}} h_{\rm II}(\tilde{r}^2), \tag{3.29}$$

$$\kappa_1(r) = \begin{cases} -L_{\rm I}(r^2)/2, & r < r_- \\ -L_{\rm II}(r^2)/2, & r > r_- \end{cases}, \tag{3.30}$$

$$\kappa_2(r) = +L_{\rm II}(r^2)/2. \tag{3.31}$$

We would like now to illustrate these features for two examples of $C(r^2)$.

$$C(r^2) = \frac{r^2}{1 - r^2} = r^2 + r^4 + r^6 + ... \tag{3.32}$$

$$C(r^2) = e^{r^2} - 1 = r^2/1! + r^4/2! + r^6/3! + ... \tag{3.33}$$

The first coefficient of the expansion in both cases is $\sigma_1 = 1$ while the radius of convergence of the functions eq(**3.32**) and eq(**3.33**) are $R = 1$ and $R = +\infty$, respectively.

As confirmed by Fig(3.2), for $\mu < \sigma_1 = 1$,$r_-(\mu), r_+(\mu)$ and $r_*(\mu)$ are identically zero. Conversely beyond this threshold, $r_*(\mu)$ (blue solid curve) is monotonically increasing and is located within the interval defined by $r_-(\mu)$ (dotted line) and $r_+(\mu)$ (dashed line). Additionally, the latter bounds both converge to R. Keeping in mind these choice for C, we choose $\mu = 3/2$ in order to have $\boldsymbol{x} = \mathbf{0}$ stable in the limit $N \to +\infty$. From fig(3.2), we have $r_*(\mu = 3/2) \approx 0.65$ for eq(3.32) and $r_*(\mu = 3/2) \approx 1.03$ for eq(3.33) respectively. We can substitute this value in the asymptotic formulae for the spherical density eq(3.20) and eq(3.21) and range r between zero and R. Fig(3.3) shows the mean number of fixed points within a ball of radius r(blue line) while the markers represent the numerical evaluation of eq(3.15) for $N = 100$. The expectation $\mathbb{E}_{\text{Gin}}\left[|\det(\boldsymbol{\Xi} - \mu\sqrt{N}\boldsymbol{D})|\right]$ is evaluated by Monte Carlo method. As we vary $r \in (0, r_*)$, the fixed points are suppressed and the only (stable) fixed point is located at the origin. As r exceeds r_*, $\mathcal{N}_\mu(r)$ grows exponentially, eventually diverging for $r \to R$ for a fixed and finite value of N. As we increase the size of the system such transition becomes steeper and steeper. This divergence is not universal and depends on the choice we made for C. In principle, we can replace the summation over k in eq(3.8) with a truncated series expansion with cut-off $\Omega > 1$, i.e. $C(r^2) = \sigma_1^2 r^2 + \cdots + \sigma_\Omega^2 r^{2\Omega}$. Clearly, the number of fixed points is bounded from above by Ω^N with probability one. This upper bound grows exponentially with N. In this case, the mean number of fixed points is related to the real zeros of a set of multivariate Kac poynomials (see section 1.2.4). Namely, we can complete this picture with the linear statistics $\mathcal{N}_\mu$, which for $N \gg 1$, is (see appendix C.4)

$$\mathcal{N}_\mu(\mathbb{R}^N) = e^{\frac{N}{2}\log\Omega}(1 + o(1)) \tag{3.34}$$

The concomitance of r_* being strictly positive and the $\boldsymbol{x} = \mathbf{0}$ being stable suggests to investigate the dynamics for initial conditions sufficiently close to the origin. More precisely, we want to check numerically whether r_* can be, somehow, used as a characteristics length of the basis of attraction of $\boldsymbol{x} = \mathbf{0}$. Clearly the algebraic polynomial in eq(3.8) makes the computation feasible only for small enough values of N. We keep, once again, the same setting $\sigma_1 = 1 < 3/2 = \mu$ and draw a single realization of the random vector field $\varphi_n(\boldsymbol{x}) = \sum_{k=1}^{\Omega} \frac{1}{\sqrt{k!}} \sum_{i_1,\ldots,i_k} \xi_{n,i_1,\ldots,i_k} x_{i_1} \cdots x_{i_k}$ with $n = 1, \ldots, N$ and $\xi_\bullet$ i.i.d. standard Gaussian random variables. Secondly, we discretize $d\boldsymbol{x}/dt = -\mu\boldsymbol{x} + \frac{1}{2}\boldsymbol{\varphi}(\boldsymbol{x})$ for a sufficiently small dt. We are left with fixing the initial condition. We consider the latter as an *initial perturbation* away from the

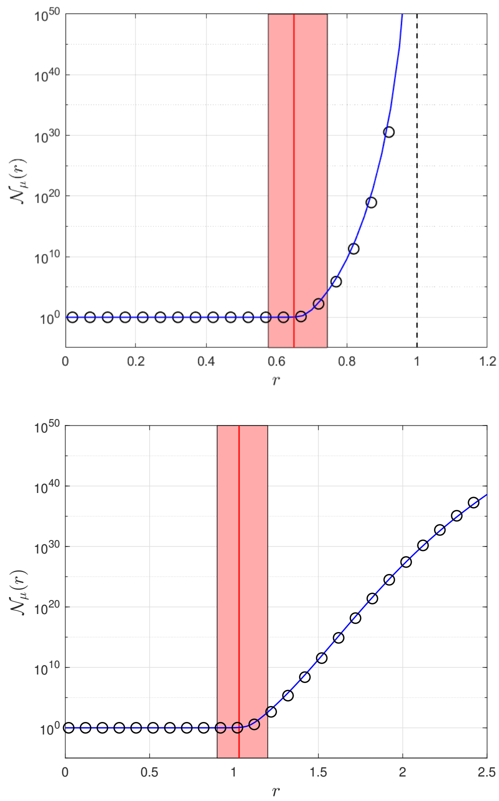

Figure 3.3: Mean number of fixed points ($N = 100, \mu = 3/2$) for eq(**3.32**)(top) and eq(**3.33**)(bottom): the blue line represents eq(**3.20**) and eq(**3.21**), the circular markers are the numerical solution of eq(**3.15**). The red line is r_*, the red region is the interval $(r_-(\mu), r_+(\mu))$.

origin. We pick up (uniformly), from the unitary $(N-1)$-sphere, p points. The j-th point defines a normalised vector $\boldsymbol{e}_j$ for $j = 1, .., p$. These are the directions of the initial conditions, i.e. $\boldsymbol{x}^1(0) = \varepsilon \boldsymbol{e}_1, \ldots, \boldsymbol{x}^p(0) = \varepsilon \boldsymbol{e}_p$ for a radial perturbation parameter $\varepsilon > 0$. According to our initial statements, we should observe that, for $\varepsilon \ll r_*$, the trajectories are attracted back to the origin, *regardless* of the direction, i.e. of the index p. In contrast to this, for $\varepsilon \gg r_*$, we expect the system to be extremely sensitive to the initial direction: some trajectories might still converge to the origin, some other might wander away. We show this is actually the case, by looking at the Euclidean norm of $\boldsymbol{x}$. In fig(**3.4**), we chose $N = \Omega = 4$ and $p = 10$. The blue solid curves, in the left plot, represent the trajectories whose initial norm are $\varepsilon = 0.5$ and $\varepsilon = 5$. The two bunches of initial conditions are separated by $r_*(\mu)$ (solid red line) contained in the interval $(r_-(\mu), r_+(\mu))$. All the initial trajectories with $\varepsilon = 0.5$ converge to the origin. Conversely, for $\varepsilon = 5$, some trajectories are not attracted by $\boldsymbol{x} = \mathbf{0}$ and eventually

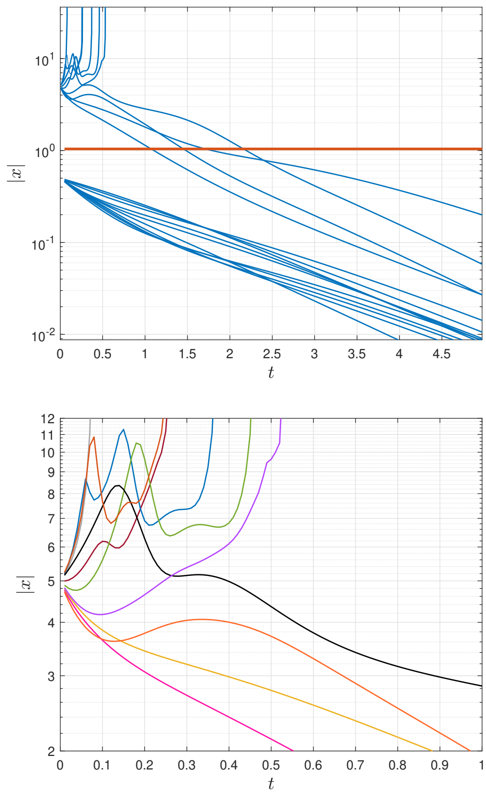

Figure 3.4: Top: numerical example of trajectories for a fixed realization of $\boldsymbol{\varphi}(\boldsymbol{x})$ with $\sigma_k = 1/\sqrt{k!}$ and $\mu = 3/2$. For $N = 4$ and cut-off $\Omega = 4$, we consider initial conditions with norms $|\boldsymbol{x}(0)|$ smaller and greater than r_*(represented as dashed line). Bottom: enhanced detail of the dotted box in the left figure.

depart from the latter as time increases. This is outlined in the plot of fig(**3.4**). We repeated this procedure several time, taking into account different values of ε, μ, N, Ω and realizations for $\boldsymbol{\varphi}(\boldsymbol{x})$. What reported above remains valid. Therefore, we come to the conclusion that r_* can be regarded as a resilience radius: an initial perturbation ε is suppressed for $\varepsilon \ll r_*$. The large time behaviour of a perturbation $\varepsilon \gg r_*$ strongly depends on the initial condition. Lastly, since we have set $N = \Omega = 4$, we necessarily have a constraint for the number of fixed points: $N_\mu \leq \Omega^N = 64$. Most of the latter (excluding the origin) are supposed to be unstable so their influence on the outer trajectories ($\varepsilon = 5$) is stronger to push them away. The assumptions of independency for the coefficient $\xi_\bullet$ in the Taylor expansion in eq(**3.8**) are surely strong but essential for the definition of $C(r^2)$ and clearly r_*. However, one might ask if such hypothesis can be relaxed and whether the results above are still valid for some ecological models. Clearly to shed light on this statement we need to choose the model we want to investigate and perform the relative numerics. One can be tempted to check if this is the case for the model in eq(**3.2**). If $\mu < \sigma$, the origin is stable *but* it's also the only fixed point for the dynamics. The next possible (and succefull) choice is a generalized Lotka-Volterra system

$$\frac{dx_i}{dt} = x_i \left(-\tilde{\mu} - x_i + \frac{\tilde{\sigma}}{\sqrt{N}} \sum_{j \neq i}^{N} \xi_{ij} x_j \right) \tag{3.35}$$

with parameters $\tilde{\mu} > 0$, $\tilde{\sigma} > 0$. The entries of the community matrix, ξ_{ij}, i.i.d. are centred Gaussian variables of unit variance. One can easily check that, for a given community matrix, the origin is a stable fix point and, therefore, it is surrounded by its basin of attraction. Clearly r_-, r_+ don't have meaning in the present model. Hence the resilience radius, r_*, cannot be estimated. However, for some $\tilde{\mu}$ and $\tilde{\sigma}$, the dynamics of eq(**3.35**) is similar to fig(**3.4**). Recovering the notations introduced above, we chose $p = 10$, $\varepsilon = 1$ and $\varepsilon = 3/2$. Trajectories with $|\boldsymbol{x}(0)| = 1$ evolve to the origin while only few trajectories with $|\boldsymbol{x}(0)| = 3/2$ follow (qualitatively) the same route (fig(**3.5**)). Although we can not provide a better mathematical consideration in this case, the observed qualitative picture provides additional support to our interpretation of r_* as the resilience radius and its relevance beyond our original model.

3.1.3.1 A final Remark on the Resilience Radius

We have exposed several features and results, lets sum them up here. We introduced a new class of nonlinear models generalizing the May's linear model and investigated the mean number of fixed points in their dynamics. We have unveiled a *local topological trivialization* once one retains all terms in the Taylor expansion of the random field. For $\mu > \sigma_1$, the origin is locally stable almost surely. Starting from this, we essentially complemented the May's model picture by showing the existence of a resilience radius $r_*(\mu) > 0$. The fixed points within such radius drastically reduce in numbers with growing number of interacting species N. In contrast to that, beyond r_*, the phase is again exponentially *studded* by saddle points. It is natural to expect that such change results into an extreme sensitivity to initial conditions and displacements. This last statement was tested numerically and lead to the conclusion that $r_*(\mu)$ can be regarded as a *resilience radius*. We observed that the system recovers from sufficiently small perturbations, with displacements compared to r_*. Such recovery occurs also for large perturbations if one takes $\mu \to \infty$, then $r_* \to R$, namely the resilience of the system

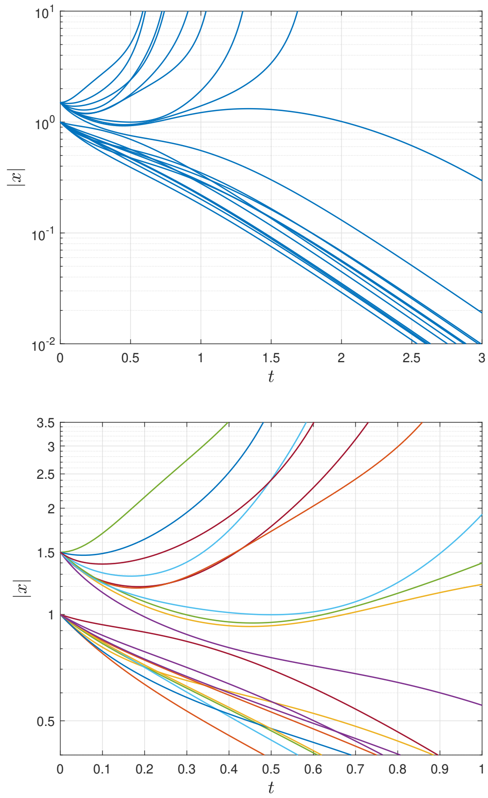

Figure 3.5: Top: numerical example of trajectories for a fixed realization of eq(**3.35**) with $\tilde{\mu} = 2$ and $\tilde{\sigma} = 4$ for random initial conditions with $|\boldsymbol{x}(0)| = 1$ and $|\boldsymbol{x}(0)| = 1.5$. Bottom: enhanced detail of the dotted box in the left figure.

increases and so does its ability to recover. For finite μ, as we impose $|\mathbf{x}(0)| \gtrsim r_*(\mu)$ the system might leave such neighbourhood and become chaotic. This last statement remains a hypothesis which we need to test. This will be the subject of the next sections. For $\mu < \sigma_1$, the origin is unstable almost surely: any finite ball containing the origin contains, on average, an exponential number of fixed points and the system experiences a loss of its resilience.

3.1.4 Chaos and Persistence for Correlations

What happen to those trajectories leaving the neighbourhood of the origin is an open question which we will try to heuristically answer in this section. For large systems, studying the dynamics still represents a challenging task. Moreover, such dynamical behaviour is not universal. As the main diffculty is the high dimensionality of the system, most of the available results in literature rely on numerics and crude approximations to decrease the size of the problem (see as an example [104]). We anticipate here the claim that such trajectories will become eventually chaotic as N increases. In natural ecosystems, the appearance of chaos is hardly observable and mostly remains observed in simulations and experiments. The main obstacles on such detection are the timescales at which this process occurs, the lack of recorded data over an extended period of time and the anthropogenic actions which alter the ecosystem. In the previous sections, we analyse the basin of attraction of $\boldsymbol{x} = \boldsymbol{0}$ by topological complexity. Conversely, to tackle the mentioned problem we need to introduce the notion of dynamical complexity. We set the feedback relaxation $\mu = 1$ without loss of generality and follow the approach in [105, 106, 107] and [108]. By introducing two auxiliary fields $\boldsymbol{b}$ and $\hat{\boldsymbol{b}}$, the generating functional for dynamical correlation functions in eq(**3.8**) is given by

$$\mathcal{Z}[\boldsymbol{b}, \hat{\boldsymbol{b}}] = \int_{\boldsymbol{x}=\boldsymbol{x}(t_0)}^{\boldsymbol{x}=\boldsymbol{x}(t)} \mathcal{D}\boldsymbol{x}\mathcal{D}\hat{\boldsymbol{x}} \exp\left(- i \int dt' \hat{\boldsymbol{x}(t')}^T \left(\partial_t \boldsymbol{x}(t') + \boldsymbol{x}(t') - \frac{1}{\sqrt{N}} \boldsymbol{\varphi}(\boldsymbol{x}(t')) \right) \right) \times$$
$$\exp\left(i \int dt' \boldsymbol{b}\hat{(t')}^T \boldsymbol{x}(t') + \boldsymbol{x}\hat{(t')}^T \boldsymbol{b}(t') \right) \tag{3.36}$$

Clearly, the external fields, $\boldsymbol{b}$ and $\hat{\boldsymbol{b}}$, allow the calculation of the correlation functions by simply computing $\frac{\delta \mathcal{Z}}{\delta \boldsymbol{b}_i^r \hat{\boldsymbol{b}}_j^s}\big|_{\boldsymbol{b},\hat{\boldsymbol{b}}=0}$. However, we will follow a different direction. Firstly, as the formulation above is valid for each single realization of $\boldsymbol{\varphi}$, we need to evaluate the average of $\mathcal{Z}$ over the latter which we will indicate with $\overline{\mathcal{Z}}$. From our work, Gaussianity of φ implies $\mathbb{E}\left[\varphi_n(\boldsymbol{x})\varphi_m(\boldsymbol{y})\right] = \delta_{nm} C(\boldsymbol{x}^T \boldsymbol{y})$. The entries of $\boldsymbol{\varphi}$ being independent, we aim to compute:

$$\prod_{n=1}^{N} \mathbb{E}_\varphi \left[\exp\left(\frac{i}{\sqrt{N}} \int dt \hat{x}_n \varphi_n(\boldsymbol{x}(t)) \right) \right] \tag{3.37}$$

This is equivalent to

$$\prod_{j=1}^{N} \mathbb{E}_\varphi \left[\exp\left(\frac{i}{\sqrt{N}} \int \hat{x}_j(t) \varphi_j(\boldsymbol{x}(t)) \right) \right] = \exp\left(\frac{-1}{2N} \int dt dt' C(\boldsymbol{x}(t)^T \boldsymbol{x}(t')) \hat{\boldsymbol{x}}(t)^T \hat{\boldsymbol{x}}(t') \right) \tag{3.38}$$

To show this, we discretize $\int dt \to \sum_a$ and $\boldsymbol{x}(n\delta t) \to \boldsymbol{x}^n$ with $t = n\delta t$ and introduce the matrices $\boldsymbol{\Phi}_{ij} = \varphi_j(\boldsymbol{x}^i)$ and $C(\boldsymbol{x}^{a,T} \boldsymbol{x}^b) = C^{ab}$, We know that

$$\int dp(\mathrm{vec}[\boldsymbol{\Phi}]) \exp\left(\frac{i}{\sqrt{N}} \mathrm{vec}[\boldsymbol{\Phi}]^T \mathrm{vec}[\hat{\boldsymbol{X}}] \right) = \exp\left(-\frac{1}{2N} \mathrm{vec}[\hat{\boldsymbol{X}}]^T \boldsymbol{C} \,\mathrm{vec}[\hat{\boldsymbol{X}}] \right) \tag{3.39}$$

Therefore

$$\prod_{j=1}^{N} \mathbb{E}_\varphi \left[\exp\left(\frac{i}{\sqrt{N}} \sum_a \hat{x}_j^a \varphi_j(\boldsymbol{x}^a) \right) \right] = \exp\left(-\frac{1}{2N} \sum_{ab} C(\boldsymbol{x}^{aT} \boldsymbol{x}^b) \hat{\boldsymbol{x}}^{aT} \hat{\boldsymbol{x}}^b \right) \tag{3.40}$$

and one simply restores the continuous limit. Before restoring the continuous limit, we take an additional step. In order to introduce a self-consistent formulation for the correlation functions, indicating $C^{ab} = C(\boldsymbol{x}^{aT}\boldsymbol{x}^b)$, we introduce a set of auxiliary variables pairs $(y^{ab}, \hat{y}^{ab})$ and the identity,

$$\exp\left(-\frac{1}{2N}C(\hat{\boldsymbol{x}}^{aT}\hat{\boldsymbol{x}}^b)\right) \propto \lim_{u\to 0^+}\int dy^{ab}d\hat{y}^{ab}\exp\left(-\frac{y^{ab}}{2}(\hat{\boldsymbol{x}}^{aT}\boldsymbol{x}^b) + i\hat{y}^{ab}\left(y^{ab} - \frac{C^{ab}}{N}\right) - u(\hat{y}^{ab})^2\right)$$

We can re-arrange the integration in eq(**3.36**) and write the generating function as

$$\overline{\mathcal{Z}}[\boldsymbol{b},\hat{\boldsymbol{b}}] = \int \mathcal{D}\boldsymbol{y}\mathcal{D}\hat{\boldsymbol{y}}e^{N\mathcal{L}(\boldsymbol{y},\hat{\boldsymbol{y}})}$$

with

$$\mathcal{L}(\boldsymbol{y},\hat{\boldsymbol{y}}) = \frac{1}{N}\log\int \mathcal{D}\boldsymbol{x}\mathcal{D}\hat{\boldsymbol{x}}\exp\left(S_1(\boldsymbol{x},\hat{\boldsymbol{x}}) + S_2(\boldsymbol{x},\hat{\boldsymbol{x}})\right)$$

and fields:

$$S_1(\boldsymbol{x},\hat{\boldsymbol{x}}) = \int_{t_0}^{t} dt' - i\hat{\boldsymbol{x}}^T(t')(1+\partial_{t'})\boldsymbol{x}(t') + i\hat{\boldsymbol{b}}^T(t')\boldsymbol{x}(t') + \boldsymbol{b}^T(t')\hat{\boldsymbol{x}}(t')$$

and

$$S_2(\boldsymbol{x},\hat{\boldsymbol{x}}) = \int_{t_0}^{t} dt'\int_{t_0}^{t} dt'' i\hat{y}(t',t'')\left(y(t',t'') - \frac{C(t',t'')}{N}\right) - \frac{y(t',t'')}{2}(\hat{\boldsymbol{x}}(t')^T\hat{\boldsymbol{x}}(t'')) - u(\hat{y}(t',t''))^2$$

We can now compute, by saddle point approximation, the large-N asymptotic behaviour of $\overline{\mathcal{Z}}$. The stationarity conditions $\frac{\delta\mathcal{L}}{\delta y^{ab}} = 0$ and $\frac{\delta\mathcal{L}}{\delta\hat{y}^{ab}} = 0$ with $u \to 0^+$ lead to

$$\begin{cases} y^{cd} = \frac{1}{N}\mathbb{E}_{\mathcal{D}}[C^{cd}] \\ i\hat{y}^{cd} = \frac{1}{2}\mathbb{E}_{\mathcal{D}}[(i\hat{\boldsymbol{x}}^c)^T(i\hat{\boldsymbol{x}}^d)] \end{cases} \tag{3.41}$$

where $\mathbb{E}_{\mathcal{D}}[...]$ is the expectation taken over the system's dynamical trajectories. The condition $\hat{\boldsymbol{y}} = \boldsymbol{0}$ is necessary to maintain the correct normalization. Therefore, the partition function reads

$$\overline{\mathcal{Z}}[\hat{\boldsymbol{b}},\boldsymbol{b}] \sim \int \mathcal{D}\boldsymbol{x}\mathcal{D}\hat{\boldsymbol{x}}\exp\left(S_1(\boldsymbol{x},\hat{\boldsymbol{x}}) + \int dt'dt''\frac{\mathbb{E}_{\mathcal{D}}[C(t',t'')]}{2N}(i\hat{\boldsymbol{x}}(t'))^T(i\hat{\boldsymbol{x}}(t''))\right) \tag{3.42}$$

The second term, in eq(**3.42**), can be written as $\mathbb{E}_\eta\left[\exp\left(i\int dt(\hat{\boldsymbol{x}}(t))^T\boldsymbol{\eta}(t)\right)\right]$ where $\boldsymbol{\eta}$ is a centered Gaussian process with covariance $\mathbb{E}_\eta[\eta_k(t)\eta_j(t')] = \frac{\delta_{kj}}{N}\mathbb{E}_{\mathcal{D}}[C(t,t')]$. Therefore we arrive at the following path integral formulation

$$\bar{\mathcal{Z}} \sim \mathbb{E}_\eta\left[\int \mathcal{D}\boldsymbol{x}\mathcal{D}\hat{\boldsymbol{x}}\exp\left(i\int dt(\hat{\boldsymbol{x}}(t))^T\boldsymbol{b}(t) + (\hat{\boldsymbol{b}}(t))^T\boldsymbol{x}(t) + S_3(\boldsymbol{x},\hat{\boldsymbol{x}})\right)\right] \tag{3.43}$$

with

$$S_3(\boldsymbol{x},\hat{\boldsymbol{x}}) = -i\int dt\hat{\boldsymbol{x}}(t)^T((1+\partial_t)\boldsymbol{x}(t) - \boldsymbol{\eta}(t))$$

The associated dynamics in the absence of external fields is equivalently described by the following Langevin equation

$$\begin{cases} \frac{dx_i}{dt} = -x_i + \eta_i(t) \\ E[\eta_i(t)\eta_i(t')] = \frac{1}{N}\mathbb{E}_{\mathcal{D}}[C(t,t')] \end{cases} \tag{3.44}$$

From all these considerations, we have

$$\left(\frac{d}{dt}+1\right)\left(\frac{d}{dt'}+1\right)\Delta(t,t') = \frac{1}{N}\mathbb{E}_{\mathcal{D}}[C(t,t')] \tag{3.45}$$

with $\Delta(t,t') = \mathbb{E}_{\mathcal{D}}[x_i(t)x_i(t')]$. To solve eq(**3.45**) we need an expression, in terms of Δ, for the r.h.s. Namely, we are looking for a self-consistent formulation. For simplicity, going back to the discrete formulation, the expectation reads as

$$\mathbb{E}_{\mathcal{D}}[C^{ab}] = \int \prod_{i=1}^{N} \frac{d\boldsymbol{y}_i e^{-1/2\boldsymbol{y}_i^T \Delta_M^{-1} \boldsymbol{y}_i}}{2\pi(\det \Delta_M)^{1/2}} C\left(\sum_{i=1}^{N} y_i^a y_i^b\right) \tag{3.46}$$

with $\boldsymbol{y}_i = \begin{bmatrix} y_i^a \\ y_i^b \end{bmatrix}$ and

$$\Delta_M = \begin{bmatrix} \Delta^{aa} & \Delta^{ab} \\ \Delta^{ab} & \Delta^{bb} \end{bmatrix} \tag{3.47}$$

With new variables $\boldsymbol{z}_i = \Delta_M^{-1/2}\boldsymbol{y}_i$, we have that

$$\mathbb{E}_{\mathcal{D}}[C^{ab}] = \mathbb{E}_{z_i^a \sim \mathcal{N}(0,1)}\left[C\left(\sum_{i=1}^{N} \Delta_0 z_i^a z_i^b + \frac{\Delta}{2}\left((z_i^a)^2 + (z_i^b)^2\right)\right)\right] \tag{3.48}$$

where $\Delta_0 = \Delta^{aa} = \Delta(t,t)$ and $\Delta = \Delta^{ab} = \Delta(t,t')$. From the equations above it is natural to re-scale $x_i \to \frac{x_i}{\sqrt{N}}$. This is equivalent to imposing $\Delta_0 \to \frac{\Delta_0}{N}$ and $\Delta \to \frac{\Delta}{N}$. We assume that the argument of C in eq(**3.48**), for $N \gg 1$, in virtue of the central limit theorem, can be replaced by a Gaussian variable $\bar{x}$ with $\mathbb{E}[\bar{x}] = \Delta$ and $Var[\bar{x}] = \Delta^2 + \Delta_0^2$. Namely,

$$\mathbb{E}\left[C\left(\Delta + \frac{\sqrt{\Delta^2+\Delta_0^2}}{\sqrt{N}}z\right)\right]_{z\sim\mathcal{N}(0,1)} \xrightarrow{N\to+\infty} C(\Delta) \tag{3.49}$$

Therefore we have $\mathbb{E}_{\mathcal{D}}[C^{ab}] \sim \sum_{k\geq 1}\sigma_k^2(\Delta^{ab})^k$. At the steady state we expect Δ to depend on times only via the difference $|t-t'| = \tau$ and to be independent from the initial conditions. Under these assumptions, $\Delta(\tau)$ can be shown to evolve according to the Newtonian dynamics

$$\partial_\tau^2 \Delta = -\partial_\Delta V(\Delta) \tag{3.50}$$

where $V(\Delta) = -\frac{\Delta^2}{2} + \int d\Delta C(\Delta) = -\frac{\Delta^2}{2} + \sum_{k=1}^{+\infty} \sigma_k^2 \frac{\Delta^{k+1}}{k+1}$ (see fig(3.6)) and with the following conditions

$$\begin{cases} \partial_\tau \Delta(0) = 0 \\ |\Delta(\tau)| \leq \Delta(0) \end{cases} \tag{3.51}$$

Solutions to eq(3.50) preserve the energy

$$V(\Delta_0) = \frac{1}{2}|\partial_\tau \Delta|^2 + V(\Delta) \tag{3.52}$$

The first boundary condition in eq(3.51) is introduced to preserve the symmetry of $\Delta(\tau)$ while the second is necessary to have a well-defined correlation function. One now may notice that our problem differs considerably from a similar one considered originally in [109] by the same technique in the neural network framework. Namely, in contrast to [109], in our case V does not parametrically depend on $\Delta(0)$. For our purpose we will only focus on the locally stable fixed point regime, assuming $\sigma_1 < 1$ (see however section 3.1.4.2 below). For $\Delta > 0$, $V(\Delta)$ forms a well, with a local maximum in $\Delta = 0$ with $\frac{d^2V}{d\Delta^2}(0) < 0$ and global minimum at $\Delta = r_+^2$, i.e. $\frac{d^2V}{d\Delta^2}(r_+^2) > 0$. These two points are fixed points for the single particle dynamics. Solutions with negative energy lead to non-vanishing average cycles while solutions corresponding to positive potential lead to centered oscillation. The potential $V(\Delta)$ can be shown to have a unique point where the second derivative $\partial_\Delta^2 V(\Delta)$ changes its sign. This occurs at $\Delta = r_-^2$. We recall that $0 < r_- < r_+$. Lastly, there is a unique point where the potential vanishes, $\Delta_0 > r_+^2$. By stability analysis of replicated dynamical mean field equation eq(3.36) (see [107] and section 3.1.4.3), this point corresponds to an exponentially time-decaying $\Delta(\tau)$ and stable attractor.

3.1.4.1 Lyapunov Exponent

The sensitivity to initial conditions and the emergence of chaotic flows is fully characterized by the maximal Lyapunov exponent λ. To define the latter we firstly introduce the mean susceptibility ([106])

$$\chi^2(\tau) = \lim_{t\to+\infty} \frac{1}{N} \sum_{ij} \mathbb{E}_{\mathcal{D}}[\chi_{ij}^2(t+\tau, t)]$$

where $\chi_{ji}(t,t') = \frac{\delta x_i(t)}{\delta x_j^0(t')}$, with $\delta x_i^0(t')$ being the initial displacement. In the limit $t \to +\infty$, the Lyapunov exponent is given by

$$\lambda = \lim_{\tau\to+\infty} \frac{\log \chi^2(\tau)}{2\tau}. \tag{3.53}$$

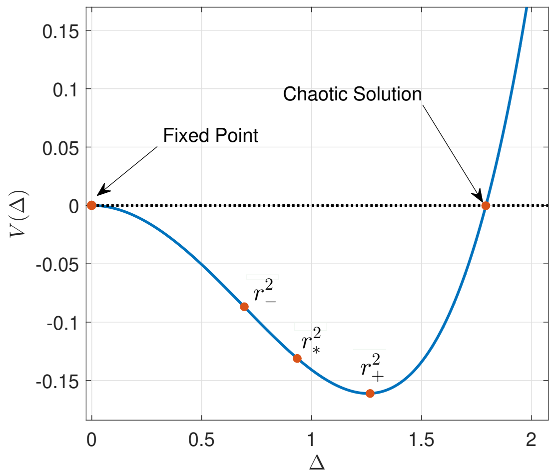

Figure 3.6: Example of profile for $V(\Delta)$ for $\mu = 1$.

The evolution of $\chi^2(t)$ is retrieved by differentiating $\frac{dx_i(t)}{dt}$ with respect to a perturbation $\delta x_j^0(t')$. The susceptibilities $\chi_{ij}(t,t')$, for the dynamics generated by sum of the feedback mechanism with $\mu = 1$ and of eq(**3.8**), satisfy the following set of coupled ODEs:

$$\left(1+\frac{d}{dt}\right)\chi_{ij}(t,t') = \frac{1}{\sqrt{N}}\sum_{u=1}^{N}\frac{\partial}{\partial x_u}\varphi_i(\boldsymbol{x}(t))\chi_{uj}(t,t') + \delta_{ij}\delta(t-t') \tag{3.54}$$

The mean susceptibility is obtained by multiplying eq(**3.54**) by itself ($N \gg 1$)

$$\left(1+\frac{d}{dt_a}\right)\left(1+\frac{d}{dt_b}\right)\frac{1}{N}\sum_{ij}\mathbb{E}_{\mathcal{D}}\left[\chi_{ij}(t_a,t_c)\chi_{ij}(t_b,t_d)\right] \simeq$$
$$+C'(\boldsymbol{x}(t_a)^T\boldsymbol{x}(t_b))\frac{1}{N}\sum_{uj}\mathbb{E}_{\mathcal{D}}\left[\chi_{uj}(t_a,t_c)\chi_{uj}(t_b,t_d)\right]+\delta(t_a-t_b-t_c+t_d)\delta(t_a+t_b-t_c-t_d) \tag{3.55}$$

The r.h.s is obtained by observing that

$$\mathbb{E}[\partial_u\varphi_i(\boldsymbol{x}(t))\partial_v\varphi_i(\boldsymbol{x}(t'))] = C''(\boldsymbol{x}(t)^T\boldsymbol{x}(t'))x_u(t')x_v(t) + C'(\boldsymbol{x}(t)^T\boldsymbol{x}(t'))\delta_{uv} \tag{3.56}$$

As in the previous section, we rescale $x_i \to \frac{x_i}{\sqrt{N}}$ and we take the limit $N \to +\infty$. With the hypothesis so far introduced, analogously to eq(**3.49**), we can assume that $C'(\boldsymbol{x}(t)^T\boldsymbol{x}(t'))$ in eq(**3.56**) is the leading term. A further change of variables, $\tau = t_a - t_b$, $\tau' = t_c - t_d$, $T = t_a + t_b$ and $T' = t_c + t_d$, leads to

$$\left[\left(1+\frac{\partial}{\partial T}\right)^2 - \frac{\partial^2}{\partial\tau^2} - C'(\Delta)\right]G(T,T',\tau,\tau') = 2\delta(T-T')\delta(\tau-\tau') \tag{3.57}$$

where $G(T,T',\tau,\tau') = \frac{1}{N}\sum_{uj}\mathbb{E}_{\mathcal{D}}\left[\chi_{uj}(\frac{T+\tau}{2},\frac{T'+\tau'}{2})\chi_{uj}(\frac{T-\tau}{2},\frac{T'-\tau'}{2})\right]$. Therefore, the mean susceptibility can be written as $G(2t,0,0,0)$ and as a series

$$\chi^2(t) = \sum_{n=0}^{+\infty}\chi_n \exp\left(2\omega_n t\right)$$

with $\omega_n = -1 \pm (1-\lambda_n)^{1/2}$. The terms λ_n are the eigenvalues of the following one dimensional Schrödinger-type equation:

$$\left[\frac{d^2}{d\tau^2} + \lambda_n + \frac{\partial^2 V}{\partial \Delta^2}(\Delta)\right]\psi(t) = 0 \tag{3.58}$$

As the large-time behaviour is controlled by the lowest eigenvalue λ_0, the maximal Lyapunov exponent is given by $\lambda = -1 + (1-\lambda_0)^{1/2}$.

3.1.4.2 Stability of Fixed Points

If Δ is constant, the Lyapunov exponent is simply $\lambda = -1 + \sqrt{C'(\Delta)}$. From the sections above, $C'(\Delta)$ is a strictly monotone function such that $C'(\Delta) > 1$ if and only if $\Delta > r_-^2$. For $\sigma_1 > 1$, $r_- = 0$ and all the fixed points are therefore unstable, including $\boldsymbol{x} = \boldsymbol{0}$ for which the Lyapunov exponent is $\sigma_1 - 1$. Conversely, for $\sigma_1 < 1$, $\boldsymbol{x} = \boldsymbol{0}$ is stable. These two regimes for the origin are in agreement with the May-Wigner instability obtained by linearization of the equations of motion. Any constant solution $\Delta > r_-^2$ is unstable, including the minimum of V at $\Delta = r_+^2$ since $r_+ > r_-$.

3.1.4.3 Chaotic Trajectories at Criticality

To find the dependence of Δ on τ requires the direct solution of eq(**3.58**). Close to criticality, i.e. $\sigma_1 = 1-\varepsilon$ with $\varepsilon \to 0^+$, we know that the basin of attraction of the fixed point located at the origin shrinks to zero. We now want to show that, depending on the initial condition, there exists a *chaotic* solution. Under these assumptions the point where the potential vanishes $\Delta_0 > r_+^2$ is sufficiently close to the origin that we can expand $V(\Delta)$ and keep the first two terms from the Taylor expansion, i.e.

$$V(\Delta_0) \simeq \frac{1}{2}(\sigma_1^2-1)\Delta_0^2 + \frac{\sigma_2^2}{3}\Delta_0^3 + \ldots \tag{3.59}$$

Therefore, $\Delta_0 \simeq \frac{3(1-\sigma_1^2)}{2\sigma_2^2}$. The evolution of $\Delta(t) \leq \Delta_0$ satisfies

$$t = \frac{1}{\sqrt{1-\sigma_1^2}}\int_{\Delta_0}^{\Delta(t)} d\Delta \frac{1}{\Delta\sqrt{1-\frac{\Delta}{\Delta_0}}} \tag{3.60}$$

By inversion $\Delta(t) \simeq \Delta_0 \cosh^{-2}(t\sqrt{1-\sigma_1^2}/2)$. The characteristic time scale is given by $\tau = (\sqrt{1-\sigma_1^2}/2)^{-1}$. We can now compute λ_0. The second derivative of the potential is given by $\frac{\partial^2 V}{\partial \Delta^2}(\Delta) \simeq (\sigma_1^2 - 1) + 2\sigma_2^2 \Delta$. With the knowledge of $\Delta(t)$, the equation eq(**3.58**) becomes (see [110])

$$\left[\frac{d^2}{dt^2} + \lambda_n - (1-\sigma_1^2) + 3(1-\sigma_1^2)\cosh^{-2}\left(t\sqrt{1-\sigma_1^2}/2\right)\right]\psi(t) = 0 \tag{3.61}$$

The term $-(1-\sigma_1^2) + 3(1-\sigma_1^2)\cosh^{-2}\left(t\sqrt{1-\sigma_1^2}/2\right)$ is, in turn, a potential with minimum for $t = 0$ and $\psi(t) = \frac{d\Delta}{dt}(t)$ is a eigenfunction with zero value for $t = 0$. The equation above can be rewritten as a Legendre equation. Its solutions can be written in terms of the generalized Legendre polynomials, with the eigenvalues given by

$$\lambda_n = -\frac{(1-\sigma_1^2)}{16}(7-(1+2n))^2 + (1-\sigma_1^2)$$

which allows to find Lyapunov exponent as $\lambda \sim -1 + \sqrt{1 + \frac{5}{4}(1-\sigma_1^2)}$. Re-introducing $\varepsilon \to 0^+$, at criticality we finally observe that the zero-energy solution corresponds to a chaotic dynamics since

$$\lambda \sim \frac{5}{4}\varepsilon$$

This is completely different from neural networks. In the latter, for $\sigma_1 < 1$, $x = 0$ is the only fixed point and *any* trajectory is attracted by it. We again observe that:

- σ_2 does not explicitly appear in $\frac{\partial^2 V}{\partial \Delta^2}(t)$, however, it is required to be non-vanishing. Lastly, we notice that the two stable solutions $\Delta = 0$ and Δ_0 are separated by the unstable solution $\Delta = r_+^2 \simeq \frac{1-\sigma_1^2}{\sigma_2^2}$.
- This result is exact if we assume the cut-off $\Omega = 2$

As all the results above have been obtained heuristically assuming validity of the mean-field approximation they have to be further tested in accurate numerical simulations. This will be the subject of future investigations, beyond the present thesis.

3.1.5 Is Topological Trivialization universal?

The results of this chapter have reflected the fact that the limiting spectral density of Ginibre matrices has compact support. This created at least three different regimes, within and out of the bulk of the spectrum, separated by a transitional edge scaling regime. We now try to answer the question addressed in the title of this subsection.

To this purpose, we suggest to consider an *ad hoc* conservative dynamics to prove that this assertion can be violated. We assume the potential is written as

$$\mathcal{V}(\boldsymbol{x}) = -\frac{\mu}{2}|\boldsymbol{x}|^2 + V(\boldsymbol{x})$$

The first (quadratic) term confines the system into a well altered by the random potential $V(\boldsymbol{x})$. The latter modifies this simple surface of the Lyapunov function by introducing local fixed points and attractors. The relative strength of the confining term and the random functions controls the appearance of a complicate energy surface featuring both stable and unstable equilibrium points. We assume $V(\boldsymbol{x})$ to be the sum of periodic potentials $V_a(\boldsymbol{x})$, i.e. $V(\boldsymbol{x}) = \sum_{a=1}^{M} V_a(\boldsymbol{x})$ with

$$V_a(\boldsymbol{x}) = u_1^{(a)} \cos(\boldsymbol{k}_a^T \boldsymbol{x}) + u_2^{(a)} \sin(\boldsymbol{k}_a^T \boldsymbol{x}) \tag{3.62}$$

The vectors $\boldsymbol{k}_a$ represent the wave numbers while $u_{1,2}^{(a)}$ are the amplitudes assumed to be normal random variables, i.e. $\mathbb{E}[u_x^{(a)} u_y^{(b)}] = \delta_{xy}\delta_{ab}$. We want to investigated the mean number of the equilibrium points $\mathcal{N}_\mu$, by the Kac-Rice formalism (see eq(**1.44**)), for the set of equations $\frac{dx_i}{dt} = -\frac{\partial V}{\partial x_i}(\boldsymbol{x})$. Our assumptions imply the following covariance structure:

$$\mathbb{E}[V(\boldsymbol{x})V(\boldsymbol{x}')] = \sum_{a=1}^{M} \cos\left(\boldsymbol{k}_a^T(\boldsymbol{x} - \boldsymbol{x}')\right), \tag{3.63}$$

$$\mathbb{E}[\partial_l V(\boldsymbol{x})V(\boldsymbol{x}')] = -\sum_{a=1}^{M} k_{ai} \sin(\boldsymbol{k}_a^T(\boldsymbol{x} - \boldsymbol{x}')), \tag{3.64}$$

$$\mathbb{E}[\partial_i V(\boldsymbol{x})\partial_j V(\boldsymbol{x}')] = \sum_{a=1}^{M} k_{ai}k_{aj} \cos(\boldsymbol{k}_a^T(\boldsymbol{x} - \boldsymbol{x}')) \tag{3.65}$$

For $\mu \gg 1$, we expect the system's dynamics to be mostly confined in the region close to $\boldsymbol{x} = \mathbf{0}$, however, as the potential V is added to the system, the origin is no longer a fixed point of the dynamics as $\partial_{x_j} V(\mathbf{0}) \neq \mathbf{0}$ almost surely. With the idea of analysing the behaviour as the size of the system become large ($N \to +\infty$), we further assume that the wave numbers $\boldsymbol{k}_a$ are centered Gaussian random variable with variance $1/N$ and we consider the number of modes $M \to +\infty$ such that $1 \leq \alpha = M/N < +\infty$. The number of fixed points for such dynamics is given by the Kac-Rice formula (see appendix C.4.1) as

$$\mathcal{N}_\mu(\mathbb{R}^N) = \frac{1}{\mu^N} \int \prod_{a=1}^{M} \frac{dT_a}{\sqrt{2\pi}} e^{-\frac{1}{2}T_a^2}\, \mathbb{E}_{\mathbf{W}}[|\det(\mu \mathbf{1}_N - \mathbf{W}\mathbf{T}\mathbf{W}^T)|] \tag{3.66}$$

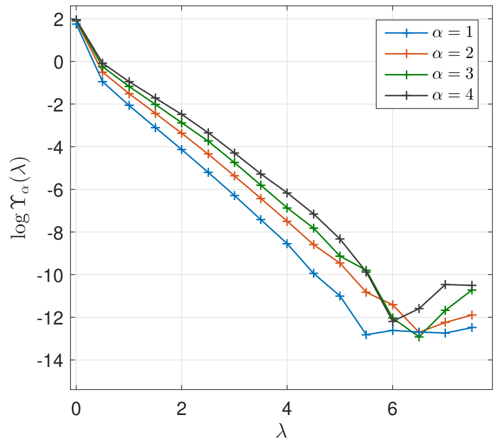

Figure 3.7: Numerical evaluation for $N = 30$ of $\Upsilon_\alpha(\lambda) = \frac{1}{N}\log \mathcal{N}_\mu$. # Samples for $\mathcal{N}_\mu$ $=10^8$.

where $\mathbf{T} = \text{diag}(T_1, .., T_M)$, $\mathbf{W}$ is a $N \times M$ real matrix whose columns, $\mathbf{w}_a$, are distributed as $p(\boldsymbol{w}_a) \propto e^{-N/2\boldsymbol{w}_a^T\boldsymbol{w}_a}$ and $\mathbb{E}_{\mathbf{W}}[g(\boldsymbol{W})] = \left(\frac{N}{2\pi}\right)^{\frac{NM}{2}} \int d\mathbf{W} e^{-\frac{N}{2}\operatorname{Tr}\mathbf{W}\mathbf{W}^T} g(\mathbf{W})$ for a sufficiently smooth function $g(x)$. Eq(**3.66**) provides a new example of connections between the study of random energy landscapes and generalised Wishart random matrices. Different examples of similar kind appeared very recently in the context of random optimization problems (see [111] [112]). The experience gained in the previous models suggests to expect $\mathcal{N}_\mu \propto e^{N\Sigma(\mu)}$ with $\Sigma(\mu)$ being the topological complexity. As before, the positive (negative) sign of $\Sigma(\mu)$ determines the exponential proliferation (suppression) of the number of fixed points. However, in contrast to the eqs(**3.4**,**3.15**) obtaining asymptotics of $\mathcal{N}_\mu$ explicitly is far from an easy task as none of the techniques of the present thesis can be directly applied. Therefore, we can only bound $\mathcal{N}_\mu$ following the results in Chapter 1 and perform numerical simulations.

3.1.5.1 Absence of Self-Averaging

For classic real RMT ensembles and $N \gg 1$, the quantity $\frac{1}{N}\log|\det(\mathbf{1}_N\mu - \mathbf{G})|$ is usually self-averaging with Gaussian fluctuation with variance of order $O(1/N^2)$ [49]. This is enough for evaluating, for large N, the complexity function since

$$\Sigma = \lim_{N\to+\infty} \frac{1}{N}\log \mathcal{N}_\mu \approx \hat{\Sigma} = \int d\rho(z)\log|\mu - z| - \log\mu \tag{3.67}$$

this fact underlies the equivalence between "quenched" and "annealed" complexity of stationary points. In such a case the topological trivialization corresponds to the

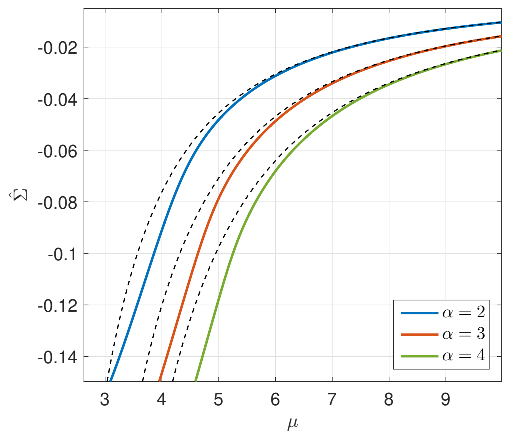

Figure 3.8: Average of $\hat{\Sigma}$ by numerical integration(coloured curves) from ρ_α and eq(**3.69**) (dashed curves).

change in sign (or vanishing) of the quantity above at some finite value of the control parameter μ. For matrices discussed in section 1.1.2, one easily checks that

$$\lim_{N\to+\infty} \frac{1}{N} \log \mathcal{N}_\mu = \begin{cases} \frac{1}{2}(\mu^2 - 1) - \log \mu \text{ for } \mu < 1 \\ 0 \text{ otherwise} \end{cases} \tag{3.68}$$

However, for $\mathcal{N}_\mu$ in eq(**3.66**), the density in the right-hand side of eq(**3.67**) is the limiting mean spectral density for matrices of the form $\mathbf{W}\mathbf{T}\mathbf{W}^T$. Such density $\rho_\alpha(x)$ is given by the inversion of eq(**1.81**). We remind here that such operation is non trivial and we only have been able to reproduce analytically the Gaussian tails of it. Namely, such limiting spectral density does not have compact support. This is the first ingredient which should be mentioned in support of our claim that a sharp trivialization transition in such a model does not occur. In the first chapter we gave few terms of the expansion, for $\mu \gg 1$, for eq(**3.67**), namely (see fig(**3.8**))

$$\hat{\Sigma} = -\frac{\alpha}{2\mu^2} - \frac{\alpha(2\alpha+3)}{4\mu^4} + o\left(\frac{1}{\mu^4}\right) \tag{3.69}$$

This will reveal to be a meaningless estimation or boundary for Σ as for sufficiently large μ, $\hat{\Sigma} < 0$ (see below). In principle, if confirmed this would correspond, on average and for $N \gg 1$, to the absence of fixed points. This result indicates that the mean of the number of equilibria may be not representative and the latter show big fluctuations from one realization of the landscape to the other. More generally, understanding complexity properly should require the control of higher moments. Those moments would involve products of characteristic polynomials, which we briefly addressed in chapter 1. Unable to estimate the fluctuations, we nevertheless are able to provide arguments that the complexity corresponding to the first moment, the mean number of equilibria, in the present model remains always positive for sufficiently large μ. To bound Σ for $N \gg 1$ and $\mu \gg 1$, from below we can use the asymptotics for $p = 1$ in section 1.3.3.6 considering :

$$\lim_{N\to+\infty} \frac{1}{N} \log \mathbb{E}[\det(\mathbf{1}_N\mu - \mathbf{WTW}^T)] = \log \mu \tag{3.70}$$

Clearly $x \leq |x|$ for any real. If one identify x with $\det(\mathbf{1}_N\mu - \mathbf{WTW}^T)$, then

$$\frac{\mathbb{E}_{\mathbf{T}}[\mathcal{Z}_{1,1}]}{\mu^N} \leq \mathcal{N}_\mu \tag{3.71}$$

which gives (for $\mu \gg 1$)

$$0 \leq \lim_{N\to+\infty} \frac{1}{N} \log \mathcal{N}_\mu$$

So far the only rigorous results are eq(**3.70**) and eq(**3.71**). However, without more details on $\mathcal{N}_\mu$, what said above is *circumstantial*. It remains to show that the first inequality in eq(**3.71**) is strict. This implies $\Sigma > 0$ *regardless* of μ. To show this is sufficent to prove that there exists an interval $U \subset (-\infty, 0)$ such that $p(U) > 0$ being p the probability density function of $\det(\mathbf{1}_N\mu - \mathbf{WTW}^T)$. In order to do this without worrying about N being large we investigate the first moment of $S = \frac{1}{2}\left(\text{sign}\left(\det(\mathbf{1}_N\mu - \mathbf{WTW}^T)\right) + 1\right)$. For $\mu \to 0^+$, we expect $\mathbb{E}[S] \simeq \frac{1}{2}$. Conversely for $\mu \gg 1$, we observe (see fig(**3.9**)) that $\log(\log(\mathbb{E}[S]))$ is linear suggesting (qualitatively) that $p(U) > 0$ for $U \subset (-\infty, 0)$. As a final remark, our intent in this section was not to fully describe this model rather to show a first example where the trivialization transition is not seen at the level of annealed complexity extracted from the mean value of equilibria, indicating towards absence of self-averaging. Clearly, more rigorous proofs of the statements above are necessary to have the last word and we postpone further investigations for the future, beyond this thesis.

3.2 Delays in May's Model

We conclude this chapter considering the stability of the May's model where the interacting terms have a delayed response. More precisely, given a vector $\boldsymbol{x} \in \mathbb{R}^N$ representing the state of the system, we want to address the local stability of $\boldsymbol{x} = \mathbf{0}$ for the system [113][114]

$$\frac{d\boldsymbol{x}}{dt} = \int_{-\infty}^{0} d\mathbf{\Pi}(\theta)\boldsymbol{x}(t+\theta) \tag{3.72}$$

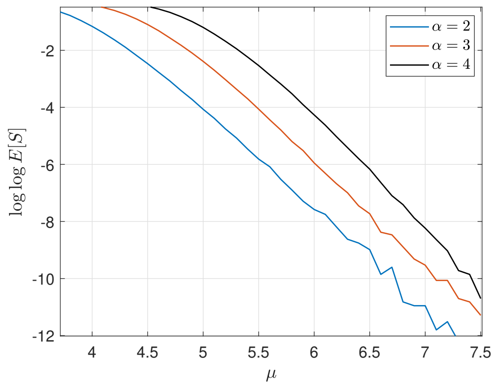

Figure 3.9: Numerical simulations of $S = \frac{1}{2}\left(\text{sign}\left(\det(\mathbf{1}_N\mu - \mathbf{WTW}^T)\right) + 1\right)$ for $N =$ 80. # Samples=10^6.

$\mathbf{\Pi}(\theta)$ is the memory kernel matrix while the integral ranges from $-\infty$ to 0 to respect causality. This generalises eq(**3.1**) which is retrieved considering

$$\mathbf{\Pi}(\theta)d\theta = \lim_{\varepsilon\to 0^+} \frac{2}{\sqrt{2\pi\varepsilon}}\left(-\mu\mathbf{1}_N + \frac{\sigma}{\sqrt{N}}\boldsymbol{\Xi}\right) e^{-\frac{\theta^2}{2\varepsilon}} d\theta$$

Similarly to the non-delayed case, to study the asymptotic stability of the origin one can introduce a small perturbation of the form $\boldsymbol{\delta x} e^{\lambda t}$ in eq(**3.72**). The latter is solution if and only if λ is a zero of the characteristic polynomial $\mathcal{Z}(\lambda)$ defined as:

$$\mathcal{Z}(\lambda) = \det\left(\lambda\mathbf{1}_N - \int_{-\infty}^{0} d\mathbf{\Pi}(\theta)e^{\lambda\theta}\right) \tag{3.73}$$

The stability of $\boldsymbol{x} = \mathbf{0}$ depends on the sign of the real part of λs such that $\mathcal{Z}(\lambda) = 0$. Adopting the terminology from [114], $\mathcal{Z}(\lambda)$ is said to be stable if $\{\lambda \in \mathbb{C}|\, \mathrm{Re}\,\lambda \geq 0, \mathcal{Z}(\lambda) = 0\} = \emptyset$. Additionally, if $\exists\eta > 0$ such that $\int_{-\infty}^{0} e^{-\eta\theta}|d\Pi_{ij}| < +\infty$ and $\mathcal{Z}(\lambda)$ is stable then $\boldsymbol{x} = \mathbf{0}$ in eq(**3.72**) is asymptotically stable. As we know, in absence of delay, the latter implication is also an *if and only if*. Lastly, given a closed and counter-clockwise oriented path γ in the complex plane, the number of zeroes of the partition function in eq(**3.73**), over the size N, contained in the region bounded by γ is given by:

$$\mathcal{N}_\gamma = \frac{1}{2\pi i N}\oint_\gamma \frac{1}{\mathcal{Z}(\lambda)}\frac{d\mathcal{Z}(\lambda)}{d\lambda}d\lambda \tag{3.74}$$

In what follows we will indicate the region of $\mathbb{C}$ with positive real part as the region bounded by γ^+. The latter is given (taking $R \to +\infty$) by the semicircle $\gamma(R)$ from $-iR$ to iR oriented counter-clockwise from argument $-\pi/2$ to $+\pi/2$ and the segment on the imaginary axis connecting iR to $-iR$. Therefore, to address the stability of eq(**3.72**) we will calculate $\mathbb{E}_{\mathbf{\Pi}}[\mathcal{N}_{\gamma+}]$:

$$\mathbb{E}_{\mathbf{\Pi}}[\mathcal{N}_{\gamma+}] = \frac{1}{2\pi i N} \lim_{R\to+\infty} \oint_{\gamma(R)} \mathbb{E}_{\mathbf{\Pi}}\left[\frac{1}{\mathcal{Z}(\lambda)}\frac{d\mathcal{Z}(\lambda)}{d\lambda}\right] d\lambda \tag{3.75}$$

over the random realizations of $\mathbf{\Pi}(\theta)$.

3.2.1 Uniform Memory Kernel

We now consider the case of uniform kernel, i.e.

$$\mathbf{\Pi}(\theta)d\theta = -2\mu\mathbf{1}_N\delta(\theta)d\theta + \frac{1}{\sqrt{N}}\mathbf{W}\nu(\theta)d\theta \tag{3.76}$$

with $W_{ij} \sim \mathcal{N}(0,1)$. The scalar function $\nu(\theta)$ is a uniform delay. Lastly, we introduce $\sigma(\lambda) = \mathcal{L}[\nu](\lambda) = \int_{-\infty}^{0} \nu(\theta)e^{\lambda\theta}d\theta$, i.e. the Laplace transform of $\nu(-\theta)$, a complex function of λ, $\mathcal{L} : \mathbb{C} \to \mathbb{C}$. With these premises, we have

$$\mathcal{Z}(\lambda) = \det\left((\lambda+\mu)\mathbf{1}_N - \frac{\sigma(\lambda)}{\sqrt{N}}\mathbf{W}\right) \tag{3.77}$$

and its derivative is given by

$$\frac{d\mathcal{Z}(\lambda)}{d\lambda} = N\frac{\dot{\sigma}(\lambda)}{\sigma(\lambda)}\mathcal{Z}(\lambda) + \sum_{j=1}^{N} \frac{\dot{\rho}(\lambda)}{\rho(\lambda) - \frac{1}{\sqrt{N}}\lambda_j}\mathcal{Z}(\lambda)$$

where $\rho(\lambda) = (\mu+\lambda)/\sigma(\lambda)$ and λ_j is the eigenvalue of $\mathbf{W}$. Hence, by taking the limit $N \to +\infty$, one retrieves

$$\lim_{N\to+\infty} \frac{1}{N}\mathbb{E}\left[\frac{1}{\mathcal{Z}(\lambda)}\frac{d\mathcal{Z}(\lambda)}{d\lambda}\right] = \left(\frac{\dot{\sigma}(\lambda)}{\sigma(\lambda)} + \dot{\rho}(\lambda)\,\mathbb{E}_X\left[\frac{1}{\rho(\lambda) - X}\right]\right)$$

where X is distributed according to the circle law. Hence, $\mathbb{E}[\frac{1}{\rho - X}] = \frac{1}{\pi}\int_{-\pi}^{+\pi} d\theta \int_0^1 dr \frac{r}{\rho - re^{i\theta}}$. The latter equals

$$\mathbb{E}_X\left[\frac{1}{\rho - X}\right] = \begin{cases} \frac{1}{\rho} & \text{if } |\rho| \geq 1 \\ \frac{|\rho|^2}{\rho} & \text{if } |\rho| < 1 \end{cases} \tag{3.78}$$

Therefore, the value of $\mathbb{E}[\mathcal{N}_{\gamma+}]$ is given by ($\omega \in \mathbb{R}$):

$$\mathbb{E}[\mathcal{N}_{\gamma+}] = \frac{1}{2} - \frac{1}{2\pi}\,\mathrm{Im}\left(\int_{|\rho(i\omega)|\geq 1} \frac{id\omega}{\mu + i\omega} + \int_{|\rho(i\omega)|<1}\left((1 - |\rho(i\omega)|^2)\frac{\sigma'(i\omega)}{\sigma(i\omega)} + i\frac{|\rho(i\omega)|^2}{\mu + i\omega}\right)d\omega\right) \tag{3.79}$$

with $\sigma'(i\omega) = \frac{d}{d\omega}\sigma(i\omega)$.

3.2.1.1 Exponential Kernel

We now write eq(**3.79**) for an exponential kernel, i.e. $\nu(\theta) = \frac{\exp(\theta/\tau)}{\tau}$ for a given time of delay $\tau > 0$. In neural networks, such delay is supposed to be inversely proportional to the axonal diameter, usually drawn from an experimentally fitted Gamma distribution (see as an example [115]). For this choice of ν, $\sigma(i\omega) = \frac{i}{i-\tau\omega}$, $|\rho(i\omega)| = \sqrt{\omega^2+\mu^2}\sqrt{1+\tau^2\omega^2}$. Clearly, $|\rho(i\omega)| \geq 1$ for $\mu > 1$, conversely for $0 < \mu < 1$ the same inequality holds whenever $|\omega| \geq \omega_*$ defined as

$$\omega_* = \sqrt{-\frac{1+\mu^2\tau^2}{2\tau^2} + \frac{1}{2}\sqrt{\frac{1+4\tau^2-2\mu^2\tau^2+\mu^4\tau^4}{\tau^4}}}$$

Substituting these relations into eq(**3.79**), we obtain

$$\mathbb{E}[\mathcal{N}_{\gamma+}] = \begin{cases} 0 & \text{if } \mu \geq 1 \\ -\frac{1}{\pi}\mu\omega_* - \frac{1}{3\pi}\mu\tau^2\omega_* + \frac{1}{\pi}\arctan\left(\frac{\omega_*}{\mu}\right) & \text{if } 0 < \mu < 1 \end{cases} \tag{3.80}$$

We can recover May's bound by taking $\tau \to 0^+$, i.e. for $0 < \mu < 1$,

$$\mathbb{E}[\mathcal{N}_{\gamma+}] = -\frac{\mu}{\pi}\sqrt{1-\mu^2} + \frac{1}{\pi}\arctan\left(\frac{\sqrt{1-\mu^2}}{\mu}\right) \tag{3.81}$$

One can easily prove that, for $N \gg 1$, eq(**3.81**) is equivalent to counting how many eigenvalues of the Ginibre matrix $\frac{1}{\sqrt{N}}\mathbf{W}$ (on average) have real part greater than μ. As we see in eq(**3.80**), the regimes depend only on the value of μ and not τ. That is to say, that the stability of the origin is unchanged and May's bound is respected. For a sufficient condition to modify this by uniform memory kernels we could proceed as follows. For a kernel $\nu(\theta;\varphi)$ for some parameter φ, the condition $|\rho(i\omega)| \geq 1$ has to be satisfies by $\mu \in U(\varphi)$ where such interval is a function of φ.

Chapter 4

Random Constrained Optimization

4.1 Introduction

Constrained Optimization plays a significant role in several and different fields of research. The problem of minimizing a cost function, $\mathcal{H}$, over a feasible set $\mathcal{X}$ arise, for example, in Finance [116][117], Physics [118][119] and Biology [120][121]. Therefore, it is natural to identify a common paradigm of solutions and equivalence classes for such problems. Frequently, regardless of the form of $\mathcal{H}$, the number and the complexity of the constraints prevent an explicit description of the feasibility space $\mathcal{X}$ and, therefore, of $\min_{\boldsymbol{x}\in\mathcal{X}}\{\mathcal{H}(\boldsymbol{x})\}$. As a particular example one may mention the financial portfolio usually constrained by budget and transaction costs. Another example is given by the folding process of proteins, from the unfolded to the native state within a thermal bath [122]. In particular, the mechanism behind the formation of extra-molecular bonds, mostly of hydrogen type among amino-acids, is still not completely understood. The folding is associated to the minimisation of a potential function, usually consisting of non-linear terms with respect to the distance between pairs of constituents. The difficulties mainly stem from the high dimensionality of the problem and in modelling such a potential. The hyper-dimensional surface given by the latter is usually studded by critical points producing an extremely complicated topology. In ecological dynamics it has been recently shown that, the dual formulation for quadratic programming of certain convex problems leads to a one-to-one correspondence with the stationary solution of the MacArthur model [121]. In the context of statistical mechanics such a problem is associated to the jamming of hard spheres. By increasing the pressure of a liquid, a glass phase appears and the space available for moving the spheres shrinks to zero, with an exponential number of metastable states and broken hergodicity [123]. The latter corresponds to disconnected clusters in the phase space. Further increase of pressure reveals an additional transition (Gadner transition) with ultrametric structures forming in the configuration space and completely suppressing diffusion [124].

A first classification regarding the optimisation problems so far mentioned is based on the definition of convexity. A problem is said to be convex if both $\mathcal{H}$ and $\mathcal{X}$ are convex when defined as a function and, respectively, a set. These problems form a large and well investigated class for which analytical results for existence and uniqueness of $\arg\min\{\mathcal{H}\}$ are known (see [125]). However, required convexity is not always present and, additionally, either $\mathcal{H}$ or $\mathcal{X}$ might be regarded as a source of randomness. Therefore, in order to have the most general mathematical framework, in the present work, we consider multiple source of randomness: we assume $\mathcal{H}$ and $\mathcal{X}$ are a random function and a random set respectively. Different level of randomness has been introduced in literature. As an example, in neural networks, the cost function has the form $\sum_{i,j} \mathbf{H}_{ij} s_i s_j$ with $\mathbf{H}_{ij}$ being the random interaction matrix coupling spin s_i and s_j [126]. $\mathbf{H}$ gives rise to multiple metastable states $s_i = \text{sign}\left(\sum_{ij} \mathbf{H}_{ij} s_j\right)$ and aging phenomena [127][126]. More simply, for $\mathbf{H} \in GOE(N)$ and the vector $(s_1, ..., s_N)$ being of a fixed unit length the minimisation problem reduces to finding the maximal eigenvalue and therefore leads to the celebrated Tracy-Widom distributions [19]. In this scenario there are $2N$ critical points in the cost function landscape. The inclusion of an additional random linear term in the cost function, $\boldsymbol{h}^T \boldsymbol{s}$, such that $\|\boldsymbol{h}\| \gg N^{-1/6}$ dramatically simplifies the set of critical points with only two (the maximum and the minimum) remaining in the cost (energy) function hence the aging phenomena mentioned above disappear [128]. One can further impose additional constraints in the form of inequalities and it was considered in modelling the perceptron [129]. The initial feasible set is partitioned into two subsets $\mathcal{S}_1$ and $\mathcal{S}_2$ according to the sign of $\boldsymbol{a}^T \boldsymbol{s} - T < 0$ where the pair $(\boldsymbol{a}, T > 0)$ is given and $\boldsymbol{s}$ is a configuration of the system [129]. By introducing M multiple constraints of this kind the problem can be satisfied (sat) or unsatisfied (unsat) whenever the set $\mathcal{X} = \emptyset$. The transition between the two phases occurs with probability $p \to 1$, in the thermodynamic limit $N \to +\infty$ with $\alpha = M/N < \infty$ [124][130]. The case $T < 0$ corresponds to the complete absence of convexity for $\mathcal{X}$ as the latter is reduced to multiple and non-connected sub-domains.

With these premises, in what follows, we introduce a general framework for investigating these systems. Therefore we consider a generic quadratic minimisation problem, belonging to the NP-family, able to reproduce most of the features described above. We assume that disorder appears in several quantities. However, this work is at an early stage and it will be completed in the incoming future.

4.2 Work in Progress

We consider the following minimisation problem:

$$\begin{cases} \min_{\boldsymbol{x}\in\mathcal{X}} \left\{ \frac{1}{2}\boldsymbol{x}^T\mathbf{H}\boldsymbol{x} + \boldsymbol{h}^T\boldsymbol{x} \right\} \\ \mathcal{X} = \{\boldsymbol{x} \in \mathbb{R}^N | \|\boldsymbol{x}\|_2^2 = N, \mathbf{A}\boldsymbol{x} \le \boldsymbol{b}\} \end{cases} \tag{4.1}$$

Where $\mathbf{H} \in GOE(N)$ with probability $dp(\mathbf{H}) \propto e^{-N/4J^2 \operatorname{Tr} \mathbf{H}^2} d\mathbf{H}$ from eq(**1.1**). The matrix $\mathbf{A}$ is a $M \times N$ real Ginibre matrix, i.e. with independent and identically distributed Gaussian entries: $\mathbb{E}[a_{ij}] = 0$ $\mathbb{E}[a_{ik}a_{jl}] = \delta_{kl}\delta_{ij}A^2$. The M-dimensional vector $\boldsymbol{b}$ has Gaussian entries with $\mathbb{E}[b_ib_j] = \delta_{ij}B^2$, $\mathbb{E}[b_i] = K$. Lastly $\boldsymbol{h}$ is a N-dimensional Gaussian vector with $\mathbb{E}[h_ih_j] = \delta_{ij}\delta^2$ and $\mathbb{E}[h_i] = 0$. We will perform the limit $N \to +\infty$ and we will consider $M/N = \alpha < +\infty$. Taking the first limit is the standard practice in the literature and allows to derive the closed form expressions ([131][132]). The second hypothesis is physical as, for the system mentioned above, α can be intepreted as the packing fraction in jamming of granual materials [133][134]. Additionally, the form of the inequality constraints, again for $N \to +\infty$, is identical to the Hopfield model presented in [135] considering the optimal storage of an infinite number of patterns. Secondly, given the randomness of the triple $(\mathbf{H}, \mathbf{A}, \boldsymbol{b})$ the problem is not convex *a priori*. In order to tackle this problem we consider the cost function as an effective energy and, given the positive parameter β, which we interpret as fictitious inverse temperature, introduce the partition function $\mathcal{Z}$ over the sphere $\|\boldsymbol{x}\|^2 = N$:

$$\mathcal{Z} = \int_{\|\boldsymbol{x}\|^2=N} d\boldsymbol{x} e^{-\beta\mathcal{H}(\boldsymbol{x})} \prod_{k=1}^{M} \theta(b_k - \boldsymbol{a}_k^T\boldsymbol{x})$$

With $\mathcal{H}(\boldsymbol{x}) = \frac{1}{2}\boldsymbol{x}^T\mathbf{H}\boldsymbol{x} + \boldsymbol{h}^T\boldsymbol{x}$. In the limit $N \to +\infty$, for $\beta = 0$, $\mathcal{Z}$ is proportional to the volume of the feasible set, i.e. $|\mathcal{X}|$ within $\mathbb{R}^N$. From now on, with the replica trick introduced in the first chapter, we consider $\mathbb{E}[\log \mathcal{Z}] = \lim_{n\to 0} \log \mathbb{E}[\mathcal{Z}^n]/n$, i.e. we will assume that such limit exists by analytic continuation (see section 1.1.1.2,[136] and [27]). For $B \to 0$, by employing the saddle point approximation, presented in some detail in appendix D, we retrieve the well known replica Gadner bound maximum storage i.e.:

$$\alpha_{max,G}(K) = \frac{1}{\sqrt{2\pi}}\Big(\int_k^{+\infty} dt e^{-\frac{1}{2}t^2}(t-K)^2\Big)^{-1}$$

In neural networks, this represents the upper limit of the storage capacity of patterns of given magnetization. However in the case $B \neq 0$, i.e. of $\boldsymbol{b}$ being random, we can't simply average $\alpha_{max,G}$ above over $\boldsymbol{b}$. Indeed, we are able to show that (see the calculation outlined in appendix D)

$$\alpha_{max}(K) = \lim_{q\to 1^-}\left((1-q)\int dx \frac{e^{-\frac{1}{2\sigma^2}(x-\mu)^2}}{\sqrt{2\pi\sigma^2}}\Big(\frac{d}{dx}\log\Big(1+\mathrm{erf}\Big(\frac{x}{\sqrt{2}}\Big)\Big)\Big)^2\right)^{-1} \tag{4.2}$$

where $\mu = K/(C\sqrt{1-q})$, $\sigma^2 = \frac{1+d^2q}{d(1-q)}$, $C=\sqrt{N}A$ and $d = C/B$. Similarly, to the definition of $\alpha_{max,G}(K)$, $\alpha_{max}(K)$ defines an upper bound for M/N for which a replica symmetry solution can be obtained. One can easily see that for $B \to 0^+$ it holds $\alpha_{max} \to \alpha_{max,G}$ while in general $\alpha_{max} \leq \alpha_{max,G}$ (see fig(**4.1**)). The variable q is introduced in the replica symmetric ansatz, i.e. as the off-diagonal entry of $Q_{a,b} = \boldsymbol{x}_a^T\boldsymbol{x}_b$. From eq(**4.2**), α_{max} clearly does not depend on β.

The free energy $f(\beta) = -\lim_{N\to+\infty, n\to 0}\frac{1}{N\beta}\mathbb{E}\left[\log\mathcal{Z}\right]$ in this case is given by:

$$f(\beta) = -\frac{\beta J^2}{4}(1-\tilde{q}^2) - \frac{\beta\delta^2}{2}(1-\tilde{q}) - \frac{1-\alpha}{2\beta}\log(1-\tilde{q})$$

Where $\tilde{q}$ solves:

$$\frac{\beta^2J^2}{2}Q_{a,b}(\tilde{q}) + \frac{\beta^2\delta^2}{2} + \frac{1}{2}(Q^{-1})_{a,b}(\tilde{q}) + \alpha\frac{\partial}{\partial Q_{a,b}}\log\mathcal{I}_n(Q)(\tilde{q}) = 0 \tag{4.3}$$

with $Q_{a,b}(q) = q + (1-q)\delta_{a,b}$ and $\mathcal{I}_n(Q) = \int_{\mathbb{R}^n}\frac{d\boldsymbol{u}}{(2\pi)^{n/2}}\mathbb{E}\left[\prod_{k=1}^n\theta(b-u_k)\right]\frac{e^{-\frac{1}{2C^2}\boldsymbol{u}^T\mathbf{Q}^{-1}\boldsymbol{u}}}{\sqrt{\det\mathbf{Q}}}$. With the considerations above we can finally formulate our main result (See fig(**4.2**)):

Result: *the average of the minimised function in eq(**4.1**), for $B\to 0^+$, is given by:*

$$\mathbb{E}\left[\min_{\boldsymbol{x}\in\mathcal{X}}\left\{\frac{1}{2}\boldsymbol{x}^T\mathbf{H}\boldsymbol{x} + \boldsymbol{h}^T\boldsymbol{x}\right\}\right] = -\sqrt{J^2+\delta^2}\sqrt{\Delta} \tag{4.4}$$

with $\Delta = 1 - \frac{\alpha}{\alpha_{max}}$

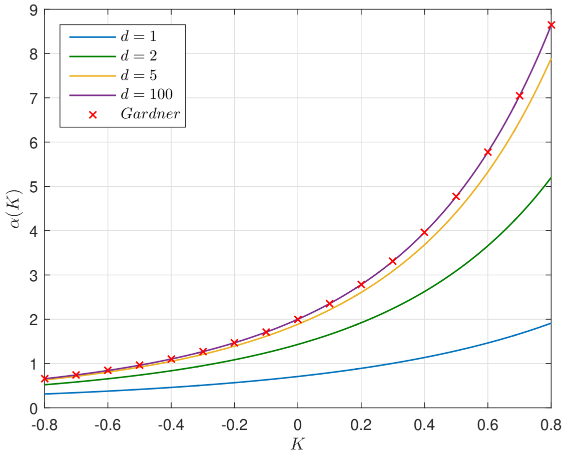

Figure 4.1: Maximum storages α_{max} and $\alpha_{max,G}$

4.3 Outline of the Calculation

The brief section above contains the early stage of my recent research. There are several interesting features worth mentioning. The maximum storage decreases upon introducing additional source of disorder in the selection of feasible points (i.e. $B \neq 0$). Secondly, for $B = 0$, the value of the minimized function increases almost linearly for sufficiently small α. As α increases even simulations fail to give reliable results (fig(**4.2**)). To find a feasible point which does not violate any constraint is a hard task. As one consider $N \gg 1$ the simulation time grows exponentially. An hypothesis to explain this behaviour could be that the well surrounding the minimum of $\mathcal{H}$ shrinks as either the dimensionality or the maximum storage increase. As shown in fig(**4.2**), this phenomenon poses significant challenges for performing numerics which would deserve a separate chapter. At present, the author is focusing on numerical evaluations of eq(**4.3**) and eq(**4.1**). The latter is approached by the RALM algorithm developed in [137]. Since eq(4.4) has been obtained in the replica symmetry ansatz, it's necessary to compute the eigenvalues of $\partial^2\varphi_n/\partial\mathbf{Q}_{a,b}\partial\mathbf{Q}_{c,d}$ to make sure $\tilde{q}$ is effectively a saddle point. However, an explicit solution for $\tilde{q}$ is not available due to the presence of the logarithmic term. Therefore the stability of $\tilde{q}$ will be performed by using the Almeida-Thouless analysis for Sherrington-Kirkpatrick spin glass [138]. At present the main difficulty is related to the amount of terms which need to be verified numerically and numerical singularities.

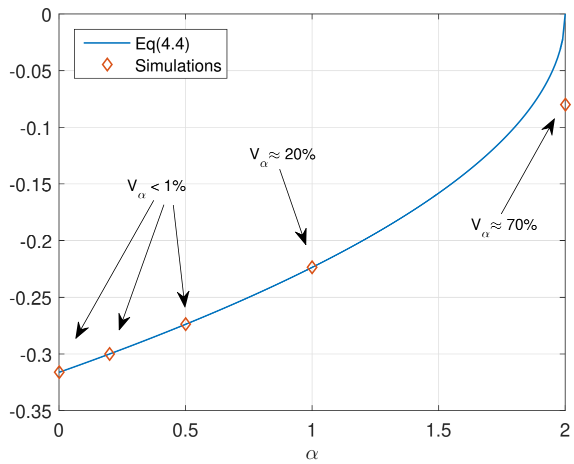

Figure 4.2: $\mathbb{E}[\min_{\boldsymbol{x}\in\mathcal{X}}\left\{\frac{1}{2}\boldsymbol{x}^T\mathbf{H}\boldsymbol{x}+\boldsymbol{h}^T\boldsymbol{x}\right\}]$ as function of α, with $B=0$, $K=0$, $\alpha_{max}=2$, $J^2+\delta^2=0.1$. V_α is the average number of violated constraints in simulations(# Samples= 10^7) with $N=70$ and $K=0$.

Chapter 5

Conclusions

In this thesis, through the lens of Random Matrix Theory, we explored several applications of characteristic polynomials and their asymptotics.

In chapter 2, we considered the characteristic function of the off-diagonal entries of the Wigner reaction matrix $\mathbf{K}_{ab}$ for quantum chaotic scattering. In presence of random Gaussian coupling channels, this quantity can be written as average of ratio of characteristic polynomials and was evaluated in the presence of absorption, representing a significant extension of the earlier result from the work by A. Nock and Y.Fyodorov [35]. For systems with broken time-reversal symmetry, the characteristic function has a determinant structure and one is able to obtain an explicit formula for the joint distribution of its real and imaginary part. In contrast, investigations of systems for which such symmetry is preserved represent a harder task. While it would be natural to expect that the characteristic function of $\mathbf{K}_{ab}$ can be expressed in a Pfaffian form, we were able to obtain the latter only as a double integral. Despite this, the second moment assumes a pretty simple form suggesting that an integrable form could be, in principle, achieved. Beyond the numerical comparison provided, the importance of these results found applications in very recent experiments with microwave networks.

In chapter 3, we described an application of Random Matrix Theory to dynamical systems governed by random Gaussian fields. This work represents the core of this thesis. The stability of randomly assembled systems, consisting of a large number of interacting species, has attracted considerable attention in biology since May's seminal work in 1972 [16]. May revealed mechanisms of inherent local instability arising when either the interaction strength or the number of constituents exceeds a certain

threshold. The introduction of non-linear velocity functions reveals a rich and diverse phase space landscape which abruptly changes from having exponentially many to a unique fixed point (topology trivialization) [128]. Starting from these premises, we were able to push forward the investigations concerning the resilience of such systems. We estimated the characteristic length of the basin of attraction of a fixed point at the origin by including all higher order terms of the Taylor expansion of the random Gaussian velocity field. In particular, it was revealed that, for a large system, there exists a (resilience) radius r^* such that, as long as the origin is asymptotically stable, all other fixed points are pushed away from it, beyond r^*. This work confirmed that the ability for a random system to recover from a disturbance resides in the high order correlations among the components. This represents a new challenge as most of the investigations and available databases merely investigated the *linear* interactions.
It is generally believed that the time-independent analysis of the dynamical systems above is universal. We challenged this statement in section 3.1.5. For a superposition of random periodic potentials, we numerically showed that the topology trivialization disappears whenever the amplitudes and the wave numbers are both Gaussian random variables. Namely, there are always exponentially many fixed points regardless of the relaxation-complexity ratio. We were not able to explicitly obtain the mean number of fixed points. This, in fact, is a very hard task. The techniques developed for this thesis were only able to scratch the surface of their complexity. The ensemble of matrices related to this problem reveals several interesting features, starting from the unbounded support of the limit spectral density, absent in the classical ensembles. At the end of these chapter, a digression on May's model with delay is included.

We conclude this work with a preliminary investigation on the minimisation of a quadratic function constrained to a set of random inequalities in chapter 4. We obtained, in the replica symmetric approach, the value of the minimum of this cost function as a function of α, i.e. the ratio between the number of constraints and the size of the system. Even the simplest numerical comparison is made difficult by the dimensionality of the problem and, as α increases, the simulations are not able to satisfy all the constraints.

5.1 Further Research

In this work we have investigated several aspects and applications of characteristic polynomials of random matrices. For each chapter, there is plenty of questions that need to be addressed in the future. This can be summarized as follow:

- In section 1.1.2, an interesting generalization of eq(**1.76**) is to replace λ with a diagonal matrix containing $(\lambda_1, ..., \lambda_N)$. This would be beneficial for addressing more realistic models of randomly assembled dynamical systems. A possible approach, at least for few independent λ_i, is to follow the steps in appendix A up to eq(**A.16**). However, a more general form for the latter is needed.

- section 1.1.3 opens the question about the bounded support for generalized Wishart matrices. Even keeping $\boldsymbol{w}$ as presented in [13], it would be interesting to analyse which conditions for $p_T(t)$ lead to bounded spectral support for $N \to +\infty$. This is likely to depend on the tail distribution of T.

- For the same ensemble mentioned above, correlations for characteristic polynomials reveals new features on the de-correlation of the eigenvalues. A general and explicit expression, even for $\beta = 2$ and any integer p, for eq(**1.86**) would shed light on this behaviour. In fact the eigenvalues surrounding the center of spectrum are "packed" in the classic sense while the maximal eigenvalue follows a un-rescaled Tracy-Widom distribution.

- For chapter 2, beyond the absence of a clear Pfaffian-determinant structures, other questions involve the statistics for the Wigner reaction matrix at the values of energy sufficiently close to the edge of the spectrum. Another completion to the present work is undoubtedly the derivation of the joint distribution for components of $\mathbf{K}_{ab}$ for systems with time reversal symmetry. It is likely that one has to devise an alternative route to what has been shown here.

  This is due to the absence of "orthogonal" Harish-Chandra integral. A further possible extension of chapter 2 could include periodically driven disturbances. To this onset one would introduce the circular ensembles given by eq(**1.66**).

- In section 3.1.3, we have used topological complexity to analyze the basin of attraction of a randomly assembled dynamical system. The path to instability for the fixed point is accompanied by the emergence of bifurcations. In particular, the Andronov-Hopf bifurcation depends on the correlations between left and right eigenvectors of real Ginibre matrices. A possible way to address the dynamics was presented although not complete.

Appendix A

Appendix for Chapter 1

A.1 Derivation of Eq(1.75) and Eq(1.76)

In this section we prove the results stated in eq(1.75) and eq(1.76). The latter is needed for evaluating the matrix expectation appearing in eq(3.15). We will first recover the exact result for any N, λ and ε. Later, we will analyse the large N behaviour. We will derive such results following the approach contained in [139, 140]. We want to investigate the following expectation

$$\mathbb{E}_{\text{GinOE}}[|\det(\lambda \mathbf{1}_N + \varepsilon \boldsymbol{h} \otimes \boldsymbol{h}^T - \boldsymbol{\Xi})|] \tag{A.1}$$

We assume that $\lambda, \varepsilon \in \mathbb{R}$ and $\boldsymbol{h} \in \mathbb{R}^N$. The expectation above is with respect to real Ginibre matrices, i.e. the entries of $\boldsymbol{\Xi}$ are i.i.d. standard Gaussian random variables. The required expectation in eq(3.15) is simply obtained with the substitution:

$$\lambda = \mu\sqrt{\frac{N}{C'(r^2)}}, \quad \varepsilon = \mu\sqrt{N\frac{C(r^2)}{\Delta(r^2)}}\left(1 - \frac{C'(r^2)}{C(r^2)}r^2\right) - \mu\sqrt{\frac{N}{C'(r^2)}}, \tag{A.2}$$

and

$$\boldsymbol{h} = (1, 0, ..., 0)^T.$$

To exploit the techniques of this thesis, we write the absolute value $|x|$ as the ratio $x^2/\sqrt{x^2}$. Hence eq(A.1) can be written as

$$\mathbb{E}_{\text{GinOE}}[|\det(\boldsymbol{\Lambda} - \boldsymbol{\Xi})|] \propto \mathbb{E}_{\text{GinOE}}\left[\frac{\det^2(\boldsymbol{\Lambda} - \boldsymbol{\Xi})}{\sqrt{\det^2(\boldsymbol{\Lambda} - \boldsymbol{\Xi})}}\right] = \mathbb{E}_{\text{GinOE}}\left[\frac{\det\begin{pmatrix} 0 & i(\boldsymbol{\Lambda}-\boldsymbol{\Xi}) \\ i(\boldsymbol{\Lambda}-\boldsymbol{\Xi})^T & 0\end{pmatrix}}{\det\begin{pmatrix} 0 & i(\boldsymbol{\Lambda}-\boldsymbol{\Xi}) \\ i(\boldsymbol{\Lambda}-\boldsymbol{\Xi})^T & 0\end{pmatrix}^{1/2}}\right]. \tag{A.3}$$

To simplify the notation we have introduced the matrix $\boldsymbol{\Lambda} = \lambda \mathbf{1}_N + \varepsilon \boldsymbol{h} \otimes \boldsymbol{h}^T$. Another essential ingredient is to observe that the numerator in eq(A.3) can be written in terms of a Berezin integral. Namely, the characteristic polynomial of any $N \times N$ matrix $\boldsymbol{A}$ can be written as (see section 1.1.1.3)

$$\det \boldsymbol{A} = \int d\boldsymbol{\psi} d\tilde{\boldsymbol{\psi}} \exp\left(\tilde{\boldsymbol{\psi}}^T \boldsymbol{A} \boldsymbol{\psi}\right) \tag{A.4}$$

The symbolic integral runs over the anti-commuting N-dimensional Grassmann vectors $\boldsymbol{\psi}$ and $\tilde{\boldsymbol{\psi}}$. The matrix appearing at the denominator of eq(A.3) is symmetric. Hence its determinant, if the real part of the eigenvalues is positive, admits the representation by Gaussian integral, i.e.

$$(\det \boldsymbol{A})^{-1/2} = \frac{1}{(2\pi)^{\frac{N}{2}}} \int_{\mathbb{R}^N} d\boldsymbol{x} \exp\Big(- \frac{1}{2}\boldsymbol{x}^T \boldsymbol{A} \boldsymbol{x}\Big), \tag{A.5}$$

The integral above, once applied to eq(A.3), requires the introduction of a regularizing parameter $p \in \mathbb{R}^+$. With all these premises, we can finally introduce

$$\begin{aligned} \mathcal{D}(\lambda, \varepsilon, \boldsymbol{h}, p) = \mathbb{E}_{\text{GinOE}}\left[\frac{\det^2(\boldsymbol{\Lambda} - \boldsymbol{\Xi})}{\sqrt{\det(2p\mathbf{1}_N + (\boldsymbol{\Lambda} - \boldsymbol{\Xi})^T(\boldsymbol{\Lambda} - \boldsymbol{\Xi}))}}\right] \propto \\ \mathbb{E}_{\text{GinOE}}\Big[\int d\boldsymbol{\psi} d\tilde{\boldsymbol{\psi}} e^{-i \begin{bmatrix}\tilde{\boldsymbol{\psi}}_1 \\ \tilde{\boldsymbol{\psi}}_2\end{bmatrix}^T \begin{bmatrix}\mathbf{0}_N & (\boldsymbol{\Lambda} - \boldsymbol{\Xi}) \\ (\boldsymbol{\Lambda} - \boldsymbol{\Xi})^T & \mathbf{0}_N\end{bmatrix} \begin{bmatrix}\boldsymbol{\psi}_1 \\ \boldsymbol{\psi}_2\end{bmatrix}} \\ \int_{\mathbb{R}^{2N}} d\boldsymbol{x}_1 d\boldsymbol{x}_2 e^{-\frac{1}{2}\begin{bmatrix}\boldsymbol{x}_1 \\ \boldsymbol{x}_2\end{bmatrix}^T \begin{bmatrix}\sqrt{2p}\mathbf{1}_N & i(\boldsymbol{\Lambda} - \boldsymbol{\Xi}) \\ i(\boldsymbol{\Lambda} - \boldsymbol{\Xi})^T & \sqrt{2p}\mathbf{1}_N\end{bmatrix} \begin{bmatrix}\boldsymbol{x}_1 \\ \boldsymbol{x}_2\end{bmatrix}}\Big]. \end{aligned} \tag{A.6}$$

As in [141], from now on we will compute the r.h.s. of eq(A.6). Eq(A.1) is obtained by imposing $p \to 0^+$. With this plan in mind, we start by combining the arguments of the exponentials. This is a sum of traces, linear in $\boldsymbol{\Xi}$ and equivalent to

$$\begin{aligned} -\frac{\sqrt{2p}}{2}\operatorname{Tr}(\boldsymbol{x}_1\boldsymbol{x}_1^T + \boldsymbol{x}_2\boldsymbol{x}_2^T) - i\boldsymbol{x}_2^T\boldsymbol{\Lambda}\boldsymbol{x}_1 + i\operatorname{Tr}\boldsymbol{\Lambda}(\boldsymbol{\psi}_2\tilde{\boldsymbol{\psi}}_1^T + \boldsymbol{\psi}_1\tilde{\boldsymbol{\psi}}_2^T) + \\ + i\operatorname{Tr}\boldsymbol{\Xi}^T\left(\frac{1}{2}\boldsymbol{x}_1\boldsymbol{x}_2^T - \boldsymbol{\psi}_1\tilde{\boldsymbol{\psi}}_2^T\right) + i\operatorname{Tr}\boldsymbol{\Xi}\left(\frac{1}{2}\boldsymbol{x}_2\boldsymbol{x}_1^T - \boldsymbol{\psi}_2\tilde{\boldsymbol{\psi}}_1^T\right). \end{aligned} \tag{A.7}$$

The last two traces involve the random matrix $\boldsymbol{\Xi}$. We now evaluate the expectation over such random matricrs, by employing the real Ginibre matrices with the identity

$$\mathbb{E}_{\text{GinOE}}\left[e^{-\operatorname{Tr}(\boldsymbol{\Xi}\boldsymbol{A} + \boldsymbol{\Xi}^T\boldsymbol{B})}\right] = e^{\frac{1}{2}\operatorname{Tr}(\boldsymbol{A}^T\boldsymbol{A} + \boldsymbol{B}^T\boldsymbol{B} + 2\boldsymbol{A}\boldsymbol{B})} \tag{A.8}$$

This identity gives rise to nonlinearities which can be circumvent by introducing a new complex integration variables, q and its complex conjugate $\bar{q}$. This allows to manage the product $(\tilde{\boldsymbol{\psi}_1}^T\boldsymbol{\psi}_1)(\tilde{\boldsymbol{\psi}_2}^T\boldsymbol{\psi}_2)$ and integrate out the anti-commuting variables. These manipulations lead to

$$\mathcal{D}(\lambda,\varepsilon,\boldsymbol{h},p) \propto \int_{\mathbb{C}} dq d\bar{q} e^{-|q|^2} \int_{\mathbb{R}^{2N}} d\boldsymbol{x}_1 d\boldsymbol{x}_2 \times \exp\left(-\frac{\sqrt{2p}}{2}(\boldsymbol{x}_1^T\boldsymbol{x}_1+\boldsymbol{x}_2^T\boldsymbol{x}_2) - i\boldsymbol{x}_2^T\Lambda\boldsymbol{x}_1 - \frac{1}{2}(\boldsymbol{x}_1^T\boldsymbol{x}_1)(\boldsymbol{x}_2^T\boldsymbol{x}_2)\right) \times \times \det\begin{bmatrix} q\mathbf{1}_N & i\boldsymbol{\Lambda}+\boldsymbol{x}_1\boldsymbol{x}_2^T \\ i\boldsymbol{\Lambda}+\boldsymbol{x}_2\boldsymbol{x}_1^T & \bar{q}\mathbf{1}_N \end{bmatrix} \quad \text{(A.9)}$$

Exploiting the Schur complement for block matrices, the determinant of the $2N\times 2N$ matrix above is given by $\det((|q|^2+\lambda^2)\mathbf{1}_N - (-2\lambda\boldsymbol{h}\boldsymbol{h}^T - (\boldsymbol{h}^T\boldsymbol{h})\boldsymbol{h}\boldsymbol{h}^T + i\boldsymbol{x}_2\boldsymbol{x}_1^T\Lambda + i\Lambda\boldsymbol{x}_1\boldsymbol{x}_2^T + (\boldsymbol{x}_1^T\boldsymbol{x}_1)\boldsymbol{x}_2\boldsymbol{x}_2^T))$. Since the matrix in the second parenthesis has rank 3, the determinant reduces to compute $(|q|^2+\lambda^2)^{N-3}((|q|^2+\lambda^2)^3 - e_1(\boldsymbol{R}_N)(|q|^2+\lambda^2)^2 + e_2(\boldsymbol{R}_N)(|q|^2+\lambda^2) - e_3(\boldsymbol{R}_N))$ where e_j is the j-th elementary symmetric polynomial, function of the 3 non-null eigenvalues of $\boldsymbol{R}_N = -2\lambda\boldsymbol{h}\boldsymbol{h}^T - (\boldsymbol{h}^T\boldsymbol{h})\boldsymbol{h}\boldsymbol{h}^T + i\boldsymbol{x}_2\boldsymbol{x}_1^T\Lambda + i\Lambda\boldsymbol{x}_1\boldsymbol{x}_2^T + (\boldsymbol{x}_1^T\boldsymbol{x}_1)\boldsymbol{x}_2\boldsymbol{x}_2^T$. In particular, by recalling $e_j(\boldsymbol{x}) = \sum_{k_{S+1}>k_S} x_{k_1}\dots x_{k_j}$ and by making use of the Newton identities we have: $e_1(\boldsymbol{R}_N) = \operatorname{Tr}\boldsymbol{R}_N$, $e_2(\boldsymbol{R}_N) = (\operatorname{Tr}\boldsymbol{R}_N)^2 - \operatorname{Tr}\boldsymbol{R}_N^2$ and $e_3(\boldsymbol{R}_N) = \frac{1}{2}(\operatorname{Tr}\boldsymbol{R}_N)^3 - \frac{3}{2}(\operatorname{Tr}\boldsymbol{R}_N)(\operatorname{Tr}\boldsymbol{R}_N^2) + \operatorname{Tr}\boldsymbol{R}_N^3$. Hence:

$$\det\begin{bmatrix} q\mathbf{1}_N & i\boldsymbol{\Lambda}+\boldsymbol{x}_1\boldsymbol{x}_2^T \\ i\boldsymbol{\Lambda}+\boldsymbol{x}_2\boldsymbol{x}_1^T & \bar{q}\mathbf{1}_N \end{bmatrix} = (|q|^2+\lambda^2)^{N-3}((|q|^2+\lambda^2)^3 - a_2(|q|^2+\lambda^2)^2 + + a_1(|q|^2+\lambda^2) + a_0) \quad \text{(A.10)}$$

with

$$a_2 = ((\boldsymbol{x}_1^T\boldsymbol{x}_1)(\boldsymbol{x}_2^T\boldsymbol{x}_2) + 2i\varepsilon(\boldsymbol{x}_1^T\boldsymbol{h})(\boldsymbol{x}_2^T\boldsymbol{h}) - \varepsilon^2(\boldsymbol{h}^T\boldsymbol{h})^2 + 2i\lambda(\boldsymbol{x}_1^T\boldsymbol{x}_2) - 2\varepsilon\lambda(\boldsymbol{h}^T\boldsymbol{h})) \quad \text{(A.11)}$$

$$\begin{aligned} a_1 = &-\varepsilon^2((\boldsymbol{x}_1^T\boldsymbol{h})^2 - (\boldsymbol{h}^T\boldsymbol{h})(\boldsymbol{x}_1^T\boldsymbol{x}_1))((\boldsymbol{x}_2^T\boldsymbol{h})^2 - (\boldsymbol{h}^T\boldsymbol{h})(\boldsymbol{x}_2^T\boldsymbol{x}_2)) + 2\varepsilon\lambda(-(\boldsymbol{x}_1^T\boldsymbol{h})(\boldsymbol{x}_2^T\boldsymbol{h})(\boldsymbol{x}_1^T\boldsymbol{x}_2) \\ &+ (\boldsymbol{x}_1^T\boldsymbol{x}_1)(\boldsymbol{x}_2^T\boldsymbol{h})^2 + (\boldsymbol{x}_2^T\boldsymbol{x}_2)(\boldsymbol{x}_1^T\boldsymbol{h})^2 - (\boldsymbol{h}^T\boldsymbol{h})(\boldsymbol{x}_1^T\boldsymbol{x}_1)(\boldsymbol{x}_2^T\boldsymbol{x}_2) + i\varepsilon(\boldsymbol{h}^T\boldsymbol{h})((\boldsymbol{x}_1^T\boldsymbol{h})(\boldsymbol{x}_2^T\boldsymbol{h}) \\ &- (\boldsymbol{h}^T\boldsymbol{h})(\boldsymbol{x}_1^T\boldsymbol{x}_2))) + \lambda^2((\boldsymbol{x}_1^T\boldsymbol{x}_1)(\boldsymbol{x}_2^T\boldsymbol{x}_2) - (\boldsymbol{x}_1^T\boldsymbol{x}_2)^2 - 4i\varepsilon(\boldsymbol{h}^T\boldsymbol{h})(\boldsymbol{x}_1^T\boldsymbol{x}_2) + 4i\varepsilon(\boldsymbol{x}_1^T\boldsymbol{h})(\boldsymbol{x}_2^T\boldsymbol{h}) \end{aligned} \quad \text{(A.12)}$$

$$\begin{aligned} a_0 = &\varepsilon(-2(\boldsymbol{x}_1^T\boldsymbol{h})(\boldsymbol{x}_1^T\boldsymbol{x}_2)(\boldsymbol{x}_2^T\boldsymbol{h}) + (\boldsymbol{x}_1^T\boldsymbol{x}_1)(\boldsymbol{x}_2^T\boldsymbol{h})^2 + (\boldsymbol{x}_2^T\boldsymbol{x}_2)(\boldsymbol{x}_1^T\boldsymbol{h})^2 + (\boldsymbol{h}^T\boldsymbol{h})((\boldsymbol{x}_1^T\boldsymbol{x}_2)^2 \\ &- (\boldsymbol{x}_1^T\boldsymbol{x}_1)(\boldsymbol{x}_2^T\boldsymbol{x}_2)))(-\varepsilon(\boldsymbol{h}^T\boldsymbol{h})\lambda^2 - 2\lambda^3) \end{aligned} \quad \text{(A.13)}$$

Eq(**A.10**) is a polynomial in $|q|$. This represents a major simplification as the integral over the complex pair $(q,\bar{q})$ can be solved explicitly in terms of the incomplete gamma function $\frac{1}{4\pi}\int d^2q e^{-|q|^2}(|q|^2+\lambda^2)^n = e^{\lambda^2}\Gamma(n+1,\lambda^2)$ for $n\geq 0$. In addition, the integrand in eq(**A.9**) is a function of a 2×2 positive definite matrix $\boldsymbol{Q}$ and vector $\boldsymbol{t}$ given by

$$\boldsymbol{Q} = \begin{bmatrix} Q_1 & Q \\ Q & Q_2 \end{bmatrix} = \begin{bmatrix} \boldsymbol{x}_1^T\boldsymbol{x}_1 & \boldsymbol{x}_1^T\boldsymbol{x}_2 \\ \boldsymbol{x}_1^T\boldsymbol{x}_2 & \boldsymbol{x}_2^T\boldsymbol{x}_2 \end{bmatrix}, \qquad \text{and} \qquad \boldsymbol{t} = \begin{bmatrix} \boldsymbol{x}_1^T\boldsymbol{h} \\ \boldsymbol{x}_2^T\boldsymbol{h} \end{bmatrix}. \quad \text{(A.14)}$$

We temporarily chose to rename such integrand with $\mathcal{F}$, so that

$$\mathcal{D}(\lambda, \varepsilon, \boldsymbol{h}, p) \propto \int_{\mathbb{R}^{2N}} d\boldsymbol{x}_1 d\boldsymbol{x}_2 \mathcal{F}(\boldsymbol{Q}, \boldsymbol{t}) \tag{A.15}$$

The r.h.s. can be re-written, up to a known proportionality constant, as (see [140])

$$\int_{\mathbb{R}^2} \int_{\boldsymbol{Q}\succ 0} \mathcal{F}(\boldsymbol{Q} + \boldsymbol{t}\boldsymbol{t}^T, h\boldsymbol{t})(\det \boldsymbol{Q})^{\frac{N-4}{2}} d\boldsymbol{Q} d\boldsymbol{t} \tag{A.16}$$

where $\sqrt{\boldsymbol{h}^T\boldsymbol{h}} = h$. The integral in $\boldsymbol{Q}$ runs over all the real 2×2 positive definite symmetric matrices. The term $\mathcal{F}(\boldsymbol{Q} + \boldsymbol{t}\boldsymbol{t}^T, h\boldsymbol{t})(\det \boldsymbol{Q})^{\frac{N-4}{2}}$ in eq(A.16) is proportional to

$$\begin{aligned}
&(Q_1Q_2 - Q^2)^{\frac{N-4}{2}}\Big(- h^2\lambda^2\varepsilon(h^2\varepsilon + 2\lambda)\Gamma(N-2,\lambda^2)(Q^2 - Q_1Q_2) - \\
&\Gamma(N,\lambda^2)(2i\lambda(ih^2\varepsilon + Q + t_1t_2) + (t_1t_2 + ih^2\varepsilon)^2 + Q_1(Q_2 + t_2^2) + Q_2t_1^2) - \Gamma(n-1,\lambda^2)(h^4\varepsilon^2(Q_1Q_2 + 2i\lambda Q) \\
&+ 2h^2\lambda\varepsilon(2i\lambda Q + Qt_1t_2 + Q_1Q_2) + \lambda^2(Q^2 + 2Qt_1t_2 - Q_2(Q_1 + t_1^2) - Q_1t_2^2)) + \Gamma(n+1,\lambda^2)\Big) \\
&\qquad \times \exp\Big[\lambda^2 + \frac{1}{2}(-2it_1t_2(h^2\varepsilon + \lambda) - \frac{1}{2}t_1^2t_2^2 - \sqrt{2p}(Q_1 + Q_2 + t_1^2 + t_2^2) + \\
&\qquad\qquad - 2i\lambda Q - Q_1(Q_2 + t_2^2) - Q_2t_1^2)\Big]
\end{aligned} \tag{A.17}$$

Before addressing the integrals in $\boldsymbol{Q}$ and $\boldsymbol{t}$, we need to introduce an additional manipulation. The bi-quadratic term in the exponent can be replaced, with the help of the Hubbard-Stratonovich transformation by

$$e^{-t_1^2t_2^2/2} \propto \int dy e^{-y^2/2 - iyt_1t_2}.$$

This simplifies our calculation as the integration over the entries of $\boldsymbol{t}$ can be computed as derivatives of a one dimensional Gaussian integral. We are therefore left with the integral over $\boldsymbol{Q}$. We chose to represent the latter as

$$\begin{bmatrix} Q_1 & Q \\ Q & \frac{r^2+Q^2}{Q_1} \end{bmatrix} \tag{A.18}$$

with $r = \det^{1/2}(\boldsymbol{Q})$ and measure $d\boldsymbol{Q} = 2\frac{dQ_1}{Q_1} r dr dQ$ with $r > 0, Q_1 > 0, Q \in \mathbb{R}$. Let introduce the rescaling $Q_1 \to \sqrt{2p}Q_1$ and $t_{1,2} \to (2p)^{1/4}t_{1,2}$ and integrate out r, Q, t_2 and y. At this stage $\mathcal{D}(\lambda, \varepsilon, \boldsymbol{h}, p)$ is a double integral in t_1 and Q_1, i.e.

$$\begin{aligned}
&\mathcal{D}(\lambda, \varepsilon, \boldsymbol{h}, p) \propto 2^{\frac{N-1}{2}}\pi^{\frac{3}{2}} \int_{\mathbb{R}^+} dQ_1 \int_{\mathbb{R}} dt_1 \exp\Big[\frac{-h^4\varepsilon^2t_1^2 - 2h^2\varepsilon\lambda t_1^2 + \lambda^2(Q_1 + t_1^2 + 2)}{2(Q_1 + t_1^2 + 1)} - p(Q_1 + t_1^2)\Big] \\
&\frac{1}{(1+Q_1)^2} Q_1^{\frac{N-3}{2}}(Q_1 + t_1^2 + 1)^{-\frac{N}{2}-4}(b_0(Q_1 + t_1^2 + 1)^2 - b_1t_1^2(Q_1 + t_1^2 + 1)(h^2\varepsilon + \lambda) + \\
&\qquad + b_2(t_1^4(h^2\varepsilon + \lambda)^2 + Q_1^2 + Q_1(t_1^2 + 2) + t_1^2 + 1))
\end{aligned} \tag{A.19}$$

where

$$
\begin{aligned}
s &= 1 + Q_1 + t_1^2 \\
u &= \lambda^2 Q_1 \Gamma(N-1,\lambda^2) - (Q_1 + t_1^2)\Gamma(N,\lambda^2) \\
v &= \lambda^2 Q_1 \Gamma(N-1,\lambda^2) - s\Gamma(N,\lambda^2) \\
b_2 &= -t_1^2 s^2 \Gamma\left(\frac{N}{2}-1\right)(\lambda^2 Q_1 \Gamma(N-1,\lambda^2) - (Q_1+t_1^2)\Gamma(N,\lambda^2)) \\
b_1 &= -2t_1^2 s\Gamma\left(\frac{N}{2}-1\right)(h^2\varepsilon+\lambda)(\lambda^2 Q_1 t_1^2 \Gamma(N-1,\lambda^2) - (t_1^2-1)s\Gamma(N,\lambda^2)) \\
b_0 &= -h^4 s^2 t_1^2 u\varepsilon^2 \Gamma\left(\frac{N}{2}-1\right) + 2h^2 s(Q_1+1)t_1^2 v\varepsilon\Gamma\left(\frac{N}{2}-1\right)(h^2\varepsilon+\lambda)+ \\
&\quad 2\lambda(Q_1+1)st_1^2 v\Gamma\left(\frac{N}{2}-1\right)(h^2\varepsilon+\lambda) - 2h^2\lambda s^2 t_1^2 u\varepsilon\Gamma\left(\frac{N}{2}-1\right) \\
&\quad + (Q_1+1)^2\Bigg(\Gamma\left(\frac{N}{2}-1\right)(\Gamma(N,\lambda^2)(s^2(h^4 s\varepsilon^2 + Ns - Q_1 - t_1^2)+ \\
&\quad + 2h^2\lambda s^2\varepsilon - \lambda^2 Q_1(s+1)) - \Gamma(N-1,\lambda^2)(h^4 Q_1\varepsilon^2(\lambda^2(s+1)+s) + 2h^2\lambda Q_1\varepsilon(\lambda^2(s+1) \\
&\quad + s) - \lambda^2 t_1^2(s-\lambda^2 Q_1)) + e^{-\lambda^2}s^2\lambda^{2N}) + 2s\Gamma\left(\frac{N}{2}\right)(h^2\lambda^2 Q_1\varepsilon(h^2\varepsilon+2\lambda)\Gamma(N-2,\lambda^2) \\
&\quad + \Gamma(N-1,\lambda^2)(-h^4 Q_1\varepsilon^2 - 2h^2\lambda Q_1\varepsilon + \lambda^2(Q_1+t_1^2)) - (Q_1+t_1^2)\Gamma(N,\lambda^2))\Bigg) \\
&\quad + Q_1 s^2 u\Gamma\left(\frac{N}{2}-1\right) - \lambda^2 s^2 t_1^2 u\Gamma\left(\frac{N}{2}-1\right) + s^2 u\Gamma\left(\frac{N}{2}-1\right).
\end{aligned}
$$

To obtain the quantities above we made use of the following identities

$$\Gamma(N+1,\lambda^2) = e^{-\lambda^2}\lambda^{2N} + N\Gamma(N,\lambda^2)$$

and we used the cancellation of the formally divergent integrals by noticing that

$$\Gamma(N+1,\lambda^2) - (N+\lambda^2)\Gamma(N,\lambda^2) + \lambda^2(N-1)\Gamma(N-1,\lambda^2) = 0.$$

One can proceed now with the remaining integrations. However, although we will report the most simplified form for $\mathcal{D}(\lambda,\varepsilon,\boldsymbol{h},p)$, to the purpose of this thesis, it's more suitable to retrieve the large N behaviour from eq(**A.19**). The only remaining step before doing so is the constant of proportionality in eq(**A.6**) which we left (intentionally) unspecified. To this end we consider the limit $p \to +\infty$ in order to observe:

$$\lim_{p\to+\infty}(2p)^{N/2}\mathcal{D}(\lambda,\varepsilon,\boldsymbol{h},p) = \mathbb{E}_{\text{GinOE}}[\det(\lambda\mathbf{1}_N + \varepsilon\boldsymbol{h}\boldsymbol{h}^T - \boldsymbol{\Xi})^2] \tag{A.20}$$

The r.h.s is obtained by introducing two Berezin integrals and follows the same procedure as outlined earlier. This time, one necessarily needs to keep track of the constants of proportionality in order to obtain

$$\mathbb{E}_{\text{GinOE}}[\det(\lambda \mathbf{1}_N + \varepsilon \boldsymbol{h}\boldsymbol{h}^T - \boldsymbol{\Xi})^2] = \lambda^{2N} + (N + h^4\varepsilon^2 + 2\lambda h^2\varepsilon)e^{\lambda^2}\Gamma(N,\lambda^2) \quad \text{(A.21)}$$

In eq(**A.19**), if we take $p \to +\infty$, necessarily the most relevant contribution to the double integral is given by $Q_1 \to 0^+$ and $t_1 \to 0$.

For these limits, the integrand eq(**A.19**) is proportional to $\mathbb{E}_{GinOE}[\det(\lambda \mathbf{1}_N + \varepsilon \boldsymbol{h}\boldsymbol{h}^T - \boldsymbol{\Xi})^2]e^{-\lambda^2}\Gamma(\frac{N}{2}-1)$. Therefore, for $p \to +\infty$, it holds

$$C_N \Gamma\Big(\frac{N}{2}-1\Big)2^{\frac{N-1}{2}}\pi^{\frac{3}{2}} \times \lim_{p\to+\infty}(\sqrt{2p})^N \int_{\mathbb{R}} dt_1 \int_{\mathbb{R}^+} dQ_1 \exp\Big[-p(Q_1+t_1^2) - \frac{1}{2}(\varepsilon^2h^4 + 2\varepsilon\lambda h^2)t_1^2\Big]Q_1^{\frac{N-3}{2}} = 1 \quad \text{(A.22)}$$

Then

$$C_N = (4\sqrt{2}\pi^{\frac{5}{2}}\Gamma(N-2))^{-1}.$$

Eq(**A.1**) is finally given, setting the limit $p \to 0^+$, namely by

$$\begin{aligned}
&\mathbb{E}_{GinOE}[|\det(\lambda \mathbf{1}_N + \varepsilon \boldsymbol{h}\boldsymbol{h}^T - \boldsymbol{\Xi})|] = \\
&\quad \frac{2^{-\frac{N}{2}-1}e^{-\lambda^2}}{\sqrt{\pi}\Gamma(\frac{N+1}{2})}\int_{\mathbb{R}} dt_1 \int_{\mathbb{R}^+} dQ_1 \exp\Big[\frac{-h^4\varepsilon^2t_1^2 - 2h^2\varepsilon\lambda t_1^2 + \lambda^2(Q_1+t_1^2+2)}{2(Q_1+t_1^2+1)}\Big] \\
&\times Q_1^{\frac{N-3}{2}}(Q_1+t_1^2+1)^{-\frac{N}{2}-2}\Big(+\lambda^{2N}(h^4\varepsilon^2Q_1 + (N-1)(Q_1+t_1^2+1)) + 2h^2\varepsilon\lambda^{2N+1}Q_1 \\
&\quad + e^{\lambda^2}\Gamma(N,\lambda^2)(\lambda^2((1-N)(Q_1+t_1^2) - h^4Q_1\varepsilon^2) + (N-1)(h^4\varepsilon^2(Q_1+1) \\
&\quad + N(Q_1+t_1^2+1)) + 2h^2\varepsilon\lambda(N-1)(Q_1+1) - 2h^2\lambda^3Q_1\varepsilon)\Big) \quad \text{(A.23)}
\end{aligned}$$

The result above is valid for any finite $N,\lambda,\varepsilon \in \mathbb{C}$ and $\boldsymbol{h} \in \mathbb{R}^N$. For completeness we observe that the integrand above is even for t_1 therefore we can reduce eq(**A.23**) to a single integral by introducing $y = Q_1 + t_1^2$ and integrating out $|t_1| < \sqrt{y}$ in order to obtain:

$$\begin{aligned}
&\mathbb{E}_{GinOE}[|\det(\lambda \mathbf{1}_N + \varepsilon \boldsymbol{h}\boldsymbol{h}^T - \boldsymbol{\Xi})|] = \frac{2^{-\frac{N}{2}}}{(N-1)\Gamma(\frac{N}{2})}\int_{\mathbb{R}^+} dy \exp\Big(-\frac{\lambda^2 y}{2(1+y)}\Big)y^{\frac{N}{2}-1} \\
&\times (1+y)^{-\frac{N}{2}-2}\Big((e^{\lambda^2}\Gamma(N,\lambda^2)((((N-1)(y+1) - \lambda^2y)(h^2\varepsilon(h^2\varepsilon+2\lambda)+N) + \lambda^2y) + \\
&\quad + \lambda^{2N}(h^4y\varepsilon^2 + 2h^2\lambda y\varepsilon + (N-1)(y+1)))F_1(y) - \frac{1}{N}h^2y\varepsilon(h^2\varepsilon+2\lambda)(\lambda^{2N} + \\
&\quad + e^{\lambda^2}(-\lambda^2+N-1)\Gamma(N,\lambda^2))F_2(y)\Big) \quad \text{(A.24)}
\end{aligned}$$

where $F_1(y)$ and $F_2(y)$ are given by the confluent hypergeometric functions

$$ {}_1F_1\left(\frac{1}{2}; \frac{N}{2}; -\frac{h^2 y\varepsilon(\varepsilon h^2 + 2\lambda)}{2(y+1)}\right) $$

and

$$ {}_1F_1\left(\frac{3}{2}; \frac{N+2}{2}; -\frac{h^2 y\varepsilon(\varepsilon h^2 + 2\lambda)}{2(y+1)}\right) $$

respectively.

A.1.1 Asymptotic for the Absolute Value in Eq(1.76)

We are now able to investigate the large-N asymptotic behaviour of eq(**A.23**). We remark here that the limiting spectral distribution of the eigenvalues of $\varXi/\sqrt{N}$, converges almost surely to the circular law, i.e. to the uniform distribution over the disc of unit radius as $N \to +\infty$. Since we want to address $N \to \infty$, this suggests, as it will be clear later, to rescale λ and ε, as $\lambda \to \sqrt{N}\lambda$ and $\varepsilon \to \sqrt{N}\varepsilon$. Without loss of generality we also impose $h = |\boldsymbol{h}| = 1$. With the application we have in mind for eq(**1.48**) in section 1.2.4 and eq(**A.23**) in section 3.1.3, this scaling arises in the parameter choice eq(**A.2**). Let consider for a moment $\varepsilon = 0$. We expect, from what stated above and [37], that $|\lambda|$ being greater or smaller than one defines different regimes for eq(**A.23**). In fact, $|\lambda| = 1$ corresponds to an evaluation at the edge discontinuity for the global spectral density and it will require an additional (edge) scaling. Setting $\varepsilon \neq 0$ introduces a rank-1 perturbation to the random matrix $\varXi$. This can create spectral outlier (see section 1.1.2) but, given its finite nature, it does not lead to further sub-regimes within and at the edge of the spectrum. The integrand in eq(**A.23**) can be re-casted in two factors. The exponential terms and the first two terms in the second line with power N of eq(**A.23**) are collected by

$$ \mathcal{L}(q,t) = \frac{-\varepsilon^2 t^2 - 2\lambda t^2 \varepsilon + \lambda^2 + \lambda^2(q+t^2+1)}{2(q+t^2+1)} - \frac{1}{2}\log(q+t^2+1) + \frac{1}{2}\log(q) \quad \text{(A.25)} $$

The (sub-leading) terms appearing in eq(**A.23**) can be presented in a form of the following function

$$ \begin{aligned} g(q,t) = {} & q^{-\frac{3}{2}}(q+t^2+1)^{-2}(\lambda^{2N}N^N(Nq\varepsilon^2 + (N-1)(q+t^2+1)) + 2\lambda^{2N+1}N^{N+1}q\varepsilon \\ & + e^{\lambda^2 N}\Gamma(N, N\lambda^2)(\lambda^2 N((1-N)(q+t^2) - Nq\varepsilon^2) + (N-1)(N(q+1)\varepsilon^2 + N(q+t^2+1)) + \\ & - 2\lambda^3 N^2 q\varepsilon + 2\lambda N(N-1)(q+1)\varepsilon) \quad \text{(A.26)} \end{aligned} $$

In order to simplify the notation we replaced Q_1 and t_1 with q and t respectively. For $N \gg 1$, the main contribution to the integrals in eq(**A.23**) is given by the neighborhood of the saddle points of $\mathcal{L}(q,t)$. It turns out that the only feasible solution to $\nabla\mathcal{L}(q,t) = \mathbf{0}$ is given by $q = \frac{1}{\lambda^2-1}$ and $t = 0$ since we need to further impose $1 + q + t^2 = 0$ for convergence. At this point

$$\mathcal{L}\left(\frac{1}{\lambda^2-1}, 0\right) = -\frac{1}{2} + \lambda^2 - \frac{1}{2}\log\lambda^2$$

while the Hessian of $\mathcal{L}(q,t)$, indicated by $\boldsymbol{H}(q,t)$, is diagonal, namely

$$\boldsymbol{H}\Big(\frac{1}{\lambda^2-1}, 0\Big) = \begin{bmatrix} -\frac{(\lambda^2-1)^4}{2\lambda^4} & 0 \\ 0 & -\frac{(\varepsilon+\lambda)^2(\lambda^2-1)}{\lambda^2} \end{bmatrix}$$

One can easily check that the Hessian $\boldsymbol{H}$ is negative definite only for $|\lambda| > 1$. This defines two regimes we need to investigate separately. As anticipated ε does not intervene in defining these regimes:

- We fix $|\lambda| > 1$. In this case, the point $(\frac{1}{\lambda^2-1}, 0)$ belongs to the domain of integration in eq(**A.23**). Hence, for $N \gg 1$, we can expand in Taylor series around such point $\mathcal{L}(q,t)$ and $g(q,t)$, namely

$$\mathcal{L}(q,t) \approx \mathcal{L}\Big(\frac{1}{\lambda^2-1}, 0\Big) + \frac{1}{2}\begin{bmatrix} q - \frac{1}{\lambda^2-1} \\ t \end{bmatrix}^T \boldsymbol{H}\Big(\frac{1}{\lambda^2-1}, 0\Big)\begin{bmatrix} q - \frac{1}{\lambda^2-1} \\ t \end{bmatrix} \tag{A.27}$$

  and

$$g(q,t) \approx g\Big(\frac{1}{\lambda^2-1}, 0\Big) \tag{A.28}$$

  After replacing the quantities above in eq(**A.23**), one can analytically perform the integrals. By retaining the leading terms of this operations, the Laplace approximation gives

$$\mathbb{E}_{\text{GinOE}}[|\det(\lambda\mathbf{1}_N + \varepsilon\boldsymbol{h}\boldsymbol{h}^T - \boldsymbol{\Xi})|] \sim N^{\frac{N}{2}}|\lambda|^{N-1}|\varepsilon + \lambda|(1 + o(1)). \tag{A.29}$$

- For $|\lambda| < 1$, one easily sees that

$$(\frac{1}{\lambda^2-1}, 0) = \arg\max\mathcal{L}(q,t) \notin \mathbb{R}^+ \times \mathbb{R} \tag{A.30}$$

  The saddle point of $\mathcal{L}(q,t)$ does not belong to the domain of integration in eq(**A.23**). To perform the asymptotics $N \gg 1$ we proceed by steps. Firstly, we restrict such domain to the subset $U(R) \subset \mathbb{R}^+ \times \mathbb{R}$ contained within the semi-circle of radius R and center $(0,0)$ in the first and fourth quadrants and the line connecting $(0, R)$ to $(0, -R)$, oriented counterclockwise. The original domain is restored by the limit $R \to +\infty$. From eq(**A.30**), the saddle point $(\frac{1}{\lambda^2-1}, 0)$ does not belong to $U(R)$. therefore $\mathcal{L}(q,t)$ hits its maximal value in correspondence of an accumulation point of $U(R)$. From eq(**A.25**) and from the parametrization of the boundary of $U(R)$, i.e. $\partial U(R)$, $\mathcal{L}(q,t)$ reaches its maximum at $(R, 0)$ where

$$\mathcal{L}(R,0) = 1/2((R+2)\lambda^2/(1+R) + \log(R/(R+1))).$$

The curve $\partial U(R)$ is smooth and differentiable with curvature R^{-1} in $(R, 0)$. The outward normal vector is simply $\boldsymbol{n} = (1, 0)$. Therefore with the help of the divergence theorem, it holds (see [40])

$$\mathbb{E}_{GinOE}[|\det(\lambda \mathbf{1}_N + \varepsilon \boldsymbol{h}\boldsymbol{h}^T - \boldsymbol{\Xi})|] = \tag{A.31}$$

$$C_{N,\lambda} \lim_{R\to+\infty} \oint_{\partial U(R)} \frac{d\ell e^{N\mathcal{L}(\ell)}}{N} \frac{g(\ell)}{|\nabla \mathcal{L}|^2} \nabla \mathcal{L}(\ell) \cdot \boldsymbol{n}(\ell) + O(e^{N\mathcal{L}(R,0)} N^{-2})$$

where $C_{N,\lambda} = \frac{2^{-\frac{N}{2}-1} e^{-\lambda^2}}{\pi^{\frac{1}{2}} \Gamma(\frac{N+1}{2})}$. Once again, if we can retain the leading terms around the point $(R, 0)$, we get

$$\mathbb{E}_{\mathrm{GinOE}}[|\det(\lambda \mathbf{1}_N + \varepsilon \boldsymbol{h}\boldsymbol{h}^T - \boldsymbol{\Xi})|] \approx \tag{A.32}$$

$$C_{N,\lambda} \lim_{R\to+\infty} \sqrt{\frac{2\pi}{N^3}} e^{N\mathcal{L}(R,0)} g(R,0) \Big(\sqrt{\big|f(R,0) + R^{-1} w(R,0))\big|}\Big)^{-1}$$

where: $w(q,t) = \big|\nabla \mathcal{L}(q,t)\big|^3$ and $f(q,t) = \frac{\partial^2 \mathcal{L}(q,t)}{\partial q \partial t} (\frac{\partial \mathcal{L}(q,t)}{\partial t})^2 - 2 \frac{\partial^2 \mathcal{L}(q,t)}{\partial q \partial t} (\frac{\partial \mathcal{L}(q,t)}{\partial t} \frac{\partial \mathcal{L}(q,t)}{\partial q}) + \frac{\partial^2 \mathcal{L}(q,t)}{\partial q \partial t} (\frac{\partial \mathcal{L}(q,t)}{\partial q})^2$. We observe that f is the leading term in the r.h.s. under the square root of eq(**A.32**). Once can easily sees that $f(R, 0) = O(R^{-5})$ whereas $w(R, 0) = O(R^{-6})$. For $N \gg 1$ and $|\lambda| < 1$, one can approximate[1]

$$\Gamma(N, N\lambda^2) \approx N^N e^{-N} \int_{\lambda^2}^{+\infty} du e^{-\frac{N}{2}(u-1)^2}$$

and

$$\mathrm{erfc}\left(\frac{\sqrt{N}(\lambda^2-1)}{\sqrt{2}}\right) \approx 2$$

If we carefully keep only the leading order terms from eq(**A.32**), we are finally left with

$$\mathbb{E}_{GinOE}[|\det(\lambda \mathbf{1}_N + \varepsilon \boldsymbol{h}\boldsymbol{h}^T - \boldsymbol{\Xi})|] \sim \sqrt{2} N^{\frac{N}{2}} e^{\frac{N}{2}(\lambda^2-1)} \sqrt{\varepsilon^2 + 2\lambda\varepsilon + 1}(1 + o(1)). \tag{A.33}$$

[1]See also the asymptotics in section 1.1.2.

- For completeness[2], it remains to address the edge of the spectrum for which $|\lambda| = 1$. To observe this regime we rescale $\lambda \to 1 + \frac{\lambda}{\sqrt{N}}$ and $\varepsilon \to 1 + \frac{\varepsilon}{\sqrt{N}}$. Now λ and ε are of order one. One can follow what done above and use the result in eq(A.31) with $N \gg 1$. This leads to:

  – for $\lambda < 0$:

$$\mathbb{E}_{GinOE}[|\det(\lambda \mathbf{1}_N + \varepsilon \boldsymbol{h}\boldsymbol{h}^T - \boldsymbol{\Xi})|] \sim \sqrt{2} N^{\frac{N}{2}} e^{\sqrt{N}\lambda + \frac{\lambda^2}{2}} \operatorname{erfc}(\sqrt{2}\lambda)(1 + o(1)) \tag{A.34}$$

  – for $\lambda > 0$:

$$\mathbb{E}_{GinOE}[|\det(\lambda \mathbf{1}_N + \varepsilon \boldsymbol{h}\boldsymbol{h}^T - \boldsymbol{\Xi})|] \sim 2\sqrt{N}(\sqrt{N} + \lambda)^{N-1}(1 + o(1)) \tag{A.35}$$

A.2 Derivation of Eq(1.87)

In order to compute the $\mathcal{Z}_{\beta,p}(\lambda; \mathbf{T})$, we rewrite the determinants as product of Berezin integrals using the Superbosonization approach. We start by rewriting the determinants by using p grassmanian pairs of $N \times 1$ vectors $\{\tilde{\boldsymbol{\psi}}_j, \boldsymbol{\psi}_j\}_{j=1}^p$. The latter symbolically satisfy the following relations (see section 1.1.1.3): $\psi_1\psi_2 = -\psi_2\psi_1$, $\int 1 d\psi = 0$, $\int \psi d\psi = 1$. Therefore, given a $N \times N$ matrix $\mathbf{A}$, its determinant is $\det \mathbf{A} = \int D\boldsymbol{\psi} \exp\left(\tilde{\boldsymbol{\psi}}^T \mathbf{A} \boldsymbol{\psi}\right)$. After some manipulations, for $\beta = 1$, we obtain:

$$\mathbb{E}_{\mathbf{W}}\left[\prod_{j=1}^{p} \det(\lambda_j \mathbf{1}_N - \mathbf{W}\mathbf{T}\mathbf{W}^T)\right] = \int D\boldsymbol{\psi} e^{-\sum_{j=1}^p \lambda_j \operatorname{Tr} \boldsymbol{\psi}_j \tilde{\boldsymbol{\psi}}_j^T} \prod_{a=1}^{m} \mathbb{E}_{\mathbf{w}_a}\left[e^{\frac{T_a}{2} \operatorname{Tr} \boldsymbol{Q}^{(s)} \mathbf{w}_a \mathbf{w}_a^T}\right] \tag{A.36}$$

where $\boldsymbol{Q}^{(s)}$ is the symmetric part of $\boldsymbol{Q} = \sum_{j=1}^p \boldsymbol{\psi}_j \tilde{\boldsymbol{\psi}}_j^T$, defined as $\boldsymbol{Q} + \boldsymbol{Q}^T$. The expectation in eq(A.36) is equal to $1/\det(\mathbf{1}_N - T_a/N\boldsymbol{Q}^{(s)})^{1/2}$. In analogy with $\log(1+x) = \sum_{n=1}^{+\infty}(-1)^{n+1}x^n/n$, the finite Taylor expansion of $\operatorname{Tr}\log(\mathbf{1}_N - T_a/N\boldsymbol{Q}^{(s)})^{1/2}$ allows to rewrite the integrand in eq(A.36) in terms of the $2p \times 2p$ matrix $\hat{\boldsymbol{Q}}$:

$$\hat{\boldsymbol{Q}} = \begin{bmatrix} \tilde{\boldsymbol{\psi}}_i^T \boldsymbol{\psi}_j & \tilde{\boldsymbol{\psi}}_i^T \tilde{\boldsymbol{\psi}}_j \\ -\boldsymbol{\psi}_i^T \boldsymbol{\psi}_j & -\boldsymbol{\psi}_i^T \tilde{\boldsymbol{\psi}}_j \end{bmatrix} \tag{A.37}$$

Since $\operatorname{Tr} \hat{\boldsymbol{Q}}^k = -\operatorname{Tr} \boldsymbol{Q}^{(s)^k}$, it follows that $-\operatorname{Tr}\log(\mathbf{1}_N - T_a/N\boldsymbol{Q}^{(s)}) = \operatorname{Tr}\log(\mathbf{1}_{2p} - T_a/N\hat{\boldsymbol{Q}})$. We replace the integration with Grassmanian variables with the integration over the group of $2p \times 2p$ unitary matrices $\mathbf{U}$ with skew symmetric sub-blocks,

[2] This regime does not play any role in eq(3.14) as it has a null measure for the spherical mean density.

satisfying:

$$\mathbf{P}^{-1}\mathbf{U}\mathbf{P} = \mathbf{U}^T$$

where we introduce:

$$\mathbf{P} = \begin{bmatrix} \mathbf{0}_p & -\mathbf{1}_p \\ \mathbf{1}_p & \mathbf{0}_p \end{bmatrix}$$

Therefore $\mathbf{U}$ has the following block form:

$$\mathbf{U} = \begin{bmatrix} \mathbf{U}_{11} & \mathbf{U}_{12} \\ \mathbf{U}_{21} & \mathbf{U}_{11}^T \end{bmatrix}$$

with $\mathbf{U}_{12}, \mathbf{U}_{21} \in Skew(\mathbb{C}^{p\times p})$. This group corresponds to the unitary matrix of the circular symplectic ensemble (CSE(p)). In a similar way one can treat the complex case ($\beta = 2$). In this case the integrand can be written as a function of $\hat{\boldsymbol{Q}}$ which only consists of the $p \times p$ left upper block of eq(**A.37**). The Berezin integral is namely replaced by an integral over group of the $p \times p$ unitary matrices (CUE(p)). We can now represent $\mathcal{Z}_{\beta,p}(\lambda; \mathbf{T})$ for both the cases, namely:

$$\mathcal{Z}_{\beta,p}(\lambda;\mathbf{T}) = \frac{\int_{C(4/\beta)E(p)} d\mathbf{U}\det(\mathbf{U})^{-\frac{\beta N}{2}} e^{\frac{\beta}{2}\operatorname{Tr}\Lambda\mathbf{U}} \prod_{a=1}^{M} \det(\mathbf{1}_{(2/\beta)p} - \frac{T_a}{N}\mathbf{U})^{\beta/2}}{\int_{C(4/\beta)E(p)} d\mathbf{U}\det(\mathbf{U})^{-\frac{\beta N}{2}} e^{\frac{\beta}{2}\operatorname{Tr}\mathbf{U}}} \tag{A.38}$$

where $\Lambda = \mathbf{1}_{2/\beta} \otimes \begin{bmatrix} \lambda_1 & 0 & \dots & 0 \\ 0 & \lambda_2 & \dots & 0 \\ \vdots & \vdots & \ddots & \vdots \\ 0 & 0 & \dots & \lambda_p \end{bmatrix}$. While the denominator of the integral form of $\mathcal{Z}_{\beta,p}(\lambda; \mathbf{T})$ is unitary invariant, the numerator does not share the same invariance due to presence of the exponential term. Therefore, for $\lambda_j \neq \lambda_i$, it's not possible to write such integrals in term of $e^{i\theta_j}$ with $\theta_j \in (0, 2\pi)$, i.e. the eigenvalues of $\mathbf{U}$. Such simplification only holds for $\lambda_j = \lambda$ for any $j = 1, ..., p$ where the numerator of eq(**A.38**) becomes a Siegel-like integral.

A.3 Derivation of Eq(1.90) and Eq(1.91)

Formulas in eqs(**1.95**,**1.96**) come from ratios of Selberg integrals (see [26]) which, after some manipulations, take the form:

$$\int_{[0,2\pi]^p} d\theta_{j=1}^p \prod_{j=1}^{p} e^{-iN\theta_j} e^{e^{i\theta_j}} \prod_{j<k} |e^{i\theta_k} - e^{i\theta_j}|^\beta =$$

$$(2\pi)^2 e^{-i\pi pN} M_p(-N, N, \beta/2)\, {}_1F_1^{(2/\beta)}(-N, -N+1+\beta/2(p-1); 1)$$

And

$$\int_{[0,2\pi]^p} d\theta_{j=1}^p \prod_{j=1}^{p} e^{-iN\theta_j} \prod_{a=1}^{M}(1-T_a e^{i\theta_j}) \prod_{j<k} |e^{i\theta_k}-e^{i\theta_j}|^\beta =$$
$$(2\pi)^p e^{-i\pi pN} M_p(-N,N,\beta/2)\, {}_2F_1^{(\beta/2)}(-p, 2/\beta N; (1-p)+2/\beta(N-1); \mathbf{T})$$

The resulst simply follow from the ratio of the latter. The case $\beta = 2$ admits a determinantal form (see [142]), i.e.:

$$\mathbb{E}_{\mathbf{W}}[\det(\mathbf{W}\mathbf{T}\mathbf{W}^\dagger)^p] = (-1)^{pN} \frac{\det\left[(T_i/N)^{M-k}_2 F_1^{(1)}(\boldsymbol{a}_k; N-p-k+1; T_i/N)\right]_{i,k=1}^{\alpha N}}{\Delta(\mathbf{T})_1 F_1^{(1)}(-N, p-N; 1)}$$

with the vandermonde determinant $\Delta(\mathbf{T}) = \prod_{j<k}(T_j - T_k)$ and $\boldsymbol{a}(k) = (-p+1-k, N+1-k)$. The case $\lambda \neq 0$ is addressed without using Jack polynomials as above. We assume that $\boldsymbol{\lambda} = (\lambda, ..., \lambda)$, for $\beta = 2$, the numerator in eq(**A.38**) is proportional to:

$$\int_{[0,2\pi]^p} d\theta_{j=1}^p \prod_{j=1}^{p} h(\theta_j) \prod_{k<j}(e^{i\theta_j}-e^{i\theta_k}) \prod_{k<j}(e^{-i\theta_j}-e^{-i\theta_k}) \tag{A.39}$$

with $h(\theta) = e^{-iN\theta+\lambda e^{i\theta}} \prod_{a=1}^{M}(1-\frac{T_a}{N}e^{i\theta})$. We then recast the Vandermonde terms in determinantal form, i.e. $\prod_{j<k}|e^{i\theta_j}-e^{i\theta_k}|^2 = \det([(e^{i\theta_j})^{k-1}]_{k,j=1}^p)\det([(e^{-i\theta_j})^{k-1}]_{k,j=1}^p)$. Eventually, after some manipulation and introducing the Andreief identity, eq(**A.39**) becomes the determinant of a Toeplitz matrix:

$$p!\det\left[\frac{1}{i}\oint \frac{dz}{z^{N-j+k+1}} e^{\lambda z} \prod_{a=1}^{M}\left(1-\frac{T_a}{N}z\right)\right]_{j,k=1}^p.$$

As the contour encircles the origin counterclockwise, for $T_a \neq 0$, the Cauchy integral formula returns

$$p!\det\left[2\pi\lambda^{N-j+k}\sum_{u=0}^{N-j+k}\frac{(-1)^u}{(N-j+k-u)!}e_u\left(\frac{\boldsymbol{T}}{\lambda}\right)\right]_{j,k=1}^p$$

where e_u is the elementary symmetric function of order u, i.e. $e_u(\mathbf{T}) = \sum_{i_S<i_{S+1}} T_{i_1}...T_{i_u}$. Replicating the same steps for the denominator of eq(**A.38**):

$$\mathcal{Z}_{\beta=2,p}(\lambda;\mathbf{T}) = \frac{\det\left[2\pi\lambda^{N-j+k}\sum_{u=0}^{N-j+k}\frac{(-1)^u}{(N-j+k-u)!}e_u\left(\frac{\boldsymbol{T}}{\lambda}\right)\right]_{j,k=1}^p}{\det\left[\frac{2\pi}{(N-j+k)!}\right]_{j,k=1}^p}$$

For $\beta = 1$, the reference ensemble in eq(**A.38**) is given by the circular symplectic matrices, the joint probability density function of the eigenvalues can be re-written with the de Brujin indentity [12] as

$$\prod_{j<k}|e^{i\theta_j}-e^{i\theta_k}|^4 = \prod_{j=1}^{p} e^{-2i(p-1)\theta_j}\det\left[e^{i(k-1)\theta_j}; (k-1)e^{i(k-2)\theta_j}\right]_{1\le k\le 2p, 1\le j\le p}.$$

Therefore the numerator of eq(**A.38**) is now proportional to:

$$\int_{[0,2\pi]^p} d\theta_{j=1}^{p} \prod_{j=1}^{p} h(\theta_j) \prod_{k<j} |e^{i\theta_j} - e^{i\theta_k}|^4$$

and it can be written as the Pfaffian of a skew-symmetric Hankel matrix:

$$(2p)!\,\mathrm{Pf}\left[(j-k)\int_0^{2\pi} d\theta h(\theta) e^{i(k+j-2p-1)\theta}\right]_{j,k=1}^{2p}$$

which is equivalent to the following Pfaffian:

$$(2p)!\,\mathrm{Pf}\left[(j-k)2\pi\lambda^{N+2p+1-(k+j)} \sum_{u=0}^{N+2p+1-(k+j)} \frac{(-1)^u}{(N+2p+1-(k+j)-u)!} e_u\left(\frac{\mathbf{T}}{\lambda}\right)\right]_{j,k=1}^{2p}$$

Again repeating the same procedure for the denominator of eq(**A.38**), we finally arrive at

$$\mathcal{Z}_{\beta=4,p}(\lambda;\mathbf{T}) = \frac{\mathrm{Pf}\left[(j-k)2\pi\lambda^{N+2p+1-(k+j)} \sum_{u=0}^{N+2p+1-(k+j)} \frac{(-1)^u}{(N+2p+1-(k+j)-u)!} e_u\left(\frac{\mathbf{T}}{\lambda}\right)\right]_{j,k=1}^{2p}}{\mathrm{Pf}\left[2\pi \frac{(j-k)}{(N+2p+1-(k+j))!}\right]_{j,k=1}^{2p}}$$

A.4 Derivation of Eq(1.97) and Eq(1.98)

Proof p=1: We fix $p = 1$. For $\beta = 2$ the result directly follows from eq(**A.38**) considering $p = 1$ as the only eigenvalue of $\mathbf{U}$ can be written as $e^{i\theta}$ with $\theta \in (0, 2\pi)$. For $\beta = 1$, the single eigenvalue $z = e^{i\theta}$ has multiplicity two and $\mathbf{U} = \begin{bmatrix} z & 0 \\ 0 & z \end{bmatrix}$. The CSE normalized Haar measure is simply given by $1/(2\pi)$. The numerator of eq(**A.38**) is therefore

$$\oint_{|z|=1} \frac{dz}{2\pi i} \frac{e^{\lambda z}}{z^{N+1}} \left(1 - \frac{\mathbb{E}[T]}{N} z\right)^{\alpha N} \tag{A.40}$$

The contour encircles the origin counterclockwise. The only pole in the integrand above being at the origin, by applying the Cauchy's integral formula, the integral above becomes $\lim_{z\to 0} \frac{1}{N!} \frac{d^N}{dz^N} e^{\lambda z} (1 - \frac{\mathbb{E}[T]}{N} z)^{\alpha N}$. Similarly, the denominator in eq(**A.38**) is simply given by $\frac{1}{N!}$. Therefore $\mathbb{E}_{\mathbf{T}}[\mathcal{Z}_{\beta,1}(\lambda;\mathbf{T})] = (\alpha N)! \sum_{k=0} \binom{N}{k} \frac{\lambda^{N-k}}{(\alpha N - k)!} \left(-\frac{\mathbb{E}[T]}{N}\right)^k$. The complex case $\beta = 2$ is similar and leads to the same result. The case $\mathbb{E}[T] = 0$ follows from eq(**A.40**).

We fix now $p = 2$ and we first consider $\beta = 2$. In this case $\mathbf{\Lambda} = \mathrm{diag}(\lambda_1, \lambda_2)$ and we need to introduce 4 variables ψ_{ij} ,with $i \leq j$ and $i, j = 1, 2$, and φ such that

$0 \leq \psi_{ij} \leq 2\pi$ and $0 \leq \varphi \leq \pi/2$. Therefore a possible parametrization of $\mathbf{U}$ is the following [47]:

$$\mathbf{U} = \begin{bmatrix} e^{i(\psi_{11}+\psi_{12})}\cos\varphi & e^{i\psi_{12}}\sin\varphi \\ -e^{i(\psi_{11}+\psi_{22})}\sin\varphi & e^{i\psi_{22}}\cos\varphi \end{bmatrix}$$

The Eucledean line element $(\mathrm{d}s)^2 = \sum_{i,j} |\mathrm{d}\mathbf{U}_{ij}|^2$:

$$(\mathrm{d}s)^2 = (d\psi_{11})^2+(d\psi_{12})^2+(d\psi_{22})^2+2(d\varphi)^2+2(\cos\varphi)^2(d\psi_{11})(d\psi_{12})+2(\sin\varphi)^2(d\psi_{11})(d\psi_{22})$$

The associated Jacobian is given by $\sqrt{2\det\mathbf{M}}$ where:

$$\mathbf{M} = \begin{bmatrix} 1 & (\cos\varphi)^2 & (\sin\varphi)^2 \\ (\cos\varphi)^2 & 1 & 0 \\ (\sin\varphi)^2 & 0 & 1 \end{bmatrix}$$

The normalised Haar measure comes from the evaluation of $\int\sqrt{\det\mathbf{M}}d\psi_{11}d\psi_{12}d\psi_{22}d\varphi$ and reads $d\mathbf{U} = \frac{1}{4\pi^3}\cos\varphi\sin\varphi d\psi_{11}d\psi_{12}d\psi_{22}d\varphi$. With this parametrization and assuming $\mathbb{E}[T] = 0$ follows that

$$\det\mathbf{U} = e^{i(\psi_{11}+\psi_{12}+\psi_{22})}, \tag{A.41}$$

$$\mathrm{Tr}\,\mathbf{\Lambda}\mathbf{U} = \cos\varphi(e^{i(\psi_{11}+\psi_{12})}\lambda_1 + e^{i(\psi_{22})}\lambda_2) \tag{A.42}$$

and

$$\mathbb{E}[\det(\mathbf{1}_2 - \frac{T_a}{N}\mathbf{U})] = 1 + \frac{\mathbb{E}[T^2]}{N^2}e^{i(\psi_{11}+\psi_{12}+\psi_{22})}. \tag{A.43}$$

The denominator of eq(A.38) is given by:

$$\frac{1}{4\pi^3}\int_0^{2\pi} d\psi_{11}\int_0^{2\pi} d\psi_{12}\int_0^{2\pi} d\psi_{22}d\varphi\cos\varphi\sin\varphi e^{\cos\varphi(e^{i(\psi_{11}+\psi_{12})}+e^{i\psi_{22}})}e^{-iN(\psi_{11}+\psi_{12}+\psi_{22})} =$$

$$= \frac{2}{(N!)^2}\int_0^{\frac{\pi}{2}} d\varphi(\cos\varphi)^{2N+1}\sin\varphi = \frac{1}{(N!)^2}\frac{1}{N+1} \tag{A.44}$$

While the numerator is:

$$\frac{1}{4\pi^3}\int_0^{2\pi} d\psi_{11}\int_0^{2\pi} d\psi_{12}\int_0^{2\pi} d\psi_{22}d\varphi\cos\varphi\sin\varphi e^{\cos\varphi(e^{i(\psi_{11}+\psi_{12})}\lambda_1+e^{i(\psi_{22})}\lambda_2)}e^{-iN(\psi_{11}+\psi_{12}+\psi_{22})}\times$$

$$\left(1+\frac{\mathbb{E}[T^2]}{N^2}e^{i(\psi_{11}+\psi_{12}+\psi_{22})}\right)^{\alpha N}$$

$$= 2\sum_{k=0}^{N}\frac{1}{k!(N-k!)!}\frac{(\lambda_1\lambda_2)^k}{(N-k)!}\frac{\alpha N!}{(\alpha N-k)!}\left(\frac{\mathbb{E}[T^2]}{N^2}\right)^k\frac{1}{2-2k+2N} \tag{A.45}$$

Lastly, the final result follows with the ratio of eq(A.45) and eq(A.44).

For $\beta = 4$, to simplify the calculation and without loss of generality we additionally fix $\mathbb{E}[T^2] = 1$. The general case is simply obtained by multiplying the result by $(\mathbb{E}[T^2])^N$

and rescale $\lambda_{1,2} \to \frac{\lambda_{1,2}}{\sqrt{\mathbb{E}[T^2]}}$. In this case $\mathbf{\Lambda} = \text{diag}(\lambda_1, \lambda_2, \lambda_1, \lambda_2)$. The parametrization of $\mathbf{U}$ is a 4×4 block matrix given by 6 variables: $h, d \in (0, 1)$ and $\varphi_{11}, \varphi_{21}, \varphi_{22}, \varphi_{14} \in (0, 2\pi)$. Namely:

$$\mathbf{U} = \begin{bmatrix} \mathbf{U}_{11} & \mathbf{U}_{12} \\ -\mathbf{U}_{12} e^{i(\varphi_{12}+\varphi_{21}-2\varphi_{14})} & \mathbf{U}_{11}^t \end{bmatrix}$$

where

$$\mathbf{U}_{11} = \begin{bmatrix} e^{i\varphi_{11}} h & e^{i\varphi_{22}} d\sqrt{1-h^2} \\ e^{i\varphi_{21}} d\sqrt{1-h^2} & -e^{-i(\varphi_{11}-\varphi_{21}-\varphi_{22})} h \end{bmatrix}$$

and

$$\mathbf{U}_{12} = e^{i\varphi_{14}} \sqrt{1-h^2}\sqrt{1-d^2} \begin{bmatrix} 0 & -1 \\ 1 & 0 \end{bmatrix}$$

In order to determine the Haar measure we start again by considering the Eucledean line element $(\mathrm{d}s)^2 = \sum_{i,j} |\mathrm{d}\mathbf{U}_{ij}|^2 = 2\sum_{i,j} |\mathrm{d}\mathbf{U}_{11;i,j}|^2 + \sum_{i,j} |\mathrm{d}\mathbf{U}_{12;i,j}|^2 + \sum_{i,j} |\mathrm{d}\mathbf{U}_{21;i,j}|^2$. In details we have that:

$$(ds)^2 = 2((dh)^2 + h^2(d\varphi_{11})^2 + 2(1-h^2)(dd)^2 - 4dh(dh)(dd) + \frac{2(dh)^2}{(1-h^2)}(dh)^2$$
$$+d^2(1-h^2)(d\varphi_{22})^2 + d^2(1-h^2)(d\varphi_{21})^2 + (dh)^2 + h^2(d\varphi_{22} + d\varphi_{21} - d\varphi_{11})^2 +$$
$$\frac{2}{(1-d^2)(1-h^2)}(d(1-h^2)(dd) + h(1-d^2)(dh))^2 + (1-d^2)(1-h^2)(d\varphi_{14})^2 +$$
$$+(1-d^2)(1-h^2)(d\varphi_{22} + d\varphi_{21} - d\varphi_{14})^2)$$

We can re-arrange the differential of the linear and angular variables such that the Jacobian of the change of variables is given by the square root of the determinant of the product of $\mathbf{M}_1$ and $\mathbf{M}_2$ defined as:

$$\mathbf{M}_1 = 4 \begin{bmatrix} 1 + \frac{h^2(1-d^2)+d^2h^2}{(1-h^2)} & 0 \\ 0 & (1-h^2) + \frac{d^2(1-h^2)}{(1-d^2)} \end{bmatrix}$$

And:

$$\mathbf{M}_2 = \begin{bmatrix} 4h^2 & -2h^2 & -2h^2 & 0 \\ -2h^2 & 2 & 2-2d^2+2d^2h^2 & -2(1-d^2)(1-h^2) \\ -2h^2 & 2-2d^2+2d^2h^2 & 2 & -2(1-d^2)(1-h^2) \\ 0 & -2(1-d^2)(1-h^2) & -2(1-d^2)(1-h^2) & 4(1-d^2-h^2+d^2h^2) \end{bmatrix}$$

The normalized Haar measure is obtained by evaluating

$$\int \sqrt{\det(\mathbf{M}_1)\det(\mathbf{M}_2)} dh dd d\varphi_{11} d\varphi_{21} d\varphi_{22} d\varphi_{14},$$

with $\det(\mathbf{M}_1) = \frac{16}{1-d^2}$ and $\det(\mathbf{M}_2) = 64d^2(1-d^2)h^2(1-h^2)^2$. It follows that $d\mathbf{U} = \frac{1}{2\pi^4} hd(1-h^2)(\mathrm{d}h\mathrm{d}d\mathrm{d}\varphi_{11}\mathrm{d}\varphi_{21}\mathrm{d}\varphi_{22}\mathrm{d}\varphi_{14})$. The denominator of eq(**A.38**) becomes:

$$\frac{1}{2\pi^3}\int_0^1 \mathrm{d}h \int_0^{2\pi} \mathrm{d}\varphi_{11} \int_0^{2\pi} \mathrm{d}\varphi_{21} \int_0^{2\pi} \mathrm{d}\varphi_{22} e^{he^{-i\varphi_{11}}(e^{2i\varphi_{11}} - e^{i(\varphi_{21}+\varphi_{22})})} e^{-iN(\varphi_{21}+\varphi_{22})} =$$

$$= \frac{4}{(N!)^2}\int_0^1 \mathrm{d}h h^{2n+1}(1-h^2) = \frac{2}{(N!)^2}\frac{1}{(2+3N+N^2)}$$

The numerator of eq(**A.38**) is given by:

$$\frac{1}{2\pi^3}\int_0^1 \mathrm{d}h \int_0^{2\pi}\mathrm{d}\varphi_{11}\int_0^{2\pi}\mathrm{d}\varphi_{21}\int_0^{2\pi}\mathrm{d}\varphi_{22} h(1-h^2)e^{-iN(\varphi_{22}+\varphi_{21})}e^{h\left(\lambda_1 e^{i\varphi_{11}}-\lambda_2 e^{i(\varphi_{22}+\varphi_{21}-\varphi_{11})}\right)}\times$$
$$\left(1-\frac{e^{i(\varphi_{22}+\varphi_{21})}}{N^2}\right)^{\alpha N}$$

by introducing and integrating out $\varphi = \varphi_{22}+\varphi_{21}$ the integral becomes:

$$\frac{2(\alpha N!)}{\pi N^{2\alpha N}}\sum_{k=0}^{N}\frac{N^{2(\alpha N-k)}}{k!(N-k)!(\alpha N-k)!}\int_0^1 \mathrm{d}h h(1-h^2)(h\lambda_2)^{N-k}\int_0^{2\pi}\mathrm{d}\varphi_{11}e^{h\lambda_1 e^{i\varphi_{11}}-i(N-k)\varphi_{11}}$$

Lastly,

$$= 2(\alpha N!)(\lambda_1\lambda_2)^N\sum_{k=0}^{N}\big((k!(\lambda_1\lambda_2 N^2)^k)((N-k)!)^2(\alpha N-k)(2+3(N-k)+(N-k)^2)!\big)^{-1}$$

The result is simply obtained by re-arranging the terms and introducing the definition of hypergeometric function.

A.5 Derivation of Eq(1.99) and Eq(1.101)

- Firstly, we address the asymptotics for the denominator of eq(**A.38**). We start by writing the denominator such that, for $N \gg 1$, the latter is proportional to terms of the form $e^{N\mathcal{L}}$. We consider the denominator of eq(**A.38**) for $\beta = 1$, which, after diagonalizing the unitary matrices, becomes:

$$\mathcal{D} = \frac{2^p}{(2\pi)^p}\frac{e^{-Np\log N}}{\Gamma(2p+1)i^p}\oint\prod_{j=1}^{p}\frac{dz_j}{z_j^{2(p-1)+1}}\prod_{j<k}(z_j-z_k)^4\prod_{j=1}^{p}e^{N\log\mathcal{L}(z_j)}$$

with $\mathcal{L}(z) = -\log z + z$. Making use of the saddle point approximation: $\frac{d\mathcal{L}}{dz}(z_{sd}) = 0 \Rightarrow z_{sd} = 1$ and $\frac{d^2\mathcal{L}}{dz^2}\Big|_{z_{sd}} > 0$. Therefore the directions of steepest descent are $\theta = \frac{\pi}{2}, \frac{3\pi}{2}$. We expand in Taylor series $\mathcal{L}$ around $z_j = 1 + i\eta_j$, i.e. $\mathcal{L}(1+i\eta) = 1 - \frac{\eta^2}{2} + O(\eta^3)$. Knowing that:

$$\int_{-\infty}^{+\infty}\prod_{j=1}^{p}d\eta_j e^{-\eta_j^2/2}\prod_{j<k}(\eta_j-\eta_k)^4 = \prod_{j=0}^{p-1}\frac{\Gamma(1+2(j+1))}{\Gamma(3)}$$

Finally, we arrive at

$$\mathcal{D} \approx \frac{e^{-Np\log N + pN}}{(2\pi)^{p/2}\Gamma(2p+1)N^{p^2-p/2}}\prod_{j=0}^{p-1}\Gamma(1+2(j+1))$$

- For $p = 1$, from the sections above, the numerator of eq(**A.38**) is

$$\mathcal{N} = \oint_{|z|=1} \frac{dz}{2\pi i} \frac{e^{\lambda z}}{z^{N+1}} \Big(1 - \frac{\mathbb{E}[T]}{N} z\Big)^{\alpha N}$$

This suggests to rescale and introduce $\mathbb{E}[T]/Nz = w$ and $x = \lambda/\,\mathbb{E}[T]$ so that:

$$\mathcal{N} = \Big(\frac{\mathbb{E}[T]}{N}\Big)^N \frac{1}{2\pi i} \oint \frac{dw}{w^{N+1}} e^{N\mathcal{L}(w)}$$

where $\mathcal{L}(w) = xw + \alpha \log(1-w) - \log w$. The saddle points of $\mathcal{L}(w)$ are given by $w_\pm = 1/(2x)(1-\alpha+x \pm \sqrt{(\alpha-1-x)^2 - 4x})$. The contribution of the latter depends on the sign of $\Delta = (\alpha-1-x)^2 - 4x$. $\Delta > 0$ correspond to $x < (1-\sqrt{\alpha})^2$ and $x > (1+\sqrt{\alpha})^2$ while $w_\pm$ lie on the real line. In particular w_- and w_+ are positive for $x > (1+\sqrt{\alpha})^2$. Additionally, for $x < 0$ we have $w_- > 0$. Lastly, for $x \in ((1-\sqrt{\alpha})^2, (1+\sqrt{\alpha})^2)$, $\frac{d^2\mathcal{L}}{dw^2}(w_\pm)$ is purely imaginary and changes its sign at $\frac{1-2\alpha+\alpha^2}{\alpha+1}$. Hence, crossing the saddle points leads to the following contributions:

$$I(w_\pm) \simeq i \frac{e^{N\mathcal{L}(w_\pm)}}{w_\pm} \left(\frac{2\pi}{N \frac{d^2\mathcal{L}}{dw^2}(w_\pm)} \right)^{1/2}$$

Conversely for $\Delta < 0$, $w_\pm$ are complex conjugate complex numbers and both contribute in encircling the pole at the origin. Therefore, for $N \gg 1$:

$$\mathcal{N} \simeq \Big(\frac{\mathbb{E}[T]}{N}\Big)^N \frac{1}{2\pi i} \begin{cases} I(w_+), & \text{if } x < (1-\sqrt{\alpha})^2 \\ -I(w_+) - I(w_-), & \text{if } 1 - 2\sqrt{\alpha} + \alpha < x < \frac{(\alpha-1)^2}{\alpha+1} \\ I(w_+) + I(w_-), & \text{if } \frac{(\alpha-1)^2}{\alpha+1} < x < (1+\sqrt{\alpha})^2 \\ I(w_-), & \text{if } x > (1+\sqrt{\alpha})^2 \end{cases}$$

For $x = 1 \pm \sqrt{\alpha} + \alpha$, the saddle points are of second order:

(i) For $x = 1+\sqrt{\alpha}+\alpha$, $w_{sd} = \frac{1}{1+\sqrt{\alpha}}$, $\frac{d^2\mathcal{L}}{dw^2}(w_{sd}) = 0$ and $\frac{d^3\mathcal{L}}{dw^3}(w_{sd}) = -2\frac{(1+\sqrt{\alpha})^4}{\sqrt{\alpha}}$. Therefore, the steepest descent direction at w_{sd} are $\theta = \{2/3\pi, 4/3\pi, 0\}$. We deform the contour by parametrizing the path, approching and leaving w_{sd} with $w = e^{i4/3\pi}t + w_{sd}$ and $w = e^{i2/3\pi}t + w_{sd}$ respectively, i.e.:

$$I(w_{sd}) \simeq \frac{e^{N\mathcal{L}(w_{sd})}}{w_{sd}} \left(e^{i2/3\pi} \int_0^{+\infty} dt e^{-N\frac{2(1+\sqrt{\alpha})^4}{3!\sqrt{\alpha}}t^3} + e^{i4/3\pi} \int_{+\infty}^0 dt e^{-N\frac{2(1+\sqrt{\alpha})^4}{3!\sqrt{\alpha}}t^3} \right)$$

Therefore:

$$I(w_{sd}) \simeq i\Gamma(1/3) \frac{\big(1 - \frac{1}{1+\sqrt{\alpha}}\big)^{\alpha N} (1+\sqrt{\alpha})^{N+1} e^{N+\sqrt{\alpha}N}}{3^{1/6}\big(N\frac{(1+\sqrt{\alpha})^4}{\sqrt{\alpha}}\big)^{1/3}}$$

(ii) Similarly, for $x = 1 - \sqrt{\alpha} + \alpha$, $w_{sd} = \frac{1}{1-\sqrt{\alpha}}$, $\frac{d^2\mathcal{L}}{dw^2}(w_{sd}) = 0$ and $\frac{d^3\mathcal{L}}{dw^3}(w_{sd}) = 2\frac{(-1+\sqrt{\alpha})^4}{\sqrt{\alpha}}$. Therefore, the steepest descent direction at w_{sd} are $\theta = \{1/3\pi, \pi, 5/3\pi\}$. We deform the contour by parametrizing the path, approching and leaving w_{sd} with $w = e^{i1/3\pi}t + w_{sd}$ and $w = e^{i5/3\pi}t + w_{sd}$ respectively. Hence,

$$I(w_{sd}) \simeq \frac{e^{N\mathcal{L}(w_{sd})}}{w_{sd}} \left(e^{i1/3\pi} \int_{+\infty}^{0} dte^{-N\frac{2(-1+\sqrt{\alpha})^4}{3!\sqrt{\alpha}}t^3} + e^{i5/3\pi} \int_{0}^{+\infty} dte^{-N\frac{2(-1+\sqrt{\alpha})^4}{3!\sqrt{\alpha}}t^3} \right)$$

Therefore:

$$I(w_{sd}) \simeq i\Gamma(1/3) \frac{(1 + \frac{1}{-1+\sqrt{\alpha}})^{\alpha N}(-1)^N(-1+\sqrt{\alpha})^{N+1}e^{N-\sqrt{\alpha}N}}{3^{1/6}\left(N\frac{(-1+\sqrt{\alpha})^4}{\sqrt{\alpha}}\right)^{1/3}}$$

We can combine the results above to obtain:

$$\lim_{N\to+\infty} \frac{1}{N} \log \mathbb{E}_{\mathbf{T}}[\mathcal{Z}_{\beta,1}(\lambda, \mathbf{T})] = \mathcal{L}(w_{sd}) + \log|\mu| - 1$$

- For $p = 2$, we restrict our attention to the case $\mathbb{E}[T] = 0$ and we start from the result of eq(**1.98**), for simplicity we impose $\mathbb{E}[T^2] = 1$ and $x = \lambda_1\lambda_2$. From the definition of hypergeometric function we have:

$$\mathbb{E}_{\mathbf{T}}[\mathcal{Z}_{\beta,2}(\boldsymbol{\lambda}; \mathbf{T})] = \sum_{k=0}^{N} \frac{\beta}{2N^{2N}} \frac{(N-k+1)_k \Gamma(\alpha N+1)\Gamma(N+\frac{2}{\beta}+1)}{\left(\frac{2}{\beta}+1\right)_k \Gamma((\alpha-1)N+1)((\alpha-1)N+1)_k} \frac{(N^2x)^k}{k!} \tag{A.46}$$

$$:= \sum_{k=0}^{N} a(k)$$

where $(b)_k = \frac{\Gamma(b+k)}{\Gamma(b)}$ is the Pochhammer symbol. We replace the summation above with an integral, by rescaling $k = N\eta$ with $\eta \in [0, 1]$. Therefore, expanding for N sufficiently large:

$$a(N\eta) \sim \frac{\beta\sqrt{\frac{2}{\pi}}\Gamma\left(\frac{2}{\beta}+1\right)\eta^{-\frac{2}{\beta}-1}\sqrt{\alpha}}{4\sqrt{N}\sqrt{1-\eta}\sqrt{(\alpha+\eta-1)}} e^{N\mathcal{L}(\eta)} \tag{A.47}$$

with:

$$\mathcal{L}(\eta) = \alpha\log(\alpha) - (\alpha+\eta-1)\log(\alpha+\eta-1) + \eta\log(x-\eta x) + 2\eta - 2\eta\log(\eta) - \log(1-\eta) - 2 \tag{A.48}$$

The maximum of $\mathcal{L}$ is located in $\eta^* \in [0, 1]$ which is given by the solution of $\frac{d\mathcal{L}}{d\eta}(\eta) = 0$, i.e.:

$$\log(x - \eta^* x) - \log(\alpha + \eta^* - 1) - 2\log(\eta^*) = 0 \tag{A.49}$$

Therefore, we want to study the roots of $p(\eta) = \eta^2(\alpha - 1 + \eta) - x(1 - \eta)$. Clearly $\lim_{\eta \to \pm\infty} p(\eta) = \pm\infty$ and $p(0) = -x$. On the interval $\eta > 0$, $p(\eta)$ is strictly increasing since $\eta^2 + 2\eta(\alpha + \eta - 1) + x > 0$. For $x \to 0^+$, the zero of p tends to 0, while for $x \to +\infty$ it tends to 1. Using Cardano's formulas we have that such root is given by ($\Delta = -2\alpha^3 + 6\alpha^2 - 6\alpha + 9\alpha x + 18x + 2, \Theta = 3x - (\alpha - 1)^2$):

$$\eta^* = \frac{1-\alpha}{3} - \frac{\sqrt[3]{2}\Theta}{3\sqrt[3]{\Delta + \sqrt{\Delta^2 + 4\Theta^3}}} + \frac{\sqrt[3]{\Delta + \sqrt{\Delta^2 + 4\Theta^3}}}{3\sqrt[3]{2}}$$

To see that η^* is actually a maximum it is sufficient to notice that:

$$\frac{d^2\mathcal{L}}{d\eta^2}(\eta) = -\frac{2}{\eta} + \frac{\alpha}{(\eta - 1)(\eta + \alpha - 1)} < 0$$

on $\eta \in (0, 1)$. To complete:

$$\mathbb{E}_{\mathbf{T}}[\mathcal{Z}_{\beta,2}(\boldsymbol{\lambda}; \mathbf{T})] \sim \frac{\beta\sqrt{\frac{2}{\pi}}\Gamma\left(\frac{2}{\beta} + 1\right)\eta^{*-\frac{2}{\beta}-1}\sqrt{\alpha N}}{4\sqrt{1-\eta^*}\sqrt{(\alpha + \eta^* - 1)}} e^{N\mathcal{L}(\eta^*)} \int_{-\infty}^{+\infty} d\eta e^{\frac{N}{2}\frac{d^2\mathcal{L}}{d\eta^2}(\eta^*)(\eta - \eta^*)^2} \tag{A.50}$$

The case $x < 0$ is less trivial as the function to maximise for $N \to +\infty$ has alternating sign near the saddle point. The hypergeometric function is given by $\sum_{k=0}^{N} \frac{(-1)^k(N-k+1)_k}{(1+\frac{2}{\beta})_k((\alpha-1)N+1)_k} \frac{(-N^2x)^k}{k!}$, let's replace $x \to -x$ such that, from now on, $x > 0$. We can separate the sum over even and odd ks so we can tackle the alternating sign terms, i.e.:

$$\begin{aligned} = \sum_{k=0}^{N/2} \frac{(N-2k+1)_{2k+1}}{(1+\frac{2}{\beta})_{2k}((\alpha-1)N+1)_{2k}} \frac{(N^2x)^{2k}}{(2k)!} + \\ - \sum_{k=0}^{N/2-1} \frac{(N-2k)_{2k+1}}{(1+\frac{2}{\beta})_{2k+1}((\alpha-1)N+1)_{2k+1}} \frac{(N^2x)^{2k+1}}{(2k+1)!} \end{aligned} \tag{A.51}$$

Here we can, again, replace the sum over k with an integral and $N/2 - 1 \approx N/2$, $k = N/2\eta$ with $\eta \in [0, 1]$. Performing now a series expansion the terms in the first and second summation above read ($N \gg 1$):

$$\mathbb{E}_{\mathbf{T}}[\mathcal{Z}_{\beta,2}(\boldsymbol{\lambda}; \mathbf{T})] \propto e^{N\mathcal{L}(\eta^*)} \tag{A.52}$$

This completes the result given in the large deviations section. As it is not essential for our goals, we did not address the subleading terms.

Appendix B

Appendix for Chapter 2

B.1 Statistics of $\mathbf{K}_{ab}$ with broken time-reversal invariance

To obtain the statistics of $\mathbf{K}_{a,b}$, we write the latter by introducing the diagonalization of $\mathbf{H}_N$. Denoting $(\lambda_n, |n\rangle)$ the eigenpairs (in bra/ket notations) of $\mathbf{H}_N$ we have:

$$\mathbf{K}_{a,b} = \sum_{n=1}^{N} \frac{w_{a,n} w^*_{n,b}}{\lambda - \lambda_n + i\alpha/N}$$

At the numerator $w_{n,a} = \langle \mathbf{w}_a | n \rangle$, $w^*_{n,b} = \langle n | \mathbf{w}_b \rangle$ are projection of the channel vectors on the eigenvectors of $\mathbf{H}_N$. The assumptions of the channel vectors being independent Gaussian random vectors are preserved for their projections. Therefore, the characteristic function of $\mathbf{K}_{a,b}$ can be written as

$$\tilde{\mathcal{R}}(q, q^*) = \mathbb{E}_{GUE(N)} \left[\overline{\exp i \left(\sum_{n=1}^{N} q^* \frac{w_{a,n} w^*_{b,n}}{\lambda - \lambda_n + i\alpha/N} + q \frac{w^*_{a,n} w_{b,n}}{\lambda - \lambda_n - i\alpha/N} \right)} \right] \tag{B.1}$$

For convenience of notation, we report here

$$\mathbb{E}_{GUE(N)}[(...)] := \int (...) d\mathcal{P}(\mathbf{H}_N)$$

and

$$\overline{[...]} = \int \int [...] \mathcal{P}(\boldsymbol{w}_a) \mathcal{P}(\boldsymbol{w}_b) d\boldsymbol{w}_a d\boldsymbol{w}_b$$

We can integrate out these last integrals over $\boldsymbol{w}_{a,n}$ and $\boldsymbol{w}_{b,n}$ to obtain

$$\tilde{\mathcal{R}}(q, q^*) = \mathbb{E}_{GUE(N)} \left[\prod_{n=1}^{N} \frac{(\lambda - \lambda_n)^2 + \alpha^2/N^2}{(\lambda - \lambda_n)^2 + \alpha^2/N^2 + |q|^2/N^2} \right] \tag{B.2}$$

$$= \mathbb{E}_{GUE(N)} \left[\frac{\det((\mathbf{H}_N - \lambda \mathbf{1}_N)^2 + \alpha^2/N^2 \mathbf{1}_N)}{\det((\mathbf{H}_N - \lambda \mathbf{1}_N)^2 + (|q|^2/N + \alpha^2/N^2)\mathbf{1}_N)} \right] := \tilde{\mathcal{R}}(|q|)$$

Such a quantity has been investigated in [87] for $N \to \infty$ in terms of the following two-point kernel $\mathbb{S}$

$$\mathbb{S}(x-y) = \begin{cases} \frac{e^{i\pi(x-y)}}{x-y}, & \text{if } \operatorname{Im} x > 0 \\ \frac{e^{-i\pi(x-y)}}{x-y}, & \text{if } \operatorname{Im} x < 0 \end{cases}$$

Back in eq(**B.2**), the characteristic function becomes:

$$\tilde{\mathcal{R}}(|q|) = \frac{\rho^2(\lambda)|q|^4}{4\alpha\sqrt{\alpha^2+|q|^2}} \det[e^{-\varphi(\lambda)(\xi_i-\eta_j)}\mathbb{S}(\xi_i-\eta_j)]_{i,j=1,2},$$

with $\xi_1 = i\rho(\lambda)\sqrt{\alpha^2+|q|^2}$, $\xi_2 = -i\rho(\lambda)\sqrt{\alpha^2+|q|^2}$, $\eta_1 = i\rho(\lambda)\alpha$ and $\eta_2 = i\rho(\lambda)\alpha$. Introducing $\mathcal{R}(|q|) = \tilde{\mathcal{R}}(|q/2|)$, from the definition of characteristic function, the probability density function of $\mathbf{K}_{ab}$ is retrieved by its Fourier-transform, namely

$$p(\mathbf{K}_{a,b}, \mathbf{K}^*_{a,b}) = \int e^{-i(\operatorname{Re} q(\mathbf{K}_{a,b}+\mathbf{K}^*_{a,b})/2+\operatorname{Im} q(\mathbf{K}_{a,b}-\mathbf{K}^*_{a,b})/2)}\mathcal{R}(|q|)\frac{d\operatorname{Re} q\, d\operatorname{Im} q}{(2\pi)^2}$$

The form of the integrand above suggests to switch to polar coordinates. After simplifying the integral above and integrating out angular the variable we can rewrite $p(\mathbf{K}_{a,b}, \mathbf{K}^*_{a,b})$ as

$$p(\mathbf{K}_{a,b}, \mathbf{K}^*_{a,b}) = \frac{\alpha^2}{\pi} \lim_{x\to 2\alpha\pi\rho(\lambda)} \int_0^\infty dr\, \frac{r}{\sqrt{1+r^2}} J_0(2\alpha|\mathbf{K}_{a,b}|r)$$

$$\times\Big(\sinh(x)\Big(1+\frac{d^2}{dx^2}\Big) - 2\cosh(x)\frac{d}{dx}\Big)\exp\left(-x\sqrt{1+r^2}\right).$$

The remaining integration over r can be re-written with the help of $y = \sqrt{1+r^2}$ and $K_{1/2}(u) = \sqrt{\frac{\pi}{2u}}e^{-u}$, where $K_\nu(u)$ is the Bessel-Macdonald function of order ν. Therefore, it is sufficient to observe (see [41])

$$\int_0^{+\infty} dr \frac{J_0(2\alpha|\mathbf{K}_{a,b}|r)r}{\sqrt{1+r^2}} \exp\left(-x\sqrt{1+r^2}\right) = \frac{e^{-\sqrt{x^2+4\alpha^2|\mathbf{K}_{a,b}|^2}}}{\sqrt{x^2+4\alpha^2|\mathbf{K}_{a,b}|^2}}.$$

This completes the proof for eq(**2.7**).

B.2 Statistics of $\mathbf{K}_{ab}$ with broken time-reversal invariance and correlated channels.

We can now relax the request of the channels being uncorrelated and introduce the 2×2 complex correlation matrix $\mathbf{C}^{-1}$. In this case, the characteristic function

$$\mathbb{E}_{GUE(N)}\overline{[\exp\frac{i}{2}(q\mathbf{K}^*_{ab} + q\mathbf{K}^*_{ab})]}$$

has the following expression

$$\mathbb{E}_{GUE(N)}\left[\prod_{n=1}^{N}\frac{N^2\det\mathbf{C}}{\pi^2}\int_{\mathbb{C}}\prod_{j=a,b}dw_{j,n}dw_{j,n}^*\exp\Bigg(-N\begin{bmatrix}w_{a,n}\\ w_{b,n}\end{bmatrix}^\dagger\mathbf{C}\begin{bmatrix}w_{a,n}\\ w_{b,n}\end{bmatrix}+\right.$$

$$\left.+\frac{i}{2}\Big(q\frac{w_{a,n}^*w_{b,n}}{\delta_n^*}+q^*\frac{w_{a,n}w_{b,n}^*}{\delta_n}\Big)\Bigg)\right] \quad \text{(B.3)}$$

where to simplify the notation we introduced $\delta_n = \lambda - \lambda_n - i\alpha/N$. The N Gaussian integrals above are readily solved yielding the characteristic function to be written as

$$\mathbb{E}_{GUE(N)}\left[\prod_{n=1}^{N}\frac{N^2\det\mathbf{C}}{N^2C_{11}C_{22}-(NC_{12}-i\frac{q}{2\delta_n^*})(NC_{12}^*-i\frac{q}{2\delta_n})}\right]$$

Replacing the definition of $\delta_n = \lambda - \lambda_n - i\alpha/N$, the characteristic function can be expressed as an average of the ratio of determinants over the GUE(N) ensemble:

$$\mathbb{E}_{GUE(N)}\left[\frac{\det((\lambda-i\alpha/N)\mathbf{1}_N-\mathbf{H})\det((\lambda+i\alpha/N)\mathbf{1}_N-\mathbf{H})}{\prod_{j=1,2}\det((\lambda\mathbf{1}_N-\mathbf{H})+\frac{i}{2N}(\tilde{k}+(-1)^j\sqrt{\tilde{k}^2+4\tilde{s}})\mathbf{1}_N)}\right]$$

with

$$\begin{cases}\tilde{k}=\frac{1}{2}\Big(\frac{C_{12}^*}{\det\mathbf{C}}q+\frac{C_{12}}{\det\mathbf{C}}q^*\Big)\\ \tilde{s}=\alpha^2+\frac{\alpha}{2}\Big(\frac{C_{12}^*}{\det\mathbf{C}}q-\frac{C_{12}}{\det\mathbf{C}}q^*\Big)+\frac{|q|^2}{4\det\mathbf{C}}\end{cases}$$

Similarly to the case of un-coupled channels we are interested in the Dyson limit. To this purpose, we recall once again eq.(4.9) in [31] so that the characteristic function is

$$\mathcal{R}(q,q^*)=-\frac{(\varepsilon_1-\mu_1)(\varepsilon_1-\mu_2)(\varepsilon_2-\mu_1)(\varepsilon_2-\mu_2)}{(\varepsilon_1-\varepsilon_2)(\mu_1-\mu_2)}(N\rho(\lambda))^2\det\left[e^{-\frac{\lambda}{2\rho(\lambda)}(\xi_i-\eta_j)}\mathbb{S}(\xi_i-\eta_j)\right]_{i,j=1,2}$$

with the following terms ($j = 1, 2$)

$$\begin{cases}\varepsilon_j=\lambda+\frac{\xi_j}{N\rho(\lambda)}\\ \mu_j=\lambda+\frac{\eta_j}{N\rho(\lambda)}\\ \xi_j=\rho(\lambda)\Big((-1)^j\frac{1}{2}\operatorname{Im}\sqrt{\tilde{k}^2+4\tilde{s}}+\frac{i}{2}(\tilde{k}+(-1)^{j+1}\operatorname{Re}\sqrt{\tilde{k}^2+4\tilde{s}}\Big)\\ \eta_j=i(-1)^j\alpha\rho(\lambda)\end{cases}$$

With few manipulations of the equalities above we obtain eq(**2.10**).

B.3 Mean $S-$matrix for non-orthogonal channels and the perfect coupling.

From [59], each entry of the $M\times M$ scattering matrix $S_{ab}(\lambda)$ in eq(**2.2**) admits the following representation:

$$S_{ab}(\lambda)=\delta_{ab}-2i\,\mathbf{w}_a^*\left(\frac{1}{\lambda\mathbf{1}_N-\mathcal{H}_{eff}}\right)\mathbf{w}_b, \quad \text{(B.4)}$$

where we introduced the effective non-Hermitian Hamiltonian as

$$\mathcal{H}_{eff} = \mathbf{H}_N - i\mathbf{\Gamma}, \quad \mathbf{\Gamma} := \mathbf{W}\mathbf{W}^\dagger = \sum_{c=1}^{M} \mathbf{w}_c \otimes \mathbf{w}_c^* \geq 0 \tag{B.5}$$

The eigenvalues of the latter are complex and of the form $\lambda_n = E_n - i\Gamma_n$. This corresponds to the poles in the complex energy plane of the scattering matrix and are usually called *resonances*. One can easily check that for $M < N$, the matrix $\mathbf{\Gamma}$ is not full rank, having exactly M positive eigenvalues γ_c for $c = 1, \ldots, M$. The remaining eigenvalue is zero with multiplicity $N - M$. With this in mind, we can perform the expectation over the GOE matrices keeping fixed the channel coupling vectors $\mathbf{w}_c$ for $c = 1, \ldots, M$. As we are interested in the limit $N \to +\infty$, we obtain

$$\lim_{N\to\infty} \mathbb{E}_{GUE(N)} \left[\frac{1}{(\lambda + i0)\mathbf{1}_N - \mathcal{H}_{eff}} \right] = \frac{g_0(\lambda)}{\mathbf{1}_N + i g_0(\lambda)\mathbf{\Gamma}}, \tag{B.6}$$

with $g_0(\lambda) = \frac{\lambda - i\sqrt{4-\lambda^2}}{2}$ for $|\lambda| < 2$. We can now plug this result in the definition for the scattering matrix to obtain its mean, namely

$$\overline{\mathbf{S}(\lambda)} = \mathbf{1}_M - 2ig_0(\lambda)\, \mathbf{W}^\dagger \frac{1}{\mathbf{1}_N + ig_0(\lambda)\mathbf{\Gamma}}\, \mathbf{W} \equiv \frac{\mathbf{1}_M - ig_0(\lambda)\mathbf{W}^\dagger\mathbf{W}}{\mathbf{1}_M + ig_0(\lambda)\mathbf{W}^\dagger\mathbf{W}} \tag{B.7}$$

One can now introduce the non-orthogonality condition of the channels in the following manner. Let's fix the scalar products $\mathbf{w}_1^*\mathbf{w}_1 = \mathbf{w}_2^*\mathbf{w}_2 =: \gamma$ while $\mathbf{w}_1^*\mathbf{w}_2 = c$ with $|c| < \gamma$. In this case

$$\mathbf{W}^\dagger\mathbf{W} = \begin{bmatrix} \gamma & c \\ c^* & \gamma \end{bmatrix}$$

The eigenvalues of the matix above are $\gamma_1 = \gamma + |c|$ and $\gamma_2 = \gamma - |c|$, with $\gamma_1 > \gamma_2$. This case can be identified with the random Gaussian correlated channels in section 2.2.1.2 if one introduce the correlation matrix $\mathbf{C}^{-1} = \mathbf{W}^\dagger\mathbf{W}$. If now, we set $\lambda = 0$, one clearly has $ig_0(0) = 1$ and the $\overline{\mathbf{S}(\lambda)}$ becomes

$$\overline{\mathbf{S}\,(\lambda = 0)} = \frac{1}{(1+\gamma)^2 - |c|^2} \begin{bmatrix} 1 - \gamma^2 + |c|^2 & -2c \\ -2c^* & 1 - \gamma^2 + |c|^2 \end{bmatrix}.$$

The spectrum of the latter is

$$s_1 = \frac{1 - (\gamma + |c|)}{1 + (\gamma + |c|)} \equiv \frac{1 - \gamma_1}{1 + \gamma_1}, \quad s_2 = \frac{1 - (\gamma - |c|)}{1 + (\gamma - |c|)} \equiv \frac{1 - \gamma_2}{1 + \gamma_2}$$

Therefore, if we take some $\gamma \in (1/2, 1)$ and we sufficiently increase the parameter $|c|$ the eigenvalue s_1 vanish for $|c| = 1 - \gamma$. This behaviour is connected with the "perfect coupling". To describe this phenomenon in full detail we start from the determinant of eq(**B.7**). The latter admits the form

$$\det\left(\overline{\mathbf{S}(\lambda)}\right) = \frac{\det\left(\mathbf{1}_M - ig_0(\lambda)\mathbf{W}^\dagger\mathbf{W}\right)}{\det\left(\mathbf{1}_M + ig_0(\lambda)\mathbf{W}^\dagger\mathbf{W}\right)}, \tag{B.8}$$

The eigenvalues of $\mathbf{W}^\dagger\mathbf{W}$ correspond to the nonvanishing eigenvalues of $\mathbf{\Gamma}$ indicated as γ_c for $c = 1, \dots, M$. Therefore, the modulus of the ratio of characteristic polynomials considered above is

$$\left|\det\left(\overline{\mathbf{S}(\lambda)}\right)\right| = \prod_{c=1}^{M}\sqrt{\frac{g_c - 1}{g_c + 1}}, \quad g_c = \frac{1}{2\pi\rho(\lambda)}\left(\gamma_c + \frac{1}{\gamma_c}\right) \tag{B.9}$$

Finally, one can easily check that by increasing parameters $\gamma_c \to 1^-$ the quantity g_c becomes 1 for $\lambda = 0$. In this onset, an eigenvalue of $\overline{\mathbf{S}(\lambda)}$ vanishes. Therefore, the determinant in eq(**B.8**) becomes equal to zero. This phenomenon is referred in literature as "perfect coupling". One of the features is worth to mention for perfect coupling is the formation of widely distributed chaotic resonances. This is described by a characteristic powerlaw tail in the density of the resonance widths [143].

B.4 Statistics of $\mathbf{K}_{ab}$ for the case of preserved time-reversal invariance

With time-reversal invariance, we need a new approach to find the characteristic function of $\mathbf{K}_{a,b}$. We start by observing that, in this case, the characteristic function of $\mathbf{K}_{a,b}$ can be written as

$$\mathcal{R}(q, q^*) = \mathbb{E}_{GOE(N)}\left[\overline{e^{i/2(q^*\mathbf{K}_{ab} + q\mathbf{K}^*_{ab})}}\right]$$

with $q = k + is \in \mathbb{C}$. Similarly to eq(**B.1**), the sum at the exponent can be re-casted with the help of the eigenvectors of $\mathbf{H}$ and is equivalent to

$$q^*\mathbf{K}_{ab} + q\mathbf{K}^*_{ab} = \sum_{n=1}^{N} w_{a,n}w_{b,n}\Big(\frac{q^*(\lambda - \lambda_n - i\alpha/N) + q(\lambda - \lambda_n + i\alpha/N)}{(\lambda - \lambda_n)^2 + \alpha^2/N^2}\Big).$$

We can easily perform the integration over the coupling variables $w_{a,n}, w_{b,n}$. The result of this integral is shown in eq(**2.11**). To simplify the derivation we fix $\lambda = 0$. We will recover the case for λ finite in the next section by universality arguments. Following [35], the matrix $\mathbf{H}_N$ can be divided in sub-blocks as

$$\mathbf{H}_N = \left[\begin{array}{cc|c} H_{11} & H_{12} & \boldsymbol{h}_1^T \\ H_{12} & H_{22} & \boldsymbol{h}_2^T \\ \hline \boldsymbol{h}_1 & \boldsymbol{h}_2 & \mathbf{H}_{N-2} \end{array}\right], \tag{B.10}$$

where $\mathbf{H}_{N-2}$ is the $(N-2)\times(N-2)$ square block obtained from $\mathbf{H}_N$ by removing the first two columns and two rows. The remaining terms $\boldsymbol{h}_1$ and $\boldsymbol{h}_2$ are $(N-2)$ dimensional vectors. With the help of the Schur complement, the numerator in eq(**2.11**), as we set $\lambda = 0$, is simply

$$\det\left(\mathbf{H}_N^2 + \frac{\alpha^2}{N^2}\mathbf{1}_N\right) = \det\left(\mathbf{H}_{N-2}^2 + \frac{\alpha^2}{N^2}\mathbf{1}_N\right)|\Delta|^2$$

where:

$$\Delta = \det\left(\begin{bmatrix} H_{1,1} - i\frac{\alpha}{N} & H_{1,2} \\ H_{1,2} & H_{2,2} - i\frac{\alpha}{N}\end{bmatrix} - \begin{bmatrix}\boldsymbol{h}_1^T \\ \boldsymbol{h}_2^T\end{bmatrix}\frac{1}{\mathbf{H}_{N-2} - i\frac{\alpha}{N}}\begin{bmatrix}\boldsymbol{h}_1 & \boldsymbol{h}_2\end{bmatrix}\right).$$

The characteristic polynomials at the denominator in eq(**2.11**) are equivalently written as Gaussian integrals, namely

$$\int_{\mathbb{R}^N} d\boldsymbol{x}\exp\left(-\boldsymbol{x}^T\mathbf{A}\boldsymbol{x}\right) \propto \frac{1}{\sqrt{\det \mathbf{A}}}$$

for $\operatorname{Re}\mathbf{A} \succ 0$. If we collect all the considerations above, the characteristic function for the imaginary part[1] of $\mathbf{K}_{ab}$ for $\lambda = 0$ is proportional to

$$\mathbb{E}_{GOE(N)}\left[\overline{e^{is\operatorname{Im}\mathbf{K}_{a,b}}}\right] \propto \mathbb{E}_{GOE(N)}\left[\int_{\mathbb{R}^{2N}} d\boldsymbol{x}_1 d\boldsymbol{x}_2 \exp\left(-\operatorname{Tr}\left\{\mathbf{H}_N^2\mathbf{Q} + \sum_{j=1,2}\frac{\omega_j^2}{N^2}\mathbf{1}_N\left(\boldsymbol{x}_j\otimes\boldsymbol{x}_j^T\right)\right\}\right)\right. \tag{B.11}$$
$$\left.\times\det\left(\mathbf{H}_{N-2}^2 + \frac{\alpha^2}{N^2}\mathbf{1}_N\right)|\Delta|^2\right]$$

We don't need to keep track of all the constant factors, but rather recover the overall factor in the end of this section using a normalization condition. In eq(**B.11**) we introduced the rank-2 symmetric matrix $\boldsymbol{Q} = \boldsymbol{x}_1\otimes\boldsymbol{x}_1^T + \boldsymbol{x}_2\otimes\boldsymbol{x}_2^T$. Such matrix has clearly two positive eigenvalues $\{q_1 > 0, q_2 > 0\}$. Therefore, it can be represented as $\mathbf{Q} = \mathbf{O}\operatorname{diag}(q_1, q_2, 0, \dots, 0)\mathbf{O}^T$ with $\mathbf{O} \in Orth(N)$. The integrand introduced above in $\boldsymbol{x}_1$ and $\boldsymbol{x}_2$ can be written as function of the full rank symmetric matrix

$$\tilde{\mathbf{Q}} = \begin{bmatrix} |\boldsymbol{x}_1|^2 & \boldsymbol{x}_1^T\boldsymbol{x}_2 \\ \boldsymbol{x}_1^T\boldsymbol{x}_2 & |\boldsymbol{x}_2|^2\end{bmatrix}$$

Indeed, one can easily check that its eigenvalues are q_1, q_2. We can use the result in eq(**1.35**) for $n = 2$ so that:

$$\mathbb{E}_{GOE(N)}\left[\overline{e^{is\operatorname{Im}\mathbf{K}_{a,b}}}\right] \propto \int_0^\infty\int_0^\infty dq_1\,dq_2(q_1q_2)^{\frac{N-3}{2}}|q_1 - q_2|\Phi(q_1, q_2; \alpha)\times \tag{B.12}$$

[1]The statistics for real part of $\mathbf{K}_{ab}$ follows a similar path (see the next section).

$$\times \int_{O(2)} d\mu(\mathbf{O}) \exp\Big(-\frac{1}{N^2}\operatorname{Tr}\begin{bmatrix}\omega_1^2 & 0\\ 0 & \omega_2^2\end{bmatrix}\mathbf{O}\begin{bmatrix}q_1 & 0\\ 0 & q_2\end{bmatrix}\mathbf{O}^T\Big),$$

with

$$\Phi(q_1, q_2, \alpha) = \mathbb{E}_{GOE(N)}[\det(\mathbf{H}_N^2 + \alpha^2/N^2)\exp(-\operatorname{Tr}\mathbf{H}_N^2\mathbf{Q})]. \tag{B.13}$$

for the purpose of this calculation $\mathbf{O}$ can be described by a real parameter $\varphi \in (0, \pi/2)$ as $\begin{bmatrix}\cos\varphi & \sin\varphi\\ -\sin\varphi & \cos\varphi\end{bmatrix}$. Hence the last integral in eq(**B.12**) can be performed by observing

$$\int_0^{\pi/2} d\varphi\, e^{\cos^2\varphi(\omega_1^2 q_1+\omega_2^2 q_2)+\sin^2\varphi(\omega_1^2 q_2+\omega_2^2 q_1)} = \frac{\pi}{2}\, e^{-\frac{\alpha^2}{N^2}(q_1+q_2)} J_0\Big(\frac{\alpha S}{N^2}(q_1-q_2)\Big), \tag{B.14}$$

where $J_0(x)$ is the Bessel function of the first kind of order 0. We still need to integrate over q_1 and q_2. We anticipate here that this is a challenging task and remains unsolved. Nevertheless we can explicitly calculate the expectation over Gaussian Orthogonal ensemble in eq(**B.13**). Re-introducing the block structure of eq(**B.10**) and the inverse matrices $\mathbf{M} = (\mathbf{H}_{N-2} - i\frac{\alpha}{N})^{-1}$ and $\mathbf{M}^* = (\mathbf{H}_{N-2} + i\frac{\alpha}{N})^{-1}$ one can re-cast $\Phi(q_1, q_2; \alpha)$ as

$$\Phi(q_1, q_2; \alpha) = \sum_{m,n,p} u_{m,n,p}(q_1, q_2, \alpha)\mathbb{E}_{GOE(N-2)}\Big[\Big(Tr(\mathbf{M})^m(\mathbf{M}^*)^n\Big)^p\Big] \tag{B.15}$$

For some coefficients $u_{m,n,p}(q_1, q_2, \alpha)$ with $0 \le m, n \le 2, 0 \le p \le 4$. To perform the average over $GOE(N)$ we need the following expressions. Firstly, $\operatorname{Tr}\left(\boldsymbol{H}_N^2(\boldsymbol{Q} + \frac{N}{4}\mathbf{1}_N)\right)$ is a quadratic polynomial in the entries of $\boldsymbol{H}_N$, namely,

$$\operatorname{Tr}\left(\boldsymbol{H}_N^2(\boldsymbol{Q} + \frac{N}{4}\mathbf{1}_N)\right) = \alpha_1 H_{11}^2 + \alpha_2 H_{22}^2 + \alpha_{12} H_{12}^2 + \beta_1|\boldsymbol{h}_1|^2 + \beta_2|\boldsymbol{h}_2|^2 + \frac{N}{4}\operatorname{Tr}\left(\boldsymbol{H}_{N-2}^2\right)$$

with

$$\begin{cases}\alpha_1 = q_1 + \frac{N}{4}\\ \alpha_2 = q_2 + \frac{N}{4}\\ \beta_1 = q_1 + \frac{N}{2}\\ \beta_2 = q_2 + \frac{N}{2}\\ \alpha_{12} = \alpha_1 + \alpha_2\end{cases} \tag{B.16}$$

Secondly,

$$\Delta\Delta^* = |H_{11}H_{22} - Z_{11}H_{22} - H_{11}Z_{22} + Z_{11}Z_{22} - H_{12}^2 - Z_{12}^2 + 2H_{12}Z_{12}|^2,$$

where $Z_{ij} = i\delta_{ij}\frac{\alpha}{N} + \operatorname{Tr}(\mathbf{M}(\mathbf{h}_j \otimes \mathbf{h}_i^T))$. We can now start calculating the expectation over the Gaussian variables H_{11}, H_{12}, H_{22} since we know

$$\int_{-\infty}^{+\infty} e^{-ax^2}|cx^2 + bx + d|^2 dx = \frac{\sqrt{\pi}}{4a^{5/2}}(3|c|^2 + 2a|b|^2 + 2a(dc^* + d^*c) + 4a^2|d|^2) \tag{B.17}$$

with $a > 0, b, c, d \in \mathbb{C}$. First we integrate out H_{11}, i.e.

$$\int e^{-\alpha_1 H_{11}^2} |\Delta|^2 dH_{11} = \frac{\sqrt{\pi}}{2\alpha_1^{3/2}} \left(|H_{22} - Z_{22}|^2 + 2\alpha_1| - Z_{11}H_{22} + Z_{11}Z_{22} - H_{12}^2 - Z_{12}^2 + 2H_{12}Z_{12}|^2\right)$$

A similar path allows one to integrate over H_{22} and H_{12}, so that, exploiting the integrals above we are left with

$$\Phi(q_1, q_2; \alpha) \propto \int d\mathbf{h}_1 d\mathbf{h}_2 d\mathbf{H}_{N-2}\, e^{-\beta_1|\mathbf{h}_1|^2 - \beta_2|\mathbf{h}_2|^2 - \frac{N}{4}\operatorname{Tr}\mathbf{H}_{N-2}^2} \det\left(\mathbf{H}_{N-2}^2 + \frac{\alpha^2}{N^2}\mathbf{1}_{N-2}\right)$$

$$\times\Big(a_1 + a_2|Z_{11}|^2 + a_3|Z_{22}|^2 + a_4|Z_{12}|^2 + 2a_5\operatorname{Re}(Z_{11}Z_{22} - Z_{12}^2) + a_6|Z_{11}Z_{22} - Z_{12}^2|^2\Big), \quad \text{(B.18)}$$

where

$$a_1 = \frac{1}{\alpha_{12}^{1/2}} + 3\frac{\alpha_1\alpha_2}{\alpha_{12}^{5/2}},\ a_2 = \frac{2\alpha_1}{\alpha_{12}^{1/2}},\ a_3 = \frac{2\alpha_2}{\alpha_{12}^{1/2}}$$
$$a_4 = \frac{8\alpha_1\alpha_2}{\alpha_{12}^{5/2}},\ a_5 = -2\frac{\alpha_1\alpha_2}{\alpha_{12}^{3/2}},\ a_6 = 4\frac{\alpha_1\alpha_2}{\alpha_{12}^{1/2}}$$

The integration over the vectors $\boldsymbol{h}_1$ and $\boldsymbol{h}_2$ in eq(**B.18**) need the following results for $\beta_1, \beta_2 > 0$:

$$\int_{\mathbb{R}^{N-2}} (\boldsymbol{h}_1^T M \boldsymbol{h}_1) e^{-\beta_1 \boldsymbol{h}_1^2} d\boldsymbol{h}_1 = \left(\frac{\pi}{\beta_1}\right)^{(N-2)/2} \frac{1}{2\beta_1} \operatorname{Tr}\mathbf{M}$$

and

$$\int_{\mathbb{R}^{N-2}} e^{-\beta_1 \boldsymbol{h}_1^2} \left(\boldsymbol{h}_1^T \mathbf{M}_1 \boldsymbol{h}_1\right)\left(\boldsymbol{h}_1^T \mathbf{M}_2 \boldsymbol{h}_1\right) d\boldsymbol{h}_1 = \frac{1}{4}\frac{\pi^{(N-2)/2}}{\beta_1^{(N-2)/2}}\frac{1}{\beta_1^2}(\operatorname{Tr}\mathbf{M}_1 \operatorname{Tr}\mathbf{M}_2 + 2\operatorname{Tr}\mathbf{M}_1\mathbf{M}_2),$$

as well as

$$\int_{\mathbb{R}^{2(N-2)}} e^{-\beta_1 \boldsymbol{h}_1^2 - \beta_2 \boldsymbol{h}_2^2} \left(\boldsymbol{h}_1^T \mathbf{M}_1 \boldsymbol{h}_2\right)\left(\boldsymbol{h}_1^T \mathbf{M}_2 \boldsymbol{h}_2\right) d\boldsymbol{h}_1 d\boldsymbol{h}_2 = \left(\frac{\pi^2}{\beta_1\beta_2}\right)^{(N-2)/2} \frac{1}{4\beta_1\beta_2} \operatorname{Tr}\mathbf{M}_1\mathbf{M}_2,$$

and

$$\int_{\mathbb{R}^{2(N-2)}} e^{-\beta_1 \boldsymbol{h}_1^2 - \beta_2 \boldsymbol{h}_2^2} \left(\boldsymbol{h}_1^T \mathbf{M}_1 \boldsymbol{h}_2\right)^2 \left(\boldsymbol{h}_1^T \mathbf{M}_2 \boldsymbol{h}_2\right)^2 d\boldsymbol{h}_1 d\boldsymbol{h}_2$$

$$= \frac{1}{16}\left(\frac{\pi^2}{\beta_1\beta_2}\right)^{(N-2)/2} \frac{1}{\beta_1^2\beta_2^2}(\operatorname{Tr}\mathbf{M}_1^2 \operatorname{Tr}\mathbf{M}_2^2 + 4\operatorname{Tr}\mathbf{M}_1^2\mathbf{M}_2^2 + 2\operatorname{Tr}^2\mathbf{M}_1\mathbf{M}_2 + 2\operatorname{Tr}(\mathbf{M}_1\mathbf{M}_2)^2),$$

and finally

$$\int_{\mathbb{R}^{2(N-2)}} e^{-\beta_1 \boldsymbol{h}_1^2 - \beta_2 \boldsymbol{h}_2^2} \left(\boldsymbol{h}_1^T \mathbf{M} \boldsymbol{h}_2\right)^2 \left(\boldsymbol{h}_1^T \mathbf{M}^* \boldsymbol{h}_1\right) d\boldsymbol{h}_1 d\boldsymbol{h}_2$$
$$= \frac{1}{8}\left(\frac{\pi^2}{\beta_1\beta_2}\right)^{(N-2)/2} \frac{1}{\beta_1^2\beta_2}(\operatorname{Tr}\mathbf{M}^2 \operatorname{Tr}\mathbf{M}^* + 2\operatorname{Tr}(\mathbf{M}^2\mathbf{M}^*))$$

and

$$\int_{\mathbb{R}^{2(N-2)}} e^{-\beta_1 \boldsymbol{h}_1^2 - \beta_2 \boldsymbol{h}_2^2} \left(\boldsymbol{h}_1^T \mathbf{M} \boldsymbol{h}_2\right)^2 \left(\boldsymbol{h}_1^T \mathbf{M}^* \boldsymbol{h}_1\right)\left(\boldsymbol{h}_2^T \mathbf{M}^* \boldsymbol{h}_2\right) d\boldsymbol{h}_1 d\boldsymbol{h}_2$$

$$= \frac{1}{16}\Big(\frac{\pi^2}{\beta_1\beta_2}\Big)^{(N-2)/2}\frac{1}{\beta_1^2\beta_2^2}(\operatorname{Tr}\mathbf{M}^2\operatorname{Tr}^2\mathbf{M}^* + 4\operatorname{Tr}\mathbf{M}^2\mathbf{M}^*\operatorname{Tr}\mathbf{M}^* + 4\operatorname{Tr}(\mathbf{M}\mathbf{M}^*)^2).$$

Using these equalities, up to a constant factor, $\Phi(q_1, q_2; \alpha)$ is given by

$$\Phi(q_1, q_2; \alpha) \propto \Big(\frac{\pi^2}{\beta_1\beta_2}\Big)^{(N-2)/2}\int d\mathbf{H}_{N-2}e^{-\frac{N}{4J^2}\operatorname{Tr}\mathbf{H}_{N-2}^2}\det(\mathbf{H}_{N-2}^2 + \frac{\alpha^2}{N^2}\mathbf{1}_{N-2})$$

$$\times\big\{u_1 + u_2\operatorname{Tr}(\mathbf{M}-\mathbf{M}^*) + u_3\operatorname{Tr}\mathbf{M}\mathbf{M}^* + 2u_4\operatorname{Re}(\operatorname{Tr}^2\mathbf{M} - \operatorname{Tr}\mathbf{M}^2) + u_5\operatorname{Tr}\mathbf{M}\operatorname{Tr}\mathbf{M}^*$$

$$+u_6\Big(\operatorname{Tr}(\mathbf{M}-\mathbf{M}^*)(\operatorname{Tr}\mathbf{M}\operatorname{Tr}\mathbf{M}^* + 2\operatorname{Tr}\mathbf{M}\mathbf{M}^*)$$

$$+\operatorname{Tr}\mathbf{M}^2\operatorname{Tr}\mathbf{M}^* + 2\operatorname{Tr}\mathbf{M}^2\mathbf{M}^* - (\operatorname{Tr}\mathbf{M}^{*2}\operatorname{Tr}\mathbf{M} + 2\operatorname{Tr}\mathbf{M}^{*2}\mathbf{M})\Big)$$

$$+u_7\Big((\operatorname{Tr}\mathbf{M}\operatorname{Tr}\mathbf{M}^* + 2\operatorname{Tr}\mathbf{M}\mathbf{M}^*)^2 + \operatorname{Tr}\mathbf{M}^2\operatorname{Tr}\mathbf{M}^{*2} + 6\operatorname{Tr}(\mathbf{M}\mathbf{M})^2$$

$$+2(\operatorname{Tr}\mathbf{M}\mathbf{M}^*)^2 - 2\operatorname{Re}(\operatorname{Tr}\mathbf{M}^2(\operatorname{Tr}\mathbf{M}^*)^2 + 4\operatorname{Tr}\mathbf{M}^2\mathbf{M}^*\operatorname{Tr}\mathbf{M}^* + 4\operatorname{Tr}(\mathbf{M}\mathbf{M}^*)^2)\Big)\Big\},$$

with:

$$u_1 = a_1 + \frac{\alpha^2}{N^2}a_2 + \frac{\alpha^2}{N^2}a_3 - 2\frac{\alpha^2}{N^2}a_5 + \frac{\alpha^4}{N^4}a_6,$$

$$u_2 = -i\frac{\alpha}{N}\frac{a_2}{2\beta_1} - i\frac{\alpha}{N}\frac{a_3}{2\beta_2} + i\frac{\alpha a_5}{(2N)}(\frac{1}{\beta_1} + \frac{1}{\beta_2}) - i\frac{\alpha^3 a_6}{(2N^3)}(\frac{1}{\beta_1} + \frac{1}{\beta_2}),$$

$$u_3 = \frac{a_2}{2\beta_1^2} + \frac{a_3}{2\beta_2^2} + \frac{a_4}{4\beta_1\beta_2} + \frac{a_6\alpha^2}{2N^2}(\frac{1}{\beta_1^2} + \frac{1}{\beta_2^2}),$$

$$u_4 = \frac{a_5}{4\beta_1\beta_2} - \frac{\alpha^2}{4N^2}\frac{a_6}{\beta_1\beta_2}; u_5 = \frac{a_2}{4\beta_1^2} + \frac{a_3}{4\beta_2^2} + \frac{\alpha^2 a_6}{4N^2}(\frac{1}{\beta_1^2} + \frac{1}{\beta_2^2}) + \frac{\alpha^2}{2N^2}\frac{a_6}{\beta_1\beta_2},$$

$$u_6 = \frac{i\alpha}{8N}a_6(\frac{1}{\beta_1^2\beta_2} + \frac{1}{\beta_1\beta_2^2}); \quad u_7 = \frac{a_6}{16\beta_1^2\beta_2^2}.$$

We have obtained the coefficients of the sum in eq(**B.15**). We are left with the evaluation of the average over $GOE(N-2)$ of polynomials of traces for $\mathbf{M} = \big(\mathbf{H}_{N-2} - i\frac{\alpha}{N}\big)^{-1}$ and its complex conjugate. Since $\mathbf{M} - \mathbf{M}^* = 2i\frac{\alpha}{N}\mathbf{M}\mathbf{M}^*$, each monomial can be rewritten as a combination of derivatives of characteristic polynomials, i.e. $\partial_\xi^m\det(\mathbf{H}_{N-2} - (\xi \pm i\alpha/N))|_{\xi=0}$ for some $m > 0$. This leave us with the expectation of characteristic polynomials over the realizations of $\mathbf{H}_{N-2}$. For this purpose, we exploit the correlation function of the product of two characteristic polynomials, for $N \gg 1$, see e.g. [34]:

$$\mathbb{E}_{GOE(N-2)}\Big[\det\Big(\mathbf{H}_{N-2} - i\frac{\alpha}{N} - \xi_+\Big)\det\Big(\mathbf{H}_{N-2} + i\frac{\alpha}{N} - \xi_-\Big)\Big]$$

$$\propto \frac{-f(\xi_+ - \xi_-)\cos\Big(f(\xi_+ - \xi_-)\Big) + \sin\Big(f(\xi_+ - \xi_-)\Big)}{f^3(\xi_+ - \xi_-)} := C_{SP}(\xi_+ - \xi_-) \qquad \text{(B.19)}$$

with $f(\xi) = 2i\alpha + N\xi$. The set of identities

$$\frac{d}{d\xi}\det(\mathbf{H}_{N-2}-(\xi\pm i\alpha/N)\mathbf{1}_N) = -\operatorname{Tr}\Big(\mathbf{H}_{N-2}-(\xi\pm i\alpha/N)\mathbf{1}_N\Big)^{-1}\det(\mathbf{H}_{N-2}-(\xi\pm i\alpha/N)\mathbf{1}_N)$$

and

$$\frac{d}{d\xi}\operatorname{Tr}\Big(\mathbf{H}_{N-2}-(\xi\pm i\alpha/N)\mathbf{1}_N\Big)^{-k} = k\operatorname{Tr}\Big(\mathbf{H}_{N-2}-(\xi\pm i\alpha/N)\mathbf{1}_N\Big)^{-(k+1)}$$

allow one to re-write Φ as:

$$\Phi(q_1,q_2;\alpha) \propto \lim_{\delta\to 0}\sum_{j=0}^{4} b_j(q_1,q_2,\alpha)\,\hat{D}_j C_{SP}(\delta) \tag{B.20}$$

where the coefficients b_j are given by the following expressions:

$$b_0 = \frac{1}{\sqrt{\alpha_{12}}} + 3\frac{\alpha_1\alpha_2}{\alpha_{12}^{5/2}} + 2\frac{\alpha^2}{N^2}\frac{\alpha_1+\alpha_2}{\sqrt{\alpha_{12}}} + 4\frac{\alpha^2}{N^2}\frac{\alpha_1\alpha_2}{\alpha_{12}^{3/2}} + 4\frac{\alpha^4}{N^4}\frac{\alpha_1\alpha_2}{\sqrt{\alpha_{12}}},$$

$$b_1 = -\frac{i}{\sqrt{\alpha_{12}}}\frac{\alpha}{N}\Big(\frac{\alpha_1}{\beta_1}+\frac{\alpha_2}{\beta_2}\Big) - i\frac{\alpha}{N}\frac{\alpha_1\alpha_2}{\alpha_{12}^{3/2}}\Big(\frac{1}{\beta_1}+\frac{1}{\beta_2}\Big) - i2\frac{\alpha^3}{N^3}\frac{\alpha_1\alpha_2}{\sqrt{\alpha_{12}}}\Big(\frac{1}{\beta_1}+\frac{1}{\beta_2}\Big)+$$
$$-\frac{iN}{2\alpha}\Big(\frac{1}{\sqrt{\alpha_{12}}}\Big(\frac{\alpha_1}{\beta_1^2}+\frac{\alpha_2}{\beta_2^2}\Big) + 2\frac{\alpha_1\alpha_2}{\alpha_{12}^{3/2}\beta_1\beta_2} + 2\frac{\alpha^2}{N^2}\frac{\alpha_1\alpha_2}{\sqrt{\alpha_{12}}}\Big(\frac{1}{\beta_1^2}+\frac{1}{\beta_2^2}\Big)\Big),$$

$$b_2 = -\frac{\alpha_1\alpha_2}{\alpha_{12}^{3/2}\beta_1\beta_2} - 2\frac{\alpha^2}{N^2}\frac{\alpha_1\alpha_2}{\sqrt{\alpha_{12}}\beta_1\beta_2} - \Big(\frac{\alpha_1}{2\sqrt{\alpha_{12}}\beta_1^2} + \frac{\alpha_2}{2\sqrt{\alpha_{12}}\beta_2^2} + \frac{\alpha^2}{N^2}\frac{\alpha_1\alpha_2}{\sqrt{\alpha_{12}}}\Big(\frac{1}{\beta_1^2}+\frac{1}{\beta_2^2}+\frac{2}{\beta_1\beta_2}\Big)\Big)$$

and

$$b_3 = i\frac{\alpha}{2N}\frac{\alpha_1\alpha_2}{\sqrt{\alpha_{12}}}\Big(\frac{1}{\beta_1\beta_2^2}+\frac{1}{\beta_2\beta_1^2}\Big) \quad \text{and} \quad b_4 = \frac{\alpha_1\alpha_2}{4\sqrt{\alpha_{12}}\beta_1^2\beta_2^2},$$

We also need a list of differential operators $\hat{\mathcal{D}}_j$:

$$\hat{\mathcal{D}}_0 = 1, \quad \hat{\mathcal{D}}_1 = -2\partial_\delta, \quad \hat{\mathcal{D}}_2 = \partial_\delta^2, \quad \hat{\mathcal{D}}_3 = -2\partial_\delta^3 + \frac{4Ni}{\alpha}\partial_\delta^2 - \frac{2N^2}{\alpha^2}\partial_\delta$$

and

$$\hat{\mathcal{D}}_4 = \partial_\delta^4 - \frac{N^2}{\alpha^2}\Big(2\partial_\delta^2 + \frac{iN}{\alpha}\partial_\delta - \frac{4Ni}{\alpha}\partial_\delta^3\Big)$$

where $\partial_\delta^k := \frac{\partial^k}{\partial\delta^k}$. As we were interested in $N\to+\infty$, we can obtain meaningful asymptotic rescaling $q_{1,2}\to N^2 q_{1,2}$ so that

$$(\beta_1\beta_2)^{N/2}\beta_1\beta_2 \approx e^{-1/4(q_1^{-1}+q_2^{-1})}(q_1q_2)^{1-N/2},$$

and $\alpha_1 \approx N^2 q_1$, $\alpha_2 \approx N^2 q_2$. We can plug all these results back into eq(**B.20**) and retrieve the proportionality constant "lost" in eq(**B.11**) by imposing

$$\mathbb{E}_{GOE(N)}\Big[\overline{e^{is\,\mathrm{Im}\,\mathbf{K}_{a,b}}}\Big] = 1$$

for either $\alpha = 0$ or $s = 0$. Since in eq(**B.12**) the limit $\alpha \to 0^+$ and the integrals over $q_{1,2}$ do not commute, the constant of proportionality is necessarily dependent on the value taken by α. One can recover, from all the steps above, the missing terms apart from the factor in eq(**B.19**). The latter can be obtained as follows. We take, in order, N to be odd for simplicity, $\xi_\pm \to 0$ and $\alpha \to 0$. Following [144], one verifies that

$$\mathbb{E}_{GOE(N-2)}\left[|\det \mathbf{H}_{N-2}|^{r-1}\right] = N^{\frac{(N-2)(r-1)}{2}}\, 2^{r-1}\frac{\Gamma(r/2)}{\Gamma(1/2)}\prod_{j=1}^{(N-3)/2} 2^{r-1}\frac{\Gamma(r+j-1/2)}{\Gamma(j+1/2)} \tag{B.21}$$

with $r > 1$. This is sufficient to replace the symbol $\propto$ with the equality in eq(**B.11**) and, therefore, to obtain the characteristic function as in eq(**2.16**). By inverting the Fourier transform we obtain the probability density function of $\mathrm{Im}\,\mathbf{K}_{a,b}$. This is possible as

$$\mathcal{F}^{-1}\Big[J_0\Big(\alpha s(q_1-q_2)\Big)\Big] := \frac{1}{2\pi}\int_{-\infty}^{+\infty} ds e^{-is\,\mathrm{Im}\,\mathbf{K}_{ab}} J_0\Big(\alpha s(q_1-q_2)\Big) =$$
$$\frac{1}{\pi}\frac{\mathbf{1}(\Omega)}{\sqrt{\alpha^2(q_1-q_2)^2 - \mathrm{Im}^2\,\mathbf{K}_{a,b}}},$$

where $\mathbf{1}(\Omega)$ is the indicator function of the set $\Omega = \{(q_1,q_2) \in \mathbb{R}^2_+ | \alpha^2(q_1-q_2)^2 > \mathrm{Im}^2\,K_{a,b}\}$. To obtain eq(**2.17**), one simply introduce $u = \alpha^{-1}\,\mathrm{Im}\,K_{a,b}$ as implicitly suggested by Ω.

B.4.1 Derivation of Eq(2.15)

What stated above can be adapted to obtain the characteristic function for $\mathrm{Re}\,\mathbf{K}_{a,b}$. Since this follows almost identically starting again by fixing $\lambda = 0$, we only report a few comments. Firstly, one need to consider

$$\mathbb{E}_{GOE(N)}\left[\overline{e^{ik\,\mathrm{Re}\,\mathbf{K}_{a,b}}}\right] = \mathbb{E}_{GOE(N)}\left[\frac{\det\left(\mathbf{H}_N^2 + \frac{\alpha^2}{N^2}\mathbf{1}_N\right)}{\Pi_{l=1,2}\det^{1/2}\left(\mathbf{H}_N^2 + (-1)^l\, i\frac{k}{N}\mathbf{H}_N + \frac{\alpha^2}{N^2}\mathbf{1}_N\right)}\right]. \tag{B.22}$$

The product of determinants appearing at the denominator is

$$\det(\mathbf{H}_N^2 + \tilde{\omega}_1^2)^{-1/2}\det(\mathbf{H}_N^2 + \tilde{\omega}_2^2)^{-1/2}$$

with

$$\begin{cases}\tilde{\omega}_1^2 = (k/2 + \sqrt{\alpha^2 + k^2/4})^2/N^2 \\ \tilde{\omega}_1^2 = (k/2 - \sqrt{\alpha^2 + k^2/4})^2/N^2\end{cases} \tag{B.23}$$

It is sufficient to explicitly obtain eq(**B.22**), to replace $\omega_{1,2}$ appearing in eq(**B.11**) with $\tilde{\omega}_{1,2}$ given above. Firstly, the integration over $\mathbf{O}$ in eq(**B.14**) has to be replaced with

$$I = \frac{\pi}{2} \exp\Big(- \frac{1}{2N^2}(k^2 + 2\alpha^2)(q_1 + q_2)\Big) J_0\Big(i\frac{k}{N^2}\sqrt{\alpha^2 + \frac{k^2}{4}(q_1 - q_2)}\Big).$$

Secondly, recovering the probability density function for $\mathrm{Re}\,\mathbf{K}_{a,b}$ is a much more challenging task in comparison with its imaginary counterpart since for

$$\frac{1}{2\pi}\int_{-\infty}^{\infty} e^{-ik\,\mathrm{Re}\,\mathbf{K}_{ab}} \exp\Big(- \frac{(q_1+q_2)}{2N^2}k^2\Big) I_0\Big(\frac{k}{N^2}\sqrt{\alpha^2 + \frac{k^2}{4}(q_1 - q_2)}\Big)\, dk$$

a known closed form is not available and one can only perform numerical evaluations.

B.5 Universality for Eq(2.18) and Eq(2.19)

To show universality and prove that the result in appendix B.4 for $\mathbb{E}_{GOE(N)}\left[\overline{e^{is\,\mathrm{Im}\,\mathbf{K}_{a,b}}}\right]$ holds for $\lambda \neq 0$ (after opportune re-scaling) we introduce an integral representation for the characteristic function(see [35]):

$$\begin{aligned}
\mathbb{E}_{GOE(N)}\left[\overline{e^{is\,\mathrm{Im}\,\mathbf{K}_{a,b}}}\right] \propto & \int_{\mathbf{Q}\succeq 0} d\mathbf{Q}(\det \mathbf{Q})^{(N-5)/2} \exp\Big(- \frac{N}{4}\,\mathrm{Tr}(\mathbf{QL})^2 + i\frac{N}{2}\,\mathrm{Tr}(\mathbf{QLM})\Big) \\
& \times \int_{\mathbb{R}} dr_1 \int_{\mathbb{R}} dr_2 \exp\Big(- \frac{N}{2}(r_1^2 + r_2^2 - i2\lambda(r_1 + r_2))\Big) \frac{(r_1 r_2)^{N-4}}{(2i\alpha)^3} \\
& \times \prod_{j=1}^{4}(r_1 + \lambda_j)(r_2 + \lambda_j) \exp\Big(N(\lambda^2 - \alpha^2/N^2)\Big) \\
& \times \Big(\frac{2i\alpha}{N(r_1 - r_2)} \cos\Big(\frac{2i\alpha(r_1 - r_2)}{2J^2}\Big) - \frac{2}{N}\sin\Big(\frac{2i\alpha(r_1 - r_2)}{2}\Big)\Big).
\end{aligned} \tag{B.24}$$

The matrix $\mathbf{Q}$ is a 4×4 positive definite real symmetric matrix, $\mathbf{L} = \mathrm{diag}(+1, +1, -1, -1)$ and $\mathbf{M} = \mathrm{diag}(\lambda + \frac{i}{N}\sqrt{\alpha^2 + i\alpha s}, \lambda + \frac{i}{N}\sqrt{\alpha^2 - i\alpha s}, \lambda - \frac{i}{N}\sqrt{\alpha^2 + i\alpha s}, \lambda - \frac{i}{N}\sqrt{\alpha^2 - i\alpha s})$. One can perform a saddle point approximation in $r_{1,2}$. Such points occur at $r_{1,2} = 1/2(i\lambda \pm 2\pi\rho)$. However one needs to expand the integral in eq(**B.24**) and include the Gaussian fluctuations as integrand vanishes once evaluated at the saddle-point . More in detail, keeping track and control of the higher orders is a non trivial task. However, here it is sufficient to observe that such integral satisfy the re-scaling introduced in eq(**2.18**).

B.6 Second Moment for $\mathbf{K}_{ab}$.

While recovering the probability density function proved to be a challenging task, interestingly, one can easily address the second moment for the components of $\mathbf{K}_{a,b}$. Hence, we report here the explicit expressions for $\mathbb{E}_{GOE(N)}[\overline{(\mathrm{Re}\,\mathbf{K}_{a,b})^2}]$ and $\mathbb{E}_{GOE(N)}[\overline{(\mathrm{Im}\,\mathbf{K}_{a,b})^2}]$. As in the sections above, $\mathbf{K}_{ab}$ can be written in terms of the eigenvalues and eigenvectors of $\mathbf{H}_N = \mathbf{O}\mathbf{\Lambda}\mathbf{O}^T$ as

$$\mathbf{K}_{ab} = \sum_{n=1}^{N} \frac{\sum_{i,j=1}^{N} w_{a,i}(\mathbf{O})_{in}(\mathbf{O})_{nj}w_{b,j}}{\lambda - \lambda_n + i\alpha/N}. \tag{B.25}$$

We can multiply real and imaginary parts in eq(**B.25**) by itself and average over the Gaussian channel vectors, obtaining after simple manipulations

$$\lim_{N\to\infty} \mathbb{E}_{GOE(N)}[\overline{(\mathrm{Im}\,\mathbf{K}_{a,b})^2}] = -\lim_{N\to\infty} \frac{\alpha}{2N}\frac{d}{d\alpha}\Big(\mathrm{Im}\,\mathbb{E}_{GOE(N)}\left[\mathrm{Tr}\,\frac{1/\alpha}{(\lambda - i\alpha/N)\mathbf{1}_N - \mathbf{H}_N}\right]\Big) \tag{B.26}$$

and:

$$\lim_{N\to\infty} \mathbb{E}_{GOE(N)}[\overline{(\mathrm{Re}\,\mathbf{K}_{a,b})^2}] = \lim_{N\to\infty} \frac{1}{2N\alpha}\frac{d}{d\alpha}\Big(\mathrm{Im}\,\mathbb{E}_{GOE(N)}\left[\mathrm{Tr}\,\frac{\alpha}{(\lambda - i\alpha/N)\mathbf{1}_N - \mathbf{H}_N}\right]\Big) \tag{B.27}$$

From now on we consider valid the exchange of the limit $N \to \infty$ with the derivative in α. If this is the case, the traces above can be written by introducing the Stieltjes transform of the semicircle law:

$$\lim_{N\to\infty} \mathbb{E}_{GOE(N)}\left[\frac{1}{N}\mathrm{Tr}\,\frac{1}{\mathbf{H}_N - z}\right] = \frac{1}{2\pi}\int_{-2}^{2}\frac{\sqrt{4-x^2}}{x-z}dx$$
$$= \frac{\lambda - i\alpha/N}{2}\left(-1 + \sqrt{1 + \frac{4}{(\alpha/N + i\lambda)^2}}\right)$$

The imaginary parts are computed by noticing $\sqrt{a+ib} = x + iy$ where (see [23])

$$x = 1/\sqrt{2}\sqrt{\sqrt{a^2+b^2}+a}$$

and

$$y = \mathrm{sign}(b)/\sqrt{2}\sqrt{\sqrt{a^2+b^2}-a}$$

One can see that the derivatives in eq(**B.26**) and eq(**B.27**) in terms of α gives:

$$\mathbb{E}_{GOE(N)}[\overline{(\mathrm{Re}\,\mathbf{K}_{a,b})^2}] = \frac{\sqrt{4-\lambda^2}}{4\alpha},$$

This result also holds for $\mathbb{E}_{GOE(N)}[\overline{(\mathrm{Im}\,\mathbf{K}_{a,b})^2}]$.

Appendix C

Appendix for Chapter 3

C.1 Joint probability density function Eq(3.14)

We want to recover, starting from eq(3.8), the joint probability density function for the random vector $\boldsymbol{\varphi}(\boldsymbol{x})$ and the random matrix $\nabla\boldsymbol{\varphi}(\boldsymbol{x})$. Since $\xi_\bullet$ are i.i.d normal random variables, the random vector field that $\boldsymbol{\varphi}(\boldsymbol{x})$ and $\nabla\boldsymbol{\varphi}(\boldsymbol{x})$ are jointly Gaussian. For the field $\boldsymbol{\varphi}(\boldsymbol{x})$ this assertion is trivial. For the gradient this result follows from the linearity of the derivative operator (in the mean square sense). While the first moment is zero, the second moment of the latter can be obtained from the derivatives of the correlation function $C(\boldsymbol{x}^T\boldsymbol{y})$. With these premises, one obtains

$$\mathbb{E}[\varphi_n(\boldsymbol{x})\varphi_m(\boldsymbol{x})] = \delta_{nm}C(\boldsymbol{x}^T\boldsymbol{x}), \tag{C.1}$$

$$\mathbb{E}[\partial_k\varphi_n(\boldsymbol{x})\varphi_m(\boldsymbol{x})] = \delta_{nm}x_kC'(\boldsymbol{x}^T\boldsymbol{x}), \tag{C.2}$$

$$\mathbb{E}[\partial_k\varphi_n(\boldsymbol{x})\partial_\ell\varphi_m(\boldsymbol{x})] = \delta_{nm}\delta_{k\ell}C'(\boldsymbol{x}^T\boldsymbol{x}) + \delta_{nm}x_kx_\ell C''(\boldsymbol{x}^T\boldsymbol{x}). \tag{C.3}$$

Fixing $\boldsymbol{x} \in \mathbb{R}^N$, we can write the joint distribution of $\boldsymbol{\varphi}(\boldsymbol{x})$ and the random matrix $\nabla\boldsymbol{\varphi}(\boldsymbol{x})$ as

$$p(\boldsymbol{v},\boldsymbol{M}) = \frac{\mathbb{P}[\boldsymbol{\varphi}(\boldsymbol{x}) \in (\boldsymbol{v},\boldsymbol{v}+d\boldsymbol{v}), \nabla\boldsymbol{\varphi}(\boldsymbol{x}) \in (\boldsymbol{M},\boldsymbol{M}+d\boldsymbol{M})]}{d\boldsymbol{v}\,d\boldsymbol{M}}. \tag{C.4}$$

This is equivalent to

$$p(\boldsymbol{v},\boldsymbol{M}) = \frac{1}{(2\pi)^{N(N+1)/2}(\det\boldsymbol{\Sigma}(\boldsymbol{x}))^{1/2}}\exp\left(-\frac{1}{2}\operatorname{vec}[\boldsymbol{v},\boldsymbol{M}]^T\boldsymbol{\Sigma}^{-1}(\boldsymbol{x})\operatorname{vec}[\boldsymbol{v},\boldsymbol{M}]\right), \tag{C.5}$$

The vectorization vec reshapes a matrix into a column vector by stacking its columns on top of each other, i.e. $\operatorname{vec}[\boldsymbol{v},\boldsymbol{M}]$ is an $N(N+1)$ column vector. The covariance matrix $\boldsymbol{\Sigma}(\boldsymbol{x})$ is an $N(N+1)\times N(N+1)$ real and symmetric matrix, i.e.

$$\boldsymbol{\Sigma}(\boldsymbol{x}) = \mathbb{E}[\operatorname{vec}[\boldsymbol{v},\boldsymbol{M}]\operatorname{vec}[\boldsymbol{v},\boldsymbol{M}]^T] \tag{C.6}$$

If we use the equalities in eqs(C.1,C.2) and eq(C.3) this can be simplified to

$$\boldsymbol{\Sigma}(\boldsymbol{x}) = \boldsymbol{\sigma}(\boldsymbol{x}) \otimes \mathbf{1}_N, \tag{C.7}$$

where $\otimes$ indicates the Kronecker (tensor) product, and

$$\boldsymbol{\sigma}(\boldsymbol{x}) = \begin{bmatrix} C(\boldsymbol{x}^T\boldsymbol{x}) & C'(\boldsymbol{x}^T\boldsymbol{x})\boldsymbol{x}^T \\ C'(\boldsymbol{x}^T\boldsymbol{x})\boldsymbol{x} & C'(\boldsymbol{x}^T\boldsymbol{x})\mathbf{1}_N + C''(\boldsymbol{x}^T\boldsymbol{x})\boldsymbol{x}\boldsymbol{x}^T \end{bmatrix} \tag{C.8}$$

which is an $(N+1)\times(N+1)$ matrix. This is enough to explicitly obtain the probability density function eq(C.5). However we need to make few checks before proceeding. Firstly, we need to prove that the covariance $\boldsymbol{\Sigma}(\boldsymbol{x})$ is invertible. To this purpose it is clearly sufficient to compute its characteristic polynomial, i.e.

$$\det\left(\boldsymbol{\Sigma}(\boldsymbol{x})\right) = \det\left(\boldsymbol{\sigma}(\boldsymbol{x}) \otimes \mathbf{1}_N\right) = \det\left(\boldsymbol{\sigma}(\boldsymbol{x})\right)^N, \tag{C.9}$$

Hence, we need to prove that $\det\left(\boldsymbol{\sigma}(\boldsymbol{x})\right)$ is non-vanishing. The latter is a block matrix. Therefore we can make use of the Schur decomposition

$$\det \begin{bmatrix} \boldsymbol{A} & \boldsymbol{B} \\ \boldsymbol{C} & \boldsymbol{D} \end{bmatrix} = \det\left(\boldsymbol{A}\right) \det\left(\boldsymbol{D} - \boldsymbol{C}\boldsymbol{A}^{-1}\boldsymbol{B}\right) \tag{C.10}$$

For any invertible $n \times n$ matrix $\boldsymbol{A}$ and any matrices $\boldsymbol{B}, \boldsymbol{C}, \boldsymbol{D}$ of sizes $n \times m$, $m \times n$, $m \times m$ respectively. If we apply this result to eq(C.9), we obtain

$$\det\left(\boldsymbol{\sigma}(\boldsymbol{x})\right) = C(\boldsymbol{x}^T\boldsymbol{x})C'(\boldsymbol{x}^T\boldsymbol{x})^N \det\left(\mathbf{1}_N + \frac{C(\boldsymbol{x}^T\boldsymbol{x})C''(\boldsymbol{x}^T\boldsymbol{x}) - C'(\boldsymbol{x}^T\boldsymbol{x})^2}{C(\boldsymbol{x}^T\boldsymbol{x})C'(\boldsymbol{x}^T\boldsymbol{x})}\boldsymbol{x}\boldsymbol{x}^T\right). \tag{C.11}$$

The last determinant appearing above is readily computed by exploiting a second identity, i.e.

$$\det\left(\mathbf{1}_n + \boldsymbol{A}\boldsymbol{B}\right) = \det\left(\mathbf{1}_m + \boldsymbol{B}\boldsymbol{A}\right) \tag{C.12}$$

for rectangular matrices $\boldsymbol{A}$ and $\boldsymbol{B}$ of size $n\times m$ and $m\times n$, respectively. Hence eq(C.9) is equal to

$$\det\left(\boldsymbol{\sigma}(\boldsymbol{x})\right) = \Delta(\boldsymbol{x}^T\boldsymbol{x})C'(\boldsymbol{x}^T\boldsymbol{x})^{N-1}. \tag{C.13}$$

where

$$\Delta(\boldsymbol{x}^T\boldsymbol{x}) = C(\boldsymbol{x}^T\boldsymbol{x})C'(\boldsymbol{x}^T\boldsymbol{x}) + \left(C(\boldsymbol{x}^T\boldsymbol{x})C''(\boldsymbol{x}^T\boldsymbol{x}) - C'(\boldsymbol{x}^T\boldsymbol{x})^2\right)\boldsymbol{x}^T\boldsymbol{x}, \tag{C.14}$$

is a scalar function, introduced for convenience of notation. Due to the rotational invariance of the covariance function (see section 3.1.3 and eq(3.11)), the determinant in eq(C.13) is a function of the squared norm in $\mathbb{R}^N$, namely, of $r^2 = \boldsymbol{x}^T\boldsymbol{x} \geq 0$. If we set $\boldsymbol{x} = \mathbf{0}$, the determinant of $\boldsymbol{\sigma}(\boldsymbol{x})$ is zero. Therefore, the latter is not invertible. However, this is not "pathological" and corresponds to the fact that $\boldsymbol{\varphi}(0) = 0$ as the origin is a non random fixed point of the dynamics, i.e. *regardless* of any realization for $\boldsymbol{\varphi}(\boldsymbol{x})$. For $\boldsymbol{x} \neq 0$, the entries of the field $\boldsymbol{\varphi}$ are purely random. The functions $C'(r^2)$ and $\Delta(r^2)$ appearing in eq(**C.13**) are positive and finite for $0 < r < R$ while for $r \to R$ they diverge. This implies that $\det(\boldsymbol{\sigma}(\boldsymbol{x}))$ is finite and positive. Therefore the covariance matrix $\boldsymbol{\Sigma}(\boldsymbol{x})$ is invertible and the probability function in eq(**C.5**) is defined for all $0 \leq |\boldsymbol{x}| \leq R$. After this check, we can invert the convariance matrix $\boldsymbol{\Sigma}(\boldsymbol{x})$ for $\boldsymbol{x} \neq 0$. We start by observing

$$\boldsymbol{\Sigma}(\boldsymbol{x})^{-1} = \boldsymbol{\sigma}(\boldsymbol{x})^{-1} \otimes \mathbf{1}_N \tag{C.15}$$

again for $\boldsymbol{x} \neq 0$. The inverse of block matrix can be calculated with the help of the Schur complement, i.e.

$$\begin{bmatrix} \boldsymbol{A} & \boldsymbol{B} \\ \boldsymbol{C} & \boldsymbol{D} \end{bmatrix}^{-1} = \begin{bmatrix} \boldsymbol{A}^{-1} + \boldsymbol{A}^{-1}\boldsymbol{B}(\boldsymbol{D} - \boldsymbol{C}\boldsymbol{A}^{-1}\boldsymbol{B})^{-1}\boldsymbol{C}\boldsymbol{A}^{-1} & -\boldsymbol{A}^{-1}\boldsymbol{B}(\boldsymbol{D} - \boldsymbol{C}\boldsymbol{A}^{-1}\boldsymbol{B})^{-1} \\ -(\boldsymbol{D} - \boldsymbol{C}\boldsymbol{A}^{-1}\boldsymbol{B})^{-1}\boldsymbol{C}\boldsymbol{A}^{-1} & (\boldsymbol{D} - \boldsymbol{C}\boldsymbol{A}^{-1}\boldsymbol{B})^{-1} \end{bmatrix} \tag{C.16}$$

where $\boldsymbol{A}, \boldsymbol{B}, \boldsymbol{C}, \boldsymbol{D}$ are $n \times n$, $n \times m$, $m \times n$, $m \times m$ matrices with $\boldsymbol{A}$ and $(\boldsymbol{D} - \boldsymbol{C}\boldsymbol{A}^{-1}\boldsymbol{B})$ invertible. It is sufficient to use this result on $\boldsymbol{\sigma}(\boldsymbol{x})^{-1}$. After some calculations one gets

$$\boldsymbol{\sigma}(\boldsymbol{x})^{-1} = \frac{1}{\Delta(\boldsymbol{x}^T\boldsymbol{x})C'(\boldsymbol{x}^T\boldsymbol{x})} \begin{bmatrix} C'(\boldsymbol{x}^T\boldsymbol{x})^2 + C'(\boldsymbol{x}^T\boldsymbol{x})C''(\boldsymbol{x}^T\boldsymbol{x})\boldsymbol{x}^T\boldsymbol{x} & -C'(\boldsymbol{x}^T\boldsymbol{x})^2\boldsymbol{x}^T \\ -C'(\boldsymbol{x}^T\boldsymbol{x})^2\boldsymbol{x} & \boldsymbol{S}(\boldsymbol{x}) \end{bmatrix} \tag{C.17}$$

where $\Delta(\boldsymbol{x}^T\boldsymbol{x})$ was introduced in eq(**C.14**) and

$$\boldsymbol{S}(\boldsymbol{x}) = \Delta(\boldsymbol{x}^T\boldsymbol{x})\mathbf{1}_N - (C(\boldsymbol{x}^T\boldsymbol{x})C''(\boldsymbol{x}^T\boldsymbol{x}) - C'(\boldsymbol{x}^T\boldsymbol{x})^2)\boldsymbol{x}\boldsymbol{x}^T \tag{C.18}$$

is a symmetric matrix-valued function. We can now write down in full detail the final expression for eq(**C.5**). For exploiting the results of section 1.1.2, we prefer to write the probability density function eq(**C.5**) as a matrix Gaussian distribution and not with the standard multivariate form. To do so, we make use of

$$\boldsymbol{A} \otimes \boldsymbol{B}\, \mathrm{vec}[\boldsymbol{X}] = \mathrm{vec}[\boldsymbol{B}\boldsymbol{X}\boldsymbol{A}^T] \tag{C.19}$$

for matrices $\boldsymbol{A}, \boldsymbol{B}, \boldsymbol{X}$ of size $k \times m$, $n \times m$, $\ell \times n$. We can apply this identity to $\boldsymbol{\Sigma}(\boldsymbol{x})$. Bearing in mind that $\boldsymbol{\sigma}(\boldsymbol{x})$ is symmetric, the argument at the exponent in eq(**C.5**) can be re-written as

$$\mathrm{vec}[\boldsymbol{v},\boldsymbol{M}]^T\boldsymbol{\Sigma}(\boldsymbol{x})^{-1}\,\mathrm{vec}[\boldsymbol{v},\boldsymbol{M}] = \mathrm{vec}[\boldsymbol{v},\boldsymbol{M}]^T(\boldsymbol{\sigma}(\boldsymbol{x})^{-1}\otimes\mathbf{1}_N)\,\mathrm{vec}[\boldsymbol{v},\boldsymbol{M}] = \mathrm{Tr}[\boldsymbol{v},\boldsymbol{M}]\boldsymbol{\sigma}(\boldsymbol{x})^{-1}[\boldsymbol{v},\boldsymbol{M}]^T, \quad \text{(C.20)}$$

where $[\boldsymbol{v},\boldsymbol{M}]$ is an $N\times(N+1)$ matrix. Therefore, substituting in eq(**C.5**), we obtain

$$p(\boldsymbol{v},\boldsymbol{M}) = \frac{1}{(2\pi)^{N(N+1)/2}(\det\boldsymbol{\sigma}(\boldsymbol{x}))^{N/2}}\exp\Big(-\frac{1}{2}\mathrm{Tr}[\boldsymbol{v},\boldsymbol{M}]\boldsymbol{\sigma}(\boldsymbol{x})^{-1}[\boldsymbol{v},\boldsymbol{M}]^T\Big). \quad \text{(C.21)}$$

We can further expand in terms of $\boldsymbol{v}$ and $\boldsymbol{M}$ while completing the square, i.e.

$$p(\boldsymbol{v},\boldsymbol{M}) = \frac{1}{(2\pi)^{N(N+1)/2}\Delta(\boldsymbol{x}^T\boldsymbol{x})^{N/2}C'(\boldsymbol{x}^T\boldsymbol{x})^{N(N-1)/2}}$$
$$\times\exp\Bigg[-\frac{\boldsymbol{v}^T\boldsymbol{v}}{2C(\boldsymbol{x}^T\boldsymbol{x})}-\frac{1}{2\Delta(\boldsymbol{x}^T\boldsymbol{x})C'(\boldsymbol{x}^T\boldsymbol{x})}\mathrm{Tr}\Big(\boldsymbol{M}-\frac{C'(\boldsymbol{x}^T\boldsymbol{x})}{C(\boldsymbol{x}^T\boldsymbol{x})}\boldsymbol{v}\boldsymbol{x}^T\Big)\boldsymbol{S}(\boldsymbol{x})\Big(\boldsymbol{M}-\frac{C'(\boldsymbol{x}^T\boldsymbol{x})}{C(\boldsymbol{x}^T\boldsymbol{x})}\boldsymbol{v}\boldsymbol{x}^T\Big)^T\Bigg], \quad \text{(C.22)}$$

C.2 Mean Number of fixed Points

With the results of the previous section and of section 1.1.2 we replace λ and ε with $\frac{\mu}{\sqrt{C'(r^2)}}$ and $\mu\sqrt{\frac{C(r^2)}{\Delta(r^2)}}(1-\frac{C'(r^2)}{C(r^2)}r^2)$ in $\mathbb{E}_{GinOE}[|\det(\lambda\mathbf{1}_N+\varepsilon\boldsymbol{h}\boldsymbol{h}^T-\boldsymbol{\Xi})|]$ in order to obtain the spherical density $\widehat{\rho}_\mu(r>0)$. Since $C(r^2)$ is a monotonically increasing function, the edge regimes (see eqs(**1.79**,**1.80**)) can be discarded as they correspond to the sets of zero measure in $\mathbb{R}^N$. Hence we can replace, in the large N limit, $\mathbb{E}_{Gin}[|\det(\boldsymbol{\Xi}-\mu\sqrt{N}\boldsymbol{D})|]$ with

(i) for $|\mu/\sqrt{C'(r^2)}|<1$: $\sqrt{2}N^{N/2}e^{\frac{N}{2}\left(\frac{\mu^2}{C'(r^2)}-1\right)}\sqrt{\mu^2\frac{C(r^2)}{\Delta(r^2)}\big(1-\frac{C'(r^2)}{C(r^2)}r^2\big)^2-\frac{\mu^2}{C'(r^2)}+1}$

(ii) for $|\mu/\sqrt{C'(r^2)}|>1$: $N^{N/2}|\frac{\mu}{\sqrt{C'(r^2)}}|^{N-1}|\mu\sqrt{\frac{C(r^2)}{\Delta(r^2)}}(1-\frac{C'(r^2)}{C(r^2)}r^2)|$

Hence, the choice of the two results above depends on the ratio μ/σ_1:

- For $\mu<\sigma_1$, after collecting all the terms for $\widehat{\rho}_\mu(r>0)$, we have, for $0<r<R$,

$$\widehat{\rho}_\mu(r)\simeq\frac{\sqrt{2N}}{\sqrt{\pi}}\frac{e^{\frac{N}{2}L_{II}(r)}}{r}\frac{\Delta^{1/2}(r^2)}{\sqrt{C(r^2)C'(r^2)}}\sqrt{\mu^2\frac{C(r^2)}{\Delta(r^2)}\Big(1-\frac{C'(r^2)}{C(r^2)}r^2\Big)^2-\frac{\mu^2}{C'(r^2)}+1} \quad \text{(C.23)}$$

with $L_{II}(r)=\log r^2-\frac{\mu^2r^2}{C(r^2)}+\log\frac{C'(r^2)}{C(r^2)}+\frac{\mu^2}{C'(r^2)}$

- Conversely for $\mu > \sigma_1$, we need to collect the two contributions of $\mathbb{E}_{Gin}[|\det(\boldsymbol{\Xi} - \mu\sqrt{N}\boldsymbol{D})|]$. We recall here the definition of the characteristic radius r_-, i.e. r_- is the solution of $C'(r^2) = \mu^2$, and we introduce the function $L_I(r) = +1 + \log \mu^2 + \log r^2 - \frac{\mu^2 r^2}{C(r^2)} - \log C(r^2)$. Hence, for $N \gg 1$:

$$\widehat{\rho}_\mu(r) \simeq \frac{\sqrt{N}}{\sqrt{\pi}} \frac{e^{\frac{N}{2}L_I(r)}}{r} \left|1 - \frac{C'(r^2)}{C(r^2)} r^2 \right| \mathbb{1}(0 < r < r_-) + \frac{\sqrt{2N}}{\sqrt{\pi}} \frac{e^{\frac{N}{2}L_{II}(r)}}{r} \times \\ \times \frac{\Delta^{1/2}(r^2)}{\sqrt{C(r^2)C'(r^2)}} \left(\sqrt{\mu^2 \frac{C(r^2)}{\Delta(r^2)} \left(1 - \frac{C'(r^2)}{C(r^2)} r^2 \right)^2 - \frac{\mu^2}{C'(r^2)} + 1} \right) \mathbb{1}(r_- < r < R) \tag{C.24}$$

  The function $\mathbb{1}(x)$ is the indicator function with value 1 if the condition x is true. For $r > r_-$ and $N \gg 1$, the second term in eq(**C.39**) is of leading order with respect to the first one as $\frac{\mu^2}{C'(r^2)} - \log \frac{\mu^2}{C'(r^2)} - 1 > 0$.

C.3 Local behaviour of fixed points around $\boldsymbol{x} = \mathbf{0}$

For $\mu < \sigma_1$, we have an exponential growth of fixed points around the origin. To show this, for $N \gg 1$, we consider the mean number of fixed points within a ball of radius r, i.e.

$$\mathcal{N}_\mu(r) \simeq \frac{\sqrt{2N}}{\sqrt{\pi}} \int_0^r dr' e^{NL(r')} \frac{\Delta^{1/2}(r'^2)}{r\sqrt{C(r'^2)C'(r'^2)}} \sqrt{\mu^2 \frac{C(r'^2)}{\Delta(r'^2)} \left(1 - \frac{C'(r'^2)}{C(r'^2)} r'^2 \right)^2 - \frac{\mu^2}{C'(r'^2)} + 1} \tag{C.25}$$

where $L(r) = \log(r) - \frac{\mu^2 r^2}{2C(r^2)} + \frac{1}{2} \log \frac{C'(r^2)}{C(r^2)} + \frac{\mu^2}{2C'(r^2)}$. We first observe that $\lim_{r \to 0^+} L(r) = 0$. For sufficiently smooth C, the Taylor expansion around this point is given by:

$$L(r) = \frac{\sigma_2^2}{\sigma_1^4}(\sigma_1^2 - \mu^2) r + O(r^3) \tag{C.26}$$

Hence, $L(r)$ is a monotonically increasing function in a neighborhood U of $\boldsymbol{x} = \mathbf{0}$. Therefore, the number of fixed points in U increases exponentially with N. In fact, let's consider a sufficiently small radius $\varepsilon > 0$ and a fixed $N \gg 1$. From the formulas above we have:

$$\mathcal{N}_\mu(\varepsilon) \simeq \int_0^\varepsilon dr e^{NL(r)} g(r) \tag{C.27}$$

where $g(r)$ collects the subleading terms. The maximum of L is achieved at ε. Therefore, around such point $L(r) = L(\varepsilon) + L'(\varepsilon)(r - \varepsilon) + O((r - \varepsilon)^2)$. Substituting the latter in eq(**C.39**) and performing the integration we obtain:

$$\mathcal{N}_\mu(\varepsilon) \simeq \frac{(1 - e^{-\varepsilon N L'(\varepsilon)})}{NL'(\varepsilon)} e^{NL(\varepsilon)} g(\varepsilon) \text{ for } \varepsilon \ll 1 \tag{C.28}$$

This poses a question: How does $\mathcal{N}_\mu(r)$ approach 0 as $r \to 0$?(we recall that$\mathcal{N}_\mu$ does not include the contribution from the trivial fixed point $\boldsymbol{x} = \boldsymbol{0}$). A Taylor expansion around the origin of $g(r)$ shows that, for $\varepsilon \ll 1$:

$$\mathcal{N}_\mu(\varepsilon) \simeq \sqrt{\frac{2N}{\pi}} \frac{\sigma_2}{\sigma_1^2} (\sqrt{\sigma_1^2 - \mu^2}) \varepsilon + O(\varepsilon^3) \tag{C.29}$$

C.4 Mean Number of Fixed Points for Truncated Correlation Function

In this section, we want to obtain the mean number of real zeros for the set of equations

$$-\mu x_n + \sum_{k=1}^{\Omega} \sigma_k \sum_{i_1,..,i_k=1}^{N} \xi_{n,i_1,...,i_k} x_{i_1} \cdots x_{i_k} = 0 \tag{C.30}$$

for $n = 1, ..., N$. As in the sections above, from eq(**C.30**), we can define the truncated correlation function, i.e.

$$C(r^2) = \sum_{k=1}^{\Omega} \sigma_k^2 r^{2k} \tag{C.31}$$

for some cut-off $\Omega > 0$. In this case, C is a finite order algebraic polynomial. The mean number of fixed points, for the dynamics generated by eq(**3.8**), corresponds to the mean number of zeros of a set of N multivariate Kac polynomials.

- If $0 < \mu < \sigma_1$, from eq(**C.25**) we have ($N \gg 1$):

$$\mathcal{N}_\mu(\mathbb{R}^N) \simeq \frac{\sqrt{2N}}{\sqrt{\pi}} \int_0^{+\infty} dr e^{NL_2(r)} \frac{\Delta^{1/2}(r^2)}{r\sqrt{C(r^2)C'(r^2)}} \times \\ \times \sqrt{\mu^2 \frac{C(r^2)}{\Delta(r^2)} \Big(1 - \frac{C'(r^2)}{C(r^2)} r^2\Big)^2 - \frac{\mu^2}{C'(r^2)} + 1} \tag{C.32}$$

  where $L_2(r) = \log(r) - \frac{\mu^2 r^2}{2C(r^2)} + \frac{1}{2} \log \frac{C'(r^2)}{C(r^2)} + \frac{\mu^2}{2C'(r^2)}$. As we increase the size of the system $N \gg 1$, the main contribution to integration over r is given by the saddle point of $L_2(r)$. We have reported in section 1.2.2 the conditions for the latter, namely, one needs to find the solutions of $\frac{dL_2}{dr}(r) = 0$ and to modify the integration path such that these points are "appropriately" crossed. However, the form of $L_2(r)$ suggests to approach such problem differently. In fact, the difficulties behind the calculation of such roots depend on the value of the cut-off Ω and on σ_ks. We notice that:

$$\begin{cases} \lim_{r \to 0^+} L_2(r) = 0 \\ \lim_{r \to +\infty} L_2(r) = \frac{1}{2} \log \Omega \end{cases} \tag{C.33}$$

As we are looking for non trivial results, we focus on the case $\Omega > 1$. For such choice clearly, $L_2(r \to 0^+) < L_2(r \to +\infty)$. We now want to show that the r.h.s. of this inequality defines an upper bound for $L_2(r)$, i.e. $\lim_{r\to+\infty} L_2(r) = \sup_{r\in\mathbb{R}^+} L_2(r)$. To see this, we fix $\mu \neq 0$ and impose $r > 0$ so that we can define the new variables $\tilde{\sigma}_k = \sigma_k/\mu$. The function $L_2(r)$ is then given by

$$L_2(r) = \frac{1}{2}\Big(\log \tilde{C}'(r^2) + \frac{1}{\tilde{C}'(r^2)} - \log \tilde{C}(r^2) - \frac{1}{\tilde{C}(r^2)}\Big) \tag{C.34}$$

with $\tilde{C}'(r^2) = r^{-2}\sum_{k=1}^{\Omega} \tilde{\sigma}_k^2 k r^{2k}$ and $\tilde{C}(r^2) = r^{-2}\sum_{k=1}^{\Omega} \tilde{\sigma}_k^2 r^{2k}$. From these definitions one can see that $\tilde{C}'(r^2) > \tilde{C}(r^2)$. Therefore, for $r \geq 0$ it holds:

$$L_2(r) \leq \frac{1}{2}\Big(\log \tilde{C}'(r^2) - \log \tilde{C}(r^2)\Big), \tag{C.35}$$

From what stated above, the r.h.s is bounded by $\frac{1}{2}\log\Omega$ as $\tilde{C}'(r^2) \leq \Omega\tilde{C}(r^2)$ as in eq(**C.33**). The leading contribution to the integral in eq(**C.32**) is obtained for $r \to +\infty$. Moreover, one observes that $\frac{dL_2}{dr}(r) \to 0$ for $r \to +\infty$. With these consideration on $L_2(r)$, the saddle point approximation is easily performed with a change of variable, i.e. $r = \frac{1}{x}$ in eq(**C.32**). Hence, now the leading contribution to the integral arises from the neighbourhood defined by $x \to 0^+$. An expansion of the subleading terms shows (for $r \gg 1$)

$$\frac{\Delta^{1/2}(r^2)}{r\sqrt{C(r^2)C'(r^2)}} \simeq \frac{\sigma_{\Omega-1}}{r^2\sigma_\Omega\sqrt{\Omega}}$$

and

$$\sqrt{\mu^2\frac{C(r^2)}{\Delta(r^2)}\Big(1 - \frac{C'(r^2)}{C(r^2)}r^2\Big)^2 - \frac{\mu^2}{C'(r^2)} + 1} = O(1)$$

In particular, the appearance of $C'''(1/x^2)$ in $\frac{d^2L}{dx^2}$ suggests to treat $\Omega = 2$ and $\Omega \geq 3$ separately.

(i) For $\Omega = 2$, one can see that

$$\lim_{x\to 0^+} \frac{dL_2^2}{dx^2}(x) = -\frac{\mu^2 + \sigma_1^2}{2\sigma_2^2} \tag{C.36}$$

and

$$\lim_{x\to 0^+} \sqrt{\mu^2\frac{C(1/x^2)}{\Delta(1/x^2)}\Big(1 - \frac{C'(1/x^2)}{x^2C(1/x^2)}\Big)^2 - \frac{\mu^2}{C'(1/x^2)} + 1} = \sqrt{1 + \frac{\mu^2}{\sigma_1^2}} \tag{C.37}$$

(ii) Conversely, for $\Omega \geq 3$, the limit in eq(**C.37**) is equal 1 while terms containing μ^2 in L_2 are negligible for the calculation of $\frac{d^2 L_2}{dx^2}(x)$. Hence, the limit in (i) above is replaced by

$$\lim_{x \to 0^+} \frac{d^2 L_2}{dx^2}(x) = -\frac{\sigma_{\Omega-1}^2}{\Omega \sigma_\Omega^2} < 0$$

One can sum up the results above so that for $\Omega \geq 1$:

$$\mathcal{N}_\mu(\mathbb{R}^N) = e^{\frac{N}{2}\log\Omega}(1 + o(1)) \tag{C.38}$$

- We now turn our attention to the case $0 < \sigma_1 < \mu$. In this regime the spherical density, $\hat{\rho}_\mu$, consists of two contribution for $\mathbb{E}_{Gin}[|\det(\boldsymbol{\Xi} - \mu\sqrt{N}\boldsymbol{D})|]$ which have to be addressed separately. To do so, we introduce (for $N \gg 1$)

$$L_1(r) = +\frac{1}{2} + \log\mu + \log r - \frac{\mu^2 r^2}{2C(r^2)} - \frac{1}{2}\log C(r^2)$$

and

$$L_2(r) = \log(r) - \frac{\mu^2 r^2}{2C(r^2)} + \frac{1}{2}\log\frac{C'(r^2)}{C(r^2)} + \frac{\mu^2}{2C'(r^2)}$$

Therefore, the mean number of roots for eq(**C.30**) reads

$$\mathcal{N}_\mu(\mathbb{R}^N) \simeq \frac{\sqrt{N}}{\sqrt{\pi}} \int_0^{r_-} dr \frac{e^{NL_1(r)}}{r} \left|1 - \frac{C'(r^2)}{C(r^2)} r^2\right| + \tag{C.39}$$

$$+ \frac{\sqrt{2N}}{\sqrt{\pi}} \int_{r_-}^{+\infty} dr \frac{e^{NL_(r)} \Delta^{1/2}(r^2)}{r\sqrt{C(r^2)C'(r^2)}} \sqrt{\mu^2 \frac{C(r^2)}{\Delta(r^2)} \left(1 - \frac{C'(r^2)}{C(r^2)} r^2\right)^2 - \frac{\mu^2}{C'(r^2)} + 1}$$

From the case investigated above (i.e. $\mu < \sigma_1$), the function $L_2(r)$ is bounded and reaches its maximum only for $r \to +\infty$. The new function $L_1(r)$ reaches its maximum for finite value of r. The point $r = 0$ represents a local minimum for $L_1(r)$, in particular

$$\lim_{r \to 0^+} L_1(r) = \frac{1}{2} + \log\mu - \log\sigma_1 - \frac{\mu^2}{2\sigma_1^2}$$

Indeed, one can observe that $\frac{dL_1}{dr} \to 0$ and $\frac{d^2 L_1}{dr^2} \to (\mu^2 - \sigma_1^2)\sigma_2^2/\sigma_1^4 > 0$ as $r \to 0^+$. For $r \gg 1$, instead, $L_1(r) \simeq +\frac{1}{2} + \log\mu + (1 - \Omega)\log r - \log\sigma_\Omega$. If we define a new variable $x = \frac{\sum_{k=1}^{\Omega} \sigma_k^2 r^{2k}}{r^2}$, L_1 reaches its maximum at $x_+ = \mu^2$ and it equals 0. The latter corresponds to r_+ since $C(r_+^2) = \mu^2 r_+^2$. Since from the definitions for r_- and r_+ it necessarily follows that $r_+ > r_-$ the leading term for $\mathcal{N}_\mu(\mathbb{R}^N)$ gives

$$\mathcal{N}_\mu(\mathbb{R}^N) = e^{\frac{N}{2}\log\Omega}(1 + o(1)) \tag{C.40}$$

C.4.1 Kac-Rice Formula For Sum of Random Periodic Potentials

In this section we obtain eq(**3.66**). To do so we make use of the Kac-Rice formula stated in eq(**1.50**). Differently from the results given by eq(**3.11**), here the random field is not equipped with rotational invariance. Therefore, we proceed as follows. From the definition of $V(\boldsymbol{x})$ and from identities in eqs(**3.63**) we have that:

$$\frac{\partial^2 V}{\partial x_i \partial x_j}(\boldsymbol{x}) = -\sum_{a=1}^{M} k_{ai}k_{aj}(u_1^{(a)}\cos(\boldsymbol{k}_a^T\boldsymbol{x}) + u_2^{(a)}\sin(\boldsymbol{k}_a^T\boldsymbol{x}))$$

is a centered random field whose variance is given by

$$\mathbb{E}\left[\frac{\partial^2 V}{\partial x_i \partial x_j}(\boldsymbol{x})\frac{\partial^2 V}{\partial x_l \partial x_m}(\boldsymbol{x})\right] = \sum_{a=1}^{M} k_{ai}k_{aj}k_{al}k_{am}$$

Therefore, the mean number of fixed points in $\mathbb{R}^N$, given the set of wave numbers $\boldsymbol{k}_a$, is given by the Kac-Rice formula (see eq(**1.50**))

$$\mathcal{N}_{tot}|\{\boldsymbol{k}_1, .., \boldsymbol{k}_M\} = \int_{\mathbb{R}^N} d\boldsymbol{x}\, \mathbb{E}\left[\prod_{i=1}^{N}\delta\Big(\lambda x_i - \frac{\partial V}{\partial x_i}(\boldsymbol{x})\Big)\Big|\det\Big(\lambda\delta_{ij} - \frac{\partial^2 V}{\partial x_i x_j}(\boldsymbol{x})\Big)_{i,j=1}^{N}\Big|\right]$$

The expectation $\mathbb{E}[...]$ is performed over the set $u_1^{(a)}, u_2^{(a)}$ for $a = 1, ..., M$. The product of Dirac delta functions can be replaced by the products of their Fourier transform, i.e.

$$\frac{1}{2\pi}\int dq_i e^{i\lambda x_i q_i - iq_i\frac{\partial V}{\partial x_i}(\boldsymbol{x})} \tag{C.41}$$

Instead of averaging directly over the realizations of $u_1^{(a)}, u_2^{(a)}$, we introduce the following change of variables:

$$\begin{cases} -(u_1^{(a)}\cos(\boldsymbol{k}_a^T\boldsymbol{x}) + u_2^{(a)}\sin(\boldsymbol{k}_a^T\boldsymbol{x})) = T_a \\ (-u_1^{(a)}\sin(\boldsymbol{k}_a^T\boldsymbol{x}) + u_2^{(a)}\cos(\boldsymbol{k}_a^T\boldsymbol{x})) = G_a \end{cases} \tag{C.42}$$

The new variables G_a can be easily integrated out, therefore, the expectation above can be re-formuated as:

$$\mathbb{E}\left[e^{-i\sum_{i=1}^{N} q_i\frac{\partial V}{\partial x_i}(\boldsymbol{x})}\Big|\det\Big(\lambda\delta_{ij} - \frac{\partial^2 V}{\partial x_i \partial x_j}(\boldsymbol{x})\Big)\Big|\right] =$$

$$= \prod_{a=1}^{M} e^{-\frac{1}{2}(\boldsymbol{q}^T\boldsymbol{k}_a)^2}\int\prod_{a=1}^{M}\frac{dT_a}{\sqrt{2\pi}}e^{-\frac{1}{2}T_a^2}\Big|\det\Big(\lambda\delta_{ij} - \sum_{a=1}^{M}T_a k_{ai}k_{aj}\Big)\Big|$$

As the second term does not depend on $\boldsymbol{x}$ we can integrate out $\boldsymbol{x}$ and $\boldsymbol{q}$ and finally obtain:

$$\mathcal{N}_{tot}|\{\boldsymbol{k}_1, .., \boldsymbol{k}_M\} = \frac{1}{\lambda^N}\int\prod_{a=1}^{M}\frac{dT_a}{\sqrt{2\pi}}e^{-\frac{1}{2}T_a^2}\Big|\det\Big(\lambda\delta_{ij} - \sum_{a=1}^{M}T_a k_{ai}k_{aj}\Big)\Big| \tag{C.43}$$

Appendix D

Appendix for Chapter 4

D.1 Derivation of $\mathbb{E}[\mathcal{Z}^n]$

We started by computing the expectations of the n-th power of the partition function, $\mathbb{E}\left[\mathcal{Z}^n\right]$, given by:

$$\mathbb{E}[\mathcal{Z}^n] = \mathbb{E}\left[\prod_{i=1}^{n} \int_{\mathbb{S}^N} d\boldsymbol{x}_i \exp\left(-\beta \mathcal{H}(\boldsymbol{x}_i) \prod_{k=1}^{M} \theta(\boldsymbol{b}_k - \boldsymbol{a}_k^T \boldsymbol{x})\right]$$

We make use of the following identities:

$$\mathbb{E}_{\mathbf{H},\boldsymbol{h}}\left[e^{-\frac{\beta}{2}(\mathrm{Tr}(\mathbf{H}\boldsymbol{x}_a \otimes \boldsymbol{x}_a^T) + \boldsymbol{h}^T \boldsymbol{x})}\right] = e^{\frac{\beta^2 J^2}{4N}\sum_{a,b}(\boldsymbol{x}_a^T \boldsymbol{x}_b)^2 + \frac{\beta^2 \delta^2}{2}\sum_{a,b}(\boldsymbol{x}_b^T \boldsymbol{x}_a)}$$

and

$$\mathbb{E}\left[\prod_{a=1}^{n} \theta(\boldsymbol{b} - \boldsymbol{a}^T \boldsymbol{x}_a)\right]_{\boldsymbol{b},\boldsymbol{a}} =$$

$$\int_{-\infty}^{+\infty} \frac{db}{\sqrt{2\pi}B} e^{-(b-k)^2/2B^2} \int du_1 ... du_n \prod_{\alpha=1}^{n} \theta(b - u_\alpha) \mathbb{E}\left[\prod_{\alpha=1}^{n} \delta(u_\alpha - \boldsymbol{a}^T \boldsymbol{x}_\alpha)\right]_{\boldsymbol{a}}$$

The expectation over $\boldsymbol{a}$ is computed by introducing the Fourier transform of the Dirac delta, i.e.:

$$\mathbb{E}_{\boldsymbol{a}}\left[\prod_{\alpha=1}^{n} \delta(u_\alpha - \boldsymbol{a}^T \boldsymbol{x}_\alpha)\right] = \int \prod_{\alpha=1}^{n} \frac{dk_\alpha}{2\pi} e^{ik_\alpha u_\alpha - \frac{1}{2}\mathbb{E}_{\boldsymbol{a}}[(\boldsymbol{a}^T \sum_{i=1}^{n} k_i \boldsymbol{x}_i)^2]}$$

The exponential can be simplified to $\mathbb{E}_{\boldsymbol{a}}\left[(\sum_{i=1}^{n} k_i(\boldsymbol{a}^T \boldsymbol{x}_i))^2\right] = \sum_{i,j} k_i k_j \mathbb{E}_{\boldsymbol{a}}[(\boldsymbol{a}^T \boldsymbol{x}_i)(\boldsymbol{a}^T \boldsymbol{x}_j)]$ and $\mathbb{E}_{\boldsymbol{a}}[(\boldsymbol{a}^T \boldsymbol{x}_i)(\boldsymbol{a}^T \boldsymbol{x}_j)]_{\boldsymbol{a}} = A^2 \boldsymbol{x}_i^T \boldsymbol{x}_j$. We also introduce the overlap matrix $\mathbf{Q}_{ab} = \boldsymbol{x}_a^T \boldsymbol{x}_b$ in order to obtain:

$$\mathbb{E}\left[\mathcal{Z}^n\right] = \int_{(\mathbb{S}^N)^n} \prod_{i=1}^{n} d\boldsymbol{x}_i e^{\frac{\beta^2 J^2}{4N}\mathrm{Tr}\,\mathbf{Q}^2 + \frac{\beta^2 \delta^2}{2}\sum_{a,b}\mathbf{Q}_{ab}} \times$$

$$\times \int_{-\infty}^{+\infty} \frac{db}{\sqrt{2\pi}B} e^{-(b-k)^2/(2B^2)} \int \prod_{i=1}^{n} du_i \prod_{\alpha=1}^{n} \theta(b-u_\alpha) \frac{e^{-1/(2A^2)\boldsymbol{u}^T\mathbf{Q}^{-1}\boldsymbol{u}}}{(2\pi A^2)^{n/2}\sqrt{\det \mathbf{Q}}}$$

Since the integrand is a function of the spectrum of $\mathbf{Q}$, $\mathbb{E}[\mathcal{Z}^n]$ can be rewritten by rescaling $\mathbf{Q} \to N\mathbf{Q}$ and $A^2N = C^2 = O(1)$ as:

$$\int_{(\mathbb{S}^N)^n} \prod_{i=1}^{n} d\boldsymbol{x}_i e^{\frac{\beta^2 J^2}{4N}\operatorname{Tr}\mathbf{Q}^2 + \frac{\beta^2\delta^2}{2}\sum_{ab}\mathbf{Q}_{ab}} (\mathcal{I}_n(\mathbf{Q}))^M =$$

$$= \frac{C_{N,n}}{N^n} \int_{\mathbf{Q}\succeq 0} e^{\frac{\beta^2 J^2}{4N}\operatorname{Tr}\mathbf{Q}^2 + \frac{\beta^2\delta^2}{2}\sum_{ab}\mathbf{Q}_{ab}} (\det \mathbf{Q})^{(N-n-1)/2} \mathcal{I}_n^M(N\mathbf{Q}) \prod_{i=1}^{n} \delta(q_{ii}-1) d\mathbf{Q}$$

With $C_{N,n} > 0$ and:

$$\mathcal{I}_n(\mathbf{Q}) = \int \prod_{a=1}^{n} \frac{du_a}{\sqrt{2\pi}} \mathbb{E}_b \left[\prod_{b=1} \theta(b-u_b)\right] F(\boldsymbol{u})$$

And:

$$F(\boldsymbol{u}) = \frac{e^{-1/(2C^2)\boldsymbol{u}^T\mathbf{Q}^{-1}\boldsymbol{u}}}{\sqrt{\det \mathbf{Q}}}$$

Therefore, collecting all the terms above, we obtain:

$$\mathbb{E}\left[\mathcal{Z}^n\right] \propto \int_{\mathbf{Q}\succeq 0} e^{N\varphi_n(\mathbf{Q})} (\det \mathbf{Q})^{-\frac{n+1}{2}} \prod_{a=1}^{n} \delta(\mathbf{Q}_{aa}-1) d\mathbf{Q}$$

With:

$$\varphi_n(\mathbf{Q}) = \frac{\beta^2 J^2}{4}\operatorname{Tr}\mathbf{Q}^2 + \frac{\beta^2\delta^2}{2}\sum_{a,b}\mathbf{Q}_{ab} + \frac{1}{2}\log\det\mathbf{Q} + \alpha\log\mathcal{I}_n(\mathbf{Q})$$

In the limit $N \to +\infty$, the integration over $\mathbf{Q}$ is substituted by a saddle point approximation. Therefore we computed $\partial\varphi_n(\mathbf{Q})/\partial\mathbf{Q}_{ab} = 0$ with $a \neq b$ as follows. Firstly, we rewrite $\mathcal{I}_n(\mathbf{Q})$ as:

$$\mathcal{I}_n(\mathbf{Q}) = \int \prod_{k=1}^{n} \frac{du_k}{\sqrt{2\pi}} \mathbb{E}_b \left[\prod_{k=1}^{n} \theta(b-u_k)\right] \int \prod_{i=1}^{n} \frac{dk_i}{\sqrt{2\pi}} e^{i\boldsymbol{k}^T\boldsymbol{u} - 1/2C^2\boldsymbol{k}^T\mathbf{Q}\boldsymbol{k}}$$

Therefore:

$$\frac{\partial \mathcal{I}_n(\mathbf{Q})}{\partial \mathbf{Q}_{a,b}} = \frac{C^2}{2} \int \prod_{k=1}^{n} \frac{du_k}{\sqrt{2\pi}} \mathbb{E}_b \left[\prod_{k=1}^{n} \theta(b-u_k)\right] \frac{\partial^2}{\partial u_a \partial u_b} F(\boldsymbol{u})$$

Since:

$$\frac{\partial F(\boldsymbol{u})}{\partial \mathbf{Q}_{a,b}} = F(\boldsymbol{u})\Big(\frac{1}{2C^2}\sum_{i,j} u_i u_j (\mathbf{Q}^{-1})_{a,j}(\mathbf{Q}^{-1})_{b,i} - (\mathbf{Q}^{-1})_{a,b}\Big)$$

The derivatives lead to:

$$\frac{\partial \mathcal{I}_n(\mathbf{Q})}{\partial \mathbf{Q}_{a,b}} = -\frac{1}{2}(\mathbf{Q}^{-1})_{ab} + \frac{1}{2C^2}\sum_{v,r=1}^{n} (\mathbf{Q}^{-1})_{av}(\mathbf{Q}^{-1})_{br} \int \prod_{k=1}^{n} \frac{du_k}{\sqrt{2\pi}} \mathbb{E}_b \left[\prod_{k=1}^{n} \theta(b-u_k)\right] F(\boldsymbol{u}) u_v u_r$$

And therefore to:

$$\frac{\partial \varphi_n(\mathbf{Q})}{\partial \mathbf{Q}_{a,b}} = \frac{\beta^2 J^2}{2}\mathbf{Q}_{a,b} + \frac{\beta^2\delta^2}{2} + \left(\frac{1}{2} - \frac{\alpha}{2}\right)(\mathbf{Q}^{-1})_{a,b} + \frac{\alpha}{2C^2}\sum_{v,r=1}^{n}(\mathbf{Q}^{-1})_{av}(\mathbf{Q}^{-1})_{br}\langle\langle u_v u_r\rangle\rangle \tag{D.1}$$

With:

$$\langle\langle u_v u_r\rangle\rangle = \frac{1}{\mathcal{I}_n(\mathbf{Q})}\int\prod_{k=1}^{n}\frac{du_k}{\sqrt{2\pi}}\mathbb{E}_b\left[\prod_{k=1}^{n}\theta(b-u_k)\right]F(\boldsymbol{u})u_v u_r$$

D.1.1 Replica Symmetry Solution

In order to find the $\mathbf{Q}_{sd}$ which satisfies eq(D.1) an ansatz for $\mathbf{Q}$ is introduced, the simplest is given by the symmetry replica solution, i.e. $\mathbf{Q}_{ab} = \delta_{a,b} + (1-\delta_{a,b})q$ to which correspond $(\mathbf{Q}^{-1})_{aa} = \frac{(1+q(n-1))}{(1-q)(1+q(n-1))}$ and $(\mathbf{Q}^{-1})_{ab} = -\frac{q}{(1-q)(1+q(n-1))}$ for $a \neq b$. For $n \to 0$ it follows $\mathcal{I}_n(\mathbf{Q}) \to 1$, $\det\mathbf{Q} \to 1$ and:

$$\langle\langle u_v^2\rangle\rangle = \int D_{t,b}\Big(\int_{-\infty}^{b}\frac{du}{\sqrt{2\pi}}e^{-u^2/(2C^2(1-q))+utR}u^2\Big)\Big(\int_{-\infty}^{b}\frac{du}{\sqrt{2\pi}}e^{-u^2/(2C^2(1-q))+utR}\Big)^{-1} \tag{D.2}$$

while, for $v \neq r$ instead:

$$\langle\langle u_v u_r\rangle\rangle = \int D_{t,b}\Big(\int_{-\infty}^{b}\frac{du}{\sqrt{2\pi}}e^{-u^2/(2C^2(1-q))+utR}u\Big)^2\Big(\int_{-\infty}^{b}\frac{du}{\sqrt{2\pi}}e^{-u^2/(2C^2(1-q))+utR}\Big)^{-2} \tag{D.3}$$

with:

$$D_{t,b} = \frac{e^{-\frac{t^2}{2}}}{\sqrt{2\pi}}\frac{e^{-\frac{(b-k)^2}{2B^2}}}{\sqrt{2\pi}B}dtdb$$

and:

$$R = \frac{\sqrt{q}}{C(1-q)}$$

$\langle\langle u_v u_r\rangle\rangle$s, in the limit $n \to 0$, don't depend directly on indices u and v. This implies that the last term in eq(D.1) can be written as:

$$\sum_{v,r=1}^{n}(\mathbf{Q}^{-1})_{av}(\mathbf{Q}^{-1})_{br}\langle\langle u_v u_r\rangle\rangle = \frac{1}{(1-q)^3}\big(-2q\langle\langle u_1^2\rangle\rangle + (1+q)\langle\langle u_1 u_2\rangle\rangle\big)$$

By rescaling $u \to uC\sqrt{1-q}$, $t \to t\sqrt{1-q}/\sqrt{q}$ and $b \to bC\sqrt{1-q}$, the integrals in eqs(D.2,D.3) can be simplified up to a single integration:

$$\langle\langle u_1^2\rangle\rangle = C^2 - C^2\frac{(1-q)}{(1+d^2q)}\Big\langle(\psi(x)\Big(2d^2q\mu + (1-d^2q)x\Big)\Big\rangle$$

And:

$$\langle\langle u_1 u_2\rangle\rangle = C^2q + \frac{2C^2}{\pi}(1-q)\langle\psi^2(x)\rangle + 2C^2d^2q\frac{(1-q)}{(1+d^2q)}\langle\psi(x)(x-\mu)\rangle$$

Where $\psi(x) = \frac{d}{dx}\log(1+\mathrm{erf}(x/\sqrt{2}))$ and $\langle ... \rangle$ is the expectation of a Gaussian random variable $\mathcal{N}(\mu, \sigma^2)$ with $\mu = k/(C\sqrt{1-q})$ and $\sigma^2 = (1+d^2q)/(d^2(1-q))$.

D.1.2 Stability of the Replica Symmetry Solution

Knowing that $\partial \mathbf{Q}_{a,b}/\partial \mathbf{Q}_{r,s} = \delta_{a,r}\delta_{b,s}$, $\partial(\mathbf{Q}_{ab})^{-1}/\partial \mathbf{Q}_{r,s} = -(\mathbf{Q}^{-1})_{ar}(\mathbf{Q}^{-1})_{s,b}$, and using the results in the previous section it holds:

$$\frac{\partial \langle\langle u_v u_r \rangle\rangle}{\partial \mathbf{Q}_{c,d}} = \frac{1}{2C^2}\sum_{i,j}(\mathbf{Q}^{-1})_{c,j}(\mathbf{Q}^{-1})_{d,i}\big(\langle\langle u_v u_r u_i u_j\rangle\rangle - \langle\langle u_i u_j\rangle\rangle\langle\langle u_v u_r\rangle\rangle\big)$$

The Hessian of $\varphi_n(\mathbf{Q})$, with $a < b$ and $c < d$, is given by:

$$\frac{\partial^2 \varphi_n(\mathbf{Q})}{\partial \mathbf{Q}_{a,b}\partial \mathbf{Q}_{c,d}} = \frac{\beta^2 J^2}{2}\delta_{a,c}\delta_{b,d} + \frac{\alpha-1}{2}(\mathbf{Q}^{-1})_{a,c}(\mathbf{Q}^{-1})_{d,b} + \tag{D.4}$$

$$-\frac{\alpha}{2C^2}\sum_{v,r}\big((\mathbf{Q}^{-1})_{ac}(\mathbf{Q}^{-1})_{dv}(\mathbf{Q}^{-1})_{br} - (\mathbf{Q}^{-1})_{av}(\mathbf{Q}^{-1})_{bc}(\mathbf{Q}^{-1})_{dr}\big)\langle\langle u_v u_r\rangle\rangle +$$

$$+\frac{\alpha}{4C^4}\sum_{v,r,i,j}(\mathbf{Q}^{-1})_{av}(\mathbf{Q}^{-1})_{br}(\mathbf{Q}^{-1})_{cj}(\mathbf{Q}^{-1})_{di}(\langle\langle u_v u_r u_i u_j\rangle\rangle - \langle\langle u_i u_j\rangle\rangle\langle\langle u_v u_r\rangle\rangle)$$

We need to evaluate 5 terms for $\langle\langle u_v u_r u_i u_j\rangle\rangle$, i.e.: $\langle\langle u_1^4\rangle\rangle$, $\langle\langle u_1^3 u_2\rangle\rangle$, $\langle\langle u_1^2 u_2 u_3\rangle\rangle$, $\langle\langle u_1^2 u_2^2\rangle\rangle$ and $\langle\langle u_1 u_2 u_3 u_4\rangle\rangle$. We also have 4 different values for $\frac{\partial^2 \varphi_n(\mathbf{Q})}{\partial \mathbf{Q}_{a,b}\partial \mathbf{Q}_{c,d}}$ according to the indices a, b, c and d:

$$\frac{\partial^2 \varphi_n(\mathbf{Q})}{\partial \mathbf{Q}_{a,b}\partial \mathbf{Q}_{c,d}} = \begin{cases} A_1, & a = c \text{ and } b = d \\ A_2, & (a = c \text{ and } b \neq d) \text{ or } (a \neq c \text{ and } b = d) \\ A_3, & a \neq c \text{ and } b \neq d \end{cases} \tag{D.5}$$

Following the idea of [138] the eigenvalues of $\frac{\partial^2 \varphi_n(\mathbf{Q})}{\partial \mathbf{Q}_{a,b}\partial \mathbf{Q}_{c,d}}$ are given by $\lambda_1 = A_1 - 4A_2 + 3A_3$ and $\lambda_2 = A_1 - 2A_2 + A_3$. We proceeded by writing a numerical scheme for evaluating $\lambda_{1,2}$s and relating them to the free parameters of the model.

Bibliography

[1] S. Belga Fedeli and Y. V. Fyodorov, "Statistics of off-diagonal entries of Wigner K-matrix for chaotic wave systems with absorption," *Journal of Physics A: Mathematical and Theoretical*, vol. 53, p. 165701, apr 2020.

[2] S. Belga Fedeli, Y. V. Fyodorov, and J. R. Ipsen, "Nonlinearity-generated resilience in large complex systems," *Physical Review E*, vol. 103, p. 022201, feb 2021.

[3] S. Belga Fedeli and Y. V. Fyodorov, "Random Superposition of Periodic Potentials and Characteristic Polynomials of Wishart Matrices," *In preparation*, 2021.

[4] B. Ławniczak Michałand van Tiggelen and L. Sirko, "Experimental investigation of distributions of the off-diagonal elements of the scattering and the Wigner's K matrices for networks with broken time reversal invariance," jul 2020.

[5] G. B. Arous, Y. V. Fyodorov, and B. A. Khoruzhenko, "Counting equilibria of large complex systems by instability index," *arxiv.org/abs/2008.00690*, aug 2020.

[6] G. Akemann, J. Baik, and P. Di Francesco, eds., *The Oxford Handbook of Random Matrix Theory*, vol. 1. Oxford University Press, aug 2018.

[7] P. J. Forrester, N. C. Snaith, and J. J. Verbaarschot, "Developments in random matrix theory," *Journal of Physics A: Mathematical and General*, vol. 36, p. R1, mar 2003.

[8] J. Wishart, "The Generalised Product Moment Distribution in Samples from a Normal Multivariate Population," *Biometrika*, vol. 20A, pp. 32–52, dec 1928.

[9] E. P. Wigner, "Characteristic Vectors of Bordered Matrices With Infinite Dimensions," *The Annals of Mathematics*, vol. 62, p. 548, nov 1955.

[10] Madan Lal Mehta, "L'emploi del polynomes orthogonaux pour calculer certain determinants," *Rapport S.P.H (Saclay)*, vol. 658, 1960.

[11] F. J. Dyson, "The threefold way. Algebraic structure of symmetry groups and ensembles in quantum mechanics," *Journal of Mathematical Physics*, vol. 3, pp. 1199–1215, nov 1962.

[12] Madan Lal Mehta, *Random Matrices.* Elsevier-Academic Press, 3rd ed., 2004.

[13] V. A. Marčenko and L. A. Pastur, "Distribution of eigenvalues for some sets of random matrices," *Mathematics of the USSR-Sbornik*, vol. 1, pp. 457–483, apr 1967.

[14] J. Ginibre, "Statistical ensembles of complex, quaternion, and real matrices," *Journal of Mathematical Physics*, vol. 6, pp. 440–449, mar 1965.

[15] H. L. Montgomery, "The pair correlation of zeros of the zeta function," *Analytic number theory, Proc. Sympos. Pure Math., XXIV. American Mathematical Society*, pp. 181–193, 1973.

[16] R. M. May, "Will a large complex system be stable?," *Nature*, vol. 238, no. 5364, pp. 413–414, 1972.

[17] D. Voiculescu, "Asymptotically commuting finite rank unitary operators without commuting approximants," *Acta Sci. Math.*, vol. 45, pp. 429–431, 1983.

[18] D. Voiculescu, "Addition of certain non-commuting random variables," *Journal of Functional Analysis*, vol. 66, pp. 323–346, may 1986.

[19] C. A. Tracy and H. Widom, "Level-spacing distributions and the Airy kernel," *Communications in Mathematical Physics*, vol. 159, pp. 151–174, jan 1994.

[20] C. A. Tracy and H. Widom, "On orthogonal and symplectic matrix ensembles," *Communications in Mathematical Physics*, vol. 177, no. 3, pp. 727–754, 1996.

[21] I. Dumitriu and A. Edelman, "Matrix models for beta ensembles," *Journal of Mathematical Physics*, vol. 43, pp. 5830–5847, nov 2002.

[22] T. Tao, “Outliers in the spectrum of iid matrices with bounded rank perturbations,” *Probability Theory and Related Fields*, vol. 155, pp. 231–263, nov 2013.

[23] G. Livan, M. Novaes, and P. Vivo, *Introduction to Random Matrices - Theory and Practice*. Springer International Publishing, dec 2017.

[24] V. Kargin, “On Pfaffian Random Point Fields,” *Journal of Statistical Physics*, vol. 154, pp. 681–704, feb 2014.

[25] J. B. Hough, M. Krishnapur, Y. Peres, and B. Virág, “Determinantal Processes and Independence,” *Probability Surveys*, vol. 3, pp. 206–229, mar 2005.

[26] P. J. Forrester, *Log-Gases and Random Matrices*. Princeton University Press, 2010.

[27] T. Shinzato, “Validation of the replica trick for simple models,” *Journal of Statistical Mechanics: Theory and Experiment*, vol. 2018, pp. 1–23, apr 2018.

[28] K. B. Efetov, “Supersymmetry and theory of disordered metals,” *Advances in Physics*, vol. 32, pp. 53–127, jan 1983.

[29] V. Varadarajan, *Supersymmetry for Mathematicians: An Introduction*, vol. 11 of *Courant Lecture Notes*. Providence, Rhode Island: American Mathematical Society, jul 2004.

[30] A. Guionnet, G. W. Anderson and O. Zeitouni, *An Introduction to Random Matrices*. Cambridge University Press, 2005.

[31] Y. V. Fyodorov and E. Strahov, “An exact formula for general spectral correlation function of random Hermitian matrices,” *Journal of Physics A: Mathematical and General*, vol. 36, pp. 3203–3213, mar 2003.

[32] P. J. Forrester, J. R. Ipsen, D. Z. Liu, and L. Zhang, “Orthogonal and symplectic Harish-Chandra integrals and matrix product ensembles,” *Random Matrices: Theory and Application*, vol. 8, oct 2019.

[33] A. Borodin and E. Strahov, “Averages of characteristic polynomials in random matrix theory,” *Communications on Pure and Applied Mathematics*, vol. 59, pp. 161–253, feb 2006.

[34] H. Kösters, “On the second-order correlation function of the characteristic polynomial of a real symmetric wigner matrix,” *Electronic Communications in Probability*, vol. 13, pp. 435–447, jan 2008.

[35] Y. V. Fyodorov and A. Nock, “On random matrix averages involving half-integer powers of goe characteristic polynomials,” *Journal of Statistical Physics*, vol. 159, pp. 731–751, feb 2015.

[36] Y. V. Fyodorov, “Complexity of random energy landscapes, glass transition, and absolute value of the spectral determinant of random matrices,” *Physical Review Letters*, vol. 92, pp. 1–4, jun 2004.

[37] T. Tao and V. Vu, “Random Matrices: The circular Law,” *Communications in Contemporary Mathematics*, vol. 10, pp. 261–307, aug 2007.

[38] Y. V. Fyodorov, “Negative moments of characteristic polynomials of random matrices: Ingham-Siegel integral as an alternative to Hubbard-Stratonovich transformation,” *Nuclear Physics B*, vol. 621, pp. 643–674, jan 2002.

[39] Y. V. Fyodorov and E. Strahov, “Characteristics polynomials of random Hermitian matrices and Duistermaat-Heckman localisation on non-compact Kähler manifolds,” *Nuclear Physics B*, vol. 630, pp. 453–491, may 2002.

[40] N. Bleistein and R. A. Handelsman, *Asymptotic Expansions of Integrals*. Dover Publications, Inc. New York, 1975.

[41] I.S. Gradshteyn and I.M. Ryzhik, *Table of Integrals, Series, and Products*. Academic Press Inc., 6th ed., 2000.

[42] M. Kac, “On the Average Number of Real Roots of a Random Algebraic Equation,” Tech. Rep. 4, 1943.

[43] J. E. Adler, R. J., Taylor, *Random Fields and Geometry*. Springer-Verlag New York, 2007.

[44] P. Littelmann, H. J. Sommers, and M. R. Zirnbauer, “Superbosonization of invariant random matrix ensembles,” *Communications in Mathematical Physics*, vol. 283, pp. 343–395, oct 2008.

[45] H.-J. Sommers, “Superbosonization,” *Acta Physica Polonica B*, vol. 38, oct 2007.

[46] C. Recher, M. Kieburg, T. Guhr, and M. R. Zirnbauer, "Supersymmetry Approach to Wishart Correlation Matrices: Exact Results," *Journal of Statistical Physics*, vol. 148, pp. 981–998, sep 2012.

[47] P. Dita, "Parametrisation of unitary matrices," *Journal of Physics A: General Physics*, vol. 15, pp. 3465–3473, nov 1982.

[48] P. Diţă, "Factorization of unitary matrices," *Journal of Physics A: Mathematical and General*, vol. 36, pp. 2781–2789, mar 2003.

[49] J. R. Ipsen and P. J. Forrester, "Kac-Rice fixed point analysis for single- and multi-layered complex systems," *Journal of Physics A: Mathematical and Theoretical*, vol. 51, pp. 1–19, oct 2018.

[50] Y. V. Fyodorov and B. A. Khoruzhenko, "Nonlinear analogue of the May-Wigner instability transition," *Proceedings of the National Academy of Sciences of the United States of America*, vol. 113, pp. 6827–6832, jun 2016.

[51] A. Auffinger, G. B. Arous, and J. Černý, "Random matrices and complexity of spin glasses," *Communications on Pure and Applied Mathematics*, vol. 66, pp. 165–201, feb 2013.

[52] Y. Y. Atas, E. Bogomolny, O. Giraud, and G. Roux, "Distribution of the ratio of consecutive level spacings in random matrix ensembles," *Physical Review Letters*, vol. 110, pp. 1–5, feb 2013.

[53] Harish-Chandra, "Differential Operators on a Semisimple Lie Algebra," *American Journal of Mathematics*, vol. 79, p. 87, jan 1957.

[54] U. Kuhl, O. Legrand, and F. Mortessagne, "Microwave experiments using open chaotic cavities in the realm of the effective Hamiltonian formalism," *Fortschritte der Physik*, vol. 61, pp. 404–419, feb 2013.

[55] G. Gradoni, J. H. Yeh, B. Xiao, T. M. Antonsen, S. M. Anlage, and E. Ott, "Predicting the statistics of wave transport through chaotic cavities by the random coupling model: A review and recent progress," *Wave Motion*, vol. 51, pp. 606–621, jun 2014.

[56] B. Dietz and A. Richter, "Quantum and wave dynamical chaos in superconducting microwave billiards," *Chaos*, vol. 25, p. 097601, mar 2015.

[57] H. Cao and J. Wiersig, "Dielectric microcavities: Model systems for wave chaos and non-Hermitian physics," *Reviews of Modern Physics*, vol. 87, pp. 61–111, jan 2015.

[58] Y. V. Fyodorov, T. Kottos, and H. J. Stöckmann, "Trends in quantum chaotic scattering," *Journal of Physics A: Mathematical and General*, vol. 38, dec 2005.

[59] J. J. Verbaarschot, H. A. Weidenmüller, and M. R. Zirnbauer, "Grassmann integration in stochastic quantum physics: The case of compound-nucleus scattering," *Physics Reports*, vol. 129, no. 6, pp. 367–438, 1985.

[60] G. E. Mitchell, A. Richter, and H. A. Weidenmüller, "Random matrices and chaos in nuclear physics: Nuclear reactions," *Reviews of Modern Physics*, vol. 82, pp. 2845–2901, oct 2010.

[61] Y. V. Fyodorov and D. V. Savin, "Resonance Scattering of Waves in Chaotic Systems," in *The Oxford handbook of random matrix theory* (G. Akemann et al., ed.), Oxford University Press, 2011.

[62] H. Schomerus, "Random matrix approaches to open quantum systems," in *Stochastic Processes and Random Matrices: Lecture Notes of the Les Houches Summer School*, vol. 104, pp. 409–473, Oxford University Press, jan 2018.

[63] V. V. Sokolov and V. G. Zelevinsky, "Dynamics and statistics of unstable quantum states," *Nuclear Physics, Section A*, vol. 504, pp. 562–588, nov 1989.

[64] Y. V. Fyodorov and H. J. Sommers, "Statistics of resonance poles, phase shifts and time delays in quantum chaotic scattering: Random matrix approach for systems with broken time-reversal invariance," *Journal of Mathematical Physics*, vol. 38, pp. 1918–1981, apr 1997.

[65] Y. V. Fyodorov, D. V. Savin, and H. J. Sommers, "Scattering, reflection and impedance of waves in chaotic and disordered systems with absorption," *Journal of Physics A: Mathematical and General*, vol. 38, pp. 10731–10760, dec 2005.

[66] Y. V. Fyodorov and D. V. Savin, "Statistics of resonance width shifts as a signature of eigenfunction nonorthogonality," *Physical Review Letters*, vol. 108, p. 184101, may 2012.

[67] S. Kumar, A. Nock, H. J. Sommers, T. Guhr, B. Dietz, M. Miski-Oglu, A. Richter, and F. Schäfer, "Distribution of scattering matrix elements in quantum chaotic scattering," *Physical Review Letters*, vol. 111, p. 030403, jul 2013.

[68] S. Kumar, B. Dietz, T. Guhr, and A. Richter, "Distribution of Off-Diagonal Cross Sections in Quantum Chaotic Scattering: Exact Results and Data Comparison," *Physical Review Letters*, vol. 119, p. 244102, dec 2017.

[69] Y. V. Fyodorov, S. Suwunnarat, and T. Kottos, "Distribution of zeros of the S-matrix of chaotic cavities with localized losses and coherent perfect absorption: Non-perturbative results," *Journal of Physics A: Mathematical and Theoretical*, vol. 50, jun 2017.

[70] T. Kottos and U. Smilansky, "Chaotic scattering on graphs," *Physical Review Letters*, vol. 85, pp. 968–971, jul 2000.

[71] O. Hul, S. Bauch, P. Pakoński, N. Savytskyy, K. Życzkowski, and L. Sirko, "Experimental simulation of quantum graphs by microwave networks," *Physical Review E - Statistical Physics, Plasmas, Fluids, and Related Interdisciplinary Topics*, vol. 69, p. 7, may 2004.

[72] O. Hul, O. Tymoshchuk, S. Bauch, P. M. Koch, and L. Sirko, "Experimental investigation of Wigner's reaction matrix for irregular graphs with absorption," *Journal of Physics A: Mathematical and General*, vol. 38, pp. 10489–10496, dec 2005.

[73] O. Ławniczak Michałand Hul, S. Bauch, P. Seba, and L. Sirko, "Experimental and numerical investigation of the reflection coefficient and the distributions of Wigner's reaction matrix for irregular graphs with absorption," *Physical Review E - Statistical, Nonlinear, and Soft Matter Physics*, vol. 77, p. 56210, may 2008.

[74] S. Lawniczak Michałand Bauch, O. Hul, and L. Sirko, "Experimental investigation of the enhancement factor for microwave irregular networks with preserved

and broken time reversal symmetry in the presence of absorption," *Physical Review E - Statistical, Nonlinear, and Soft Matter Physics*, vol. 81, p. 46204, apr 2010.

[75] S. Hemmady, X. Zheng, E. Ott, T. M. Antonsen, and S. M. Anlage, "Universal impedance fluctuations in wave chaotic systems," *Physical Review Letters*, vol. 94, p. 014102, jan 2005.

[76] S. Hemmady, X. Zheng, J. Hart, T. M. Antonsen, E. Ott, and S. M. Anlage, "Universal properties of two-port scattering, impedance, and admittance matrices of wave-chaotic systems," *Physical Review E - Statistical, Nonlinear, and Soft Matter Physics*, vol. 74, p. 036213, sep 2006.

[77] X. Zheng, S. Hemmady, T. M. Antonsen, S. M. Anlage, and E. Ott, "Characterization of fluctuations of impedance and scattering matrices in wave chaotic scattering," *Physical Review E - Statistical, Nonlinear, and Soft Matter Physics*, vol. 73, p. 046208, apr 2006.

[78] Y. V. Fyodorov, "Induced vs. spontaneous breakdown of S-matrix unitarity: Probability of no return in quantum chaotic and disordered systems," *JETP Letters*, vol. 78, no. 4, pp. 250–254, 2003.

[79] Y. V. Fyodorov and D. V. Savin, "Statistics of impedance, local density of states, and reflection in quantum chaotic systems with absorption," *JETP Letters*, vol. 80, no. 12, pp. 725–729, 2004.

[80] D. V. Savin, H. J. Sommers, and Y. V. Fyodorov, "Universal statistics of the local green's function in wave chaotic systems with absorption," *JETP Letters*, vol. 82, no. 8, pp. 544–548, 2005.

[81] R. A. Méndez-Sánchez, U. Kuhl, M. Barth, C. H. Lewenkopf, and H. J. Stöckmann, "Distribution of reflection coefficients in absorbing chaotic microwave cavities," *Physical Review Letters*, vol. 91, p. 174102, oct 2003.

[82] L. Ławniczak Michałand Sirko, "Investigation of the diagonal elements of the Wigner's reaction matrix for networks with violated time reversal invariance," *Scientific Reports*, vol. 9, dec 2019.

[83] I. Rozhkov, Y. V. Fyodorov, and R. L. Weaver, "Variance of transmitted power in multichannel dissipative ergodic structures invariant under time reversal," *Physical Review E - Statistical, Nonlinear, and Soft Matter Physics*, vol. 69, pp. 1–10, mar 2004.

[84] I. Rozhkov, Y. V. Fyodorov, and R. L. Weaver, "Statistics of transmitted power in multichannel dissipative ergodic structures," *Physical Review E - Statistical Physics, Plasmas, Fluids, and Related Interdisciplinary Topics*, vol. 68, no. 1, p. 12, 2003.

[85] H. Nishioka and H. A. Weidenmüller, "Compound-nucleus scattering in the presence of direct reactions," *Physics Letters B*, vol. 157, pp. 101–104, jul 1985.

[86] D. V. Savin, M. Richter, U. Kuhl, O. Legrand, and F. Mortessagne, "Fluctuations in an established transmission in the presence of a complex environment," *Physical Review E*, vol. 96, sep 2017.

[87] E. Strahov and Y. V. Fyodorov, "Universal Results for Correlations of Characteristic Polynomials: Riemann-Hilbert Approach," *Communications in Mathematical Physics*, vol. 241, pp. 343–382, sep 2003.

[88] L. Pauling, "The diamagnetic anisotropy of aromatic molecules," *The Journal of Chemical Physics*, vol. 4, pp. 673–677, oct 1936.

[89] S. Allesina and S. Tang, "The stability–complexity relationship at age 40: a random matrix perspective," *Population Ecology*, vol. 57, pp. 63–75, jan 2015.

[90] P. Landi, H. O. Minoarivelo, Å. Brännström, C. Hui, and U. Dieckmann, "Complexity and stability of ecological networks: a review of the theory," *Population Ecology*, vol. 60, pp. 319–345, oct 2018.

[91] R. M. May, *Stability and Complexity in Model Ecosystems.* Princeton University Press, 1973.

[92] S. Johnson, V. Domínguez-García, L. Donetti, and M. A. Muñoz, "Trophic coherence determines food-web stability," *Proceedings of the National Academy of Sciences of the United States of America*, vol. 111, pp. 17923–17928, dec 2014.

[93] J. Grilli, T. Rogers, and S. Allesina, "Modularity and stability in ecological communities," *Nature Communications*, vol. 7, pp. 1–10, jun 2016.

[94] L. Stone, "The feasibility and stability of large complex biological networks: A random matrix approach," *Scientific Reports*, vol. 8, dec 2018.

[95] J. W. Baron and T. Galla, "Dispersal-induced instability in complex ecosystems," *Nature Communications*, vol. 11, pp. 6032–6032, dec 2020.

[96] I. Neri and F. L. Metz, "Spectral theory for the stability of dynamical systems on large oriented locally tree-like graphs," *arXiv: 1908.07092*, 2019.

[97] E. Bairey, E. D. Kelsic, and R. Kishony, "High-order species interactions shape ecosystem diversity," *Nature Communications*, vol. 7, aug 2016.

[98] J. Grilli, G. Barabás, M. J. Michalska-Smith, and S. Allesina, "Higher-order interactions stabilize dynamics in competitive network models," *Nature*, vol. 548, pp. 210–213, aug 2017.

[99] C. K. Fisher and P. Mehta, "The transition between the niche and neutral regimes in ecology," *Proceedings of the National Academy of Sciences of the United States of America*, vol. 111, pp. 13111–13116, sep 2014.

[100] G. Biroli, G. Bunin, and C. Cammarota, "Marginally stable equilibria in critical ecosystems," *New Journal of Physics*, vol. 20, p. 083051, aug 2018.

[101] G. Wainrib and J. Touboul, "Topological and dynamical complexity of random neural networks," *Physical Review Letters*, vol. 110, p. 118101, mar 2013.

[102] M. Scheffer, S. Carpenter, J. A. Foley, C. Folke, and B. Walker, "Catastrophic shifts in ecosystems," *Nature*, vol. 413, pp. 591–596, oct 2001.

[103] L. Dai, D. Vorselen, K. S. Korolev, and J. Gore, "Generic indicators for loss of resilience before a tipping point leading to population collapse," *Science*, vol. 336, pp. 1175–1177, jun 2012.

[104] I. Ispolatov, V. Madhok, S. Allende, and M. Doebeli, "Chaos in high-dimensional dissipative dynamical systems," *Scientific Reports*, vol. 5, p. 12506, jul 2015.

[105] H. Sompolinsky, A. Crisanti, and H. J. Sommers, "Chaos in random neural networks," *Physical Review Letters*, vol. 61, pp. 259–262, jul 1988.

[106] J. Kadmon and H. Sompolinsky, "Transition to chaos in random neuronal networks," *Physical Review X*, vol. 5, p. 041030, nov 2015.

[107] A. Crisanti and H. Sompolinksy, "Path integral approach to random neural networks," *Physical Review E*, vol. 98, p. 062120, dec 2018.

[108] F. Roy, G. Biroli, G. Bunin, and C. Cammarota, "Numerical implementation of dynamical mean field theory for disordered systems: Application to the Lotka-Volterra model of ecosystems," *Journal of Physics A: Mathematical and Theoretical*, vol. 52, p. 484001, nov 2019.

[109] H. Sompolinsky, A. Crisanti, and H. J. Sommers, "Chaos in random neural networks," *Physical Review Letters*, vol. 61, pp. 259–262, jul 1988.

[110] L. D. Landau and E. M. Lifshitz, *Quantum Mechanics Non-relativistic Theory.* Pergamon Press, 1991.

[111] Y. V. Fyodorov and R. Tublin, "Counting stationary points of the loss function in the simplest constrained least-square optimization," *Acta Phys. Pol. B*, vol. 51, pp. 1663–1672, nov 2019.

[112] A. Maillard, G. B. Arous, and G. Biroli, "Landscape Complexity for the Empirical Risk of Generalized Linear Models," *Proceedings of The First Mathematical and Scientific Machine Learning Conference*, pp. 287–327, aug 2020.

[113] J. H. Park, T. H. Lee, Y. Liu, J. Chen, J. H. Park, T. H. Lee, Y. Liu, and J. Chen, "Basics and Preliminaries of Time-Delay Systems," in *Dynamic Systems with Time Delays: Stability and Control*, pp. 23–58, Springer Singapore, 2019.

[114] G. Stepan, *Retarded Dynamical Systems: Stability and Characteristic Functions.* Longman Scientific & Technical, 1989.

[115] M. R. García, B. A. Pearlmutter, P. E. Wellstead, and R. H. Middleton, "A Slow Axon Antidromic Blockade Hypothesis for Tremor Reduction via Deep Brain Stimulation," *PLoS ONE*, vol. 8, p. e73456, sep 2013.

[116] S. Sharifi, M. Crane, A. Shamaie, and H. Ruskin, "Random matrix theory for portfolio optimization: A stability approach," *Physica A: Statistical Mechanics and its Applications*, vol. 335, pp. 629–643, apr 2004.

[117] H. R. Golmakani and M. Fazel, "Constrained portfolio selection using particle swarm optimization," *Expert Systems with Applications*, vol. 38, pp. 8327–8335, jul 2011.

[118] G. Parisi, "Constraint Optimization and Statistical Mechanics," *arxiv.org/abs/cs/0312011*, dec 2003.

[119] M. T. Oakley, D. J. Wales, and R. L. Johnston, "Energy landscape and global optimization for a frustrated model protein," *Journal of Physical Chemistry B*, vol. 115, pp. 11525–11529, oct 2011.

[120] S. Ranganathan, P. F. Suthers, and C. D. Maranas, "OptForce: An Optimization Procedure for Identifying All Genetic Manipulations Leading to Targeted Overproductions," *PLoS Computational Biology*, vol. 6, p. e1000744, apr 2010.

[121] P. Mehta, W. Cui, C. H. Wang, and R. Marsland, "Constrained optimization as ecological dynamics with applications to random quadratic programming in high dimensions," *Physical Review E*, vol. 99, p. 052111, may 2019.

[122] Z. Li and H. A. Scheraga, "Monte Carlo-minimization approach to the multiple-minima problem in protein folding.," *Proceedings of the National Academy of Sciences of the United States of America*, vol. 84, pp. 6611–6615, oct 1987.

[123] M. Mezard, G. Parisi, and M. Virasoro, *Spin Glass Theory and Beyond*, vol. 9 of *World Scientific Lecture Notes in Physics*. World Scientific, nov 1986.

[124] S. Franz and G. Parisi, "The simplest model of jamming," *Journal of Physics A: Mathematical and Theoretical*, vol. 49, p. 145001, feb 2016.

[125] G. C. Calafiore and L. . El Ghaoui, *Optimization models — Control systems and optimization*. Cambridge University Press, 2014.

[126] S. Kirkpatrick and D. Sherrington, "Infinite-ranged models of spin-glasses," *Physical Review B*, vol. 17, pp. 4384–4403, jun 1978.

[127] E. Vincent, V. Dupuis, M. Alba, J. Hammann, and J.-P. Bouchaud, "Aging phenomena in spin-glass and ferromagnetic phases: Domain growth and wall dynamics," *Europhysics Letters (EPL)*, vol. 50, pp. 674–680, jun 2000.

[128] Y. V. Fyodorov and P. Le Doussal, "Topology Trivialization and Large Deviations for the Minimum in the Simplest Random Optimization," *Journal of Statistical Physics*, vol. 154, pp. 466–490, sep 2014.

[129] F. Rosenblatt, "The perceptron: A probabilistic model for information storage and organization in the brain," *Psychological Review*, vol. 65, pp. 386–408, nov 1958.

[130] G. Biroli, R. Monasson, and M. Weigt, "A variational description of the ground state structure in random satisfiability problems," *European Physical Journal B*, vol. 14, pp. 551–568, apr 2000.

[131] E. Gardner and B. Derrida, "Optimal storage properties of neural network models," *Journal of Physics A: General Physics*, vol. 21, pp. 271–284, jan 1988.

[132] M. Shcherbina and B. Tirozzi, "On the volume of the intersection of a sphere with random half spaces," *Comptes Rendus Mathematique*, vol. 334, pp. 803–806, may 2002.

[133] P. Charbonneau, J. Kurchan, G. Parisi, P. Urbani, and F. Zamponi, "Glass and Jamming Transitions: From Exact Results to Finite-Dimensional Descriptions," *Annual Review of Condensed Matter Physics*, vol. 8, pp. 265–288, mar 2017.

[134] A. O. Siemens and M. Van Hecke, "Jamming: A simple introduction," *Physica A: Statistical Mechanics and its Applications*, vol. 389, pp. 4255–4264, oct 2010.

[135] E. Gardner, "Structure of metastable states in the Hopfield model," *Journal of Physics A: Mathematical and General*, vol. 19, p. L1047, nov 1986.

[136] V. Dotsenko, *Introduction to the Replica Theory of Disordered Statistical Systems.* Cambridge University Press, nov 2000.

[137] C. Liu and N. Boumal, "Simple Algorithms for Optimization on Riemannian Manifolds with Constraints," *Applied Mathematics and Optimization*, vol. 82, pp. 949–981, dec 2020.

[138] J. R. De Almeida and D. J. Thouless, “Stability of the Sherrington-Kirkpatrick solution of a spin glass model,” *Journal of Physics A: Mathematical and General*, vol. 11, pp. 983–990, may 1978.

[139] Y. V. Fyodorov, “On Statistics of Bi-Orthogonal Eigenvectors in Real and Complex Ginibre Ensembles: Combining Partial Schur Decomposition with Supersymmetry,” *Communications in Mathematical Physics*, vol. 363, pp. 579–603, oct 2018.

[140] Y. V. Fyodorov, “A Spin Glass Model for Reconstructing Nonlinearly Encrypted Signals Corrupted by Noise,” *Journal of Statistical Physics*, vol. 175, pp. 789–818, jun 2019.

[141] Y. V. Fyodorov, P. Le Doussal, A. Rosso, and C. Texier, “Exponential number of equilibria and depinning threshold for a directed polymer in a random potential,” *Annals of Physics*, vol. 397, pp. 1–64, oct 2018.

[142] A. Y. Orlov, “New solvable matrix integrals,” in *International Journal of Modern Physics A*, vol. 19, pp. 276–293, World Scientific Publishing Company, may 2004.

[143] Y. V. Fyodorov and H. J. Sommers, “Statistics of S-matrix poles in few-channel chaotic scattering: Crossover from isolated to overlapping resonances,” *Journal of Experimental and Theoretical Physics Letters*, vol. 63, pp. 1026–1030, jun 1996.

[144] R. Delannay and G. Le Caër, “Distribution of the determinant of a random real-symmetric matrix from the Gaussian orthogonal ensemble,” *Physical Review E - Statistical Physics, Plasmas, Fluids, and Related Interdisciplinary Topics*, vol. 62, pp. 1526–1536, aug 2000.